International Workshop on Duration of Load in Lumber and Wood Products

[illegible]

Proceedings

Forintek Canada Corp.

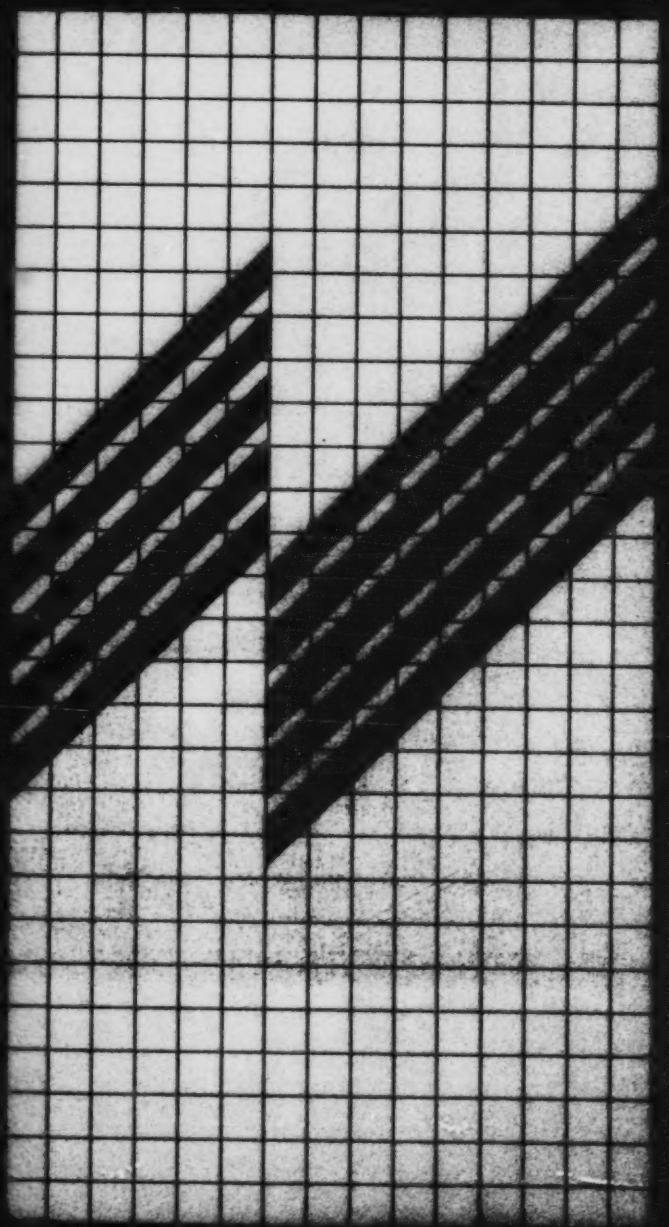

86-03970/

PROCEEDINGS OF THE INTERNATIONAL WORKSHOP ON DURATION OF LOAD IN LUMBER AND WOOD PRODUCTS

VANCOUVER, CANADA
SEPTEMBER 12 - 13, 1985

FORINTEK CANADA CORP.
Western Region
6620 N.W. Marine Dr.
Vancouver, B.C.
V6T 1X2

March, 1986

SPECIAL PUBLICATION NO. SP-27

ISSN 0824-2119

PREFACE

The International Workshop on Duration of Load in Lumber and Wood Products was held in Vancouver, B.C., Canada on September 12 and 13, 1985. The idea for this workshop arose from a request from the Canadian Standards Association, responsible for the Canadian Code of Engineering Design in Wood, CSA 086, to bring together scientists from around the world working on duration of load studies. The objective was to exchange information and ideas on experimental methodology, modelling alternatives and engineering code implementation problems, particularly in relation to reliability based design.

The invitation to participate in the workshop was well received by scientists in all parts of the world, and a total of 57 scientists and engineers attended. This volume contains all the papers presented.

The organizing committee wishes to acknowledge the financial support received from the Canadian Forestry Service and the Canadian Wood Council, and the help and collaboration of the staff of Forintek Canada Corp., without which the conference could not have taken place.

J.D. Barrett
R.O. Foschi
H.P. Vokey
E. Varoglu

TABLE OF CONTENTS

	Page
PREFACE	i
Duration of Load Effects, 2 x 8 Spruce Lumber in Bending: Data Analysis and Modelling R.O Foschi and J.D. Barrett	1
Duration of Load Research on Lumber at the U.S. Forest Products Laboratory Charles C. Gerhards	14
Testing and Analysis Carried Out as Part of the Princes Risborough Laboratory's Programme to Examine the Duration of Load Effect on Timber A.R. Fewell	22
Rate of Loading and Duration of Load Tests in Tension and in Compression P. Glos	33
Results of Pair-Matching of Wood for Long-Term Loading Bengt Norén	39
Duration of Load Tests with Notched Spruce Beams at Two Moisture Levels P. Hoffmeyer, H.J. Krebs and L.F. Nielsen	45
Prediction of Short- and Long-Term Behavior of Truss-Plate Joints in Tension L.D. Palka	51
Creep and Creep-Rupture in Reconstituted Panel Products Theodore Laufenberg	61
Wood as a Cracked Viscoelastic Material Part I: Theory and Applications Lauge Fuglsang Nielsen	67
Wood as a Cracked Viscoelastic Material Part II: Sensitivity and Justification of a Theory Lauge Fuglsang Nielsen	79
Reliability of Wood Structural Systems Ricardo O. Foschi	90
Application of Duration of Load Information to Timber Design Codes Borg Madsen	103
Duration of Load Tests at U.B.C. Borg Madsen	109
LIST OF PARTICIPANTS	115

DURATION OF LOAD EFFECTS, 2 x 8 SPRUCE LUMBER IN BENDING: DATA ANALYSIS AND MODELLING

R.O. Foschi and J.D. Barrett

Professor, Civil Engineering Dept., and Professor and Head, Wood Science and Harvesting Dept., Faculty of Forestry, respectively, University of British Columbia, Vancouver, B.C.

INTRODUCTION

A wood member which survives the application of a load may fail over time if the same load is sustained. This phenomenon has a direct and important influence on the safety and reliability of wood structures, affecting the use of lumber and other wood products in applications from housing to heavy timber construction. Little is known about this phenomenon, and the rules that are presently followed to adjust the short-term strength of lumber for loads of longer duration were derived many years ago mainly from tests on small, clear Douglas-fir specimens in bending.

Codes for engineering design practice are being transformed from the traditional "Allowable Unit Stress Design" procedure to a "Limit States Design" (LSD) or reliability-based format. Introduction of LSD Codes offers the opportunity of providing more uniform levels of safety across structures and across materials. The transformation of the design recommendations for wood structures to a reliability-based format cannot be readily accomplished without information on the effect of load duration: the strength of a wood element cannot be estimated independently of the type and duration of the load which such an element will undergo during its service life.

The expense and time required to obtain experimental data on duration of load effects for all grades, sizes and species of dimension lumber produced in North America would be prohibitive. A cooperative research effort has been undertaken between Canada and the U.S.A. to develop duration of load information on selected species, wood qualities, sizes and types of loading. The cooperative plan outlines a series of studies on three species which account for a large proportion of the dimension lumber used in North America: Douglas-fir, Southern pine and Canadian white spruce. The plan includes examinations to be conducted in bending, tension and compression, for two sizes (2 x 4 and 2 x 8), and two lumber qualities (low and high). The Canadian contribution to the coordinated project refers exclusively to Canadian white spruce, and this report includes a first analysis of the Canadian data for 2 x 8 spruce in bending.

MATERIALS, SAMPLE SELECTION AND EXPERIMENTAL PROCEDURES

One of the objectives of the research program was to assess the effect of quality on the long-term performance of 2 x 8 spruce lumber in bending. Accordingly, the experimental plan called for the identification of two lumber qualities, Q1 (High) and Q2 (Low), from the entire production of 2 x 8 spruce. "Quality" was taken to mean "bending strength." Thus, non-destructive bending strength predictors were used to separate the two desired experimental populations. A full description of the procedures followed for the non-destructive evaluation of the material is given by Samson (1983).

A total of 750 kiln-dried specimens were selected for each quality category from a single British Columbia mill. The specimens corresponding to each quality were separated into five groups of 150 specimens each. These five groups were used for four different experimental conditions:

1 Group (150 specimens) for "short-term strength evaluation" (control group);

1 Group (150 specimens) for a constant load test with a duration of three years;

2 Groups (300 specimens) for a constant load test with a duration of one year;

1 Group (150 specimens) for a rapid ramp load strength test.

Table 1 shows the characteristics of the qualities Q1 and Q2, both planned and as actually obtained during the testing of the control groups.

For each quality, the assignment of specimens to each of the five groups was conducted following a procedure which ensured (as much as possible) matching of the predicted short-term bending strength distributions for the individual groups. This procedure is outlined in detail by Samson (1983).

The sample sizes of 150 and 300 were obtained on the basis of computer simulation, using data from a previous experiment on hemlock lumber (Foschi and Barrett, 1982). The smaller sample size (150) was used for a constant load test where the load level was taken as 62.5 percent of the corresponding median control (short-term) strength. The larger sample of 300 was used for a second constant load test with a load level equal to 75 percent of the corresponding median control strength. These levels were chosen to result in the failure of at least 50 percent of the sample in, respectively, three and one years.

For both quality levels, the samples for each constant load level were further subdivided as follows: 1) half of the specimens were positioned in the testing frame with the worst edge defect appearing on the tension side, and 2) the other half was tested with the worst edge defect appearing on the compression side. These two sub-groups were referred to, respectively, as the Tension and Compression subgroups.

All specimens were tested at the Long-Term Loading Facility which Forintek Canada Corp. maintains in Richmond, B.C. Existing test frames (138-in. or 3.50-m span) from a previous hemlock experiment were used to load each specimen. The load was applied by means of a dead weight, adjusted to induce the planned bending stress in the specimen. The dead weight was applied by a hydraulic mechanism which allowed the lowering of the weight at a constant rate. This rate was adjusted to equal the one in the control ramp test used for short-term strength evaluation: approximately one minute was taken to reach a stress equal to the median control short-term strength.

Table 2 shows the constant stress levels applied to each quality, including the tension and compression sub-groups, and the corresponding median short-term strengths and applied stress ratios. The applied stress ratio ϕ is defined as the applied stress divided by the median control short-term strength for the sub-group. Table 2 also shows that, for each duration, the same stress level was applied to each quality. This resulted in the planned stress ratios of 0.75 and 0.625 being achieved only when all specimens for each quality are considered, but in different applied stress ratios for each sub-group.

Some specimens failed prior to the full application of the load. In such instances, the load reached was measured by means of a load cell attached to the loading mechanism. Since the rate of loading was specified, knowledge of the maximum load permitted the calculation of the time-to-failure for those specimens that broke during loading. Time-to-failure for specimens that survived loading was measured automatically by a microcomputer-based data acquisition system. All times-to-failure in the data include the time taken to apply the constant load.

One-year tests were discontinued after all specimens in the group had been loaded for one year. Surviving specimens were then unloaded to be tested to failure using a ramp loading identical to that of the control group. Such tests provide a partial check on the matching of the short-term strength distributions of long-term and short-term (control) groups.

TEST STATUS

At the time of this report, all three-year tests were underway and had been under load for approximately two years. Thus, the three-year results are available for preliminary analysis with their full sample size of 150.

The one-year tests are incomplete. Only 150 specimens have been loaded for one year in the Q2 quality, with 150 still remaining to be tested to complete the full sample of 300. For quality Q1, 75 specimens have been tested in the tension sub-group, and another 75 will be finished in the compression sub-group by April, 1986. By this date, therefore, 150 Q1 specimens will have been tested for one year, and 150 will still remain to complete the full sample of 300.

The deflection of the specimens has been monitored at regular intervals in order to estimate creep. These data are not included in the present report.

DATA ANALYSIS: EXPERIMENTAL RESULTS

at the lower probabilities. These two curves should match each other up to the percent (or cumulative probability) corresponding to the The times-to-failure for the controls and for the different constant load groups were ranked in order to construct the corresponding cumulative probability distribution functions. These are shown in Figures 1 through 6, where the times-to-failure in hours are expressed on a logarithmic scale.

Figure 1 shows the control, one-year and three-year results for Q1, tension sub-group. The sample sizes are 75 for the control and 75 for each of the constant load tests shown. Of particular interest is the lack of agreement between the control and the three-year curve specimens breaking during load application. Lack of agreement implies a lack of matching between the control sample and that used for the three-year Q1 tension test. Since matching was done initially with a carefully planned scheme based on non-destructive testing (Samson, 1983), it may be hypothesized that the short-term strength of the three-year sample changed during the waiting period until this sample could be loaded. Such change could have occurred because of moisture content variations.

Figure 2 shows the results for Q1, compression sub-group. Here the one-year test has not been completed, and the sample sizes are 75 for the control and 75 for the three-year test.

Figure 3 shows the combined results for Q1, which can only include the three-year test and the control, with sample sizes of 150 each.

Figure 4 presents the control, one-year and three-year results for Q2 in the tension sub-group. The sample sizes are, respectively, 75 and 75 for each of the two long-term tests.

Figure 5 shows the corresponding results for Q2, compression sub-group, also with sample sizes of 75 for the control and 75 for each of the two constant load tests.

Finally, Figure 6 shows the combination of all results for Q2, including the control, one-year and three-year tests. Corresponding sample sizes are now 150 for each.

As can be seen in Figure 6, the "one-year" test did in fact achieve failure of approximately 50 percent of the sample, as planned. Thus, the experiment behaved approximately as predicted on the basis of simulations using previous hemlock data. Similarly, the "three-year" test will achieve 50 percent failure in about three years, also as planned. Given that the test was designed using data from a different species, these results point to a relative insensitivity of duration of load effects to species differences when the applied stress ratio is kept constant.

If such insensitivity is present with respect to species differences, it may also be present with respect to quality variations within the same species. The comparison must be made at the same applied stress ratio and for tests with the full sample size (complete experiment). The present experiment status permits this comparison only for the control and the three-year tests.

Figure 7 shows the comparison between Q1 and Q2. The applied stress ratio is, in both cases, 0.625 (Table 2). It is apparent that the results are insensitive to quality effects if the applied stress ratio is constant.

The discrepancy between the controls in Figure 7 is due to a slight difference in the obtained median time-to-failure for the Q1 and Q2 short-term ramp test. These tests were conducted under load control, estimating the loading rate to produce a median failure time of one minute. The median time for Q1 was very close to one minute while that for Q2 was approximately 50 seconds.

The agreement between the three-year curves in Figure 7 is quite remarkable, given the very different characteristics of the qualities Q1 and Q2 shown in Table 1.

The same comparison cannot be made for the three-year tests broken down by tension or compression sub-groups, since the applied stress ratios are not the same (as shown in Table 2).

DATA ANALYSIS: MODELLING

The experimental results include only two types of loadings: a ramp used for short-term strength determination and a constant stress used in the long-term tests. Since actual service loads are seldom ramp or constant, the experimental results must be interpreted to extrapolate conclusions valid for a general loading situation.

Analysis of fatigue data in other materials has been based on essentially two types of models: 1) an accumulation of damage process or 2) a slow crack growth process. The first is based on the definition of a state variable "damage", normalized to be zero at the initiation of the control short-term test and one at the time of failure. The damage accumulation model prescribes the rate of growth in damage as a function of the applied stress and, in general, the already accumulated damage. The slow crack growth approach is based on the theory of fracture mechanics, and it prescribes the rate of crack growth as a function of the applied stress and the current crack length. Both approaches are thus similar, and both require calibration of model constants to the test results.

Whatever modelling technique is used, the resulting model must be able to make reliable predictions for all types of loadings.

This report presents the calibration of a damage accumulation model to the preliminary test results. Since the calibration must be made using the full sample size for completed experiments, only the results shown in Figure 7 were used to determine the model parameters. Furthermore, since the Q1 and Q2 results in Figure 7 can be taken to be identical, a single model was calibrated to the data combined for the two qualities.

The model decribes, for a given specimen, the rate of growth in the damage α:

$$\frac{d\alpha}{dt} = a\, e^{\omega_1 R_N} \left(\frac{\tau(t)}{\tau_s} - \sigma_o \right)^b + \lambda e^{\omega_2 V_N} \alpha \qquad [1]$$

where a, b, λ, ω_1, ω_2 and σ_o are model parameters to be found by calibration. τ_s is the short-term strength of the specimen, and R_N and V_N are standard random normal variables.

The parameter determination proceeded as follows (Foschi and Barrett, 1982): A set of parameters was chosen and the corresponding predicted times-to-failure were obtained by computer simulation using an integrated form of Equation 1. The difference between these predictions and the curves of Figure 7 was computed and minimized, in the least-squares sense, by searching for a best set of parameters. For each set, the predictions were obtained by simulating a control and a three-year experiment with 800 specimens.

The "best" set of parameters obtained was:

$$\left.\begin{array}{ll} a & = 0.305067 \times 10^{15} \\ b & = 36.0 \\ \lambda & = 0.250 \times 10^{-2} \\ \sigma_o & = 0.50 \\ \omega_1 & = 0.21 \\ \omega_2 & = 1.20 \end{array}\right\} \qquad [2]$$

The parameters ω_1 and ω_2 relate, respectively, to the variability in short- and long-term time-to-failure, while the parameter σ_o is a threshold stress ratio. The value $\sigma_o = 0.50$ means that no damage accumulates until the applied stress ratio exceeds 50 percent of the specimen's short-term strength.

The cumulative probability functions for times-to-failure, as predicted by the calibrated model, are shown in Figure 8 against the results for Q1 and Q2 of Figure 7. It is apparent that a good representation of the data is possible with the same model, both for the control tests and the three-year tests for the two qualities.

Figures 9, 10 and 11 show a comparison between model predictions and other Q2 tests. These comparisons were made taking into account the corresponding applied stress ratio shown in Table 2. Figure 9, for example, shows the agreement with Q2, one-year test. The agreement is not very good, but this comparison can only be called preliminary, since the data contains only 150 samples out of the 300 required. Figure 10 shows the agreement for the Q2 tension sub-group. The agreement is not very good, but this comparison is shown only for completeness, since the sample sizes are too small: 75 in each case. For good comparisons, the samples in a tension Q2 population should have been 300 for the one-year test and 150 for the three-year test. The same comment applies to Figure 11,showing the comparison between model and the Q2 compression sub-group. The agreement is now better t an for the tension sub-group, even at the small sample size of 75, but this is due to the relatively small ϕ levels (Table 2) and to the fact that results at low applied stress ratio are less sensitive to sample size.

Figures 12 and 13 show comparisons between model predictions and other Q1 tests. Figure 12 shows the Q1 compression sub-group, for which the agreement is satisfactory, and Figure 13 shows the Q1 tension sub-group for which, again, the agreement is not good for the one-year test. The sample sizes are 75 in each case and the same comments apply as discussed in the case of quality Q2.

The damage accumulation model, with parameter values from Equation 2, can be used to predict the shape of the relationship between applied

stress ratio and median time-to-failure in a constant load test. This type of graphical representation is directly comparable with the standard "Madison Curve" in use in Codes today.

Figure 14 shows the results for the 2 x 8 Spruce tests. The presence of the threshold stress ratio is now in evidence, since the curve in Figure 14 has a lower bound at the 0.50 level. The curve goes through 1.0 at a time of one minute, the median time adopted for the short-term test.

For comparison purposes, Figure 15 shows the spruce curve of Figure 14 superimposed on that corresponding to hemlock, from the experiment reported earlier (Foschi and Barrett, 1982). It is apparent that there is little difference between them, pointing to lack of sensitivity of the results (at least on the median) to species differences. Differences between the two experiments exist when variability in the results is considered: the hemlock test was performed on "No.2 and Better" grade, with a short-term strength coefficient of variation of 0.40; while the spruce tests were conducted on separate qualities with narrower strength distributions.

CONCLUSIONS

1. Test results to date show no significant differences in damage accumulation between lumber qualities when each is loaded to the same applied stress ratio.

2. There appear to be no significant differences between species when each is loaded to the same applied stress ratio.

3. A single damage accumulation model may be calibrated to results for both qualities.

RECOMMENDATIONS

1. Complete the one-year testing of both spruce lumber qualities to achieve the full sample size of 300 in each.

2. Carry the three-year testing of both qualities to full term.

3. Complete the ramp testing of the surviving specimens in all groups, to compare short-term strength distributions with initial control tests. Measurement of moisture contents prior to these ramp tests is required.

4. Compare moisture content in specimens at time of failure under constant load, with moisture content at time of control ramp load test. These moisture content comparisons should be performed to normalize all strength distributions to a uniform moisture content prior to final data analysis.

5. Consolidate creep measurement data.

REFERENCES

Foschi, R.O. and J.D. Barrett. 1982. Load-duration effects in western hemlock lumber. Journal of the Structural Division, ASCE, ST7, 108:1494-1510.

Samson, M. 1983. Duration of Load Effects in Spruce Lumber in Bending: Data Report-First Year. Forintek Canada Corp., Report to the Canadian Forestry Service.

Table 1

Characteristics of the Two Qualities
Used in the Experiment

Characteristic		Quality Category	
		Q1 (High)	Q2 (Low)
Planned strength range	(Mpa)	41.4 to 52.8	16.6 to 30.0
	(Psi)	6000 to 7659	2400 to 4350
Median strength from tests	(Mpa)	48.7	24.8
	(Psi)	7058	3600
Coefficient of variation from control tests (%)		17.1	27.7
Strength ratio range		0.60 to 0.95	0.20 to 0.60
Modulus of elasticity range ($\times 10^6$ Psi)		1.50 to 1.90	0.90 to 1.25

Table 2

Applied Constant Stess Levels, Mpa (Psi)

Quality	Group	Median Control Strength	1 Year N = 300 Stress	ϕ	3 Years N = 150 Stress	ϕ
	All Specimens	48.7 (7058)	36.5 (5294)	0.75	30.4 (4411)	0.625
Q1	Tension	46.7 (6768)	36.5 (5294)	0.78	30.4 (4411)	0.65
	Compression	50.5 (7320)	36.5 (5294)	0.72	30.4 (4411)	0.60
	All Specimens	24.8 (3600)	18.6 (2700)	0.75	15.5 (2250)	0.625
Q2	Tension	21.9 (3178)	18.6 (2700)	0.85	15.5 (2250)	0.71
	Compression	27.3 (3960)	18.6 (2700)	0.68	15.5 (2250)	0.57

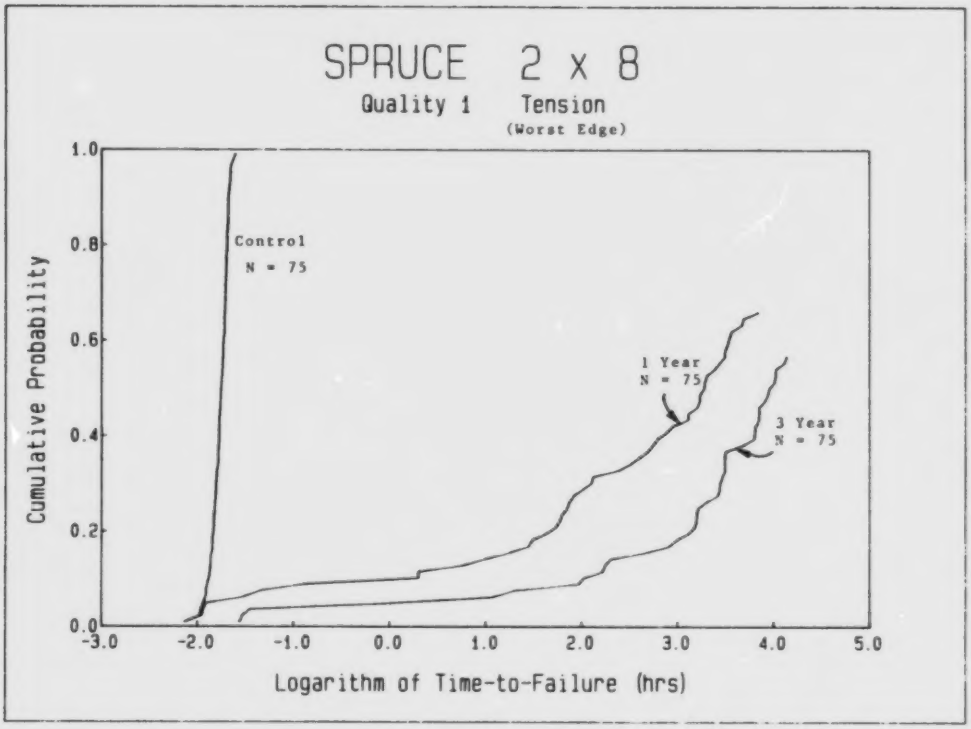

Figure 1.

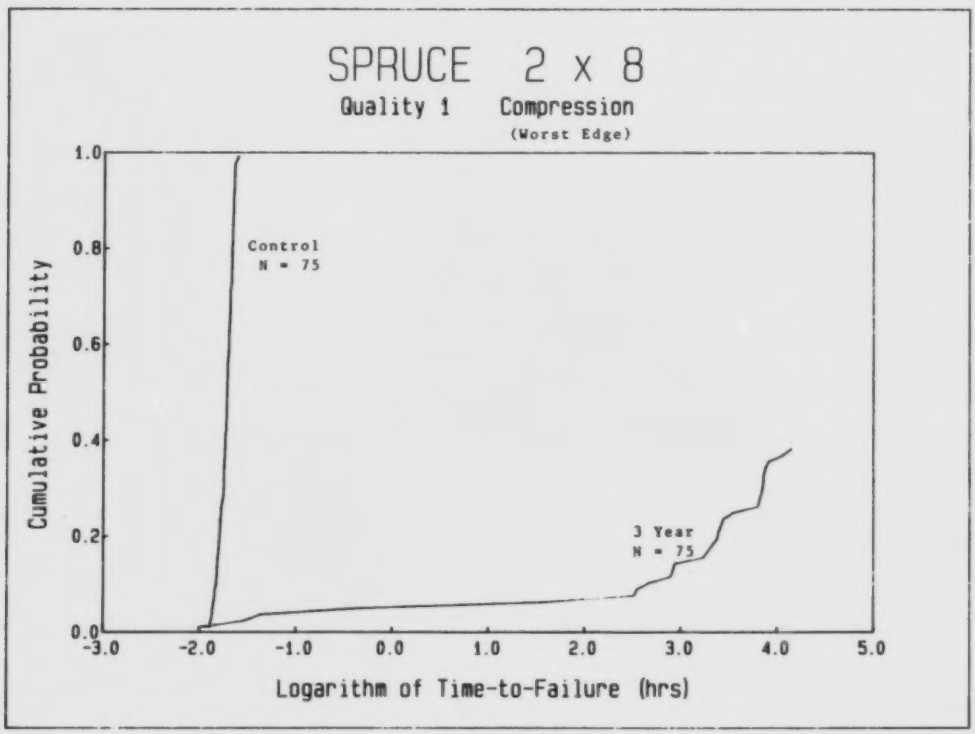

Figure 2.

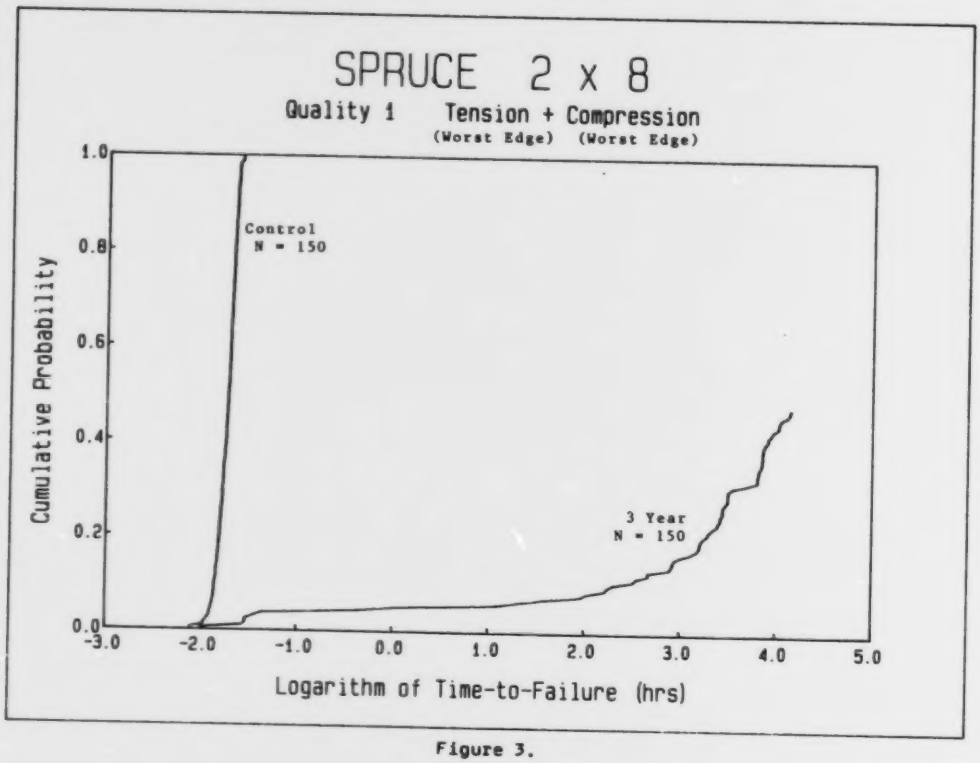

Figure 3.

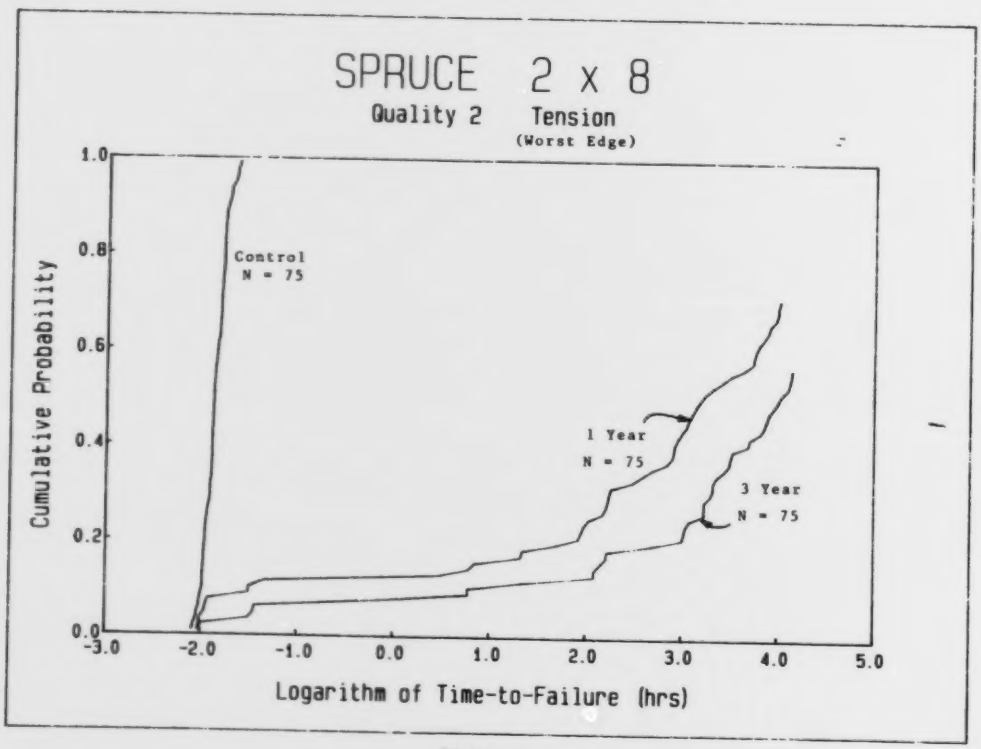

Figure 4.

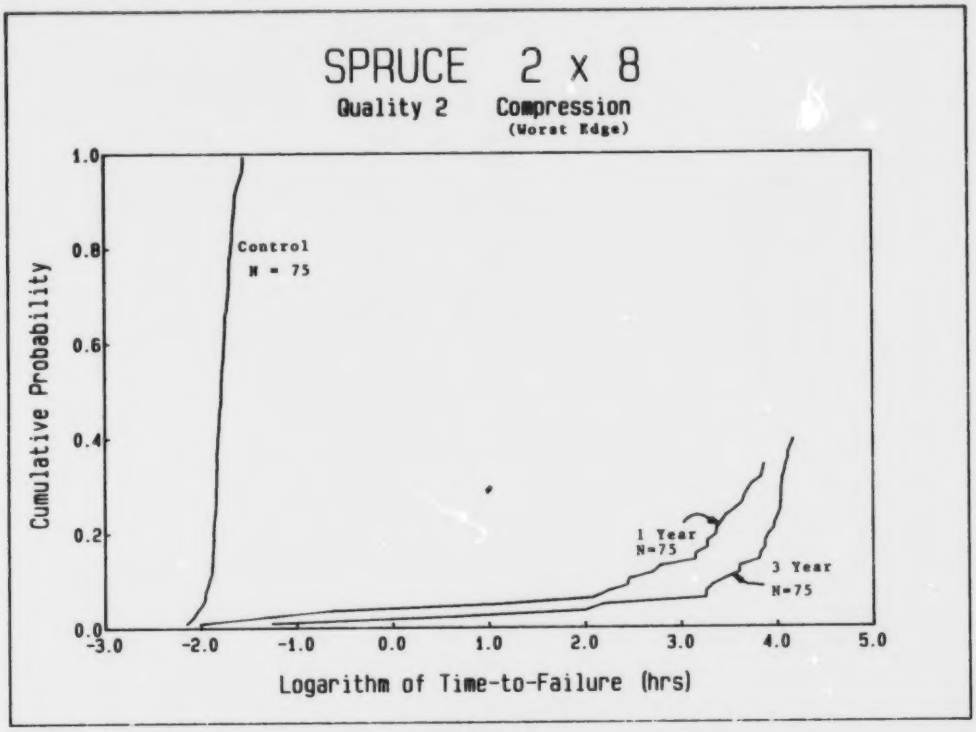

Figure 5.

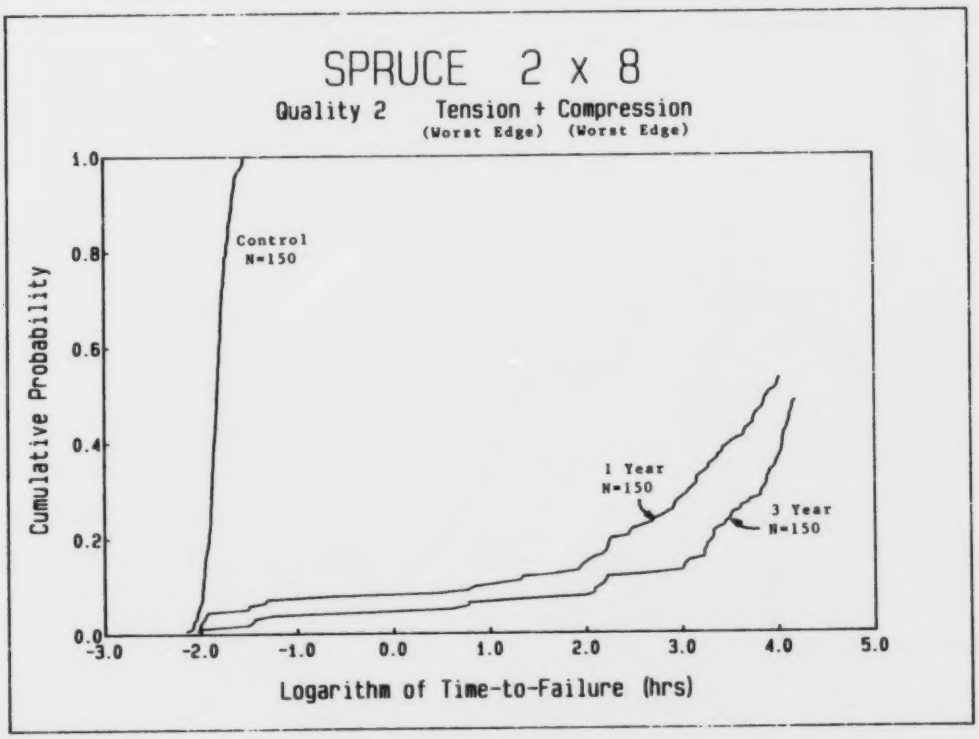

Figure 6.

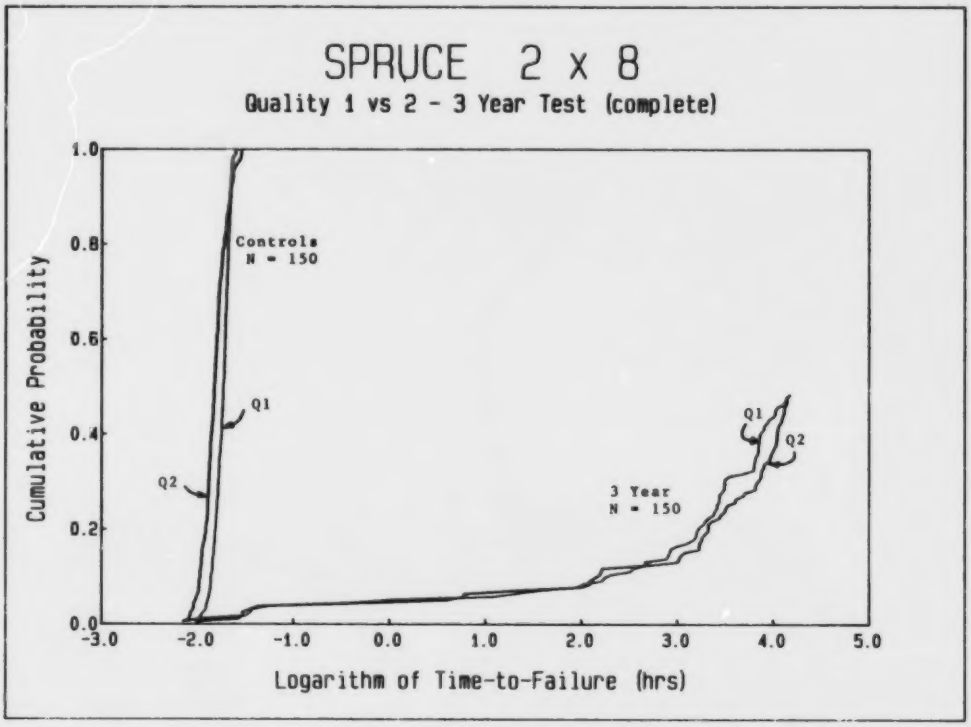

Figure 7.

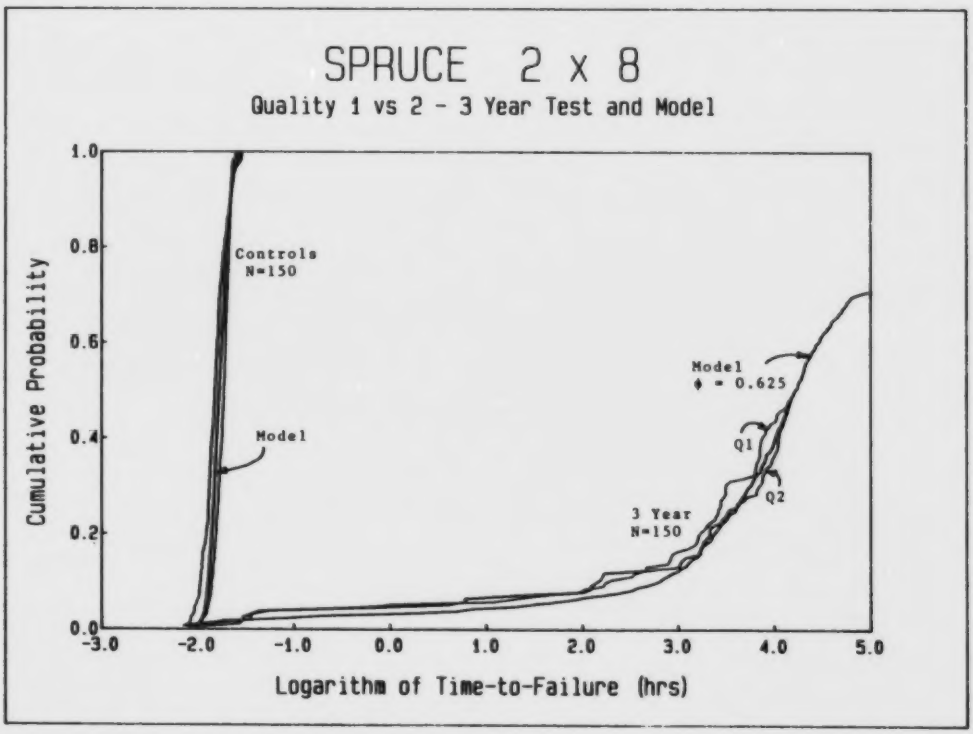

Figure 8.

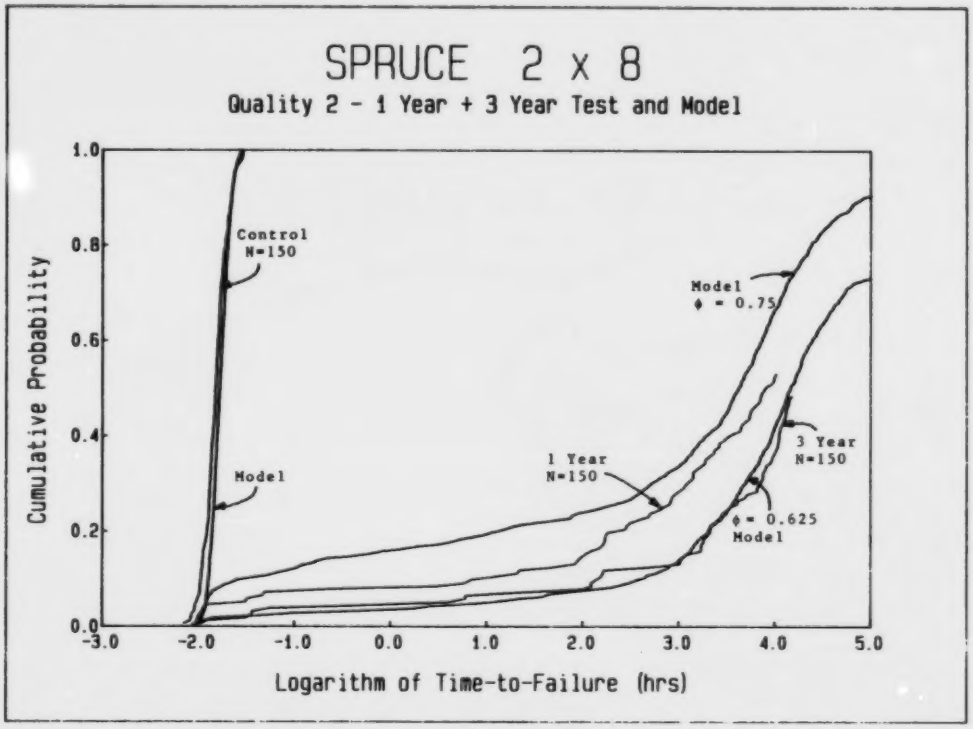

Figure 9.

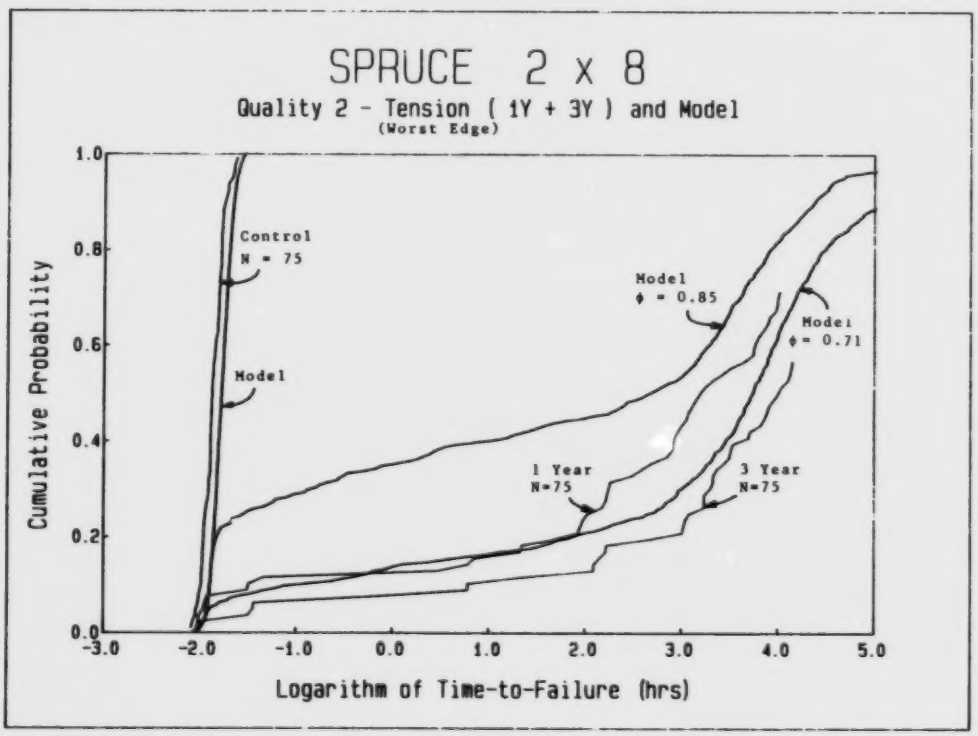

Figure 10.

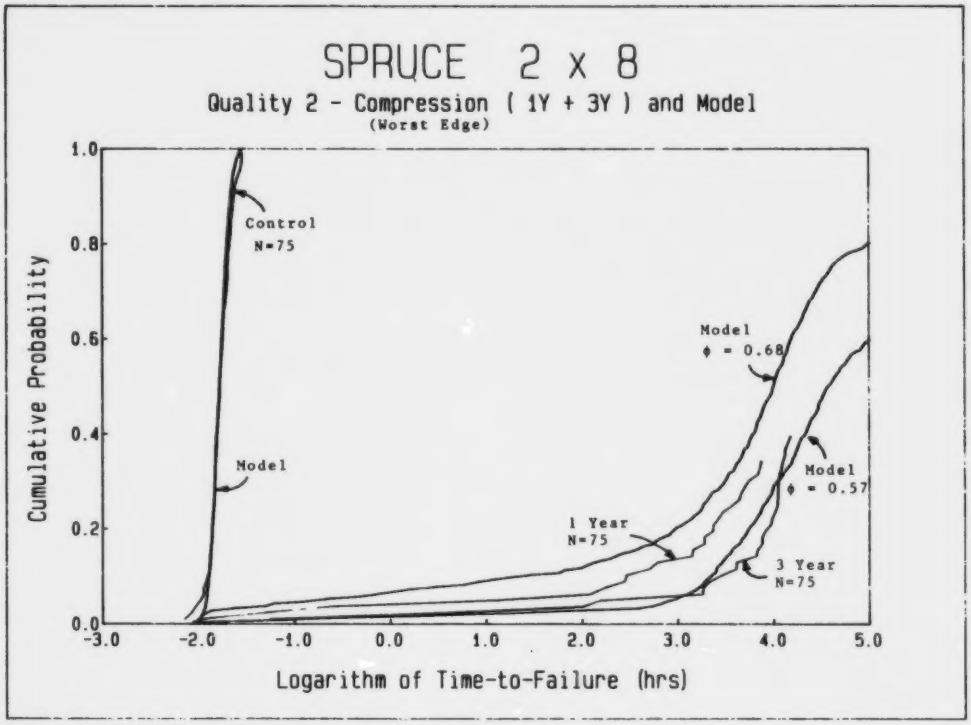

Figure 11.

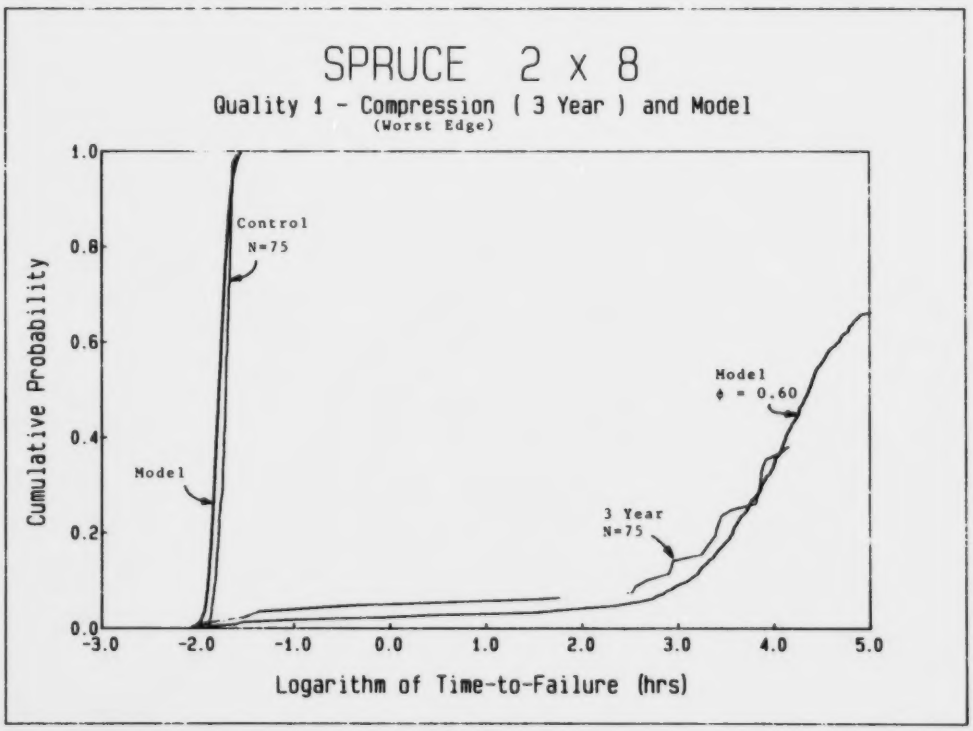

Figure 12.

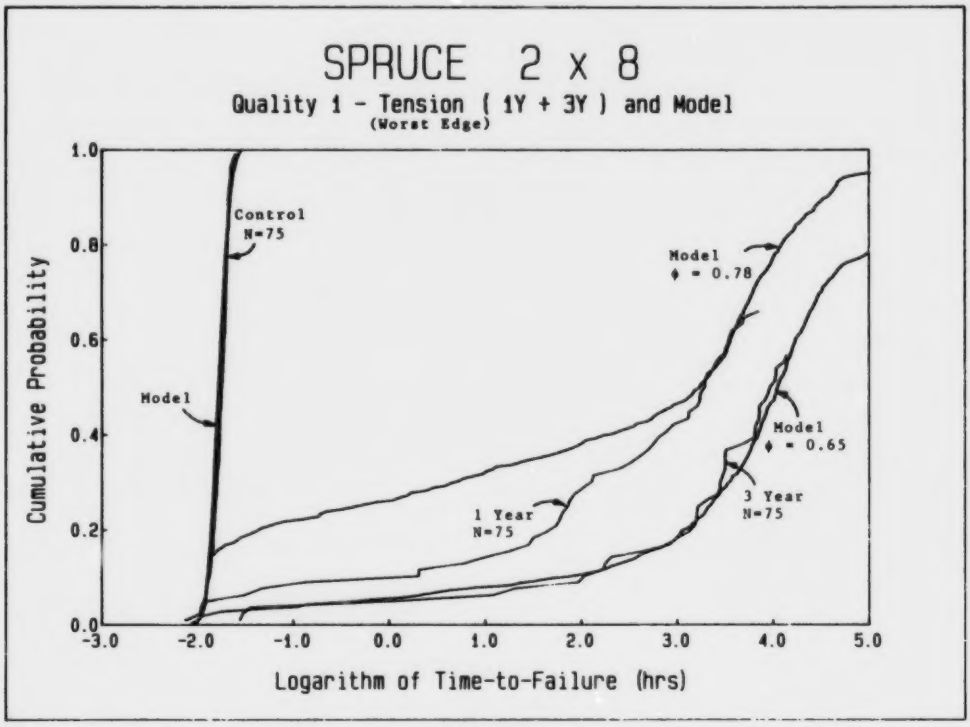

Figure 13.

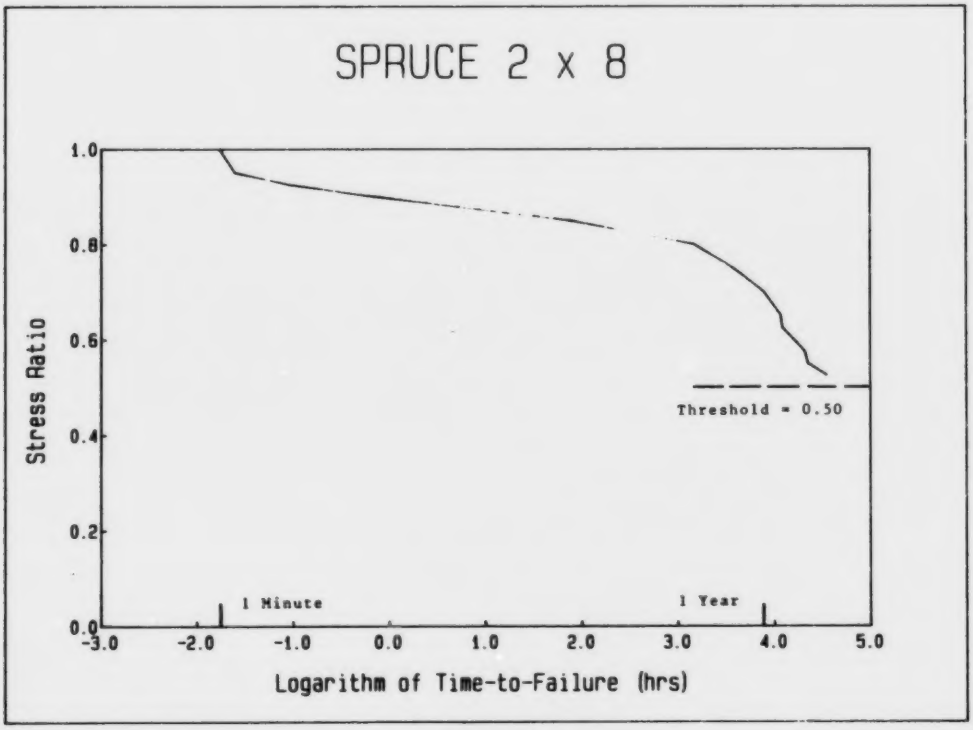

Figure 14.

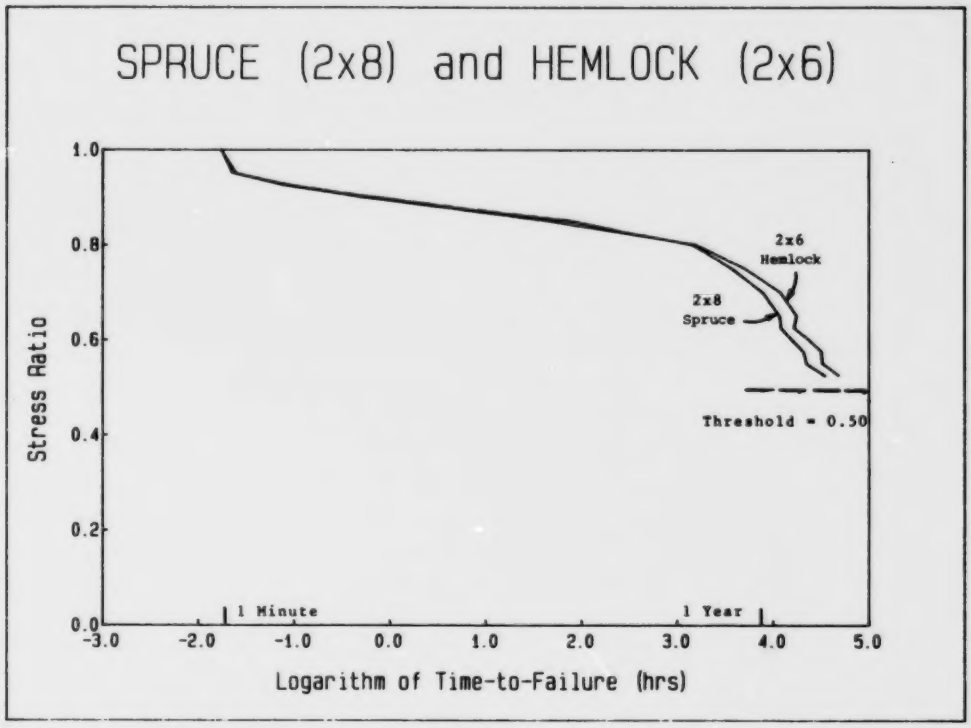
SPRUCE (2x8) and HEMLOCK (2x6)
Stress Ratio
1.0
0.8
0.6
0.4
0.2
0.0
2x6
Hemlock
2x8
Spruce
Threshold = 0.50
1 Minute
1 Year
-3.0
-2.0
-1.0
0.0
1.0
2.0
3.0
4.0
5.0
Logarithm of Time-to-Failure (hrs)

Figure 15.

DURATION OF LOAD RESEARCH ON LUMBER AT THE U.S. FOREST PRODUCTS LABORATORY

Charles C. Gerhards
Research Engineer, Forest Products Laboratory, USDA, Madison, WI

Several factors can affect the load duration behavior of lumber. These factors are generally ignored in wood engineering design criteria. Moreover, the existing design criteria is based on a load duration curve developed from tests of clear wood in bending (Wood, 1951). To evaluate these possible factors, the Forest Products Laboratory's (FPL) objectives for conducting duration of load (DOL) research are severalfold.

1. Establish a duration of load (DOL) curve for lumber;
2. Determine the effect of grade on the load duration curve;
3. In cooperation with Forintek, determine the effect of species on the load duration curve;
4. Determine the effect of loading mode on the load duration curve (also being done at Forintek Canada Corp.);
5. Evaluate the effect of processing variables on load duration;
6. Evaluate the effect of temperature and relative humidity (RH) on load duration; and
7. Evaluate the effect of repeated loads on load duration.

All of the above objectives except for item 4 are associated with loading in the bending mode. Item 4 includes tension and compression. Four different types of machines were developed and several samples of lumber were obtained to conduct the necessary studies. The experimental techniques are discussed in this document.

This report does not cover research on load duration or creep of edge knot lumber as these have been reported elsewhere (Gerhards and Link, 1983; Gerhards, 1985).

EXPERIMENTAL TECHNIQUES

TEST MACHINES

The test machines consist of 150 pneumatic load bending machines, 100 dead load bending frames, 50 dead load cable-pulley tension machines, and 50 dead load cable-pulley compression machines. All of these machines are designed to test 2 x 4 lumber.

The pneumatic loading machines (Figure 1) are designed to test 2 x 4's on a support span of 84 inches, with a two-point loading bar spanning 24 inches. Total load up to 3,000 pounds (14,700 psi bending stress equivalent) can be applied at a maximum rate of about 750 pounds per minute. The pneumatic loading system is flexible in that a variety of loading histories can be imposed on specimens, e.g. ramp, constant, step-constant, and repeated loads.

Ramp loading is controlled by a computer, while constant load is maintained with a precision pressure regulator. The computer also records load-deflection-time data. It is programmed to read deflections every 1/10 second but only saves data when the new deflection exceeds the last saved deflection by a set amount.

The 150 pneumatic bending machines are divided into three groups so that 50 specimens can be tested simultaneously for a given load history. Each group of 50 machines has a master cylinder-load cell frame (Figure 2) which is used to monitor bending load. Each of the three groups of 50 machines also has at least two 20-gallon air tanks as well as system piping to maintain air pressure/bending load when any one specimen fails. These machines and associated tanks and piping are located in two rooms (100 in one, 50 in the other) maintained at constant temperature and RH.

The 100 dead load bending frames (Figure 3) are located in a building that is vented but does not have air conditioning equipment, i.e. temperature and RH are not controlled. Loading span and support span are the same as for the pneumatic machines. Deflections of the loaded 2 x 4's are monitored with a digital electronic gauge mounted in a stainless steel cage (Figures 3 and 4). A precision-ground granite rail (Figure 4) is used as a reference for zeroing the deflection gauge-cage system.

The 50 DOL tension machines (Figure 5) were built according to a design by Glos and Barrett (1980) with slight modification. These machines were designed to test 12-foot-long 2 x 4 to 2 x 8 lumber with an upper specimen load of 40,000 pounds. The machines apply a tensile force to a specimen through a system of cables and pulleys and a dead weight. The system has a theoretical magnification of about 105 to 1; however, calibration of the FPL machines shows this factor to vary, depending on weight and height of the dead load and whether the load is being jacked up or let down. Specimens to be tested in these machines were only recently acquired. In the meantime the machines are being used to study creep of pin-connected wood joints.

The DOL compression machine (Figure 6) is based on a modification of the design developed by Forintek (personal communication). As with the tension machine, the compression machine uses a system of cables and pulleys to magnify a dead load; the theoretical magnification ratio is 72 to 1. The FPL compression machines are designed for a maximum compression load of 23,500 pounds, and are on order from a fabricating shop.

LUMBER SPECIMENS

Several samples of lumber have been purchased by FPL for load duration studies. These include a 3,600-specimen sample, 1,849-specimen sample, and some smaller samples used to study kiln drying or treatment effects.

3,600-Specimen Sample

The major DOL effort at FPL has been spent working with portions of a 3,600-specimen sample of Douglas-fir 2 x 4's. The lumber was purchased surfaced green with the specification that the central two-foot length in an eight-foot length contain the strength-controlling defect (knot or slope of grain) for the piece, with half of the specimens to be No. 2 and the other half Select Structural with an upper strength ratio (SR) of about 80 percent. Actual ASTM D245 (ASTM 1974) strength ratios ranged from below 25 percent to above 80 percent based on measurements at FPL.

At FPL the lumber was kiln dried by a mild schedule. As the lumber had been surfaced green, it was not surfaced after drying.

After a long period of shed storage and conditioning for several months at 70°F and 55 percent RH, the following properties of each specimen were measured:

- Length to 1/10 inch.
- Width to 1/100 inch, based on average of third-point values.
- Thickness to 1/100 inch, based on average of third-point values.
- Type of limiting knot (see Figure 7).
- Knot size by displacement to nearest 1/100 inch.
- Knot distance from end to nearest inch for limiting knot.
- Knot distance from edge to nearest 1/100 inch for limiting knot.
- Deflection to 1/10,000 inch for a 55-pound total load (equivalent bending stress = 282 psi).
- Bow to 1/10 inch.
- Crook to 1/10 inch.
- Twist to 1/10 inch.
- General slope of grain in central one-third length--inches distance for one-inch deviation.

For the deflection measurement, specimens were tested in edgewise bending on a span of 84 inches with symmetric loading at two points, two feet apart. Modulus of elasticity (E) calculated from the load-deflection data and SR calculated from the knot or slope of grain data were used to sort the specimens. Warp measurements and any unusual characteristics were used to cull specimens from further DOL use. Data were recorded for 3,564 specimens. The remainder were culled because warp was excessive or lumber had unusual characteristics or was damaged.

Wood moisture content averages about 9 to 10 percent for the storage conditions. Since the lumber was surfaced green, presumably to 1-9/16 x 3-9/16 and then dried, it is not surprising that width averaged less than 3.5 inches because four percent shrinkage could be expected.

The maximum controlling knot size in the 3,564 specimens ranged from about 1/4 to 2-1/2 inches by the displacement method, with strength ratio ranging from 95 percent to eight percent. Equations for strength ratio are given in ASTM D245 for edge knots and centerline knots. The only knot type that can be a true centerline knot is type 22 (Figure 7). Except for the type 10, all other knot types contact a narrow face. ASTM D245 is not specific in identifying which knot types should be considered edge and which types should be considered nonedge, except for the provision that a knot whose center is within two-thirds of the knot size from the lumber edge is to be considered an edge knot. Consequently, all knot types except for type 22 (no type 10's were found) were assumed to be edge knots, and the size of the edge knot was determined by the displacement method of ASTM D245. For the type 22 knot, an equivalent edge knot size was iteratively determined. Then knot strength ratios were calculated from the ASTM D245 strength ratio formulas for edge knots, depending on whether SR was greater or less than 45 percent. ASTM D245 also contains a table relating slope of grain to strength ratio. The equation with slope of grain (Z) in degrees

$$SR = 100 - [(Z-2.84)/0.001871]^{1/2}$$

fits the slope of grain strength-ratio table values for bending members within 3-1/2 percent or less. The equation was used to calculate strength ratio when slope of grain was limiting. The distribution of specimen strength ratios is summarized as:

	SR class in percent							
	<25	25-35	35-45	45-55	55-65	65-75	75-85	85-95
Number of specimens	103	353	265	649	689	856	626	23

Width and thickness of the 3,564 specimens are summarized as:

	Mean	Standard deviation	Min.	Max.
		---(inches)---		
Width	3.41	0.028	3.32	3.56
Thickness	1.51	.014	1.40	1.57

Because of the large spread in strength ratio, the lumber was sorted into four grades: Select Structural for SR $\geq$ 65 percent, No. 1 for 55 $\leq$ SR < 65 percent, No. 2 for 45 $\leq$ SR < 55 percent, and No. 3 for 26 $\leq$ SR < 45 percent. Note that the sort was based on the strength ratio limitations rather than knot size limitations of the National Grading Rule.

Modulus of elasticity was calculated on the basis of a 1.5-inch by 3.5-inch cross-section. Statistics of E by grade are:

Grade	Number of Specimens	E in 10^6 pounds per square inch			
		Mean	Standard deviation	Minimum	Maximum
SS	1,505	1.86	0.293	0.71	2.81
No. 1	689	1.57	.293	.76	2.91
No. 2	649	1.39	.271	.76	2.65
No. 3	721	1.32	.258	.69	2.20

The modulus of elasticity statistics show a trend toward higher average values as grade quality increases; however, the overlap in moduli of elasticity among the grades is large, based on minimum and maximum values.

Sorting of specimens into groups proceeded after some further culling. First, specimens with bow > 0.3 inch and crook > 0.5 inch were culled. Also culled were specimens with SR > 85 percent or < 25 percent. Then the specimens in each grade were ranked by modulus of elasticity. A few additional specimens having extreme values of modulus of elasticity were culled from each of the four grades to make the total number of specimens per grade exactly divisible by 25. After culling, the number of usable specimens was:

1,475 Select Structural
675 No. 1
625 No. 2
600 No. 3

Thus, the number of groups of 25 specimens that could be formed were:

59 Select Structural
27 No. 1
25 No. 2
24 No. 3

For each grade with the usable specimens ranked by modulus of elasticity, the ranked specimens were divided into sets, each set containing the number of groups to be formed. Then for each grade the specimens in each set were randomly assigned group numbers. The group numbers assigned were:

1 through 59 for Select Structural
60 through 86 for No. 1
87 through 111 for No. 2
112 through 135 for No. 3

Through this scheme and because of the narrow width of SR classes, the groups for any one grade were reasonably matched in distributions of E and SR. Random choice from among the groups of any one grade was made for tests at different DOL histories.

1,849-Specimen Sample

This lumber set of Douglas-fir was selected by Western Wood Products Association personnel. Specifications called for specimens 12 to 16 feet long, with a No. 2 grade strength controlling knot or slope of grain with its position no closer than 30 inches from either lumber end. (Similar restrictions were placed on spruce lumber sampled for Forintek's DOL research, allowing an evaluation of species effects.) These specimens are undergoing final equilibrium moisture content (EMC) conditioning at FPL prior to nondestructive evaluation for E and SR. The lumber will be sorted into groups similar to those for the 3,600-specimen sample and will be used in bending, tension and compression DOL research, allowing those properties to be compared for load duration effect.

High-Temperature Drying Southern Pine Sample

316 green, rough-sawn southern pine eight-foot-long 2 x 4's were obtained from a Mississippi mill with the specification that none contain the tree pith. They were to be No. 2 and better quality overall with a strength-controlling knot in the central two-foot length with all Select Structural excluded. Specimens were dip treated to prevent blue stain and wrapped to prevent drying during shipping.

At FPL, specimens were nondestructively tested for E flatwise (EF) on a span of 45 inches with two symmetrical load points located 18 inches apart. The central strength-controlling characteristic was located between the load points.

The lumber was then sorted into four groups, after setting aside four specimens for kiln control samples. The sorting was done by ranking the specimens according to EF, blocking the ranked specimens into sets of four, and then randomly assigning the four specimens in a set to the four groups. This resulted in four groups of 78 specimens each, with each group having a like distribution of EF's.

Two groups selected at random were dried with a conventional low temperature schedule (180°F maximum dry-bulb temperature). The other two groups were dried with a high-temperature schedule (240°F dry-bulb for 21 hours). Each kiln run had a 90 psf top loading for drying restraint.

After kiln drying the lumber was further conditioned for about four months at 70°F and 50 percent relative humidity (the conditions of strength and duration of load testing). Then the specimens were surfaced to the 1.5- by 3.5-inch standard size and graded for SR of knots and slope of grain in the central 28-inch length and for warp overall (Southern Pine Inspection Bureau, 1977). Lumber grade for SR was more variable than originally sought. Only 64 percent qualified as No. 1 and No. 2, 25 percent were Select Structural and 11 percent were No. 3. Also, 11 percent contained the tree pith. Lumber grade for warp was good to excellent--96 percent of high-temperature drying (HTD) and 87 percent of conventional drying met Select Structural requirements for straightness, and only one HTD specimen and four conventional specimens failed to meet No. 2 for straightness.

Due to changes in grade from drying and surfacing, additional sorting was required to select 50 specimens in each group to make the groups match qualitywise. Thus, specimens having 100 percent SR in the central 28-inch length or with too much warp (bow > 0.3 in., crook > 0.4 in., twist > 0.5 in.) were culled. The remaining specimens were remeasured for EF using the same procedure as for the rough, green condition.

Final selection decisions were based on predicted modulus of rupture (PMOR). The predicting equation (Ethington, 1970) was:

$$PMOR = \exp(7.58 + 0.377EF + 0.00947SR)$$

where EF (dry) is in 10^6 psi and SR is in percent. The PMOR's were ranked within each group and compared across groups. A few specimens were switched between groups 1 and 2 so that 50 specimens in group 1 matched 50 specimens in group 3 and 50 specimens in group 2 matched 50 specimens in group 4 for distribution of PMOR, with specimens having low EF from all groups excluded in average PMOR between the four groups. Selected specimens differed by less than one percent. Overall, PMOR averaged 6,890 psi, EF (dry) ranged from 1.0 to 2.6 million psi and SR ranged from 28 to 94 percent.

High-Temperature Drying Douglas-fir Sample

1,000 green, rough sawn Douglas-fir eight-foot-long 2 x 4's were obtained from an Oregon mill. Specifications required No. 2 or better grade with any that would make Select Structural or that had the tree pith excluded from

the sample. Specimens were coated to prevent mold and wrapped in a vapor barrier for shipment to FPL.

At FPL each specimen was tested for E edgewise (EE) on a five-foot span under centerpoint loading. The EE data for the 1,000 specimens were ordered, and the ordered values were divided into 200 sets of five values per set. Specimens in each of the five-valued sets were randomly assigned to two groups: two specimens in group 1 and three specimens in group 2, resulting in 400 specimens in group 1 and 600 specimens in group 2 with an equal distribution of E's between the two groups.

Group 1 was dried by a conventional kiln schedule where maximum dry-bulb temperature was 160°F. Group 2 dried by a high-temperature schedule where maximum dry-bulb temperature was 230°F (maintained for the first 19 hours of the 25-hour run). All specimens were sticker-stored at 75°F, 50 percent RH for several months, following which they were machined to 1.5 by 3.5 inches.

Specimens are now undergoing nondestructive evaluations (E, knot or slope of grain strength ratio, warp) which will be used to select four groups of 50 conventionally dried specimens, and six groups of 50 high-temperature dried specimens, such that each group is equally matched by E and strength ratio distributions. Final selected specimens will be used to compare static strengths and durations of loads at two constant levels.

Preservative Treatment Southern Pine Sample

550 southern pine eight-foot-long 2 x 4's were selected from a local (Madison, WI) house builders supply. These were graded No. 2 KD. Specimens were stored several months at 75°F, 50 percent RH. They were then nondestructively measured for E (same as for high-temperature Douglas-fir sample), knot or slope of grain strength ratio and warp. First, excessively warped specimens were culled. From the remainder, the specimens were ordered by E. The data were divided by E classes with a class increment in E of 100,000 psi. Next, with each E class, specimens were grouped into sets of eight specimens with like strength ratios. These eight specimens were randomly assigned to eight different groups. This sorting provided eight groups of 50 specimens with like distributions of E and strength ratio. The same routine will be used for the final sorting of Douglas-fir in the high-temperature drying study.

Four of the groups will be treated to 0.6 pcf with Type C CCA (AWPB FDN Standard) and redried with a mild kiln schedule. These and the controls will be tested for static strengths and DOL's at two constant levels.

LOAD HISTORIES

The different samples of lumber are or will be subjected to different load histories, depending on the particular study objective.

3,600-Specimen Sample

Parts of this sample are being used in, or are being planned for use in several different studies in bending. The primary study forms the base for the other studies. In the primary study, the objectives are severalfold: (1) develop a load duration curve for lumber, (2) evaluate grade effect, (3) evaluate repeated loads, and (4) evaluate effect of temperature and relative humidity. Results will be evaluated with a damage model.

The base study involves SS, No. 2, and No. 3 grades of Douglas-fir tested in an environment maintained at 73°F, 50 percent relative humidity. Load histories include three rates of ramp loading and three levels of step constant loading. The three rates include: static, 0.01 static and 0.0001 static, with approximate mean failure times of five minutes, eight hours, and one month, respectively. The three constant load levels include tests starting at the 5th, 15th, and 40th percentiles of static strength with steps to higher load levels after one year, seven weeks and seven days, respectively. All of the rates and levels were done on SS and No. 2 specimens. No. 3 specimens were subjected to only a part of these load histories. The longest duration of these tests (5th percentile) is 1-1/2 years.

Other studies using this sample include a 10-year dead load test (static 5th percentile divided by 1.62) in an uncontrolled environment using SS and No. 2 specimens, and two tests under controlled environment (73°F, 50 percent RH) using repeated loads on SS specimens. One of the repeated loads consists of several cycles of one week at the 5th percentile static strength, followed by one week at the 15th percentile static strength. The other repeated loads consist of several cycles of one week at the 15th percentile static strength, followed by one week at the 5th percentile static strength, followed by one week with no load.

The temperature and relative humidity effects tests are dependent on getting funding. The plan is to test SS and No. 2 at the 15th percentile static strength at a few different constant and variable levels of temperature and relative humidity.

1,849-Specimen Sample

No tests are yet underway with this set, but the objective of the study using this specimen set is to evaluate the effect of loading mode on load duration. Duration of load tests will be conducted in the bending mode, tension mode, and compression mode. Plans are to determine static strength (one rate of loading) in each of these modes, and then test at three levels of constant loading in each of these modes.

316-Specimen Sample

The objective of this study was to evaluate the effect of high-temperature drying on load duration for southern pine. One rate of loading was used to determine static strength distributions for conventionally dried and high-temperature dried specimens. One level of step constant loads was used to determine if load durations differed for the two types of drying. Results of this completed study indicated that high-temperature drying did not have any significant effect on static strength or load duration.

1,000-Specimen Sample

The objective of this study is the same as for that using the 316-specimen sample, except Douglas-fir is being used here. Plans are to use one rate of load to determine static strength distributions for conventionally dried and high-temperature dried Douglas-fir. Then both types of lumber will be tested at two different levels of constant load (10th and 40th percentile static strengths of the conventionally dried lumber). In addition, specimens of high-temperature dried lumber will be tested at the 10th and 40th percentile static strengths of the high-temperature dried lumber.

550-Specimen Sample

The objective of this study is to evaluate the effect of foundation level of CCA treatment on strength and load duration of southern pine. Plans are to treat 60 percent of the specimens to 0.6 pcf using Type C CCA, with the remainder serving as controls. One rate of loading will be used to determine static strength distributions of control and treated specimens. Both specimen types will be tested at two levels of constant load (10th and 40th percentiles of control static strength distribution).

RESULTS

Results will include strength distributions from ramp load tests and time-to-failure distributions from constant load tests. The data will be evaluated with some form of damage model, probably more than one, so that results can be used in engineering reliability analysis for wood structures.

REFERENCES

American Society for Testing and Materials. 1974. Standard methods of establishing structural grades and related allowable properties for visually graded lumber. ASTM D245. Philadelphia, PA.

Ethington, R. L. 1970. Some stress-grading criteria and methods of grade selection for dimension lumber. USDA, Forest Serv., Forest Products Laboratory. Res. Pap. FPL 148.

Gerhards, C. C. 1985. Time-dependent bending deflections of Douglas-fir 2 x 4's. Forest Prod. J. 35(4):18-26.

Gerhards, C. C. and C. L. Link. Use of a cumulative damage model to predict load duration characteristics of lumber. 1983 Madison, WI, IUFRO Wood Engineering Group Conference Proc.

Glos, P. and J. D. Barrett. 1980. Machine for duration-of-load tension tests of dimension lumber. Forintek Canada Corp. Western Lab. Tech. Rep. No. 15.

Southern Pine Inspection Bureau. 1977. Grading Rules. Pensacola, FL.

Wood, L. W. 1951. Relation of strength of wood to duration of load. USDA, Forest Serv., Forest Products Laboratory. Rep. No. 1916, Madison, WI.

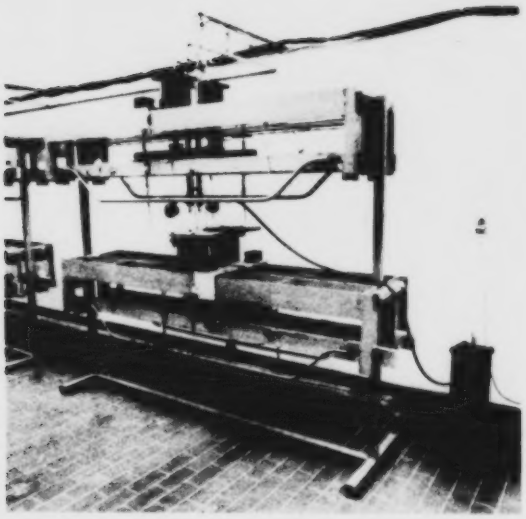

Figure 1. Duration of load pneumatic bending test frames. (M83 0172-10)

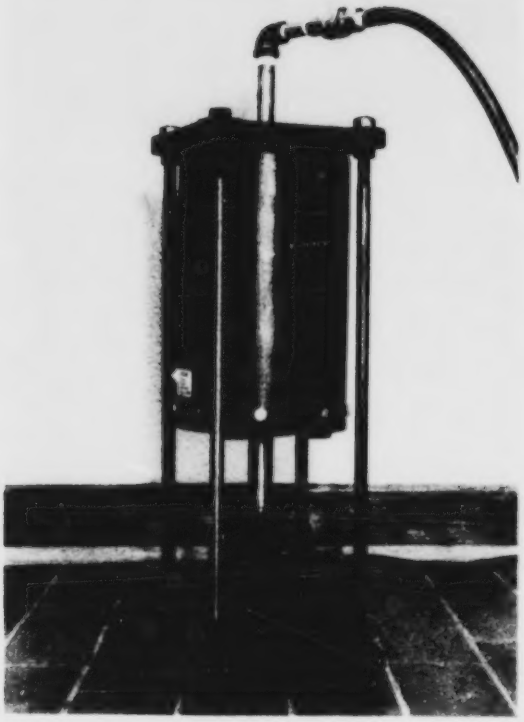

Figure 2. Master air cylinder-load cell frame. (M85 0159-3)

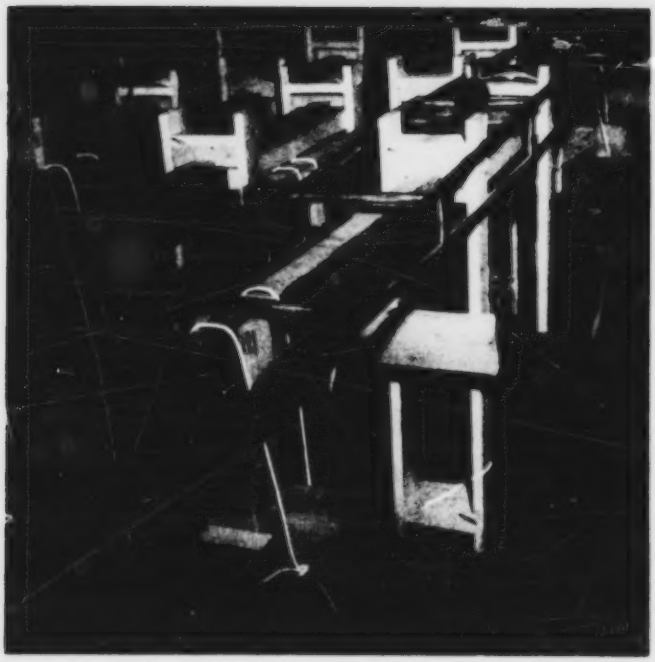

Figure 3. Dead load bending test frames. (M85 0244-6)

Figure 4. Deflection gauge-cage system on zero-reference precision ground granite rail. (M85 0244-3)

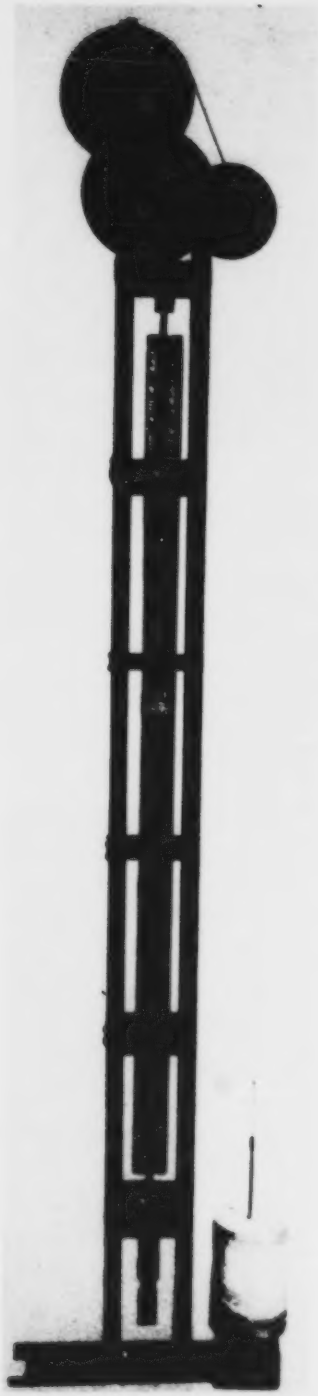

Figure 5. Duration of load tension test machines. (M151 634)

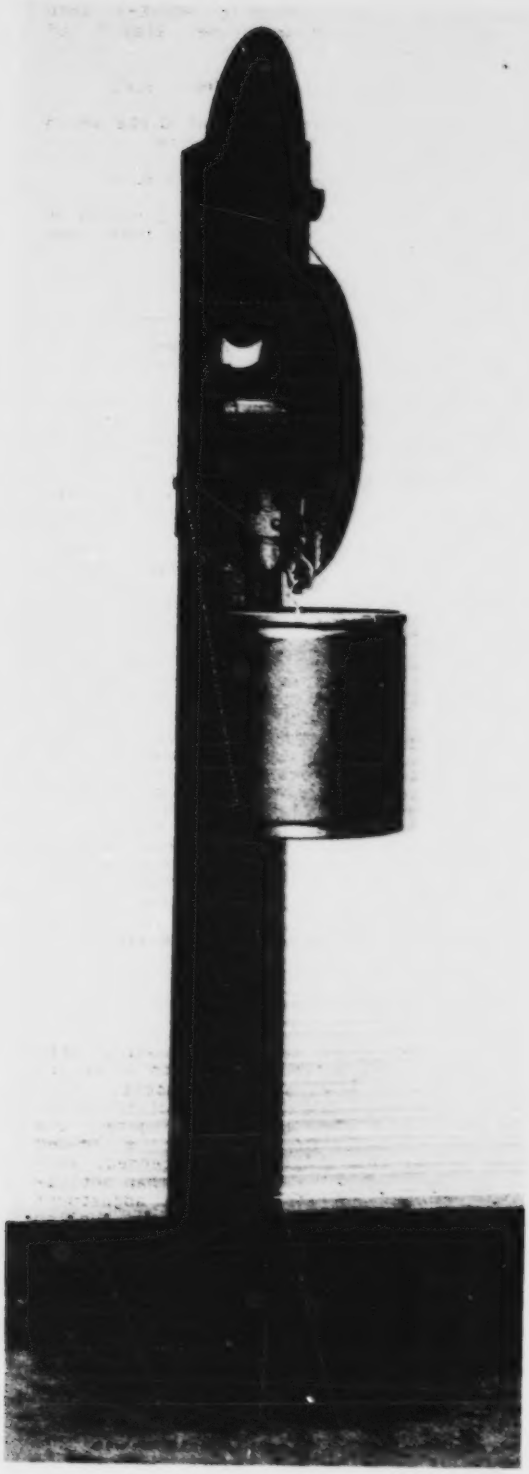

Figure 6. Duration of load compression test machines. (M85 0331-2)

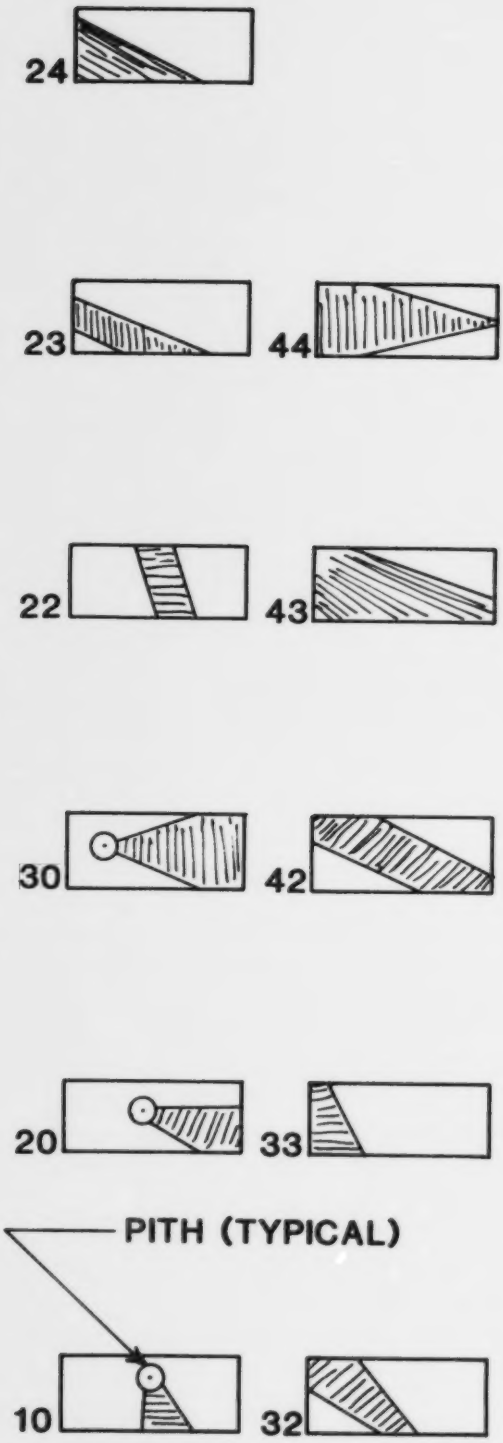

Figure 7. Knot types and associated identification numbers. (ML85 5391)

TESTING AND ANALYSIS CARRIED OUT AS PART OF THE PRINCES RISBOROUGH LABORATORY'S PROGRAMME TO EXAMINE THE DURATION OF LOAD EFFECT ON TIMBER

A.R. Fewell
Building Research Establishment,
Princes Risborough Laboratory,
Princes Risborough, Aylesbury,
Buckinghamshire, England

INTRODUCTION

Lacking the resources needed to carry out duration of load (DOL) tests on a whole range of properties, humidity conditions, species and sizes, the Princes Risborough Laboratory (PRL) decided to limit its involvement in DOL research. Their efforts will be directed to determining if differences in the DOL effect exist between the timber of North America and that of Europe, with their inherent differences in knot size and orientation. At the same time, researchers at the Technical University of Denmark were proposing to carry out DOL tests with varying humidity on a single species. It was realized that we should endeavour to match the test specimens used for both projects. The Swedish Institute for Wood Technology Research agreed to supply the test samples and carry out considerable initial testing to ensure matching of the British (UK) and Danish samples.

This paper is an interim report on an unfinished project and presents the results of analyses carried out to date.

TEST PROCEDURE

The UK tests are being carried out at PRL in a constant controlled environment to give 10 to 11 percent estimated moisture content (EMC) on 42 x 95 mm European whitewood specimens in bending. The test procedure, detailed in Appendix A, closely follows the procedure used by Forintek Canada Corp. The major difference is in the method of selecting the test samples.

A pilot project using 310 specimens was carried out in Sweden to determine the limiting values of Cook-Bolinder MOE(E_{CB}) and tension margin knot area ratio (TMK) to be used in selecting the quality samples. These are shown diagrammatically in Figure 1 with contour lines to relate them to the basic material sample. The multiple regression equations to be used for ranking the specimens for strength were also determined from the pilot project.

The equation referred to in Item 4 of Appendix A is:

$$f_m = 4.322\ E_{CB} - 0.293\ TMK + 7.30$$

with a correlation coefficient of 0.816.

By refining the E_{CB} readings, an improved equation was developed:

$$f_m = 4.312\ E_{CB} - 0.294\ TMK + 7.29$$

Means and standard deviations of predicted strength for the samples sent to the UK and Denmark are given in Table 1 with the cumulative distributions plotted in Figures 2, 3, 4 and 5. The similarity between the UK and Danish samples is evident although it must be remembered that the figures are based on predicted and not actual strength.

The final sample matching was carried out by incorporating a pure bending MOE(E_T) into the regression equation (see Item 8 of Appendix A) as follows:

$$f_m = 1.909E_T + 2.241E_{CB} - 0.265TMK + 6.61$$

with a correlation coefficient of 0.828 which was later improved by refining E_{CB} to

$$f_m = 1.982E_T + 2.144E_{CB} - 0.265TMK + 6.73$$

The control samples were broken as directed in Item 9 of Appendix A and the constant load stress levels determined as follows:

	SR_{15}	SR_{30}
Q_1	31.97 N/mm^2	35.24 N/mm^2
Q_2	41.12 N/mm^2	45.01 N/mm^2

It was realized that the difference in strength between the two qualities was not as large as we would have liked and that the existence of a quality effect on DOL might be difficult to determine. However, the introduction of a strength class system in the new UK Code, BS 5268, prevents the use of a quality effect.

The UK, which imports 90 percent of its structural timber, permits the use of many species and grades in order to maintain competition and keep prices as low as possible. The strength class system greatly facilitates the use of these alternatives, as illustrated below. Table 2, taken from the Code, gives the strength properties for nine strength classes to be used by a designer or engineer. Classes SC6 to SC9 are primarily for hardwoods. Having used the properties for SC3, for example, a designer would specify that strength class and could be offered any of a number of alternative grades and species which meet that class, as listed in tables in the Code, of which Tables 3 and 4 are typical. A high grade of a weak species can therefore be classified with a low grade of a strong species making the use of a DOL quality effect unworkable. A strength class system is also included in the draft Eurocode which will be used by all countries in the European Common Market.

ANALYSIS

The specimens which broke on loading were compared with the control samples to ascertain The accuracy of the matching process. Figures 6, 7, 8 and 9 are cumulative distribution plots which show that apart from Figure 7 the matching was incorrect. Therefore, the applied stress levels were higher than intended, with more specimens breaking on loading than anticipated. It was decided that some adjustment was necessary in order to predict the applied stress ratios.

Many simulations of the sample matching procedure were carried out on an unrelated sample of European whitewood. While there was considerable variation in the results, Figure 10 is fairly typical and was used to justify the linear displacement of the control samples to match exactly the specimens which broke on loading.

A strength ratio for each specimen was then calculated assuming equal rank between the strength of short term and constant load samples. Figures 11 and 12 show strength ratio against log T (hours) and in each case the line for the higher stressed sample is above that for the lower stressed sample.

While this is opposite to the quality effect found by Madsen, the difference is well within what could be expected due to experimental variability, since at these high stress levels the Madsen model shows only a minimal effect.

The higher than intended stress levels and the low coefficient of variation of the samples resulted in high stress ratios. Consequently, most of the test specimens have failed by now.

The results from fitting the Madsen model are shown in Figures 13, 14, 15 and 16. It can be seen that the model (dotted line) fits the data well using the parameters recommended by Madsen, except for parameter "b" which was changed from 0.45 to 0.33. The effect of changing "b" from 0.45 to 0.33 can be judged from Figure 17.

Efforts were also made to fit the Foschi/ Barrett model which fitted less well, as can be seen from Figure 18. However, the fit may be improved by the use of Foschi's curve-fitting computer programme.

To further examine the effect of quality, and at the same time avoid the assumption of equal rank, the mean values of strength ratio and log T, ignoring pieces which broke on loading, were plotted in Figure 19. A significant quality effect is not evident.

This paper reports on a project which is incomplete in terms of testing and analysis. When completed, a full report will be made available, linked to the work about to begin in Denmark.

APPENDIX A

DURATION OF LOAD PROJECT PROCEDURE

Items 1 to 4 to be carried out by the Swedish Forest Products Laboratory. Items 5 to 14 to be carried out by Princes Risborough Laboratory.

1. The test samples will be 3.3 m long, selected from a sufficient quantity of European whitewood obtained from one source and planed to 42 x 95 mm cross section. Moisture content to be approximately 15 to 16 percent.

2. Machine grade each piece using a Cook-Bolinder machine and examine visually to establish a critical section at least 900 mm from either end. Critical section to be marked with an arrow pointing to tension edge. Reject pieces with abnormal defects or distortion or where E_{CB} and TMK for critical section are outside the limits for Q_1 and Q_2. Add identifying number to accepted pieces and record the cross section dimensions, TMK and grading machine reaction forces for 1.4 m equi-spaced about the critical section. Nine hundred pieces are required in each quality group.

Quality Group	Min E_{CB}	Max E_{CB}	Min TMK	Max TMK
Q_1	6500	11400	0.27	1.00
Q_2	10000	14000	0.10	0.48

3. Cut specimens to 1.8 m length with critical section at the centre.

4. Rank specimens for strength using predictive equation with E_{CB} and TMK as independent variables. Divide into two populations assigning alternate specimens to Teknologisk Institut and PRL.

5. Kiln dry to 12 percent moisture content.

6. Determine E_T as specified in BS 5820 clause 11.1 at the critical section with arrow pointing to tension edge.

7. Record for critical section and weakest section within the length, knot plots, fibre angle and average width of growth rings (excluding first five rings from pith).

8. Rank specimens in each quality group for strength using predictive equation with E_T, E_{CB} and TMK (other variables may be included) as independent variables. Divide the ranked specimens into consecutive sub-groups of nine specimens. From each sub-group of nine specimens select at random two specimens for strength ratio sample SR_{15}, three for strength ratio sample SR_{30} and four for the control sample. This will result in matched distributions of 200 specimens in the control sample, 150 specimens in the SR_{30} sample and 100 pieces in the SR_{15} sample for each quality group.

9. Break control sample using loading configuration shown in Figure A1 by ramp loading with median time to failure of one minute and with arrow pointing to tension edge. Record failure load, time to failure and knot plot if different from critical section. Measure and record specific gravity and moisture content from small, clear prisms.

10. Use control sample test results to check the predictive equation and the sample variability.

11. Load SR_{15} and SR_{30} samples of quality Q_1, and SR_{15} sample of quality Q_2 to constant stress levels of the lower 15 percent and 30 percent exclusion values of the control sample strength distributions. Test configuration to be as in Figure A2 with arrows on specimens at centre and pointing to tension edge. Loading to be carried out at same speed as that used for control samples using a special hydraulic device which will also record the time to failure of specimens which break during loading. When loading begins, a long term timer will be started for each specimen, which will indicate times to failure. Record time to failure for specimens which break during loading and record knot plot if different from critical section. Monitor relative humidity of test area.

12. Each specimen will have location points (see Figure A3) from which a gauge can measure the beam deflections. Deflections will be measured immediately after loading and then at pre-determined intervals.

13. Inspect specimens at intervals of time (yet to be determined) and record the times to failure. Record knot plots if failure is not at critical section. Take a photograph of each failure cross section to clearly show the defects and indicate, for example, the extent of grain distortion around knots.

Table 1

Allocation of Sample Material

Name of file	No. of data	Mean (f_m pred)	Stand dev.	Remarks
FMPR1987	1987	41.92	6.75	Alla
ZQ1DATA	907	36.53	4.70	Alla Q1
Q1DkDATA	454	36.54	4.73	Denmark Q1
Q1GBDATA	453	36.53	4.68	England Q1
ZQ2DATA	903	47.37	4.05	Alla Q2
Q2DKDATA	451	47.36	4.03	Denmark Q2
Q2GBDATA	452	47.39	4.07	England Q2

Table 2

Grade Stresses and Moduli of Elasticity for Strength Classes:
for the Dry Exposure Condition

Strength class	Bending parallel to grain	Tension parallel to grain	Compression parallel to grain	Compression perpendicular to grain		Shear parallel to grain	Modulus of elasicity		Approximate density
							Mean	Minimum	
	(N/mm^2)	(N/mm^2)	(N/mm^2)	(N/mm^2)	(N/mm^2)	(N/mm^2)	(N/mm^2)	(N/mm^2)	(kg/m^3)
SC1	2.8	2.2	3.5	2.1	1.2	0.46	6800	4500	540
SC2	4.1	2.5	6.3	2.1	1.6	0.66	8000	5000	540
SC3	5.3	3.2	6.8	2.2	1.7	0.67	8800	5800	540
SC4	7.5	4.5	7.9	2.4	1.9	0.71	9900	6600	590
SC5	10.0	6.0	8.7	2.8	2.4	1.00	10700	7100	590/760
SC6	12.5	7.5	12.5	3.8	2.8	1.50	14100	11800	840
SC7	15.0	9.0	14.5	4.4	3.3	1.75	16200	13600	960
SC8	17.5	10.5	16.5	5.2	3.9	2.00	18700	15600	1080
SC9	20.5	12.3	19.5	6.1	4.6	2.25	21600	18000	1200

Table 3

North American Softwood Species/Grade Combinations Which Satisfy the Requirements for Strength Classes: NLGA and NGRDL Joist and Plank Grades

Standard Name and Origin	Strength Class				
	SC1	SC2	SC3	SC4	SC5
Douglas-fir-larch (Canada)	No.3		No.1, No.2	Sel	
Douglas-fir-larch (USA)	No.3		No.1, No.2	Sel	
Hem-fir (Canada)	No.3		No.1, No.2	Sel	
Hem-fir (USA)	No.3		No.1, No.2	Sel	
Spruce-pine-fir (Canada)	No.3		No.1, No.2	Sel	
Western whitewoods (USA)	No.3	No.1, No.2	Sel		
Southern pine (USA)			No.1, No.2, No.3		Sel

Table 4

Softwood Species/Grade Combinations Which Satisfy the Requirements for Strength Classes: Graded to BS 4978

Standard Named Origin	Strength Class				
	SC1	SC2	SC3	SC4	SC5
Imported					
Parana pine			GS	SS	
Pitch pine (Caribbean)			GS		SS
Redwood			GS/M50	SS	M75
Whitewood			GS/M50	SS	M75
Western red cedar	GS	SS			
Douglas-fir-larch (Canada)			GS	SS	
Douglas-fir-larch (USA)			GS	SS	
Hem-fir (Canada)			GS/M50	SS	M75
Hem-fir (USA)			GS	SS	
Spruce-pine-fir (Canada)			GS/M50	SS/M75	
Western whitewoods (USA)	GS		SS		
Southern pine (USA)			GS	SS	
British Grown					
Douglas-fir		GS	M50/SS		M75
Larch			GS	SS	
Scots pine			GS/M50	SS	M75
Corsican pine		GS	M50	SS	M75
European spruce	GS	M50/SS	M75		
Sitka spruce	GS	M50/SS	M75		

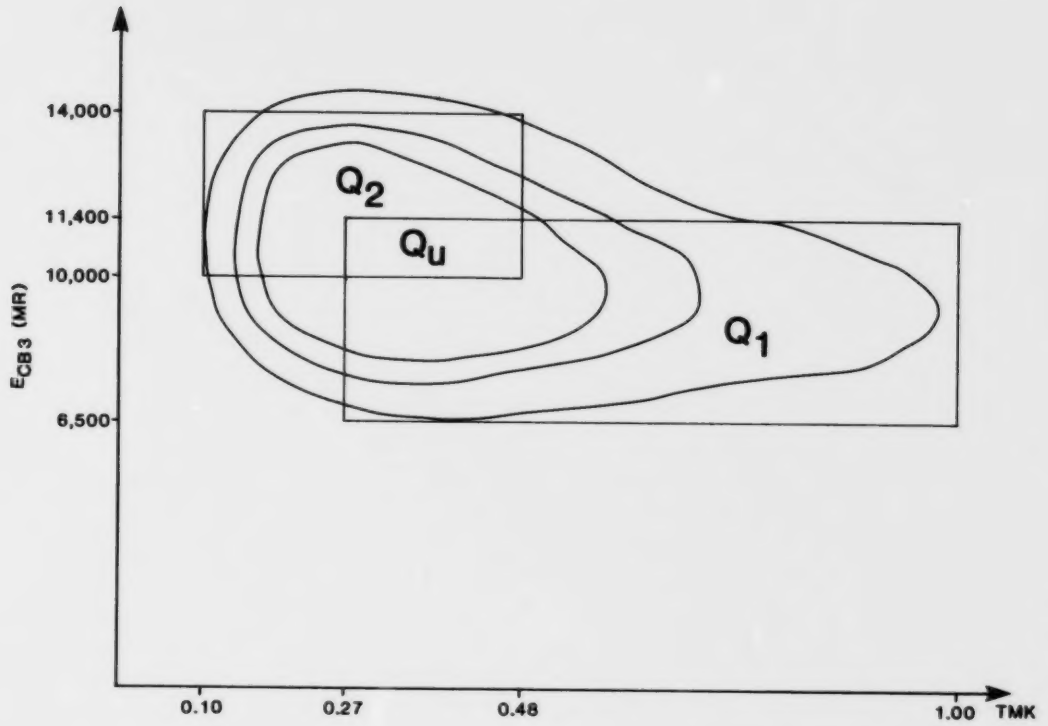

Figure 1.

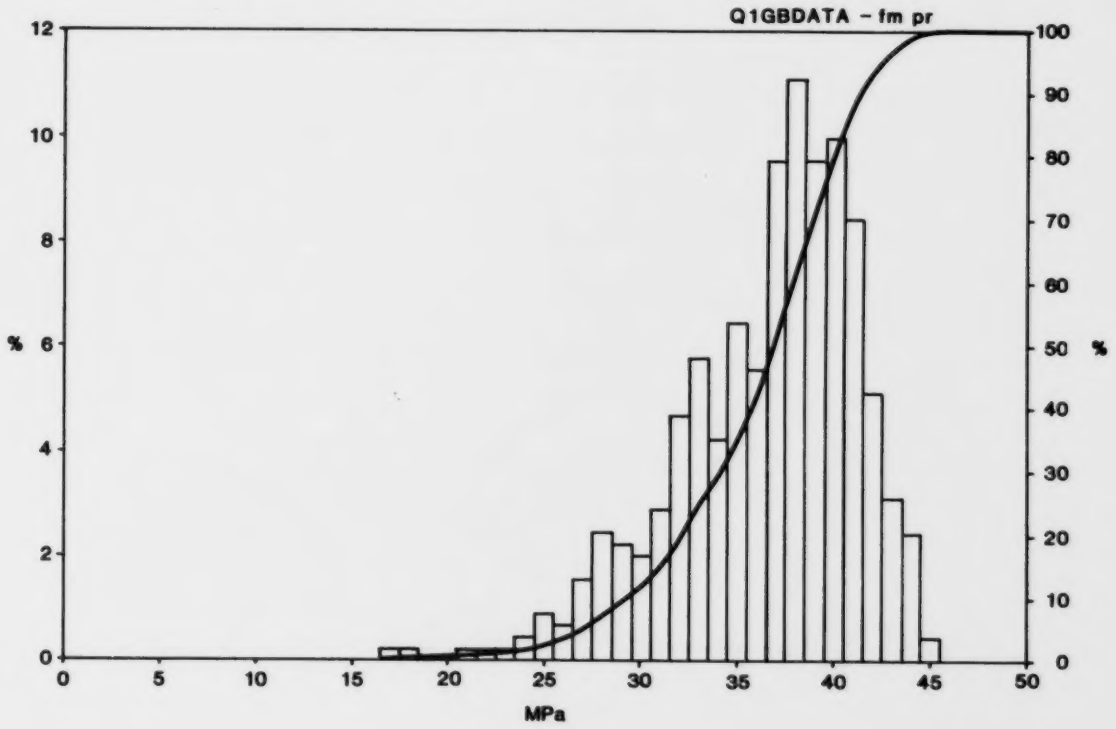

Figure 2.

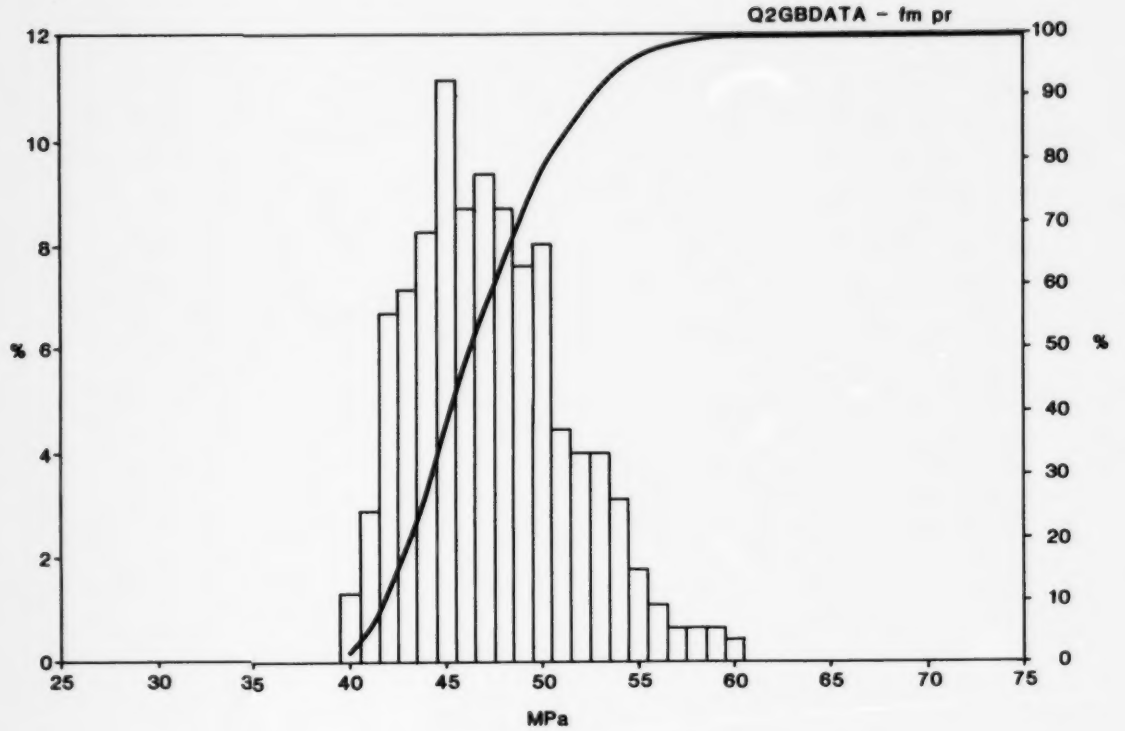

Figure 3.

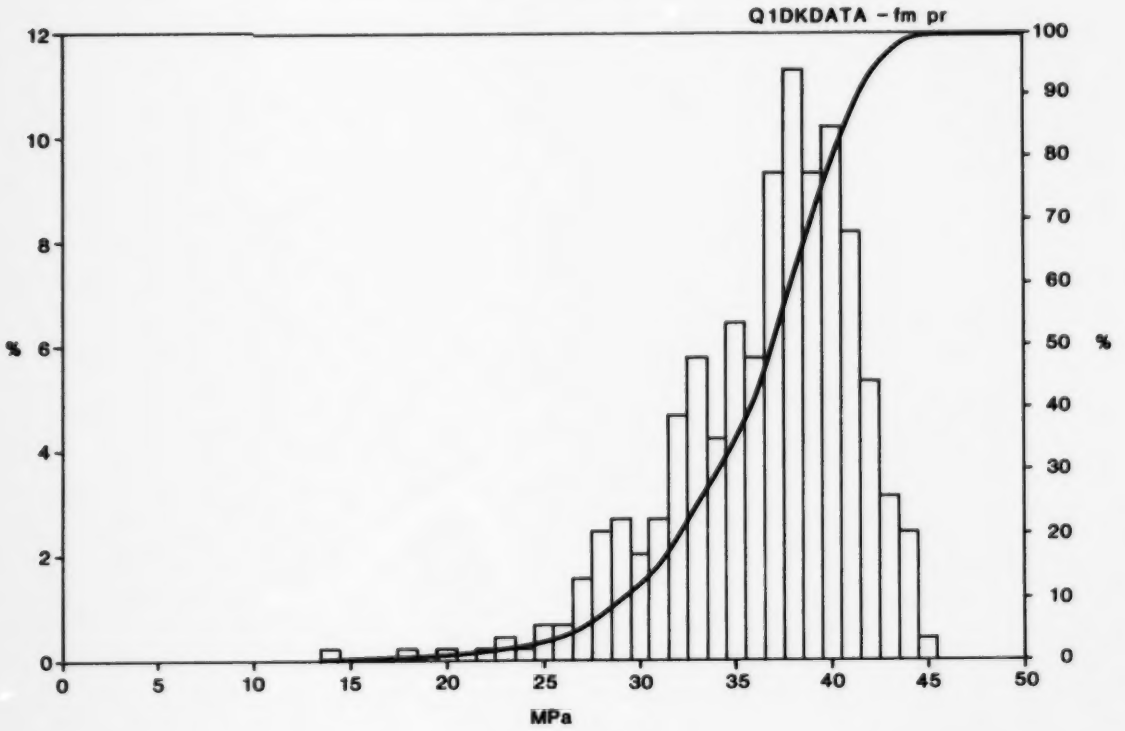

Figure 4.

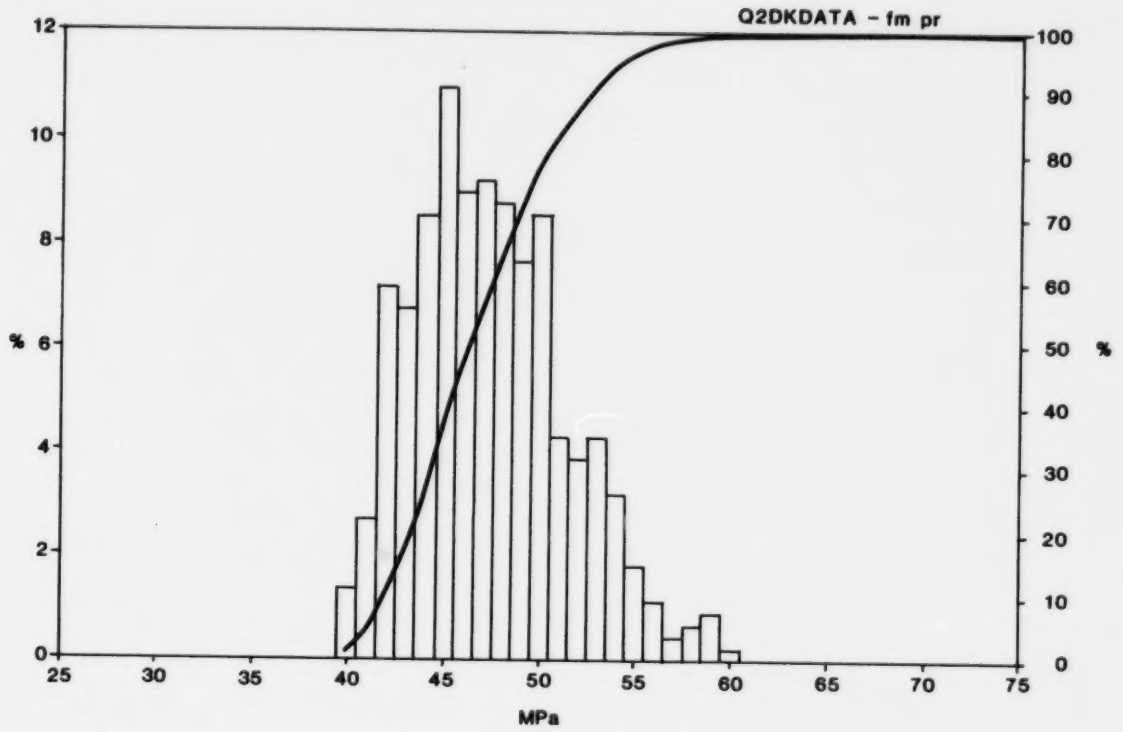

Figure 5.

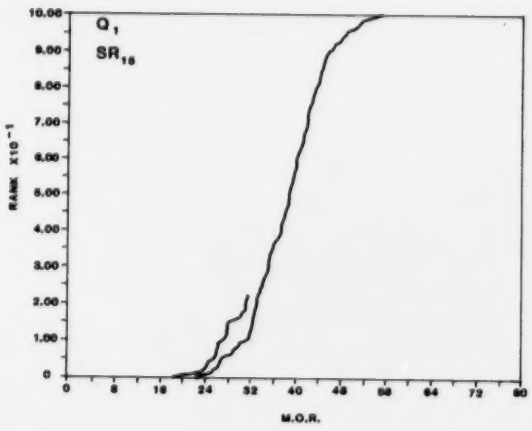

Figure 6.

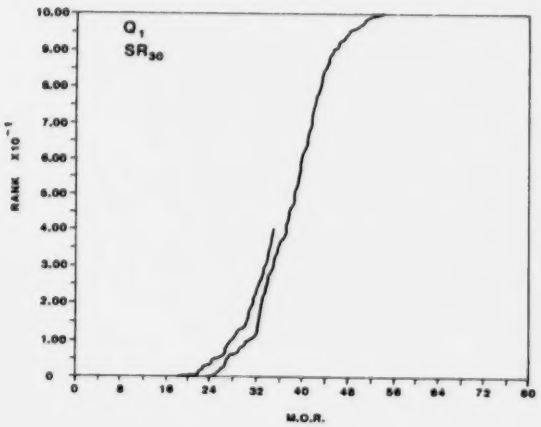

Figure 7.

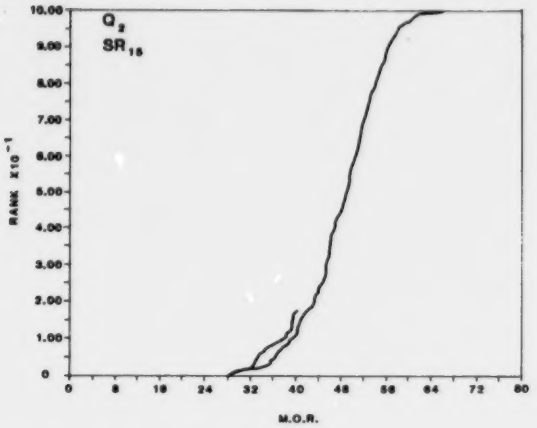

Figure 8.

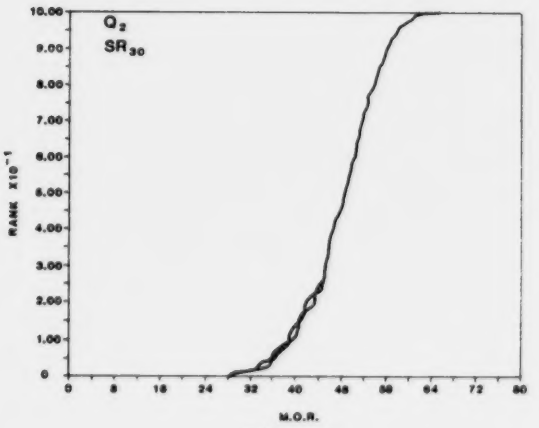

Figure 9.

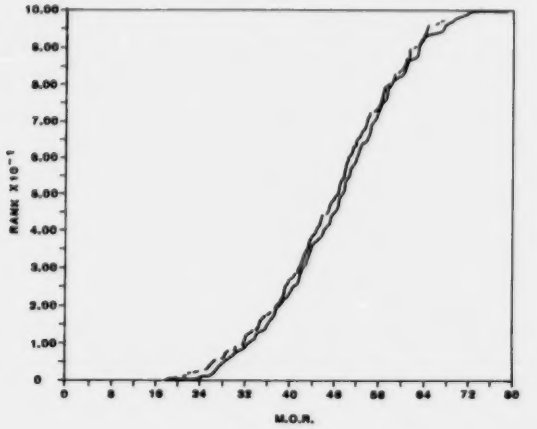

Figure 10.

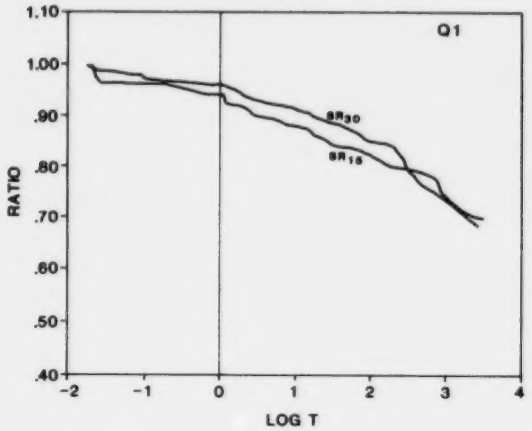

Figure 11.

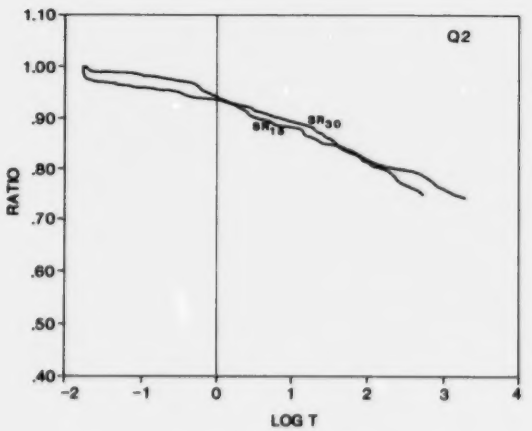

Figure 12.

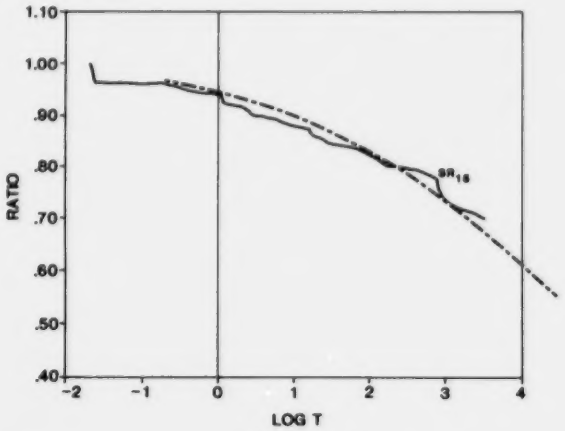

Figure 13.

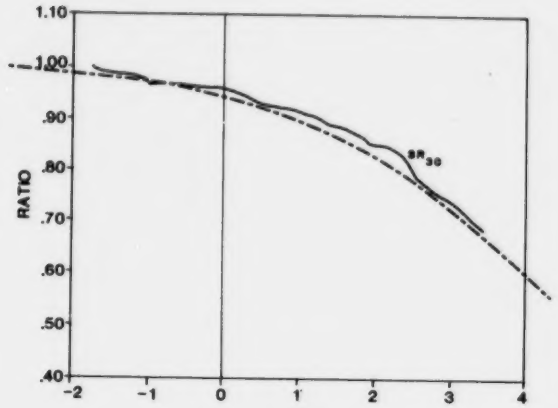

Figure 14.

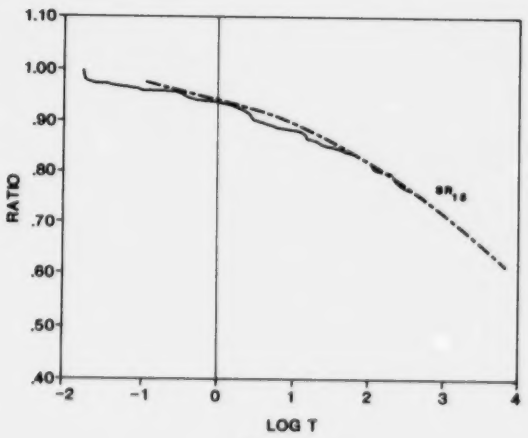

Figure 15.

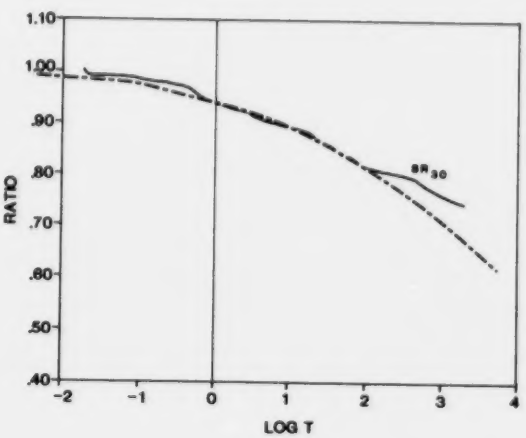

Figure 16.

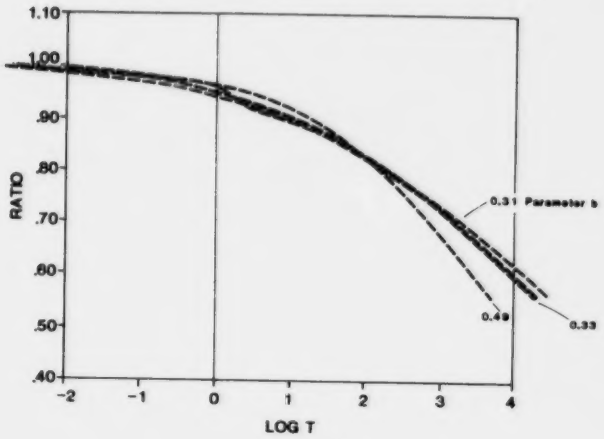

Figure 17.

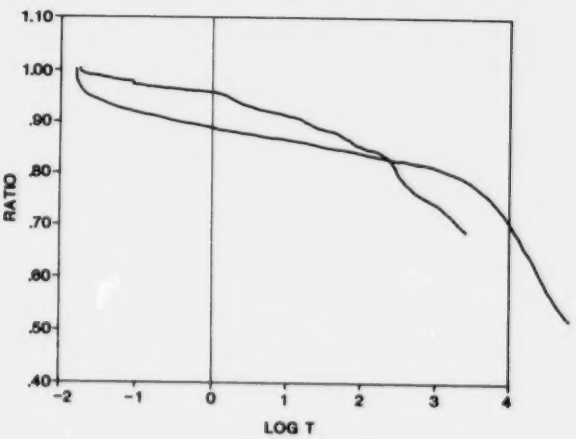

Figure 18.

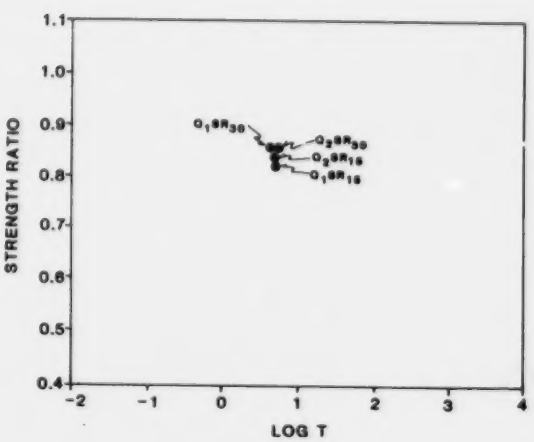

Figure 19.

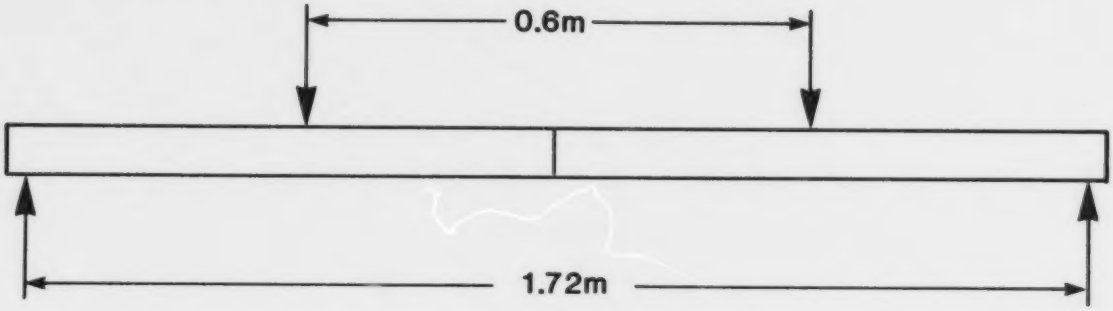

Figure A1. Loading configuration for control samples.

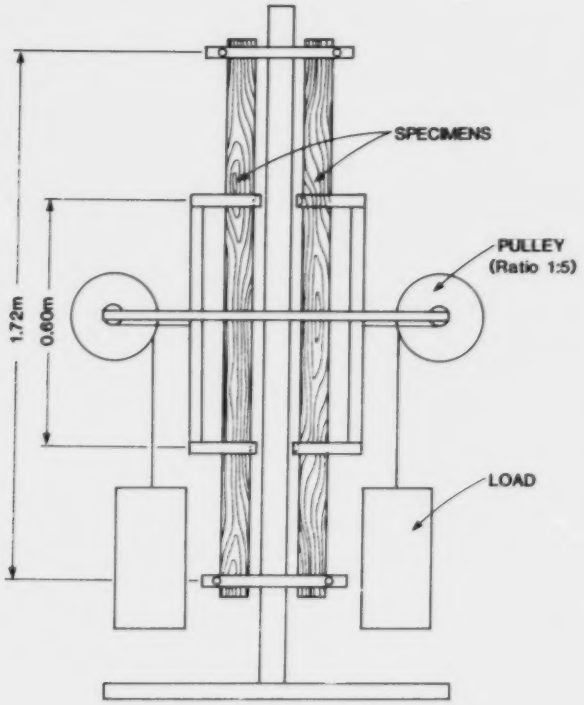

Figure A2. Section through test frame showing one pair of specimens.

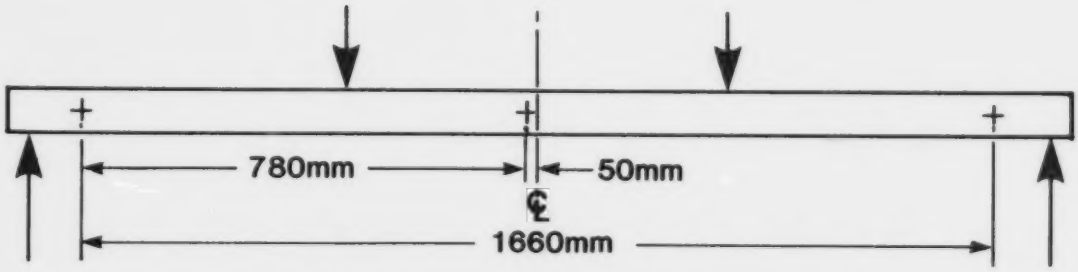

Figure A3. Points for creep deflection measurements.

RATE OF LOADING AND DURATION OF LOAD TESTS IN TENSION AND IN COMPRESSION

P. Glos
Institut für Holzforschung der Universität München, München, Federal Republic of Germany

INTRODUCTION

That wood strength is dependent on load duration has been well-known in German-speaking countries. Among the scientists who have studied this problem some 50 years ago are Baumann, Graf, Kraemer, Roth and Staudacher. From small clear specimens they found, among other things, that in dynamic tests a duration of load effect may already become noticeable at stress levels of approximately 20 percent of short-term strength, whereas with static tests no duration of load effects were detected at stress levels below 40 to 50 percent.

Despite the knowledge of these relationships, the existing German structural timber design codes do not explicitly mention a duration of load factor. Nevertheless, these codes have been effective; at least no relevant failures have become known which were not attributed to other causes. One reason for this is that the probability of a duration of load effect occurring is a function of the entire code system, including the loading codes and grading rules as well as the grading and design errors.

It can be assumed that the German structural timber design codes which do not specify any explicit safety factor at all, implicitly contain a global safety factor of about 2.5 to 3.0. Keeping in mind that duration of load effects do not occur unless the applied stress exceeds a threshold of about 40 to 50 percent of short-term strength, this explains why in conventional statically loaded timber structures a strength reducing duration of load factor is generally not experienced (Figure 1).

Nevertheless, it appears necessary to systematically study the duration of load effect for the reasons listed below:

1. A better understanding of the relation between time and strength will provide the key to the solution of many hitherto unsolved problems and contribute towards a wider use of wood as a construction material.

2. The transition to reliability-based structural design which will inevitably have to be made in the field of timber construction also, requires an exact knowledge of the relationship between load and strength as a function of time.

3. Only the knowledge of the actual duration of load effect can form the basis for an international harmonization of structural design codes.

When discussing duration of load, it should be helpful to distinguish between the duration of load effect as such and the way in which this effect will be implemented in a design code.

The present study aims to examine the duration of load effect in tension and compression for lumber, and to determine to what extent this differs from that of the much more comprehensively studied duration of load effect in bending. The scope of the test program was limited by the funds available for this project. An extension of the program is planned.

EXPERIMENTAL PROCEDURE

Results from two studies are presented here. The first project dealt with long-term tension and compression tests under constant climate conditions of 20°C and 65 percent relative humidity (r.h.). The material tested consisted of glulam laminates made from European spruce (Picea abies). The test plan, both for tension and compression, comprised two constant load test series (stress level 14 and 21 N/mm^2; loading time six months) and three ramp load test series (time to failure 10 sec., one hr. and 360 hrs.*), i.e. a total of 2 x 5 = 10 test series. The test plan with sample sizes is outlined in Table 1. Sample sizes for each series varied from 10 to 40 specimens, the total being 210 tests.

The material tested was three m long European spruce lumber collected as a representative sample from 15 out of approximately 40 German glulam plants. Shape and dimensions (mm) of the specimens are given in Figure 2. After conditioning to normal climate (20°C/65 percent r.h.) the three meter long boards were planed to the largest possible size of either 30 x 180 or 30 x 120 mm^2 and cut to a length of 2.40 m so that the presumably weakest cross section (biggest knot) was situated in the gauge length of 1.65 m. From each of these trimmed boards bending modulus of elasticity, knot size and density were determined. Using these characteristics as well as regression functions available from former test work, short-term tension and compression strength were predicted for each board. The boards were then grouped into subsamples for the 10 test series so that each subsample exhibited equal reference strength distribution (predicted short-term strength) as well as equal distribution of modulus of elasticity, knot size and density. Finally the test specimens were produced from the selected boards by nailing the shoulders to the tension specimens or cutting compression specimens at both ends down to the test length of 1.65 m.

In order to obtain comparable results, all the ramp load tests and all constant load tests were carried out in the same load frames. The test load was applied by an oil-hydraulic system. In the compression tests the load was transferred directly to specimen ends, lateral buckling of the specimen was prevented by lateral supports spaced every 30 cms. In the tension tests the load was transferred to the specimen by shoulders attached to each end (Figure 2). An electric load cell recorded the load. For each test the ultimate load and time to failure, if applicable, were recorded by producing a time-load diagram. For each

* For tension tests, time to failure was approximately 240 hrs.

constant load test, time to failure was recorded automatically via an electric clock and a switch connected to the board. Creep deformation was measured both in constant load tension and compression tests. Specimens that survived the constant load tests were subsequently subjected to a 10-sec. ramp load test.

This project has not yet been completed. Thus, only the test results available so far can be discussed here.

The second project comprised long-term tension tests under cyclic environmental conditions. The object of this study was to evaluate the duration of load effect in tension under realistic climate conditions that exist in an unheated building (e.g. in a skating rink). The material tested was a sample of 100 European spruce glulam laminates. It was subject to a constant load tension test (stress level 14 N/mm^2; loading time one year). Prior to the creep test, these boards were conditioned to normal climate (20°C/65 percent r.h.). From each board a section 50 cm long including the grade determining defects was cut. Five randomly chosen sections were connected by finger-jointing (finger joint A 7.5 mm DIN 68140) to form one board which was planed to a uniform cross section of 120 x 25 mm^2 (Figure 3). In this way 100 specimens were accomodated in the 20 available load frames.

Ten of the 20 load frames--each accomodating 10 x 5 = 50 specimens--were installed in one of two climate rooms. As shown in Figure 10 the climate in both rooms was cycled stepwise between 10°C/80 percent r.h. and 22°C/50 percent r.h. at intervals of four weeks for the first six months. Due to technical problems in one room, the climate had to be held constant at 20°C/65 percent r.h. for the latter part of the test period (series No. 1). In the second room (series No. 2) the climate was changed back to 10°C/80 percent r.h. after eight months for a period of roughly four weeks (Figure 9).

RESULTS

The results available for the first project, i.e. ramp load and constant load tension and compression tests under constant climate conditions of 20°C/65 percent r.h., are shown in Figures 4 to 8. In all cases these results indicate a significant duration of load effect.

The results of the ramp load tension tests are shown in Figure 4 whereas the results of the ramp load compression tests are shown in Figure 5, presented in ranked order throughout.

It can be seen that both tension and compression strength are being reduced when time to failure is increased. This effect is clearly evident also in the lower range of the strength distribution in both tension and compression.

This result contrasts with that for bending tests carried out in Canada earlier. One of the findings from the latter was that the duration of load effect is less pronounced for the lower range of strength distribution as compared to high strength material (e.g. Madsen, 1973 and 1975; Spencer, 1979; and Figure 8). In Figure 6 the results of the tension and compression tests reported here are compared with those of Spencer's (1979) bending tests. The discrepancy in the lower range of the strength distribution is obvious.

The results of the constant load tests in tension and in compression are shown in Figures 7 and 8 respectively, again presented in ranked order. These figures show the number of specimens that failed during the constant loading period of six months, together with their corresponding times to failure. Also shown is the residual short-term strength (10-sec. ramp load test) of those specimens that survived the constant load test. For comparison, the predicted short-term strength and the test results of a control group (time to failure 10 sec.) are also given.

The test results indicate a significant duration of load effect. Test specimens are shown to fail under constant tensile or compressive load in a constant climate of 20°C/65 percent r.h. when a stress level of roughly 14/21 or 21/36, i.e. approximately 0.6, related to short-term strength (10-sec. ramp load test) is reached or exceeded. For a constant compressive stress of 14 N/mm^2 the critical stress level was not reached and therefore no failures were experienced in this test series.

The test results for the second project, i.e. constant load tension test under cyclic climate conditions, are shown in Figure 9, separate for the two subsamples tested in two climate rooms under partly different climate conditions. Along a time axis, Figure 9 shows how the climate was varied and when failures occurred. Immediately upon failure of one of the five sections connected to one another and loaded in one frame, it was repaired so that the remaining sections in that frame could be reloaded after a short time, generally after a period of two to three days.

Figure 9 shows that many of the failures occurred with a change of climate. These results lead to the assumption that the duration of load effect is not independent of environmental conditions, despite or beyond a possible interaction between adjacent sections, based on the failure of one of them and the subsequent reloading process.

CONCLUSIONS

All test results presented here are based on a limited number of tests on European spruce. With this reservation in mind, the following conclusions can be drawn:

1. Structural lumber exhibits a significant duration of load effect in tension and in compression under constant climate conditions. The test results indicate that this effect is more pronounced in the lower range of strength distribution than was the case for bending tests carried out in Canada. Whether this difference is partly due to differences between wood species or grading rules will have to be determined in current investigations in various North American and European countries.

2. The duration of load effect seems to be eqully pronounced in both tension and compression despite different creep behavior.

In the particularly interesting lower range of strength distribution (Figure 1) the magnitude of the duration of load effect both for ramp load and constant load tests corresponds approximately to the Madison curve.

3. The constant load tensile tests carried out under cyclic climate conditions imply that for structural lumber also, the duration of load effect is influenced and probably increased by changing environmental conditions.

REFERENCES

Madsen, B. 1973. Duration of load tests for dry lumber in bending. For. Prod. J. 23(2):21-28.

Madsen, B. 1975. Duration of load test for wet lumber in bending. For. Prod. J. 25(5):33-40.

Spencer, R. 1979. Rate of loading effect in bending for Douglas-fir lumber. IN: Proc. of the First International Conference on Wood Fracture, August 1978, Banff, Canada. pp.259-279.

Table 1

Test Plan, First Project

Ramp load tests

Series No.	Property	Loading time to failure	Sample size
1	tension	10 sec	40
2		1 hr	40
3		360 hr	20
4	compression	10 sec	20
5		1 hr	20
6		240 hr	10

Constant load tests (load duration up to six months

Series No.	Property	Stress level	Sample size
7	tension	14 N/mm^2	20
8		21 N/mm^2	20
9	compression	14 N/mm^2	10
10		21 N/mm^2	10

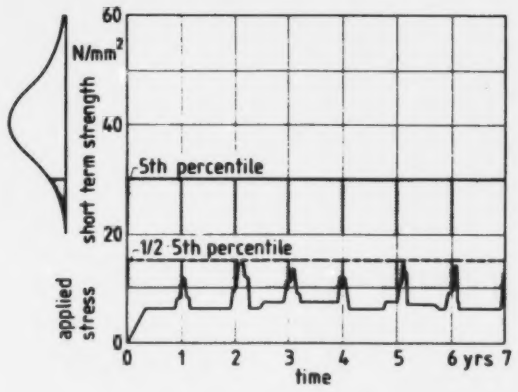

Figure 1. Short-term strength and temporal progress of applied stress in a roof structure (schematic).

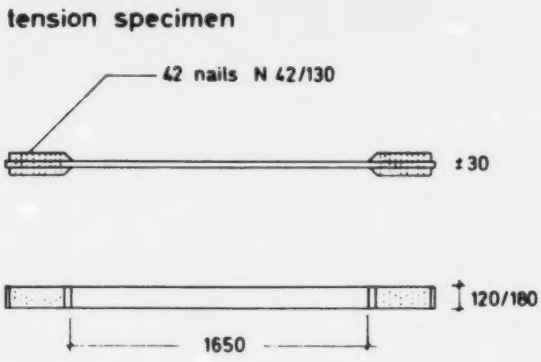

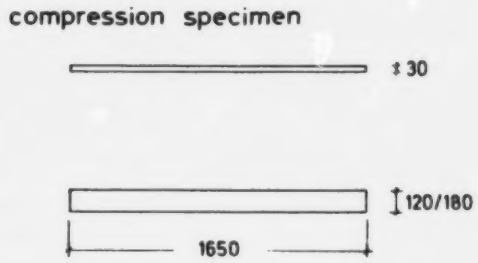

Figure 2. Specimens for tension and compression ramp load and constant load tests (first project).

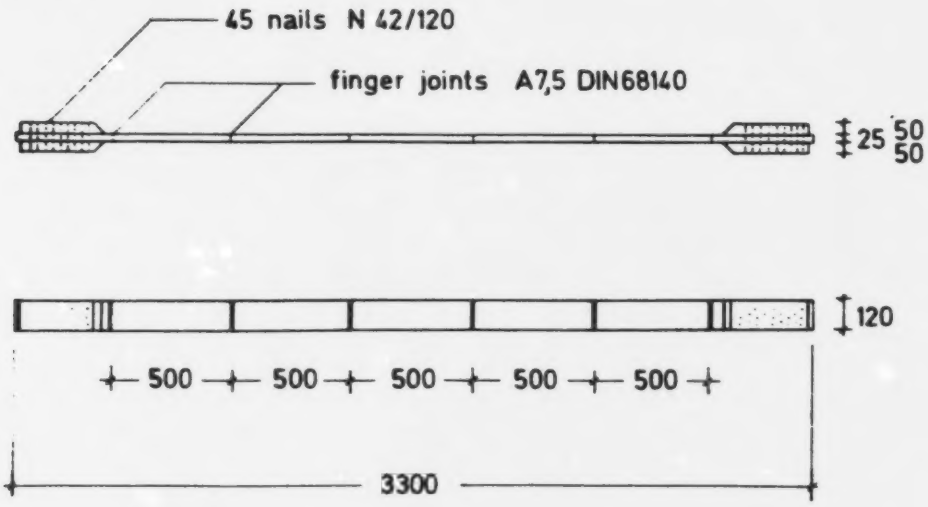

Figure 3. Specimens for tension constant load test (second project), comprising five samples.

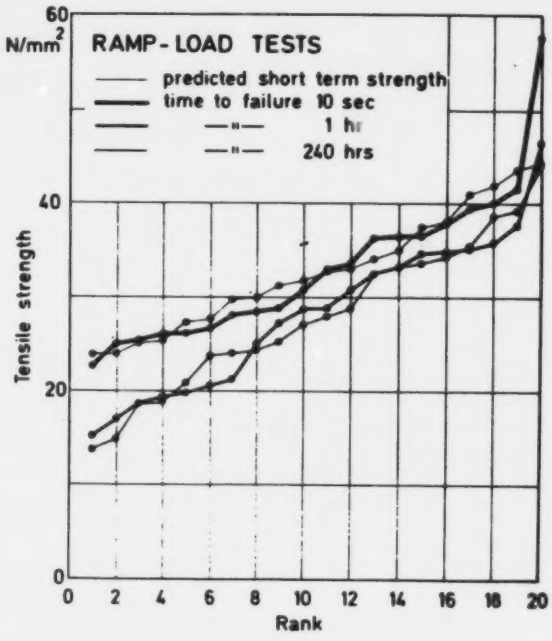

Figure 4. Ramp load tension tests in constant climate 20°C/65% r.h.

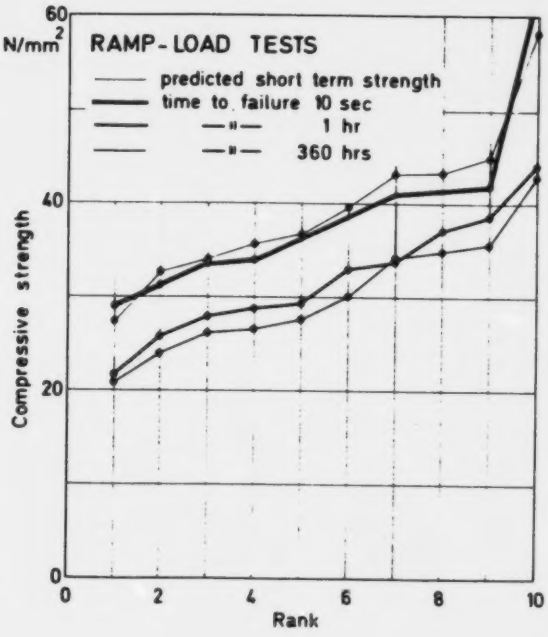

Figure 5. Ramp load compression tests in constant climate 20°C/65% r.h.

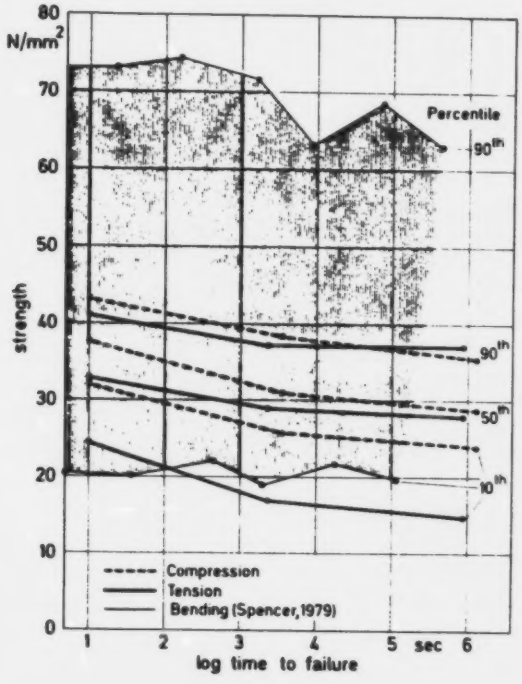

Figure 6. Comparison of results of ramp load tension, compression and bending tests. Bending tests by R. Spencer, 1979.

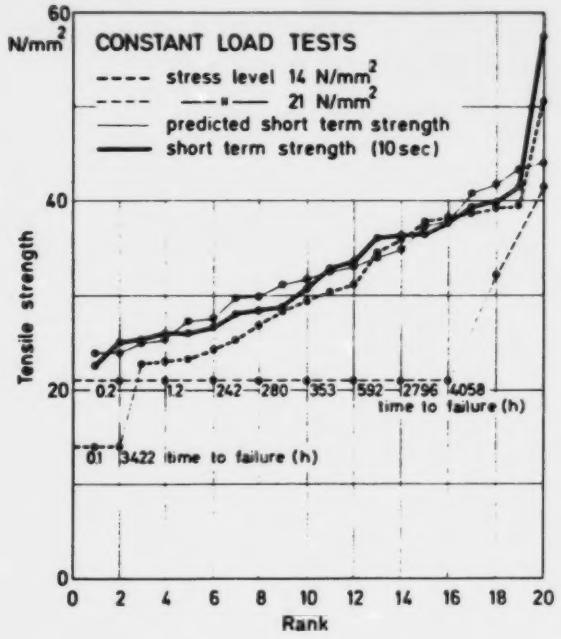

Figure 7. Constant load tension tests and short term strength of a control group. Constant climate 20°C/65% r.h.

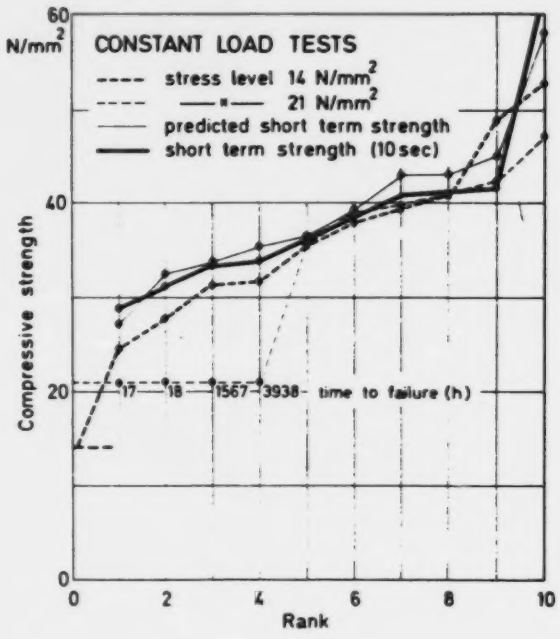

Figure 8. Constant load compression tests and short term strength of a control group. Constant climate 20°C/65% r.h.

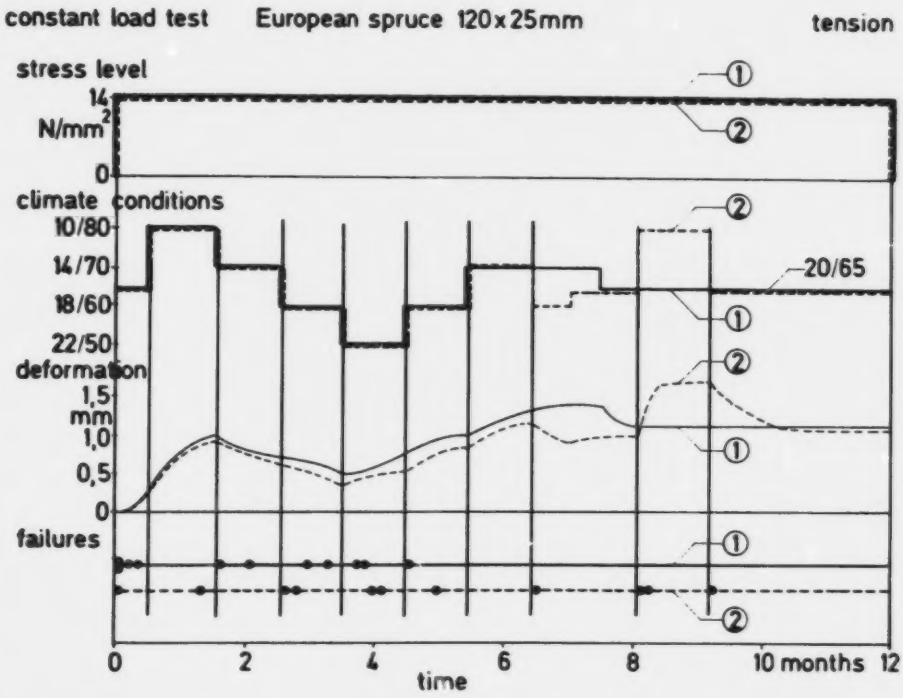

Figure 9. Constant load tension test (stress level 14 N/mm²; loading time 1 year) under cyclic climate conditions. Temporal progress of climate conditions, creep deformation, number of failures.

RESULTS OF PAIR-MATCHING OF WOOD FOR LONG-TERM LOADING

Bengt Norén
Swedish Institute for Wood Technology Research,
Stockholm, Sweden

INTRODUCTION

The aim of the matching was originally to produce specimens of structural size and grade for long-term loading within a joint European Programme (Norén, 1983 and 1984). The test method used or possible alternative methods will not be discussed here. Neither will the general aspects of predicting strength of structural timber in connection with matching be dealt with. These topics are appropriately described by Gerhards (1976).

A matching study, similar to the one examined here, was carried out at the laboratory in 1977 (Norén, 1977). Planks (45 x 145 mm), considered to match, were sampled at the saw in the mill, and local bending stiffness was used to improve prediction of strength. Although the results were satisfactory (Table 1), a complete report was never issued since the structural grade was too high for application to the common low grade level.

TESTING METHOD

The timber was loaded on edge for critical constant moment in the middle of the span, where the critical knot was placed. The rate of deflection at the loading points was six mm/min. and the correspondent load was continously recorded.

The curvature was measured over 300 mm length at three positions: (Position 1) immediately to the left of the knot; (Position 2) with the knot at centre and; (Position 3) immediately to the right of the knot. Additionally, the curvature on 600 mm gauge length was measured with the knot at the centre (Position 4). The possible difference in curvature at the four positions has not yet been analyzed. The E_{beam}-ratios in Table 2, Column 2, are calculated from the Position 4 deflection curves. The values in Column 3 of the table originate from the stiffness recording (Position 4), which was carried out to judge the thickness adjustment at planing the specimens. For several reasons, they deviate some from the final values.

The local curvature in the four positions was recorded to a load level exceeding the proportional level. In several cases the first crack is clearly identified in the curve. However, as the gauge had to be removed well before collapse, only E_{beam}, the load at the proportional limit, FP, (and possibly a load defined by a small fraction of non-Hookian curvature) can be derived. Studies at higher load levels including the definition of failure are reduced to the recordings of the displacement at the loading points, recorded to failure.

The local stiffness (gauge length 900 mm) in bending flatwise (E_{flat}) was pre-recorded in a Cook-Bolinder Stress-Grader machine.

The knot-area-ratio for the total cross section (KAR) and 1/4 of the section at the tension side (TMKAR) was also measured before testing. The density of the corresponding (clean) sections (D resp. MD) was measured after testing.

RESULT

The result from the pilot test of eight pairs is reproduced in Table 1, the result of an additional 46 pairs in Table 2. Columns 2 to 8 in both tables give ratios of the various properties of the specimens in the pair when they are arranged to give a strength ratio F (Column 8) of at least unity. By this arrangement, a predominant number of values in the columns should be expected to exceed unity. This will simplify a first judgement of whether it is meaningful to apply an adjustment of the F-ratio based on its possible correlation with one or more of the parameters involved. (The influence on deviation of the arrangement must be considered when the probability of predicted values is derived.)

A difference between Tables 1 and 2 is that the ratios E_{flat} are missing from Table 2, because they are not yet derived for all material. Instead, the ratios E_{beam} from the central curvature (Position 4) are added (Column 2). The difference between these two ratios E^1_{beam} has not yet been analyzed, nor have possible differences between values from the curvature in other positions (Positions 1-3). New in Table 2 is the ratio of proportional limits, FP (Column 9), also based on the curvature in the central position (Position 4).

Preliminary effort is concentrated on the use of the ratios E_{beam}, $TMKAR^{-1}$ and FP to adjust the prediction beyond the accuracy expected from simple pair-matching.

First of all, four pairs must be excluded when the F-ratio is analyzed. The reason is that one of the pieces failed far from the matched section. The corresponding rows in Table 2 have been marked "o". It is further recommended to define limits for the ratios within which the F-ratio may be adjusted. Among the measured factors it seems adequate to put such limits on the ratios of E_{beam}, $TMKAR^{-1}$ and, possibly, FP.

Three alternatives have been applied so far:

1. Acceptable range of E_{beam}-ratio 0.800 to 1.250
2. Acceptable range of $TMKAR^{-1}$ 0.667 to 1.500
3. 1 + 2.

Alternative 1 will exclude another four pairs and Alternative 2 three pairs.

ADJUSTMENT BY CORRELATION

For the previous matching study (Norén, 1977) a simple adjustment based on E_{beam} was used: $F = Const.*E_{beam}$. If the same approach is used on the values of F-ratios in Table 2, the values in Table 3 (Column 8a) result.

Several models for multicorrelation involving other factors have been presented, for example, in connection with the sampling of timber for the current DOE-project at the Princes Risborough Laboratory (PRL). The ratios in Table 2 cannot be used to design such models, as they lack the information on deviation between the pairs. Possible prediction improvement by applying multicorrelation models on the material will be looked into next.

The possibility to improve the matching, assuming proportionality between E_{beam} and F, may be alternatively illustrated by comparing the difference in strength within pairs. The effect of using $F_B^* = F_A(E_B/E_A)$ instead of F_A as predicted value follows from Table 3, Columns 10 to 13.

CONCLUSION

The conclusion is that a single correlation of strength to the elastic modulus, derived from the deflection measured at a gauge length of 600 mm, will not help to predict a difference in strength between the matched specimens within a pair. Neither can the prediction be improved by reducing the accepted range of the difference (ratio) of elasticity moduli within a pair.

The possibility of improving the prediction from differences in stiffness measured at 300 mm gauge length and in the stress at the proportional limit will be dealt with in the final report. The conclusion with regard to using the knot area ratio (TMKAR) is similar to that with regard to the elastic modulus. Preliminary studies of differences in fibre disturbance within pairs have not offered any real improvement so far.

Thus, if the very matching is not improved, suggested methods involve a considerable increase in sampling cost, and should further analyses not bring any essential improvements in predicting the strength difference between the matched specimens, then, according to Table 4, a standard deviation (and coefficient of variation) of 0.19 should be anticipated for the strength ratio within the pair. If the distribution is normal, the specimens in 70 percent of the pairs will have a strength ratio between 0.80 and 1.20. Consequently, at the 0.80 load level, 15 percent of the specimens should fail during loading. According to the "real" distribution (Table 4, Figure 2), however, only three out of 38, or eight percent of the specimens, will break "immediately" during loading.

REFERENCES

Norén, B. 1977. Side-matching of structural timber. STFI Report to CIB/IUFRO S5.02-03.

Norén, B. 1983. The strength of structural timber at long-term loading. STFI. Contractor's meeting, European R&D Programme Wood, Brussels.

Norén, B. 1984. Matching of structural timber. CEC R&D Programme Contract Report No.3. TräteknidCentrum, Stockholm.

Gerhards, C.C. 1976. Pair matching and strength prediction of lumber. Wood Science 8(3).

Table 1

Ratio of Parameters Within Pairs of Specimens

Pairs Nos.	E^{1}_{beam}	E_{flat}	D	MD	KAR^{-1}	$TMKAR^{-1}$	F
1	2	3	4	5	6	7	8
52/51	1.00	0.97	0.97	0.98	1.12	1.08	1.06
111/112	0.97	0.83	1.01	1.01	0.50	0.80	1.26
162/161	1.04	0.98	0.98	1.04	1.70	1.00	1.09
321/322	1.01	0.98	1.01	1.01	0.95	0.93	1.40
411/412	1.01	1.11	1.01	1.03	1.25	0.92	1.20
602/601	1.00	1.01	1.02	1.00	1.81	1.06	1.15
731/732	0.93	1.00	1.02	0.98	1.51	1.09	1.43*
821/822	1.05	0.98	1.01	1.01	1.13	1.03	1.34
Mean	1.00	0.98	1.00	1.01	1.07	1.00	1.24

*Secondary failure (1.20 at primary failure)

Table 2

Ratio of Parameters and Strength Within Pairs

Pairs Nos.	E_{beam}	E^{1}_{beam}	D	MD	KAR^{-1}	$TMKAR^{-1}$	F	FP	FR	
1	2	3	4	5	6	7	8	9	10	
11 K/12 K	1.046	1.000	0.985	1.021	1.822	0.897	1.142	1.05	11494	
32 K/31 K	1.074	1.000	1.007	0.993	1.488	1.000	1.695	-	17842	(0)
42 K/41 K	1.296	1.268	1.152	1.137	1.312	0.983	1.634	1.09	13022	(1)
71 /72	0.980	1.013	1.171	1.082	0.477	0.603	1.035	1.22	8641	(2)
81 K/82 K	0.925	0.961	0.997	1.019	0.589	0.938	1.143	0.83	8864	
92 K/91 K	1.236	1.160	1.056	1.094	0.929	0.848	1.181	0.96	15145	
101K/102K	0.974	1.019	1.032	1.027	1.170	1.042	1.048	0.71	12494	
122K/121K	1.094	1.050	0.972	1.003	0.812	1.115	1.192	1.13	12111	(0)
132K/131K	1.042	1.022	0.971	0.942	0.961	0.947	1.125	1.27	11830	
141K/142K	0.843	1.010	1.010	0.984	0.748	0.925	2.132	-	8261	(0)
152 /151	1.067	1.000	1.095	1.128	0.860	0.517	1.565	1.05	9800	(2)
172K/171K	0.965	0.955	0.983	0.984	0.836	1.127	1.208	1.00	6013	
181K/182K	1.026	0.976	0.997	0.995	0.805	1.003	1.109	1.05	10020	
192K/191K	0.977	0.951	1.012	1.008	1.372	1.279	1.066	0.82	11643	
202K/201K	0.853	0.831	0.990	0.997	0.632	0.976	1.138	0.76	5269	
222K/221K	1.149	1.150	0.985	0.954	1.160	0.973	1.036	1.57	11802	
232 /231	0.946	0.917	1.105	1.048	0.936	1.046	1.232	1.32	11928	
241K/242K	1.153	1.043	1.020	0.986	2.924	1.000	1.194	-	15090	
251 /252	1.020	0.985	0.977	0.995	1.049	0.963	1.017	0.89	8558	
261 /262	0.829	0.967	0.951	1.015	0.822	0.975	1.158	0.95	9874	
271 /272	1.078	1.058	1.038	1.035	1.178	0.859	1.012	0.96	12147	
331K/332K	1.131	1.091	1.018	1.003	0.994	1.035	1.049	1.03	9558	
351K/352K	0.875	1.000	0.959	0.986	1.370	1.232	1.229	1.11	9099	(0)
362 /361	1.000	0.982	0.984	0.997	1.055	1.565	1.096	1.25	15141	(2)
372 /371	0.963	0.940	1.059	1.066	1.159	0.671	1.059	0.97	13565	
391 /392	0.995	0.973	1.042	1.046	0.848	0.847	1.084	0.75	7642	
442 /441	1.341	1.040	0.974	0.974	1.393	1.466	1.289	1.88	9308	(1)
452K/451K	0.958	0.920	1.012	0.989	0.909	1.311	1.031	0.89	9632	
472 /471	0.914	0.957	1.027	1.015	1.038	1.135	1.145	0.69	7447	
501 /502	1.025	0.985	1.054	1.067	0.858	1.000	1.086	-	10128	
541 /542	1.136	1.100	1.075	1.081	0.930	0.845	1.257	1.06	10049	
571K/572K	1.059	1.049	0.916	0.914	0.421	0.918	1.356	1.19	15301	
582 /581	0.921	0.977	1.000	0.941	0.889	0.883	1.410	1.16	9158	
591K/592K	-	1.022	0.989	1.017	0.922	0.726	1.179	-	8337	
611 /612	0.801	0.965	1.020	1.010	1.344	1.049	1.205	0.84	8492	
631 /632	1.133	1.069	1.026	0.941	1.672	1.182	1.123	0.82	9587	
642K/641K	1.019	1.028	1.003	0.995	1.122	0.791	1.211	1.39	9036	
682 /681	1.026	0.923	1.022	1.027	0.513	0.910	1.020	-	9195	
691K/692K	1.008	1.065	0.980	0.976	1.418	0.841	1.062	1.01	5929	
702K/701K	0.973	1.012	1.012	0.980	0.794	0.880	1.052	0.98	8023	
741 /742	1.325	0.968	0.901	0.876	1.000	0.769	1.242	0.86	11127	(1)
752K/751K	0.858	0.978	1.015	1.002	1.043	1.046	1.213	0.84	5088	
761 /762	1.193	1.075	0.974	1.008	1.730	1.068	1.633	1.11	8769	
772K/771K	1.000	0.986	1.033	1.074	0.919	0.971	1.509	-	8316	
782K/781K	0.869	0.968	0.977	1.051	1.036	1.314	1.159	-	5559	
811 /812	0.796	0.963	0.927	0.978	0.618	1.063	1.582	1.05	5403	(1)

(0) Failure at different defects
(1) E out of bounds (.800 - 1.250)
(2) 1/TMKAR out of bounds (.667 - 1.500)

Table 3

Adjustment

	Pairs Nos.	E=EA/EB	F	F_{adj}	FA N	FB N	FA-FB N	FB-FB* N
	1	2	8	8a	10	11	12	13
	11 K/12 K	1.046	1.142	1.092	11494	10061	1433	928
(1)	42 K/41 K	1.296	1.634	1.261	13022	7971	5051	2077
	71 /72	0.980	1.035	1.056	8641	8352	289	465
	81 K/82 K	0.925	1.143	1.236	8864	7754	1110	719
	92 K/91 K	1.236	1.181	0.956	15145	12829	2316	-576
	101K/102K	0.974	1.048	1.076	12494	11925	569	903
	132K/131K	1.042	1.125	1.080	11830	10517	1313	836
	152 /151	1.067	1.565	1.467	9800	6260	3540	2925
	172K/171K	0.965	1.208	1.252	6013	4978	1035	1253
	181K/182K	1.026	1.109	1.081	10020	9037	983	729
	192K/191K	0.977	1.066	1.091	11643	10926	717	991
	202K/201K	0.853	1.138	1.334	5269	4632	637	1545
	222K/221k	1.149	1.036	0.902	11802	11338	464	-1066
	232 /231	0.946	1.232	1.302	11928	9680	2248	2929
	241K/242K	1.153	1.194	1.036	15090	12636	2454	452
	251 /252	1.020	1.017	0.997	8558	8411	147	-21
	261 /262	0.829	1.158	1.397	9874	8526	1348	3385
	271 /272	1.078	1.012	0.939	12147	12005	142	-737
	331K/332K	1.131	1.049	0.928	9558	9111	447	-660
	362 /361	1.000	1.096	1.096	15141	13819	1322	1322
	372 /371	0.963	1.059	1.100	13565	12806	759	1280
	391 /392	0.995	1.084	1.092	7642	7052	590	628
(1)	442 /441	1.341	1.289	0.961	9308	7220	2088	-279
	452K/451K	0.958	1.031	1.076	9632	9341	291	713
	472 /471	0.914	1.145	1.253	7447	6502	945	1646
	501 /502	1.025	1.086	1.060	10128	9330	798	551
	541 /542	1.136	1.257	1.107	10049	7996	2053	850
	571K/572K	1.059	1.356	1.281	15301	11283	4018	3166
	582 /581	0.921	1.410	1.531	9158	6496	2662	3448
	591K/592K	-	1.179	-	8337	7070	1267	-
	611 /612	0.801	1.205	1.504	8492	7047	1445	3555
	631 /632	1.133	1.123	0.991	9587	8534	1053	-72
	642K/641K	1.019	1.211	1.188	9036	7459	1577	1409
	682 /681	1.026	1.020	0.994	9195	9013	182	-51
	691K/692K	1.008	1.062	1.054	5929	5582	347	300
	702K/701K	0.973	1.052	1.081	8023	7629	394	617
(1)	741 /742	1.325	1.242	0.937	11127	8960	2167	-562
	752K/751K	0.858	1.213	1.414	5088	4193	895	1737
	761 /762	1.193	1.633	1.369	8769	5369	3400	1981
	772K/771K	1.000	1.509	1.509	8316	5510	2806	2806
	782K/781K	0.869	1.159	1.334	5559	4795	764	1602
(1)	811 /812	0.796	1.582	1.987	5403	3416	1987	3372
	Mean	M	1.193	1.156			1430	1148
	Stand. dev.	s	0.172	0.246			1131	1267
	Number	n		41			42	41
	If rows denoted (1) are disregarded:							
		M	1.167	1.142			1283	1148
		s	0.150	0.213			1002	1218
		n		37			38	37

FB* =(EB/EA)FA

Table 4

Ratio of Strength Within Pairs
Specimens in Random Order

Pair No. 1	F 8	Continued 1	8
1	1.142	33	1.049
7	1.035	36	0.912
8	1.143	37	0.944
9	0.847	39	1.084
10	1.048	45	0.970
13	0.889	47	0.873
15	0.639	50	1.086
17	0.828	54	1.257
18	1.109	57	1.356
19	0.938	58	0.709
20	0.879	59	1.179
22	0.965	61	1.205
23	0.812	63	1.123
24	1.194	64	0.826
25	1.017	68	0.980
26	1.158	69	1.062
27	1.012	70	0.951
		75	0.824
		76	1.633
		77	0.663
		78	0.863
		Mean M	1.005
		Stand. Dev. s	0.193
		Number n	38

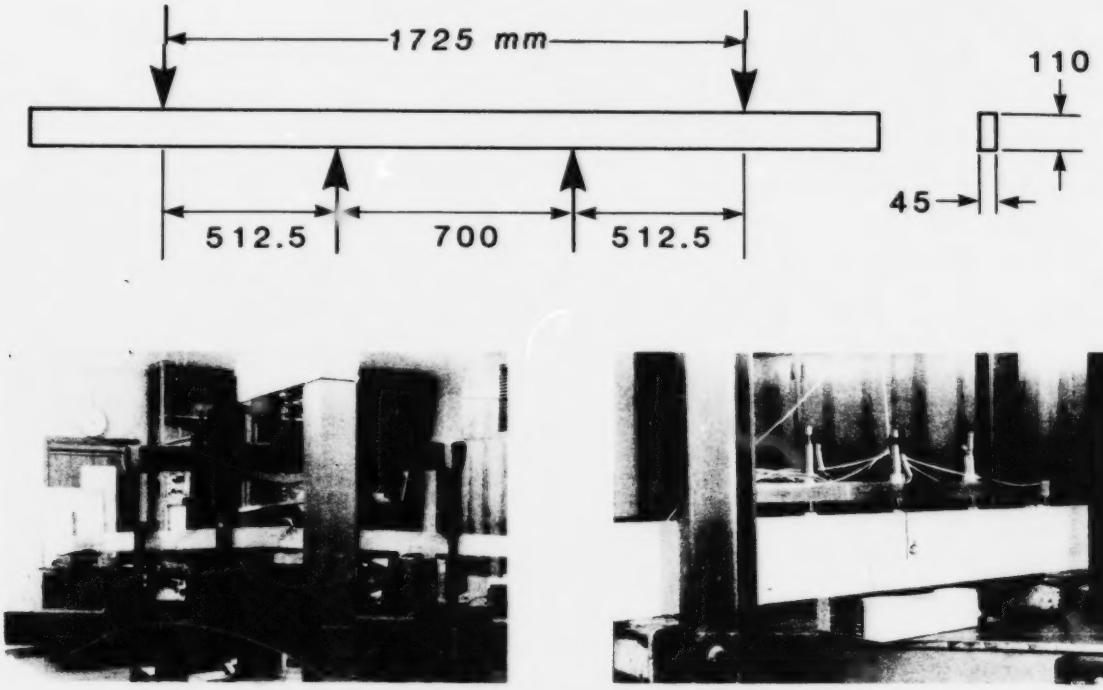

Figure 1. Testing arrangement.

Figure 2. Distribution of strength ratios within pairs.

DURATION OF LOAD TESTS WITH NOTCHED SPRUCE BEAMS AT TWO MOISTURE LEVELS

P. Hoffmeyer, H.J. Krebs, L.F. Nielsen
Building Materials Laboratory, Technical University of Denmark, Lyngby, Denmark

INTRODUCTION

The work presented here is an extension of the research carried out by Krebs (1984) for a duration of load program at the Building Materials Laboratory at the Technical University of Denmark. The report describes only lifetime observations for small clear notched specimens subjected to bending, whereas the creep measurements will be the subject of a separate paper.

MATERIALS

SAMPLING

Fifteen slow grown spruce trees (Picea abies) were chosen. The trees were straight grown and approximately 100 years old. From the butt of each tree four 2.2-m-long slabs were cut. Each slab was then split to form the basis of the final specimen selection.

The specimens were cut as 28 x 28 mm pairs from the sapwood (Figure 1). Then they were conditioned to 20°C, 65 percent relative humidity (RH), and cut and planed to their final dimensions of 20 x 20 x 600 mm.

When all pieces with excessive reaction wood and fiber angle had been rejected, 255 pairs of specimens were left. Only 132 pairs were included in the present test series.

SPECIMEN GEOMETRY

The specimens were loaded in bending. In order to obtain brittle failure typical of structural wood, a 3.5-mm-deep notch was introduced (Figure 2) on the tension side. In this way, the tension side of the beams failed before the compression side. The two holes served the purpose of arresting failure as soon as a crack reached them.

CONDITIONING

The specimens were dried from green condition to approximately 15 percent moisture content over a two and a half month period. After planing, 66 pairs were kept at 20°C and 65 percent RH, and 66 pairs were rewetted using vacuum treatment.

METHODS

TEST RIGS

The test rigs (Figure 3) introduce a constant (time independent) moment along the 400 mm free span of the specimen, and provide simple support.

DEFORMATION MEASUREMENTS

The time dependent deformations were constantly monitored. A presentation and discussion of creep data will be given in a separate paper.

CLIMATE CONDITIONS

The climate of the environment throughout the two years was 21 $\pm$ 3°C and 64 $\pm$ 1 percent RH.

All specimens, dry as well as wet, were sealed in plastic tubing. Frequent injection of water into the plastic tubing ensured constant water saturation of the wet specimens.

LOAD LEVELS AND NUMBER OF SPECIMENS

The average short-term strength was established, and three groups of long-term specimens were loaded at stress levels (SL) corresponding to 78 percent, 72 percent and 66 percent of the corresponding average short-term strength. The number of pairs of specimens is shown in Table 1.

SHORT-TERM TEST PROCEDURE

In order to test the quality of the pair matching, 30 pairs were tested at each of the two climate conditions.

The tests were carried out in one of the long-term test rigs (Figure 3) to ensure that the short-term load configuration was identical to the long-term load configuration. Average time to failure was 3.0 minutes.

LONG-TERM TEST PROCEDURE

One specimen of each pair was tested in the green condition, and the other was tested in the dry condition. Both specimens of one pair were tested at the same stress level. The long-term load was applied within five to 10 seconds.

RESULTS

SHORT-TERM TESTS

The average failure loads ($\bar{F}$) are given in Table 2. The load is equivalent to the weight attached to the lever. These results represent 30 pairs of specimens for each of the two climate conditions. The distribution of failure loads and the type of failure are also presented in Figure 4.

There are two possible failure modes (Figure 5). Type 1 is the anticipated mode of failure with the crack starting at the notch and progressing as a combined shear and tension perpendicular to the grain failure. Type 2 starts as a tension parallel to the grain failure under one of the two holes. Out of 120 specimens, only five (four percent) failed as Type 2 failure (Figure 4).

LONG-TERM TESTS

The long-term tests were started in August, 1982, and terminated in October, 1984. At the end of the loading period, nearly all specimens from the two higher stress levels had failed, while four wet and 10 dry specimens still remained at the low stress level (Figure 6).

The failure type frequency is also shown in Table 3.

ESTIMATION OF AVERAGE TIME TO FAILURE

There is no way to assess the true short-term strength of the long-term loaded specimens in the present experiment. For this reason, the duration of load curves are represented here only by the mean time to failure of each of the samples tested.

For the samples in which not all specimens have failed it is necessary to estimate the mean time to failure based on a censored distribution. This is done by assuming a logarithmic normal distribution and using the statistical methods described by Gupta (1952). The results are shown in Table 4.

The estimated time to failure as a function of stress level is depicted in Figure 7. As the short-term strength is based on ramp loading, the time to failure is not directly comparable to the dead load results. Theoretical considerations (Nielsen and Kousholt, 1980) indicate a -0.5 shift of the ramp load time to failure to equate dead load time to failure. This shift is also indicated in Figure 7.

DISCUSSION

TYPES OF FAILURE

The Type 2 failure appears more frequently in long-term loading than in short-term loading for the dry specimens (Figure 6 and Table 3). This is probably caused by a more severe time factor for the Type 2 failure mechanism. For this to be true, the time factor involved in tension parallel to grain (Type 2) should be more severe than that of a combined shear and tension perpendicular to grain failure (Type 1). This, however, is not in agreement with results of other investigations.

The observation that the frequency of Type 2 failures drops dramatically for wet specimens seems to indicate less moisture dependency for tension parallel to grain than for a combination of shear and tension perpendicular to grain.

MATCHING

The pair-wise matching of specimens does not result in any significant improvement of short-term strength predictability.

An estimate of short-term strength based on the strength of the corresponding twin results in coefficient of variations of 6.9 and nine percent for dry and wet specimens, respectively (Table 2). An estimate based on the average strength of a reference distribution results in corresponding coefficients of variation of approximately eight percent.

The variations are very small, and the lack of advantage of matching has probably to do with the fact that the sampling from the outset has secured a very uniform material from similar trees (same age, growing conditions, etc.).

TIME TO FAILURE

The technique used in order to predict mean time to failure based on a censored distribution seems adequate, which is illustrated by the predicted mean time to failure for the dry specimens at SL = 66 percent.

After 98 days, 33 percent of the specimens had failed, and the predicted mean logarithmic time (hours) to failure was 4.2 (Krebs, 1984). After 630 days, 75 percent of the specimens had failed, and the predicted mean logarithmic time was 3.7. The logarithmic time to failure when exactly 50 percent of the specimens had failed was 3.9.

In spite of the complications caused by the occurrence of two different failure modes, it is safe to assume a difference between time to failure for wet and dry specimens equal to or larger than that illustrated in this paper (Figure 7).

As mentioned earlier, the Type 2 failure supposedly has a more severe time factor than Type 1. Samples including Type 2 failures should thus be expected to have shorter mean times to failure. Since, at the same time, dry samples show significantly more numerous Type 2 failures than wet samples, the difference betweeen time to failure for the two conditions can only widen.

It may be noted that the difference between mean logarithmic time to failure for dry and wet samples is nearly the same ($\Delta \log_{10} t_c = 1.3$) at all three stress levels.

The duration of load curves (Figure 7) seem to be bent slightly upwards. However, as no further evidence is available to substantiate this observation, a straight line is adopted as a first approximation (Figure 8).

Very few duration of load experiments including different moisture content levels have been reported. McDowall (1982) carried out tests on Douglas-fir in tension perpendicular to grain at moisture content levels of six and 60 percent. The mean logarithmic times to failure were calculated by Krebs (1984) and are shown in Figure 8 together with the "Madison curve". This figure shows a remarkable agreement between the different investigations, especially when considering the three different failure modes involved: bending parallel to grain (Madison tests), tension perpendicular to grain (McDowell), and a mixture of tension perpendicular, shear and tension parallel to grain (present investigation).

CONCLUSION

The present investigation shows that:

- Short-term bending strength for a particular specimen is predicted with the same accuracy by the mean strength of a large sample as by the strength of the twin of a matched pair. Matching technique for specimens of the present type is therefore superfluous.
- Wood, which is loaded to the same relative stress level, shows significantly shorter times to failure when wet than when dry. The difference in mean logarithmic time to failure is of the order 1.3.
- Time to failure for dry wood subjected to a combination of shear, tension perpendicular to grain, and tension parallel to grain failure is very well predicted by the Madison curve.

REFERENCES

Gupta, A.K. 1952. Estimation of the mean and standard deviation of a normal population from a censored sample. Biometrica 39.

Krebs, H.J. 1984. Vandindholdets betydning for traes mekaniske langtidsegenskaber. Building Materials Laboratory, Technical University of Denmark, Technical Report No. 105/84.

McDowall, B.J. 1982. The Duration of Load Effect in Tension Perpendicular to the Grain for Douglas Fir. Department of Civil Engineering, University of British Columbia, Vancouver, Canada.

Nielsen, L.F. and K.K. Kousholt. 1980. Stress-strength-lifetime relationship for wood. Wood Science 12(3).

Table 1

Number of Pairs of Specimens

Condition	Short-term	Long-term stress level (SL)		
		78%	72%	66%
65% RH	30	16	16	40
green	30			

Table 2

Average Short-term Failure Load ($\bar{F}$) for 60 Pairs of Specimens

	Twin No.1			Twin No.2			$\bar{F}_1/\bar{F}_2$		
	$\bar{F}_1$ (N)	s (N)	c.v. (%)	$\bar{F}_2$ (N)	s (N)	c.v. (%)		s	c.v. (%)
Dry	71.2	5.9	8.3	70.1	5.6	8.0	1.018	.071	6.9
Wet	48.6	3.9	8.1	48.8	3.9	8.1	1.000	.090	9.0

Table 3

Percentage of Failed Specimens Showing Type 2 Failure

Stress Level		100%	78%	72%	66%
Condition	Dry	3	7	29	33
	Wet	5	0	0	11

Table 4

Mean Logarithmic Time to Failure and Standard Deviation of Mean*

Condition	Wet			Dry		
Stress Level	78%	72%	66%	78%	72%	66%
Total number of specimens	16	16	40	16	16	40
Number of broken specimens	16	15	36	15	14	30
Mean logarithmic time to failure	0.59	1.27	2.32	1.96	2.60	3.72
Standard deviation of mean	0.40	0.39	0.26	0.56	0.53	0.19

* Except for stress level 78% (wet), the calculations are based on statistics for censored distributions (Gupta, 1952).

Time to failure in hours.

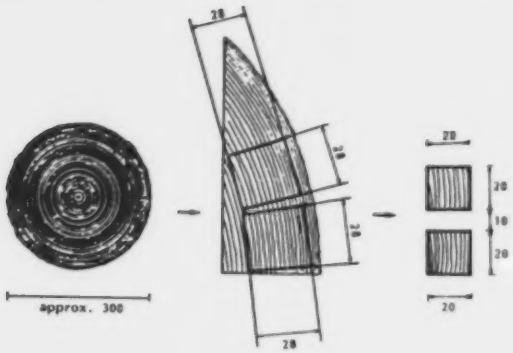

Figure 1. From the butt of each tree four 2.2 m long slabs were cut. Each slab was then split to form the basis for the final specimen selection. The specimens were cut as pairs from the sapwood.

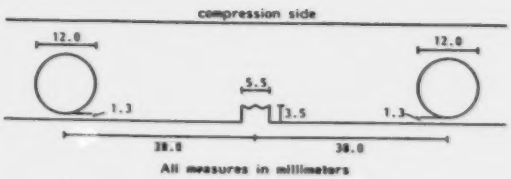

Figure 2. Specimen geometry showing notch and the two holes.

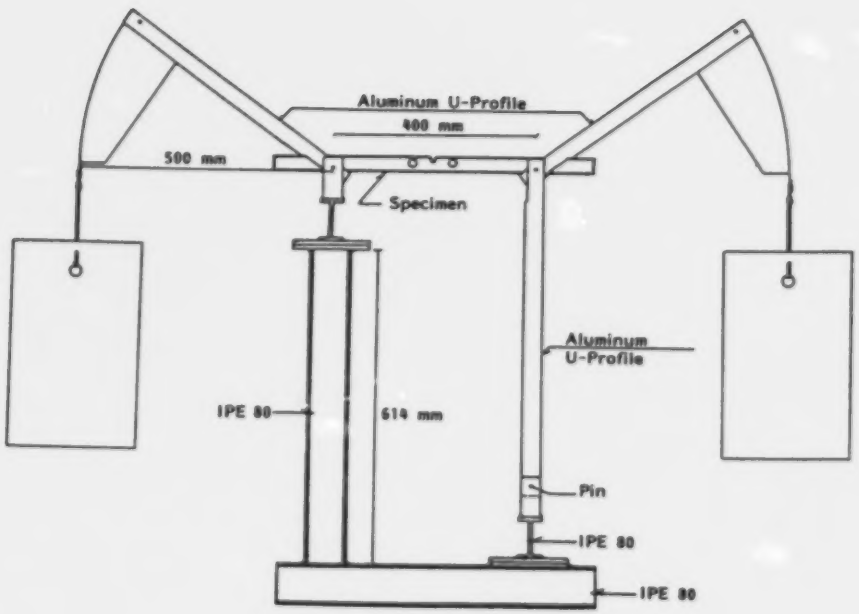

Figure 3. The test rigs introduce a constant moment along the 400 mm free span of the specimen.

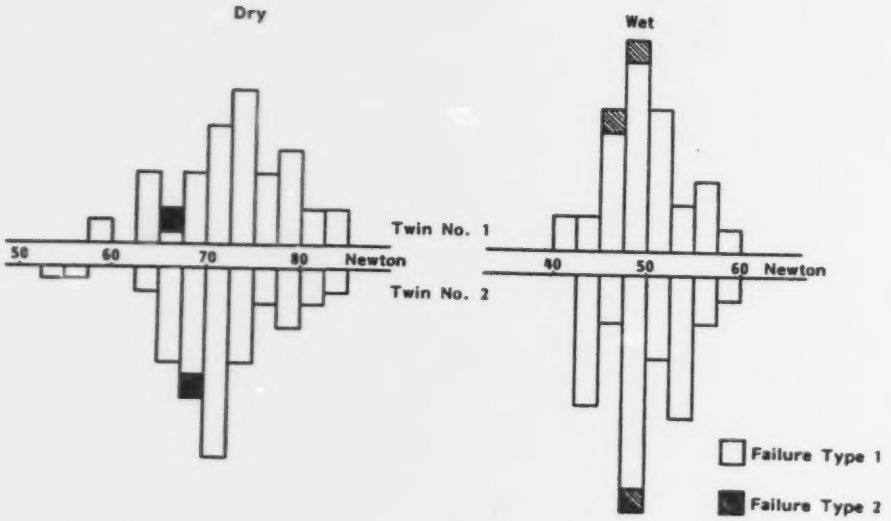

Figure 4. Distribution of failure load and type of failure for short-term tests.

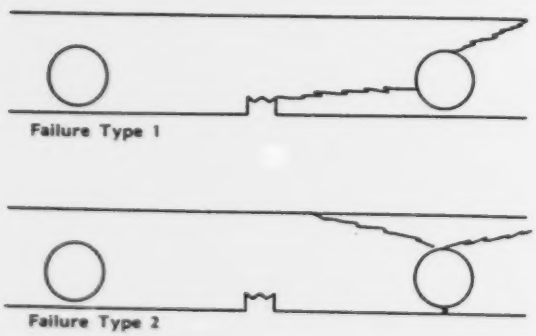

Figure 5. The two possible failure modes.

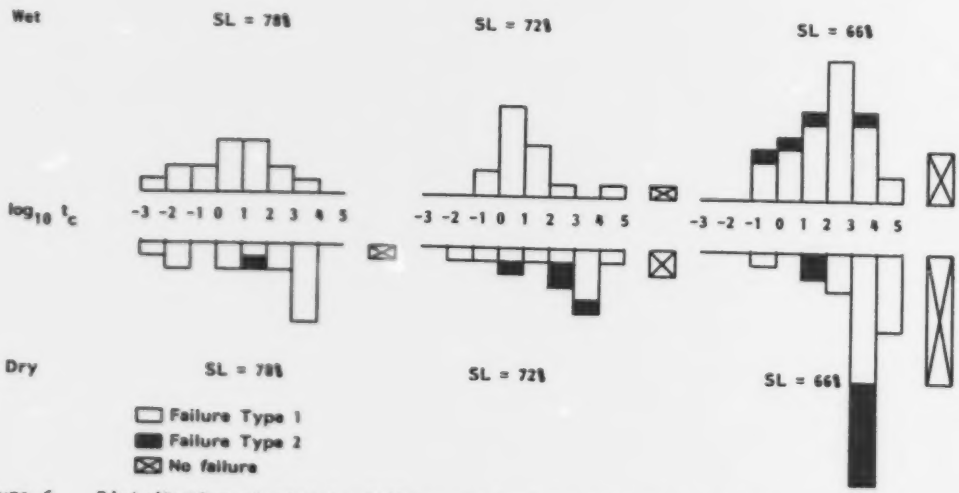

Figure 6. Distribution of time to failure and type of failure for long-term loaded specimens. t_c = time to failure in hours.

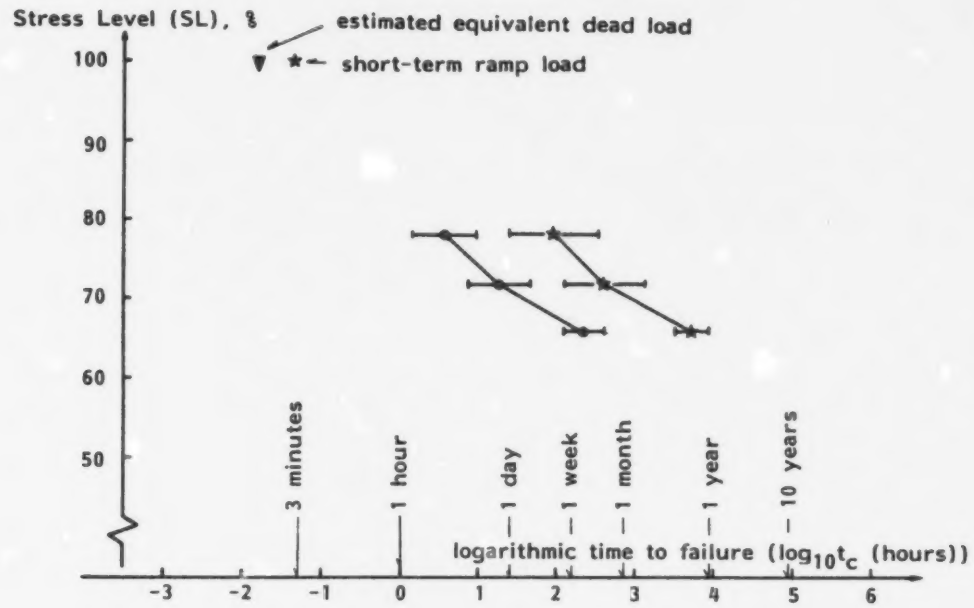

Figure 7. Estimated logarithmic mean time to failure for dry (✱) and wet (●) specimens as a function of stress level. Standard deviation (s) of estimate is indicated as $\vdash\frac{s}{}+\frac{s}{}\dashv$.

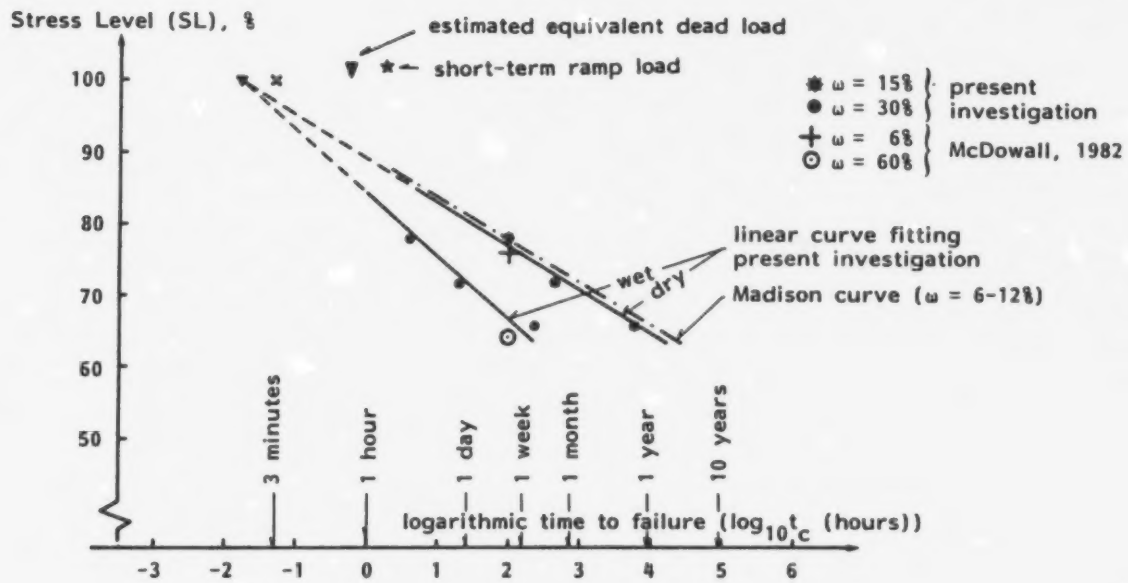

Figure 8. Estimated logarithmic time to failure as a function of stress level. The results from McDowall (1982) have been calculated by Krebs (1984).

PREDICTION OF SHORT- AND LONG-TERM BEHAVIOR OF TRUSS-PLATE JOINTS IN TENSION

L.C. Palka
P. Eng., Forintek Canada Corp., Western Laboratory, Vancouver, B.C.

INTRODUCTION

Wood structural systems are assemblies of individual lumber pieces and panel products interconnected by means of mechanical fasteners or adhesives. The objectives of this exploratory study were to develop an understanding and reliable design equations for both the short-term and long-term behavior of truss-plate joints in tension. To achieve these goals, development of both analytical models and supporting experimental data is needed. A general review of the problem, past results and possible solutions was outlined by Palka (1981).

The experimental design (Table 1) for the initial truss-plate joint tests was developed next (Palka, 1982), together with appropriate specimen dimensions (Figure 1) and both short- and long-term tests. The selection of kiln-dried, 2 x 4 in. (38 x 89 mm) 1650f-1.5E, machine stress graded spruce lumber and the specifications of the 3 x 5 in. (76 x 127 mm), 80 tooth, 20 gauge, galvanized steel TTS-LT truss-plate has also been discussed elsewhere (Palka, 1983). The short-term testing of 150 specimens and the initial development of closed-form, non-linear analytical models for describing the static behavior of truss-plate joints in tension were then completed (Palka, 1983).

Creep and creep-rupture tests of 300 truss-plate joint specimens in tension were initiated in 1984 (Palka, 1984).

A detailed data report summarizing all short-term and the first seven months of long-term test results was recently prepared (Palka and Rovner, 1985). Similarly, all short- and long-term test methods, special instrumentation and improved data acquisition systems developed for and used in the study have been described elsewhere (Palka, 1983 and 1984; Rovner, 1985). Therefore, only the highlights or most interesting implications of this exploratory investigation will be discussed here.

RESULTS AND DISCUSSION

In the past, engineers attempted to break complex problems into simple components, for ease of understanding and analysis. Consequently, the static, creep and creep-rupture (time-to-failure) properties of materials were evaluated from completely independent tests by unrelated analytical models (Palka, 1981). The resulting database was fairly extensive--and expensive to collect--but highly fragmented, as were the corresponding predicting equations for various material properties. Therefore, an accurate assessment of the relationships between various material parameters needed in modern analyses of structural systems would be difficult, if not impossible, from past information.

Current load-duration studies require the evaluation of static, creep and creep-rupture behavior of matched material samples (Table 1). The resulting database is suitable for an accurate assessment of relationships between various material parameters, in addition to supporting the development of conventional (individual) predicting functions. It is hoped that, ultimately, the most important material parameters will be predicted from a single static or short-duration creep test in the future. For example, static behavior may be described by creep parameters, and selected creep parameters could also predict time-to-failure under constant loads.

SHORT-TERM BEHAVIOR OF TRUSS-PLATE JOINTS

Model Development and Calibration

Failure by tooth withdrawal--in a plane normal to the axial tension force--is a characteristic of truss-plate joints not observed in any other connector types (Palka, 1981). Therefore, the load/slip (P/S) behavior of truss-plate joints was approximated here by a metal beam (E, I), clamped at one end ($\eta = 1.0$), resting on a wood foundation (k) and subject to an axial tensile (withdrawal) force (N). The non-linear P/S behavior of truss-plate joints in tension (Figure 2) could be readily described by a conventional elastic model (Hetenyi, 1962) when beam and foundation moduli were replaced by appropriate secant moduli (Palka, 1981):

$$P/S = K = (k/\eta\lambda)\,([3\alpha^2 - \beta^2]/2\alpha\lambda)c$$

with,

$\lambda = (k/4EI)^{0.25}$,
$\alpha = \lambda(1 + \lambda^{2}N/k)^{0.5}$,
$\beta = \lambda(1 - \lambda^{2}N/k)^{0.5}$, and,
c = empirical adjustment factor.

For estimating the secant moduli of metal teeth, two alternatives were evaluated (Palka, 1983): (1) a complex non-linear equation $E \cong E_o \cdot f(1,s)$ incorporating the effects of changing tooth length (l) and slip (s), and (2) a simple bi-linear model $E \approx \sigma_o/\epsilon$ based on knowledge of yield stress (σ_o) and strain (ϵ) calculated from tooth slip (s). The fit between measured (triangles) and predicted (i = dashed lines, ii = solid lines) P/S is depicted in Figure 2. Apparently, both alternatives yielded answers adequate for truss-plate design.

The proposed model was also used for predicting the load/slip behavior of glulam-rivet joints (Figure 3), as an independent check on the validity of the assumptions made in the derivation of the truss-plate joint design equations: P/S = K. Large deflections indicated by the solid lines in Figure 3 had been observed only recently (Karacabeyli, 1985, personal communication). Even at low slip values, the secant moduli estimated from $E = \sigma_o/\epsilon$ seemed to yield a better fit to experimental data. The good agreement between observed and predicted values for both truss-plate and glulam-rivet joints suggests the absence of any major error or bias in the proposed non-linear load/slip model for a single tooth- or dowel-type joint. Consequently, the model can be used to predict the effect of many tooth (or dowel) and wood variables upon the behavior of truss-plate or glulam-rivet joints in tension (Palka, 1983). Indeed, the model could be used to estimate the four strength values of truss-plate joints (Pa: P, P', Q, Q' in Figure 4) required by the Canadian design code (CAN3-086-M84). This would eliminate the need for experimental determination of these four basic values (S-347-M1980) for each combination of lumber species, grades and sizes with various types and sizes of truss-plate teeth.

Joint Design and Reliability

Based on the test results, the allowable design load for a TTS-LT type truss-plate joint in air-dry spruce lumber may be estimated as:

$$Pa = 22.5 \times \text{rows} \times \text{columns (lbs)}$$

$$= 100 \times \text{rows} \times \text{columns (N)}$$

where,

$Pa \leqslant$ plate tension strength,
$\text{row} \leqslant 8$, and
rows x columns = total number of teeth in a truss-plate

The graphical equivalent of this design equation is depicted in Figure 5. The graph permits the quick selection of the smallest truss-plate size--to carry a given load--by simple inspection.

The cumulative probability of the static tensile strength (P') of the sample joints is depicted in Figure 6. This allows speculation about the reliability of truss-plate joints in tension, in the following manner: the allowable design load for these joints is

$$Pa = \bar{P}'/3 = 67.17 \text{ lb}/3 = 22.36 \text{ lb } (99.5 \text{ N})$$

per tooth, which is less than the location parameter

$$b = 35.51 \text{ lb } (157.9 \text{ N})$$

of their Weibull distribution. Thus, if the truss-plate joints "recognize" that their tensile strength constitutes a Weibull distribution, they will never fail in simple static (short-term) tension under the allowable design load. Were these joints designed according to rules applied to dimension lumber, the allowable joint loads would be

$$Pa = P'_{0.05}/2.1 = 53.90 \text{ lb}/2.1 = 25.65 \text{ lb } (114.1 \text{ N}).$$

Again, this is less than the location parameter b (Figure 6), although it exceeds the value obtained by the previous method. Consequently, the probability of truss-plate joint failure is marginally smaller than that of lumber failure under identical tensile loads and load duration factors, when the proposed design procedure is followed.

LONG-TERM BEHAVIOR OF TRUSS-PLATE JOINTS

Load Duration Factors

An important parameter required for structural design is the loss in joint strength under prolonged loads, identified as the "load duration effect" in building codes. In the past, the relationship between strength and load duration has been generally described by the "Madison curve" (Wood, 1951) depicted by the solid line in Figure 7, which was derived from small, clear wood specimens in bending. For in-grade lumber in bending, the relationship between strength and load duration is more complex (Foschi and Barrett, 1982), with a threshold at about 50 percent of the static strength.

The simplest prediction of load duration effects would be obtained by extending, for long periods of time, a linear regression between load level and the logarithm of time (Dinwoodie et al., 1984). A similar model, fitted to selected segments of the available experimental data for truss-plate joints in tension is depicted in Figure 8. Projection of this trend line beyond one year is purely speculative; no experimental data are available in that range yet. The corresponding tentative load duration factors and load ratios are listed in Table 2 and depicted in Figure 7 (dashed line). These tentative values will have to be revised, as long-term truss-plate joint failure data continue to accumulate.

Median failure times, at each constant long-term load level, needed to fit the more complex damage accumulation models (Foschi and Barrett, 1982) to develop load duration factors for truss-plate joints in tension are not yet available from the current study.

Truss-plate Joint Creep

The creep of truss-plate joints during the service life of trusses is also of interest to structural engineers. In the present study, the effect of only two load levels ($PR = P/P_0 = 0.60$ or 0.85) upon joint slip (s) have been experimentally determined, during a test period (t) of seven months. Creep was automatically recorded in 3/1000 inch (0.076 mm) increments, together with the corresponding time (to the nearest second) and date, by a microcomputer controlled data acquisition system. After suitable manipulations, conventional creep responses could be plotted for each joint, as shown in Figure 9.

Analytically, a six-parameter function (Marin, 1962) was chosen to describe joint creep S(t), or creep-rupture S(t = FT),

$$S(t) = [K + K_1(1-e^{-K_2 t}) + K_3 t]\,(P/P_0)^{\eta}$$

In fitting this function to individual joint creep data, the load level (P/P_0) was also assumed to be an unknown parameter. A commercial computer program (SAS Institute, 1982) was used to estimate the six parameters for each joint by a non-linear least-squares method. The goodness of fit between observed and predicted slip can be judged from an inspection of Figure 9, for a specific joint. A summary of creep (surviving specimens) and creep-rupture (failed specimen) parameters is given in Table 3, together with the last measured slip (LS) or failure slip (FS) and last measured time (LT) or failure time (FT).

Relations Between Creep and Failure Parameters

A few of the possible relationships between static, creep and creep-rupture parameters will be examined here, in light of the available experimental data and proposed models for describing truss-plate joint behavior in tension. For example, the average maximum joint slip in static tension was 0.136 inch (3.45 mm) at a moisture content of 9.5 percent, while the average joint creep at rupture was 0.144 inch (3.66 mm) at a moisture content of about 12 percent (Palka, 1985). The good agreement between these independent observations suggests that truss-plate joints in tension tend to fail at a critical slip value (0.140 inch or 3.55 mm), regardless of load history under comparable environmental conditions.

Inspection of Table 3 reveals that the average parameters of the proposed non-linear viscoelastic model depend on both load level and failure status. Surviving and failed specimens have different parameters even under the same constant load. Apparently, these viscoelastic parameters do not represent truly independent material properties, but rather

interactions of several basic wood and metal variables. Establishment of relationships between basic material properties and viscoelastic parameters has not been attempted in this study.

Inspection of Table 3 also reveals that the slip of surviving creep specimens is dominated by elastic (K_0) and viscoelastic (K_1 and K_2) components, while the slip of failed creep specimens is dominated by the viscous (K_3) component. The same tendency has been observed for particle-boards (Dinwoodie et al., 1984) and for plastics and metals (Marin, 1962). These arguments were used to justify prediction of creep-rupture time (FT) from the following simplified formula:

$$FT \simeq \frac{1}{K_3 \eta \, (P/P_0)^{\eta}}$$

The resulting relationship between constant loads ($y = P/P_0$) and logarithm of failure time ($x = \log FT$) is depicted in Figure 10, for truss-plate joints with $K_3 = 0.0036$ inch/hour and $\eta = 25$ or $\eta = 10$. Although these theoretical predictions asymptotically approach zero load at infinitely large times, the magnitude of shape parameter η may be considered as a measure of load threshold values at a service life of about 10^{16} hours or 10^{12} years. As indicated by the dashed lines in Figure 10, the observed behavior of truss-plate joints in creep-rupture is more complicated than the pattern suggested by the simple model.

The difference between observed and predicted behavior of truss-plate joints could be reduced by several empirical methods. For example, predicted failure times could be modified by a time-dependent correction factor; or both K_3 and η could be estimated as functions of load level and load duration or damage accumulation. The accuracy of predicted load/time relationship may be more simply improved by specifying an arbitrary value of the shape parameter, ray $\eta = 25$, and a shift in the load axis, say $y = (P/P_0 - 0.2)$ from the original $y = P/P_0$. The resulting prediction, with a small error on the conservative side, is depicted in Figure 11. While empirical modification factors may be appealingly simple for the truss-plate joint tested, they cannot be readily generalized for other joint types. Clearly, much more basic research is needed to establish general relations between material properties of wood and truss-plate, and the conventional creep and creep-rupture parameters in the future.

CONCLUSIONS

From a modified elastic model, based on a metal beam (tooth) subject to axial withdrawal force and resting on a wood foundation--using secant moduli to account for the observed non-linearity of the system--the effect of major wood and truss-plate variables upon the short-term (static) load/slip behavior of truss-plate joints in tension can be predicted.

The proposed model is able to answer many practical "what if" questions, not only for truss-plate joints in static tension but for glulam-rivet joints as well. Based on this model, a simple design procedure has been proposed.

The creep behavior of truss-plate joints in tension was described by a conventional four-parameter linear viscoelastic spring and dash-pot model, subject to non-linear load effects. The agreement between measured and predicted creep values was excellent for most specimens.

A limited number of joints failed under the constant loads in the first seven months of the experiment. Failure time was, however, predicted from appropriate creep parameters for all test specimens. Measured and predicted failure times showed good agreement for large failure times (>1000 hours) only. Tentative load duration factors were proposed from measured failure times.

Truss-plate joint failure seems to be dominated by a critical slip value, under both ramp loads and constant loads.

The potential benefits, and difficulties, of establishing general relations between basic material properties and model parameters describing static, creep or creep-rupture behavior of truss-plate joints have been briefly indicated.

REFERENCES

Canadian Standards Association. 1984. CAN3-086-M84: Engineering Design in Wood (Working Stress Design). Canadian Standards Assoc., Rexdale, Ont. 206p.

Canadian Standards Association. 1980. S-347-M1980: Method of Test for Evaluation of Truss Plates Used in Lumber Joints. Canadian Standards Assoc., Rexdale, Ont. 20p.

Dinwoodie, J.M., B.M. Paxton, C.B. Pierce and E.J. Aloysius. 1984. Quantification and Prediction of Creep in Particleboard. DOE, Building Research Establishment, Princes Risborough Laboratory, UK. Paper presented at FESYP Technical Conference. 19p.

Foschi, R.O. and J.D. Barrett. 1982. Load-duration effects in western hemlock lumber. Journal of Structural Division, Proceedings of the American Society of Civil Engineers, 108(ST7, July):1494-1510.

Hetenyi, M. 1962. Beams on elastic foundations, (Chapter 3). IN: Handbook of Engineering Mechanisms by Flugge. McGraw-Hill Book Co., New York, NY. 10p.

Karacabeyli, E. 1985. Glulam rivet joints under excentric loading. Experimental data for Masters Thesis, Department of Engineering, University of British Columbia, Vancouver, B.C. Personal Communication.

Marin, J. 1962. Mechanical Behavior of Engineering Materials. Prentice-Hall, Inc., Englewood Cliffs, N.J. 502p.

Palka, L.C. 1985. Effect of Load Duration Upon Timber Fasteners: Short- and Long-term Models. Report to the Canadian Forestry Service. Forintek Canada Corp., Vancouver, B.C. 38p.

Palka, L.C. 1984. Effect of Load Duration Upon Timber Fasteners: I. Building a Long-Term Tension Test Frame. II. Influence of Loading Rates on Joint Slip. Report to the Canadian Forestry Service. Forintek Canada Corp., Vancouver, B.C. 40p.

Palka, L.C. 1984. Effect of Load Duration Upon Timber Fasteners: I. Load/Slip Characteristics of Toothed Truss-Plate Joints in Static Tension. II. Prediction of Load/Slip Characteristics of Timber Joints Made With Metal Plate Connectors. III. Development of an Economical Test System for Automatic Measurement and Recording of Long-Term Slip in Timber Joints. Report to the Canadian Forestry Service. Forintek Canada Corp., Vancouver, B.C. 75p.

Palka, L.C. 1982. Effect of Load Duration Upon Timber Fasteners: Assessment of the Problem, Identification of Research Needs and a Proposal for Initial Experimental Work. Report to the Canadian Forestry Service. Forintek Canada Corp., Vancouver, B.C. 28p.

Palka, L.C. 1981. Effect of Load Duration Upon Timber Fasteners: A Selective Literature Review. Report to the Canadian Forestry Service. Forintek Canada Corp., Vancouver, B.C. 58p.

Palka, L.C and B. Rovner. 1985. Effect of Load Duration Upon Timber Fasteners: First Data Report. Report to the Canadian Forestry Service. Forintek Canada Corp., Vancouver, B.C. 65p.

Rovner, B. 1985. Low cost measurement of mechanical joint deformation. For. Prod. J. 35(1):36-38.

SAS Institute. 1982. SAS User's Guide: Statistics. SAS Institute, Inc., Cary, N.C. 589p.

Wood, L.W. 1951. Relation of Strength of Wood to Duration of Load. USDA, Forest Service, Forest Products Laboratory, Madison, WI. Report No. 1916. 26p.

Table 1

Initial Truss-Plate Joint Tests

Load Duration	Load Type	Joint Type	Test Conditions	Load Levels			Replicates
				Nominal (%)	Code	Actual (lb.)	
Short-time	Ramp, Tension	Single	Ambient	100	0	5370	150
Long-time	Constant, Tension			85	2	4600	150
Long-time	Constant, Tension			60	1	3200	150

Long-time: The smaller of five years or the time needed to fail 50% of the test specimen.

Single: Joints made with MSR SPF lumber of one grade, and 20-gauge, 3 x 5 in. steel plate with 3/8 in. deep teeth.

Ambient: Ambient laboratory temperature and humidity conditions during the test period.

100%: Average load at failure under short-term ramp loading.

Lumber: 1650f-1.5E MSR spruce.

Truss-plate: TTS-LT 20-gauge.

Table 2

Tentative Load Duration Factors for a Specific Truss-Plate Joint in Axial Tension

Load Duration Definitions	Code Load Duration Factors	Experimental Estimates*	
		Sustained Load Level	Duration Factors
Continuous (50 years)	0.90	0.46	0.85
Normal (10 years)	1.00	0.54	1.00
Two Month (0.167 year)	1.15	0.76	1.41
Seven Day (0.019 year)	1.25	0.815	1.51
One Day (0.0027 year)	1.33	0.825	1.53
Static	-	1.000	1.85
Instantaneous	2.00	?	?

* Based on limited number of joint failures within the first seven months of creep-rupture testing.

Table 3

Summary of Creep and Creep-Rupture Parameters by Load Levels

Variable	N	Minimum Value	Maximum Value	Mean	STD Error of Mean	Standard Deviation	C.V.	Skewness
			Surviving Specimens (Nominal load level of 0.60)					
K_o	127	1.0000	300.0000	45.8155	8.5837	96.7335	211.137	2.0723
K_1	127	1174.8250	17500.0000	11062.9976	459.1923	5174.8340	46.776	0.0154
K_2	127	2.5000	45.0000	12.1920	0.8275	9.3260	76.493	0.7299
K_3	127	1.0000	7.5000	1.8558	0.1051	1.1841	63.808	2.3228
P/P_o	127	0.6560	0.7230	0.6890	0.0012	0.0139	2.013	-0.0164
η	127	14.4660	18.7570	16.5729	0.0765	0.8621	5.202	-0.0096
LS	127	7.0000	129.0000	34.1024	1.4529	16.3735	48.013	2.1789
LT	127	528.2000	4285.3000	3324.7472	60.1669	678.0461	20.394	-1.3871
			Surviving Specimens (Nominal load level of 0.85)					
K_o	87	1.0000	300.0000	130.9961	14.0951	131.4702	100.362	0.3088
K_1	87	250.0000	17500.0000	8377.2019	595.3080	5552.6631	66.283	0.7095
K_2	87	2.5000	26.0780	7.2160	0.4988	4.6523	64.472	1.9866
K_3	87	1.0000	7.5000	1.6456	0.1392	1.2984	78.902	2.6921
P/P_o	87	0.6770	0.8270	0.7186	0.0021	0.0195	2.711	1.7203
η	87	8.4870	17.3570	14.7551	0.1253	1.1688	7.922	-1.4858
LS	87	18.0000	149.0000	91.7356	3.2051	29.8950	32.588	-0.0061
LT	87	25.8000	4222.9000	3546.6494	66.4534	619.8361	17.477	-3.7421
			Failed Specimens					
K_o	56	1.0000	300.0000	68.7869	12.7586	95.4766	138.801	1.4369
K_1	56	250.0000	17500.0000	3039.4210	624.5769	4673.9056	153.776	2.3222
K_2	56	2.5000	45.0000	5.9512	0.7894	5.9076	99.267	5.4752
K_3	56	1.0000	7.5000	3.5820	0.3963	2.9654	82.784	0.4795
P/P_o	56	0.7040	0.9140	0.7909	0.0076	0.0567	7.166	0.4870
η	56	5.0000	15.6970	10.6198	0.4166	3.1179	29.359	-0.3592
FS	56	68.0000	225.0000	143.8750	4.6223	34.5901	24.042	-0.1888
FT	56	0.3000	3819.4000	1236.2161	175.2437	1311.4034	106.082	0.7381

Note: Slip (LS or FS) in 1/1000 inch; time (LT or FT) in hours.

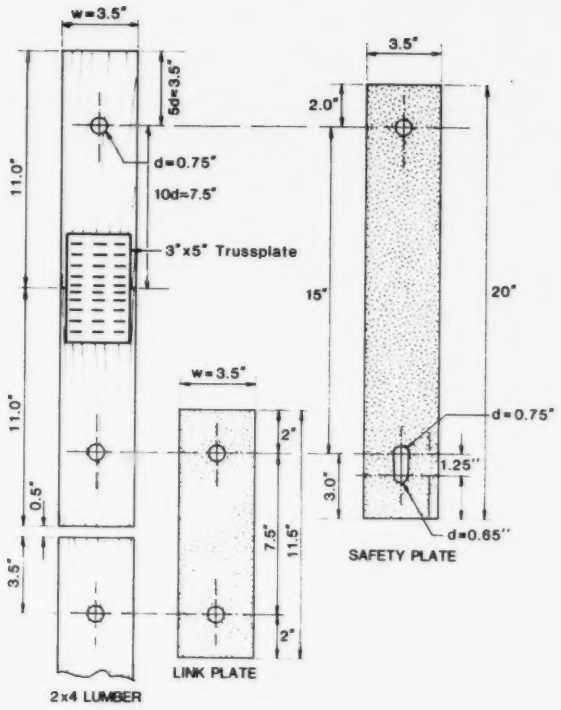

Figure 1. Specimen and linkage dimensions for testing truss-plate joints in tension.

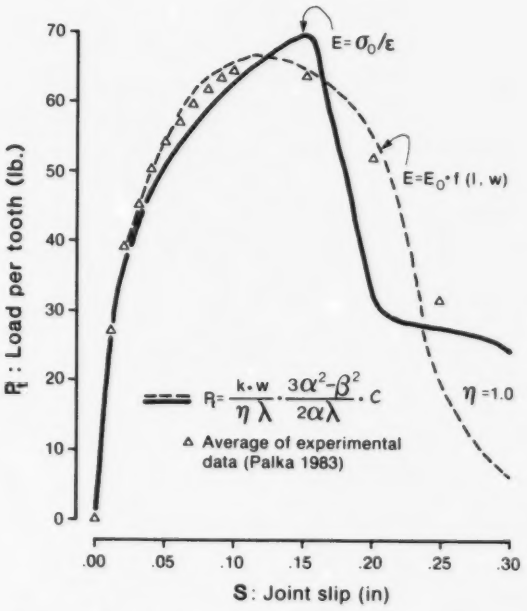

Figure 2. Measured and predicted behavior of a specific truss-plate tooth when the joint is subjected to static tension parallel to the grain in air-dry spruce lumber.

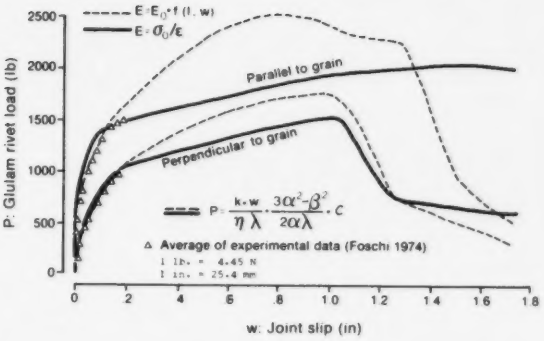
E=E0*f (l, w)
E=σ0/ε
Parallel to grain
Perpendicular to grain
P=k*w/η λ · (3α²-β²)/2αλ · c
Δ Average of experimental data (Foschi 1974)
P: Glulam rivet load (lb)
w: Joint slip (in)

Figure 3. Measured and predicted behavior of a specific glulam rivet joint subjected to static tension in air-dry Douglas-fir lumber.

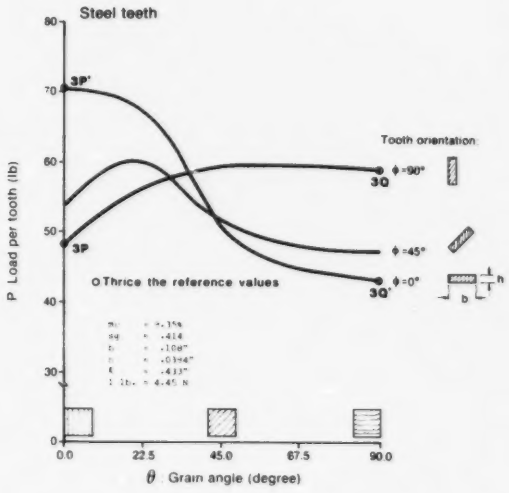

Figure 4. Predicted effect of grain angle and tooth orientation on maximum truss-plate joint strength in air-dry spruce lumber.

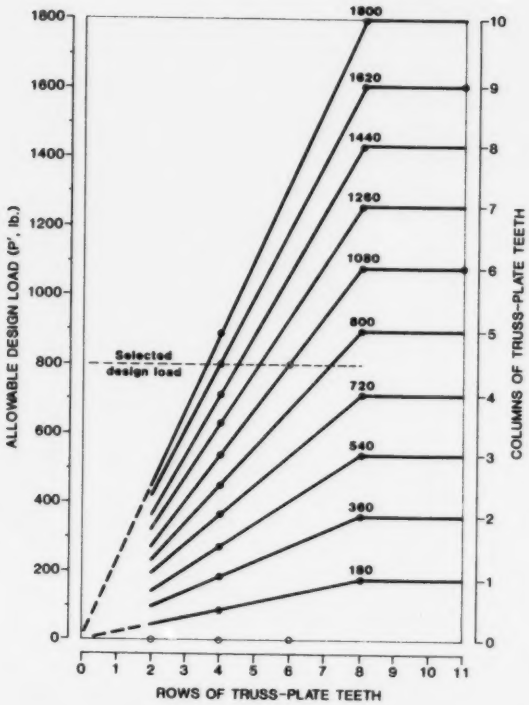

Figure 5. Allowable design loads for a specific truss-plate joint type in tension.

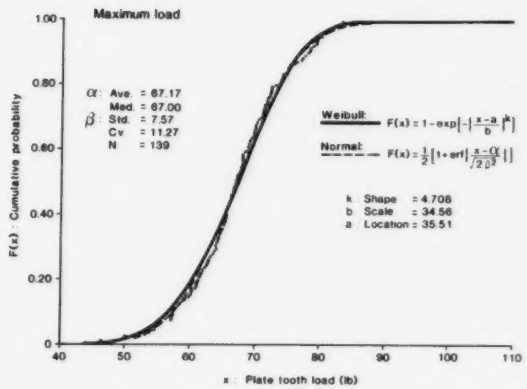

Figure 6. Cumulative distribution of maximum tooth load in 80-tooth truss-plate joints in spruce lumber.

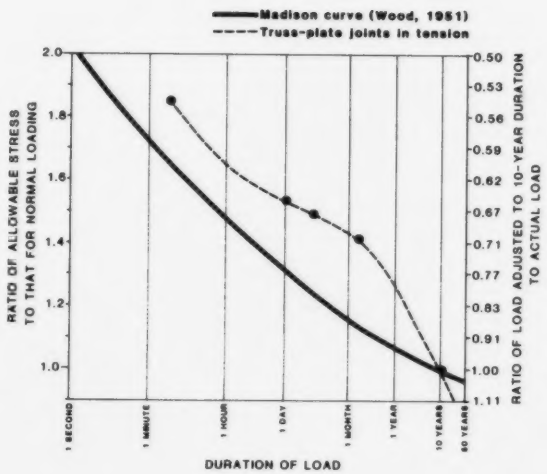

Figure 7. Relation of strength to load duration.

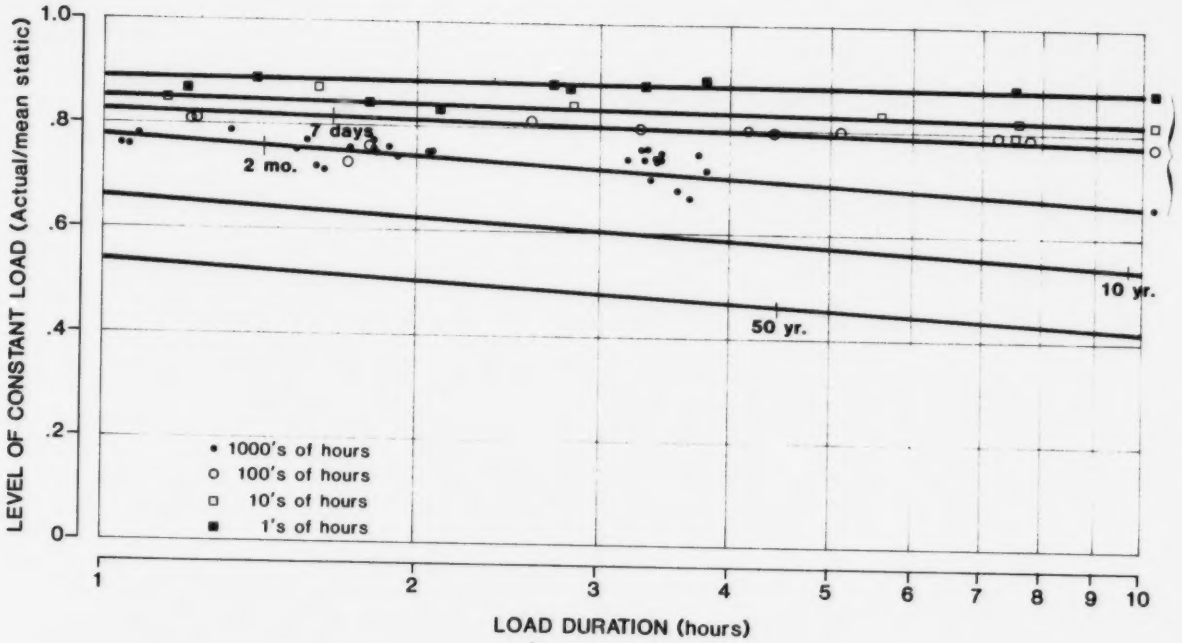

Figure 8. Load duration as a function of constant loads based on experimental data collected in the present study.

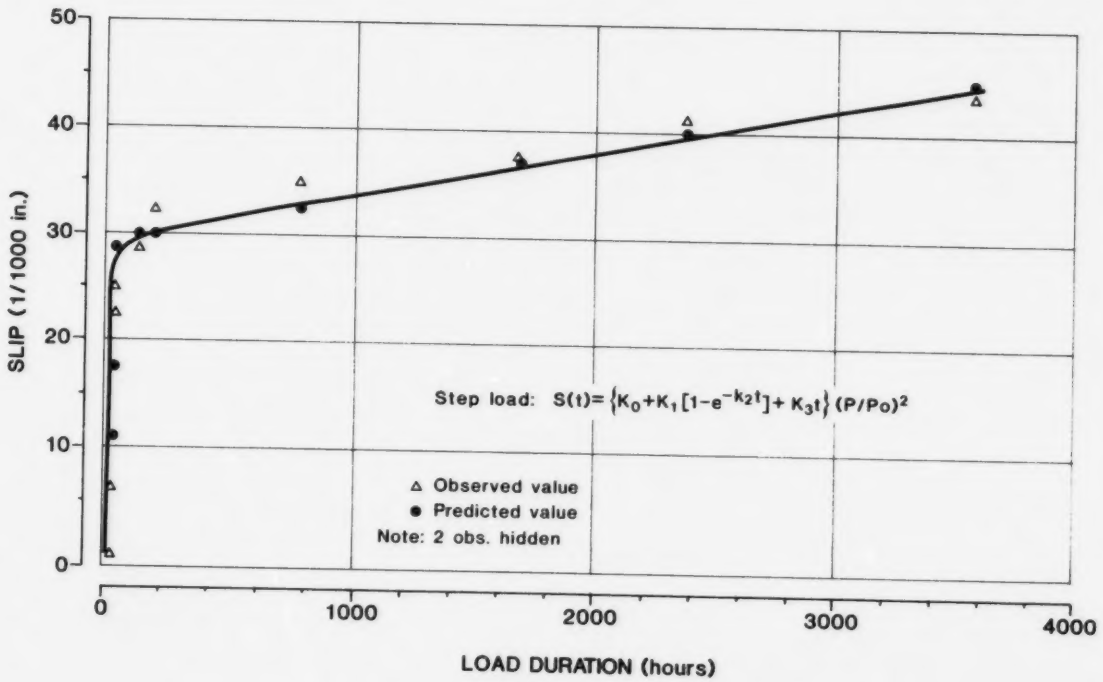

Figure 9. Creep of Joint No.379.

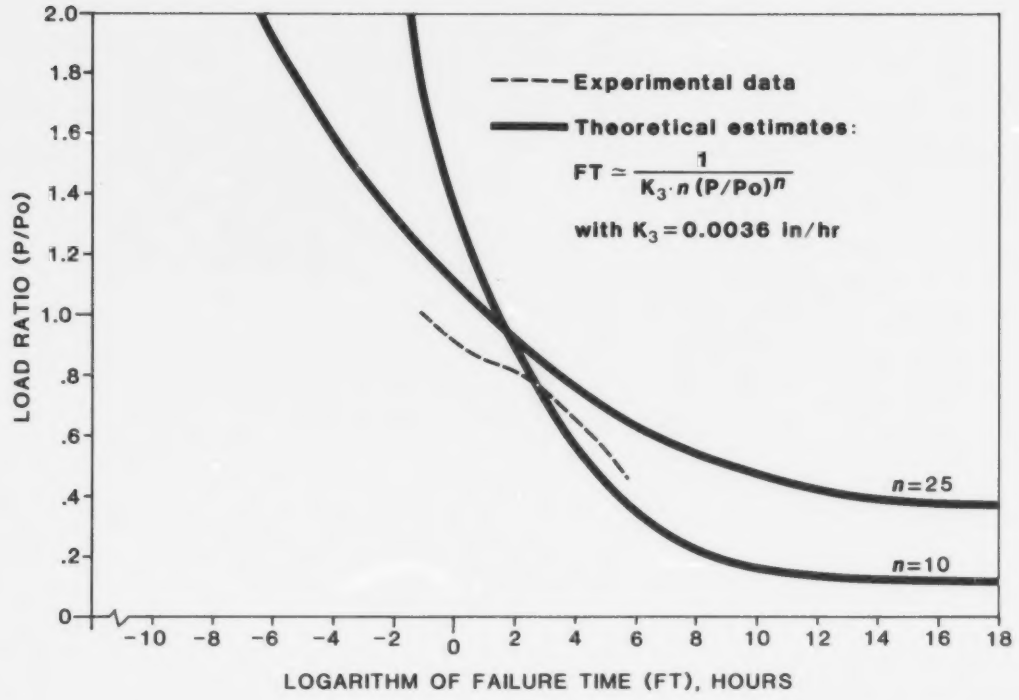

Figure 10. Theoretical and observed relations between load ratio and failure time for truss-plate joints.

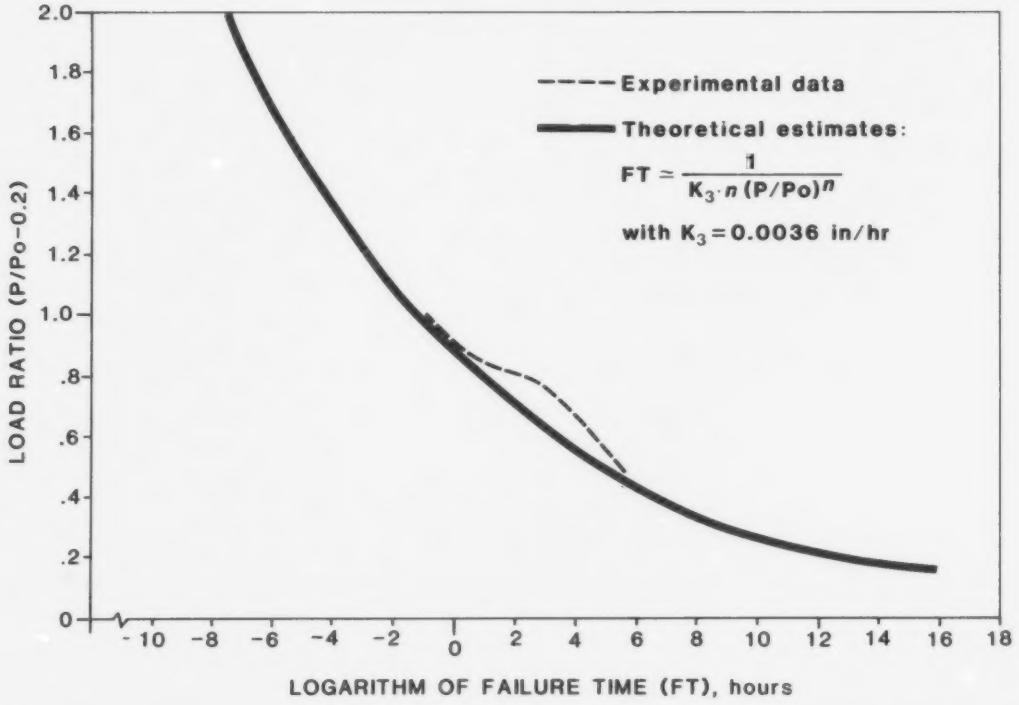

Figure 11. Theoretical and observed relations between modified load ratio and failure time for truss-plate joints.

CREEP AND CREEP-RUPTURE IN RECONSTITUTED PANEL PRODUCTS

A cooperative study by:
Forintek Canada Corp. and
Forest Products Laboratory, USDA

Theodore Laufenberg
Research General Engineer, Forest Products Laboratory, USDA, Madison, WI

ABSTRACT

Commercially produced plywood, oriented strandboard, and waferboard of varying constructions are being tested to identify the variables most influential in their flexural creep and creep-rupture performance. The tests will be completed in late 1987. Environmental conditions will be varied for creep tests but held constant for creep-rupture tests. The test program is intended to provide a broad data base on the rheological properties and duration-of-load behavior of panel products for preliminary design usage.

OBJECTIVES

The objectives for this pilot study of flexural creep and creep-rupture in reconstituted panel products are

(a) To characterize the rheological behavior of common commercial reconstituted panel products at several load levels and loading rates

(b) To apply or modify analytical methods for characterizing the rheological behavior of panels

(c) To provide guidance for future experiments in such areas as load levels and environmental conditions

(d) To provide guidance for future research on the effect of manufacturing process parameters on creep performance.

BACKGROUND

Reconstituted panel products produced from wafers and strands are rapidly becoming accepted as replacements for traditional materials such as plywood and solid wood boards in a variety of structural applications. Manufacturers can produce products to meet the requirements of each end use by varying the characteristics of the wood raw material (furnish), the volume and type of adhesive, and other production parameters.

Strength and stiffness characteristics are among the important properties considered in assessing the adequacy of wood products for any structural end use application. Methods for assessing the "static" strength and stiffness of panel products are provided in standards such as ASTM D 1037, Standard Methods for Evaluating the Properties of Wood-Base Fiber and Particle Panel Materials; ASTM E 661, Standard Test Methods for Performance of Wood and Wood Based Floor and Roof Sheathing under Concentrated Static and Impact Loads; and CSA Standard CAN3-0188.0, Standard Test Methods for Mat-Formed Wood Particleboards and Waferboard. Product requirements for waferboard panels are given in standards such as CSA CAN3-0188. The American Plywood Association has established "Performance Standards and Policies for APA Structural-Use Panels."

Reconstituted panel products are relatively new to structural uses. Thus, a long-time performance history based on common building practices has not been established for these products. Moreover, their rheological properties are inadequately characterized within the research community. This lack of information not only hinders development of empirical design guidelines such as would be used in a limit-states design code, but also precludes development of any reliability-based design codes.

The work outlined in this paper will provide a baseline of information needed to characterize the reliability, or safety, of wood-frame structures sheathed in reconstituted wood panels. These measures of reliability will come directly from application of models for viscoelastic behavior and damage accumulation developed using the experimental data obtained during this study.

SCOPE

Three reconstituted panel product types are included in this study: Plywood (PLY), oriented strandboard (OSB), and waferboard (WFB). All materials satisfy the performance requirements for 20-inch-on-center, single-layer flooring (ASTM E 771). Primary emphasis is on evaluation of flexural creep and creep-rupture performance using a large test specimen of dimensions, 5/8 x 11.8 x 39.4 inches (16 x 300 x 1,000 mm). Two steady-state conditions and a cyclic environment are being used for the creep tests, whereas the creep-rupture tests are limited to a single steady-state condition.

Experimental work was initiated in early 1986, with completion expected late in 1987. Forintek Canada Corp. is to evaluate the waferboard product; the Forest Products Laboratory will examine oriented strandboard and plywood products. Additional research being conducted independently at both facilities greatly expands the scope of rheological studies on reconstituted panel products.

TEST MATERIALS AND PROCEDURES

Three manufacturers' panels were chosen within each product type (PLY, OSB, and WFB). Manufacturers were selected based on a small-scale preliminary screening of panels (Laufenberg, manuscript in preparation) for their creep performance and on panel property data bases maintained by the American Plywood Association and the Waferboard Association. The three manufacturers of each product type were chosen as having panels with high-, median-, and low-creep performance, respectively.

SPECIMEN SIZE

Two sizes of specimens are being cut for the experiments. Large specimens for the ramp tests and constant load tests were 300 mm (11.8 in.) wide, 1,000 mm (39.4 in.) long, and had a test span of 900 mm (35.4 in.). The

300-mm width is compatible with the RILEM/CIB-3TT Committee recommendations for testing of plywood and particleboard (Lee, 1980). A specimen thickness of 5/8 inch is assumed for the subsequent discussion.

Specimens for the ASTM D 1037 flexure test are also being cut from the panels.

TEST METHODS

Ramp Tests

Ramp tests are being carried out at three target median times to failure: 10 hours, 20 minutes, and one minute (the control test). These are done on a testing machine capable of carrying such experiments under load control, thus ensuring that the loading function is a ramp of constant rate until the specimen's failure. The specimens are positioned in the testing machine over a span of 900 mm and subjected to loads at the 1/3 points. The measurements taken in these tests include the failure load, the time to failure, and a complete plot of the load versus deformation relationship.

Constant-load Tests

Constant-load tests are being carried out in specially built frames (Figure 2). Specimen load positioning and measurements taken are identical to those of the ramp tests. Three constant-load levels have been chosen to correspond to median times to failure of 2,000 hours, 400 hours, and 10 hours. Loading is achieved by means of dead weights, acting on a pulley mechanism, designed to amplify the force actually applied by the weights. These weights are applied to the specimen at a controlled rate equal to that used for the control ramp test. This rate is dictated by a loading apparatus equipped with a load cell to record the actual failing load for those specimens which fail during the application of the weights. Similarly, the loading apparatus is equipped to record the time to failure of those specimens failing during the application of the weights. Measurements made during the long-term tests are time to failure and bending creep deflections of the specimens.

The deflections of the ramp and constant-load specimens are measured by linear potentiometers attached to the test frames and to the specimens at midspan. These measuring devices are scanned automatically at short intervals during the first part of the test and then at longer intervals until the completion of the experiment. A data acquisition system stores the data in a magnetic device from which it can be retrieved for analysis.

Specimens surviving constant-load tests are up-loaded to failure by the ramp test procedure. These residual strength data will be used in the interpretation and characterization of creep-rupture for the test materials.

Static bending and thickness swelling according to ASTM D 1037 and density and moisture content tests are being performed on material cut from each panel (Figure 1).

CREEP METHODOLOGY

SAMPLING

The creep experiment includes two constant stress levels (Table 1) and is being carried out under three environmental conditions (Table 2). For each case, a sample of specimens is matched with respect to the distribution of control ramp test strength. Matching is checked by nondestructively evaluating all specimens for stiffness using ultrasonics and dead loading (Gerhards and Floeter, 1982).

SAMPLE SIZE

Because creep is related mainly to serviceability performance requirements, the sample size was chosen recognizing that mean deformation behavior, rather than lower fractile values, is required for design.

Nine panels of each product type (three for each manufacturer) were cut into eight bending test specimens each (Figure 1): one specimen from each panel is used at each environment and load level. The two remaining specimens per panel are used to provide control strength data.

LOAD LEVELS

Load levels were chosen to allow determination of creep characteristics under conditions comparable to those encountered in service.

Load level factors of 15 and 30 percent of expected failure load (ψ = 0.15 and ψ = 0.30) were selected. Load levels in this range are not expected to cause any failure on loading or during the period of the creep test. For the matched distribution approach, all specimens in the group should be subjected to the same stress chosen to produce the specified deflection, based on mean flexural stiffness, for the intended end use application. However, it is unlikely that initial deflection limits larger than 1/45 of span will be used in design.

DURATION OF THE TESTS

The creep tests are to be carried out for as long as possible, in order to facilitate the analysis and the choice of a mathematical model to represent the phenomenon. These initial studies are planned to last as long as the creep-rupture study (15 months).

DATA ANALYSIS

The experiment will provide data for the determination of the creep function for the material, as it relates to the environmental conditions and the level of applied stress. A mathematical form representing such creep functions will be developed, investigating both empirical relationships and functions based on the assumptions of underlying models of linear viscoelasticity (combinations of springs and dashpots). The coefficients

present in such mathematical representations will be random variables, and their distribution will be assessed on the basis of the variability measured in creep, across specimens, at a given time. Tests at load levels factors $\psi = 0.15$ and $\psi = 0.30$ will permit assessment of validity of the linear viscoelasticity assumption.

CREEP-RUPTURE METHODOLOGY

SAMPLING

Both ramp tests and constant-load tests are included in the experiments for creep-rupture. Tests are conducted at 68°F (20°C) at relative humidity of 50 percent. The one-minute ramp tests are used as the control sample, and the load levels applied during the constant-load tests are chosen as fractions of the median strength established with the control. The group matching is performed in a manner identical to that described for creep.

SAMPLE SIZE

Seventy-five panels of each product type (25 from each manufacturer) were cut into six specimens (Figure 1) of which each bending test receives one specimen. For each constant-load test all specimens have a load level equal to a fraction of the median short-term strength measured in the control group.

DURATION AND LOAD LEVEL

The target duration of each test has been chosen to be sufficiently long so that the median time to failure is achieved with a sufficient margin of assurance. This allows more failures to take place providing a broader data base to describe the distribution of time to failure.

Table 3 shows the estimated duration for each test, such that 80 percent of the specimens tested would achieve failure. The three estimated load level factors for each material type are also shown in Table 3. The corresponding test durations will then be seven months, 2.5 months, and 15 days.

DATA ANALYSIS

For each load level, the times to failure (failure may be rupture or excessive deflection) will be ranked to obtain their cumulative distribution functions. Using these, the parameters of models for damage accumulation will be calibrated to models presented by Foschi and Barrett (1982) and Gerhards and Link (1983). Any other models of interest such as Caulfield (1983) will also be evaluated. The models thus obtained could be used to predict the material's response under loading conditions different from those used in the tests. For example, they could be used to estimate the behavior under varying, random loads, as encountered in service, allowing the estimation of the reliability (against rupture) and reliability (against excessive deflection) of waferboard, oriented strandboard, and plywood for flexural end use conditions.

SUMMARY

Ramp and constant-load load flexural tests are being conducted by Forintek and the Forest Products Laboratory to identify what variables are most influential in composite panel products' creep and creep-rupture performance. Plywood, oriented strandboard, and waferboard materials of varying constructions are being tested. Experimental tests will be completed in late 1987 after six months of screening tests and 15 months of larger specimen testing. Environmental conditions will be constant for creep-rupture tests, whereas two conditioning levels and a cyclic environment will be explored for creep behavior. A tabular summary of this jointly sponsored composite panel test program is shown in Tables 4 and 5. The test program will provide a broad data base of information on the duration of load properties of panel products for preliminary design usage and to determine what follow-on test programs may be required.

REFERENCES

American Plywood Assocation. 1980. Performance standards and policies for APA structural-use panels. American Plywood Association, Tacoma, WA.

American Society for Testing and Materials. 1978. Standard test methods of evaluating the properties of wood-base fiber and particle panel materials, ASTM Desig. D 1037; Standard test methods for performance of wood and wood-based floor and roof sheathing under concentrated static and impact loads, ASTM Desig. E 661. American Society for Testing and Materials, Philadelphia, PA.

Canadian Standards Association. 1978. Standard test methods for mat-formed wood particleboards and waferboard. CAN-30188. O-M78. Canadian Standards Association, Rexdale, ON, Canada.

Caulfield, D. F. 1983. A chemical kinetics approach to the duration of load problem in wood. Presented at IUFRO Div. 5 Conf., Madison, WI.

Foschi, R. O. and J. D. Barrett. 1982. Duration of load effects in western hemlock lumber. J. Struct. Div. ASCE 108(ST7): 1494-1510.

Gerhards, C. C. and L. H. Floeter. 1982. Nondestructive evaluation of mechanical properties of a structural flakeboard made from forest residues. USDA Forest Serv. Res. Pap. FPL 414. Forest Prod. Lab., Madison, WI.

Gerhards, C. C. and C. L. Link. 1983. Use of a cumulative damage model to predict load duration characteristics of lumber. Presented at IUFRO Div. 5 Conf., Madison, WI.

Laufenberg, T. L. Industry-wide screening of composite panel creep performance. Manuscript in preparation. Madison, WI: U.S. Department of Agriculture, Forest Service, Forest Products Laboratory

Lee, I.D.G. 1980. Tentative proposals for testing particleboard for use in load-bearing structures. Report to Working Commission W18-Timber Structures of the International Council for Building Research Studies and Documentation. June 1980. Helsinki, Finland.

Table 1

Creep Experiment

Load level factor ↓	Sample size	Bending stress[1]	Load[1]	Mean initial deflection[1]
		lb/in.^{2}	lb	in.
0.15	9	480.0	62.5	0.410 or L/91
.30	9	960.0	125.0	0.820 or L/45

[1]Note: Median short-term strength = 3,200 lb/in.^{2}.
Mean modulus of elasticity = 500,000 lb/in.^{2}.

Table 2

Environmental Conditions for Creep Testing

Test	Temperature	Relative humidity	Cycle
	°C	Pct	
Dry test	20	50	Constant
Wet test	20	85	Constant
Cyclic test	20	85	48 hours
	20	50	48 hours

Table 3

Creep-rupture: Recommended Sample Sizes and Test Durations

Estimated load level factor ↓[1]					
Plywood	Oriented strand-board	Waferboard	Sample size	Median time to failure	Duration of test (failure of 80 percent of sample)
				----------Hr----------	
0.72	0.65	0.55	75	2,000 (2.75 months)	5,000 (7 months)
.78	.73	.66	75	400 (.5 months)	1,800 (2.5 months)
.83	.80	.75	75	10 (.4 day)	300 (15 days)

[1]Load levels are based on limited data used in a damage accumulation model (Foschi and Barrett 1982).

Table 4

Matrix of Creep and Creep-rupture Testing

Bending test	Waferboard specimens			Oriented strand-board specimens			Plywood specimens			Loading frames	Median time to failure
	(number)										(min)
	CREEP										
Constant load	Dry	Wet	Cyclic	Dry	Wet	Cyclic	Dry	Wet	Cyclic		
[1]ψ = 0.15	9	9	9	9	9	9	9	9	9	27	NA
ψ = 0.30	9	9	9	9	9	9	9	9	9	27	NA
	CREEP RUPTURE										
Ramp											
10-hour	75			75			75			NA[2]	600
20-minute	75			75			75			NA	20
1-minute	75			75			75			NA	1.
ASTM D 1037	150			150			150			NA	1.
											(hr)
Constant load											
7-month	75			75			75			114	2,000
2.5-months	75			75			75			45	400
15-day	75			75			75			9	10
Totals											
Specimens	654			654			654				
Panels	84			84			84				
Frames										222	

[1]ψ = load level factor.
[2]Not applicable.

Table 5

Matrix of Load Level Factors ψ

Bending test	Waferboard	Oriented strand-board	Plywood
Constant load			
7-month	0.55	0.65	0.72
2.5-month	.66	.73	.78
15-day	.75	.80	.83
Creep			
Low	.15	.15	.15
High	.30	.30	.30

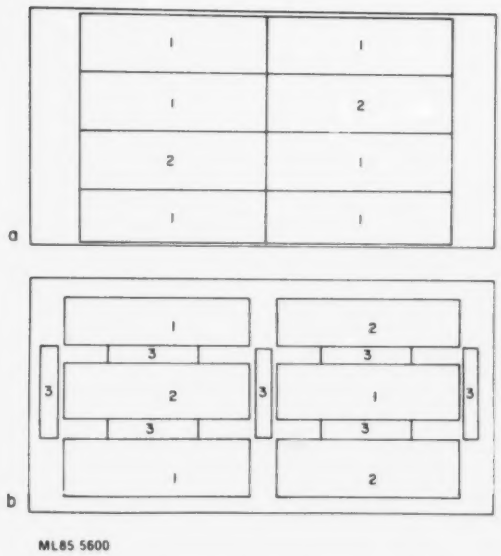

Figure 1. Cutting plan for 4- x 8 foot panels to provide (a) creep and (b) creep-rupture specimens: 1--constant-load tests, 2--ramp load tests, 3--ASTM D 1037 tests. (ML85 5600)

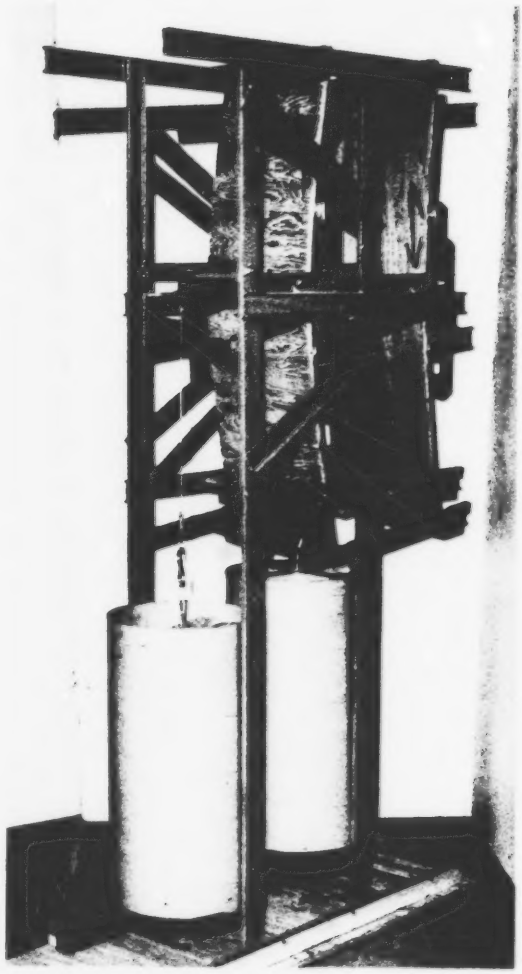

Figure 2. Panel flexure test machine for creep and creep-rupture testing. (Overall height = 75 in. Floor dimensions: 15 x 38 in.) Two specimens are mounted in each test machine with this design. (M85 0395)

WOOD AS A CRACKED VISCOELASTIC MATERIAL

PART 1: THEORY AND APPLICATIONS

Lauge Fuglsang Nielsen
Building Materials Laboratory
Technical University of Denmark
Lyngby, Denmark

INTRODUCTION

Wood is a material with significant viscoelastic mechancial properties. Thus, wood under a constant load exhibits time dependent deformation in a relatively short time (months) which is of the same order of magnitude as the initial elastic deformation, see Figure 1.

Wood is also a material which contains cracks and other defects (e.g., knots) which may cause a considerable strength reduction. This reduction is time dependent just like the deformation. One speaks about short-time strength which is the load the wood can maintain for about five minutes--and long-time strength which is the load which can be maintained for 10 years, for example, before failure appears. A 10-year strength which is about 60 percent of the short-time strength is typical for wood, see Figure 2.

To consider wood as a viscoelastic material is an old idea. For a long time deformation of wood has been calculated on the basis of viscoelastic theory. There is also nothing new in considering wood as a cracked material on which elastic fracture mechanics can be applied to determine strength.

However, the previous models cannot consistently explain a number of phenomena which are very important features characterizing the mechanical behavior of wood. For example, lifetime and lifetime dependency of wood quality, short-time strength as influenced by time under load, tertiary creep, strength-stiffness relations (MOE-MOR graphs), etc. may be mentioned.

An explanation of these significant materials properties was first made possible when an integrated materials concept for the behavior of wood was established by the present author (Nielsen, 1978, 1979, 1982a, 1983): Wood is a cracked viscoelastic material the mechanical behavior of which can only be described in sufficient detail by coupling the theories of viscoelasticity and fracture mechanics. One cannot (as it was done previously) consider wood either as a cracked elastic material or as a homogeneous viscoelastic material without losing the possibility of a unified description of wood behavior.

The scope of the present paper is to demonstrate the variety of features of wood behavior which can be explained and described on the basis of the new concept. It is hereby suggested how we may consider the influence of climatic conditions.

The subject is divided into two parts: A part (I) which is mainly theoretical with some applications, and a part (II) which confronts the theoretical predictions with experimental evidence.

The present part is the theoretical one. The expressions needed here are taken from Nielsen (1982a and 1982b) mainly and presented in the introductory sections together with the basic viscoelastic and fracture mechanics models. Readers who are mostly interested in application of the theory are referred to the "Application" section, especially the figures of that section.

VISCOELASTICITY

Consider two bodies which are identical at any time in shape and boundary conditions. One body is linear elastic. The other one has the same elastic properties. In addition, however, it performs linear-viscoelastically. This means that the following linear expression relates deformations, δ, of the two bodies

$$\delta_{visc}(t) = \int_{-\infty}^{t} C(t-\eta) \frac{d\delta_{el}(\eta)}{d\eta} d\eta \qquad (1)$$

Time is denoted by t. The viscoelastic properties in question are defined by the normalized creep function, C(t), which is proportional by Young's modulus, E, to the real creep function, c(t). That is,

$$C(t) = Ec(t) = 1 + \phi(t) \qquad (2)$$

where $\phi(t)$ is the so-called creep factor.

The creep function is the viscoelastic counterpart to the inverse Young's modulus of an elastic material. That is, strain response due to a stress, $\sigma = 1$, applied at $t = 0$. The creep factor gives the fraction of strain which is time dependent.

WOOD

There is experimental evidence (Krebs, 1984; Nielsen, 1972 and 1981) that wood behaves approximately like a linear viscoelastic material exhibiting creep according to the following normalized creep function

$$C(t) = 1 + (t/\tau)^b \qquad (3)$$

where b is a constant, and τ is the so-called doubling time.

Both creep parameters appearing in Equation 3 are easily determined from experimental creep data, see Krebs (1984) and Nielsen (1984) for examples.

According to Nielsen (1984) the following orders of magnitude apply for wood at moisture equilibrium, $u = 0.15$ (by weight), and $T = 20°C$: $(b_\perp, b_\parallel) = (.33\text{-}.25, .25\text{-}.20)$ and $(\tau_\perp, \tau_\parallel) = (10\text{-}100, 10000\text{-}100000)$ days. The symbols $\perp$ and $\parallel$ mean perpendicular and parallel to grain, respectively.

Apparently b is not very dependent on climatic variations. However, the doubling time, τ, is extremely sensitive such that its value decreases at increasing humidity and increasing temperature. The following factor on τ has been suggested (Nielsen, 1984) to estimate the influence of equilibrium climatic conditions different from $(u,T) = (0.15, 20°C)$

$$a = 10^{10(0.15-u)+(20-T)/15}; (u \leq 0.30 \text{ and wet}) \qquad (4)$$

It is noticed that Equation 3 predicts no threshold on wood creep. The existence of a limit on wood creep has often been the topic of discussions. However, it has never been observed. Equation 3 is based on experiments some of which have run for more than 10 years. No threshold value was indicated in this period of time, although the rate of creep diminished appreciably at long times. Nielsen (1972 and 1981) investigated the creep behavior of timber

used in very old structures and found that Equation 3 still seems to predict creep reasonably well even after 100 years with (b,τ) = (0.25,100 days) at an average. Naturally, however (because of the long time span with varying moisture and temperature histories), the scatter in Nielsen's data was so large that they did not disprove the existence of a threshold some time after more than 10 years. Generally, the practical importance of such a threshold is limited. In the subsequent lifetime analysis of wood, however, it is of some interest to know how a threshold will potentially influence long-time strength. For this purpose a generalized version of Equation 3 is given below

$$C(t) = 1 + \alpha\left[1-\exp\left\{-\frac{1}{\alpha}\left(\frac{t}{\tau}\right)^{D}\right\}\right] \qquad (5)$$

This relation expresses a normalized creep function with a threshold of $C(\infty) = 1 + \alpha$, where α is a constant, the value of which is probably no less than three. Equation 3 is approached when $\alpha \longrightarrow \infty$ and/or when $t \longrightarrow 0$.

CRACK MECHANICS

Single Crack Model

The strength of a cracked material may be described by the so-called Dugdale model (Dugdale, 1960) shown in Figure 3. It is a tunnel crack centrally placed in a large elastic body which is loaded at infinity by a uniformly distributed stress, σ, perpendicular to the crack plane.

The crack is prevented from spreading out by a uniformly distributed stress of coherence, σ_L, at the front zones of the crack. The stress of coherence represents the theoretical strength of the material. That is, σ_L, relates to surface forces acting across an empty crack front when brittle materials are considered; and yield stress when more ductile materials are considered where material is pulled out into the front zone.

The Dugdale model applies strictly only to elastic materials. Experiments (Dugdale, 1960), however, have shown that the model is a good approximation also in the case of ductile materials as long as $\sigma/\sigma_L < 0.9$. This limitation is of no practical importance in the present study.

The strength, σ_{cr}, of the Dugdale model having a half crack length of L_o, is given by

$$\sigma_{cr} = \frac{2\sigma_L}{\pi}\arccos\left\{\exp\left(-\frac{\pi E \Gamma_{cr}}{L_o \sigma_L^2}\right)\right\}$$

$$\cong \sqrt{\frac{E\Gamma_{cr}}{\pi L_o}}\,; \qquad \text{(plane stress)} \qquad (6)$$

where the following failure condition has been introduced: Crack propagation appears when the crack front opening, δ, approaches a critical value, δ_{cr}. This failure criterion is identical to saying that the so-called strain energy release rate, $\Gamma = \sigma_L\delta$, approaches a critical value, $\Gamma_{cr} = \delta_L\delta_{cr}$. The approximation in Equation 6 which applies when $\sigma_{cr}/\sigma_L < 1/3$ is recognized to be the well-known Griffith load capacity (Griffith, 1920).

The mathematics of the Dugdale model implies the following relation between two crack states, (σ,L,δ) and the reference fracture state $(\sigma_{cr},L_o,\delta_{cr})$

$$A = \frac{\log_e \cos\left(\frac{\pi}{2}\frac{\sigma_{cr}}{\sigma_L}\right)}{\log_e \cos\left(\frac{\pi}{2}\frac{\sigma}{\sigma_o}\right)} = \frac{L}{L_o}\frac{\delta_{cr}}{\delta}$$

$$\cong \left(\frac{\sigma_{cr}}{\sigma}\right)^2 \qquad (7)$$

where the approximation applies at $\sigma_{cr}/\sigma_L < 1/3$.

The parameter, A, formed by the first term in Equation 7 was introduced into lifetime analysis by the present author in 1982 (Nielsen, 1982a). It plays an important role in simplifying and normalizing the results obtained. Among other things, it eliminates the fracture mechanics parameters, δ_{cr} or Γ_{cr}, by introducing the actual strength, σ_{cr}, and at the same time it takes away the assumptions of a special stress-strain situation (like plane stress for example) by eliminating the Young's modulus.

It is convenient in this paper to rewrite Equation 7 using another terminology and approximate $\cos x = 1 - (2x/\pi)^2$. That is

$$A = \frac{\log_e(1 - FL^2)}{\log_e(1 - FL^2\cdot SL^2)} = \kappa\frac{\delta_{cr}}{\delta} \cong SL^{-2} \qquad (8)$$

where

$$FL = \sigma_{cr}/\sigma_L \qquad \text{(strength level)} \qquad (9)$$

$$SL = \sigma/\sigma_{cr} \qquad \text{(load level)} \qquad (10)$$

$$\kappa = L/L_o \qquad \text{(defect ratio)} \qquad (11)$$

$$\kappa_{cr} = L_{cr}/L_o \qquad \text{(critical defect ratio)} \qquad (12)$$

The latter symbol denotes the relative crack length $L/L_o = L_{cr}/L_o$, at which the material will fail when subjected to load level, $SL = \sigma/\sigma_{cr}$. That is, according to Equation 8 letting $\delta \longrightarrow \delta_{cr}$

$$\kappa_{cr} = A \cong SL^{-2} \qquad (13)$$

where the approximation applies when $FL < 1/3$.

Multi-Crack Model

The single-crack model presented in the preceding section applies to materials having cracks with inter-crack distances large in comparison with crack lengths. When cracks are more densely packed in a material, serious interaction effects will result which cannot be predicted by a single-crack model.

It is, however, possible to generalize the single-crack model in such a way that interaction effects are modelled approximately, in a relatively simple manner. Such a generalization has been developed by Nielson (1982b) where the underlying simplified multi-crack model is a system of parallel cracks placed in a rhombic lattice with the distance between crack planes at $\vartheta/4$ (> ca. 1) of the in-plane crack center distance. The crack intensity, ρ, is defined as the number of cracks per unit area.

The result of the analysis (Nielsen, 1982b) is that we may consider multi-crack systems using the single-crack relations only by multiplying σ_{cr} and σ with the square root of the following interaction factors, f_o and f, respectively

$$f_o = \frac{1-\sigma_{cr}/\sigma_L}{1-\sigma_{cr}/\sigma_L - \theta\rho L_o^2} = \frac{1-FL}{1-FL-\theta\rho L_o^2} \leq \frac{1}{FL} \qquad (14)$$

$$f = \frac{1-\sigma/\sigma_L}{1-\sigma/\sigma_L - \theta\rho L^2}$$

$$= \left\{1 - \frac{1-FL}{1-FL\cdot SL}\left(1-\frac{1}{f_o}\right)\kappa^2\right\}^{-1} \leq \frac{1}{FL\cdot SL} \qquad (15)$$

When the limits indicated are violated, we have f_o and $F = \infty$, respectively.

The generalization of the single-crack relations may also be formulated in terms of strength and load levels

$$FL \Rightarrow FL\sqrt{f_o} \qquad (16)$$

$$SL \Rightarrow SL\sqrt{f/f_o} \qquad (17)$$

As an example of generalization, the critical defect ratio, $\kappa = \kappa_{cr}$, for a multi-cracked material is determined implicity by Equations 8 and 14-17. We get

$$\kappa_{cr} = \text{Min}\left\{\frac{\log_e(1 - f_o FL^2)}{\log_e(1-f\,FL^2\cdot SL^2)}, \quad (1 - FL\cdot SL)\sqrt{\frac{f_o}{1-FL)(f_o-1)}}\right\} \qquad (18)$$

where f is introduced with $\kappa = \kappa_{cr}$.

For <u>small loads</u> we get

$$f_o = \frac{1}{1-\theta\rho L_o^2} \quad ; \quad (\theta\rho L_o^2 \leq 1) \qquad (19)$$

$$f = \frac{f_o}{f_o-(f_o-1)\kappa^2} \quad : \kappa \leq \sqrt{\frac{f_o}{f_o-1}} \qquad (20)$$

which implies the following analytical solution of Equation 18

$$\kappa_{cr} = \frac{2f_o}{SL^2}\left(1+\sqrt{1+4\,\frac{f_o(f_o-1)}{SL^4}}\right)^{-1} \qquad (21)$$

The corresponding $f = f_{cr}$ is given by

$$f_{cr} = \frac{1}{2}\left(1+\sqrt{1+4\,\frac{f_o(f_o-1)}{SL^4}}\right) \qquad (22)$$

<u>Stiffness and Stiffness/Strength Relation</u>

Still considering the multi-crack model defined in the preceding section, the following relation was developed by Nielson (1982b) for Young's modulus, E*, of a cracked material

$$E^*/E \cong \frac{1}{1+\frac{5}{\theta}\log_e(f)} = D\{f\}^{-1} = D(\sigma,\kappa)^{-1} \qquad (23)$$

where E as before denotes Young's modulus of the uncracked material. The interaction factor, f, is given by Equation 15. Thus, E* is generally load dependent.

At a fracture state (σ_{cr}, L_o) we have $f = f_o = (\sigma_{cr,o}/\sigma_{cr})^2$, where $\sigma_{cr,o}$ is the strength at very low crack intensities (Griffith load capacity). Introducing this interaction factor into Equation 23, we get the following expression relating strength and stiffness (at $J = \sigma_{cr}$) for cracked materials

$$\sigma_{cr}/\sigma_{cr,o} = \exp\left\{\frac{\theta}{10}\left(1-\frac{E}{E^*}\right)\right\} \qquad (24)$$

Both Equations 23 and 24 apply at any strength level, FL.

VISCOELASTIC FRACTURE RELATIONS

The viscoelastic and single-crack fracture models presented above were combined earlier (Nielsen, 1978, 1979 and 1982a) to form a material's lifetime theory. The basic relations developed (Nielson, 1982a) are given below in generalized versions.* That is, they consider also multi-cracked systems as suggested by Nielsen (1982b) and the preceding crack mechanics chapter.

The relations are presented in two sections: 1) general relations applying to any strength level, $FL < 1$, and 2) relations applying at low strength levels, that is when $FL < 1/(3\sqrt{f})$. It should be mentioned that the crack velocity expressions presented are valid only when non-negative velocities are predicted. Thus, the effects of fast cyclic loads (fatigue) cannot be considered without further generalizations (Nielsen, 1985).

The functions appearing in the relations presented below are the normalized creep function, C(t), of the material and the inverse of this function,

$$F = C^{-1} \quad ; \quad (F(X) = \tau(X-1)^{1/b}) \qquad (25)$$

the "weighted" creep function

$$\bar{C}(t) = 1 + \int_o^t \left(1-\frac{\eta}{t}\right)^2 \frac{dC}{d\eta}\,d\eta \quad ;$$

$$(\bar{C}(t) = C(t/q)) \qquad (26)$$

and the inverse of this function

$$\bar{F} = \bar{C}^{-1} \quad ; \quad (\bar{F}(X) = qF(X)) \qquad (27)$$

The functions in parenthesis are the respective relations associated with the power type creep function given in Equation 3. The constant, q, depends on the power, b, in the following way

$$q = ((b+1)(b+2)/2))^{1/b} \qquad (28)$$

<u>Any Strength Level</u>

Time to start of crack propagation:

When the material considered is first loaded at time, $t = 0$, crack propagation will start at time, $t = t_s$, determined by

$$\int_o^{t_s} C(t_s-\eta)\,\frac{d(A_o^{-1})}{d\eta}\,d\eta = 1 \qquad (29)$$

*Readers of Nielson (1982a) will notice that the following simplifying features have been introduced: $B \Rightarrow 1$ and $\cos\theta \Rightarrow 1 - (2\theta/\pi)^2$.

where

$$A_o = \frac{\log_e (1 - f_o\, FL^2)}{\log_e (1 - f_L\, FL^2 \cdot SL^2)} \quad ;$$

$$f_L = \left\{ 1 - \frac{1-FL}{1-FL \cdot SL} \left(1 - \frac{1}{f_o}\right) \right\}^{-1} \qquad (30)$$

is the interaction modified A-parameter given by Equations 8, 16 and 17 with $L = L_o$.

Figure 4 illustrates the history of a crack during a fracture process. The crack state at $t < t_s$ is named Phase 1. Phases 2 and 3 are explained below.

Crack Velocity;

When the crack front opening has reached its critical value at $t = t_s$, the crack starts propagating. A characteristic feature is now that the front opening is constantly δ_{cr} while the crack length is increasing. This situation is illustrated in Figure 4 as Phase 2. At Phase 3 catastrophic failure occurs because the crack propagates extremely fast.

The rate of propagation is determined by

$$\frac{dt}{d\kappa} = \frac{\bar{F}\,(A/\kappa)/\kappa}{f \cdot FL^2 \cdot SL^2} \qquad (31)$$

where the interaction force, f, is given by Equation 15, and

$$A = \frac{\log_e (1 - f_o\, FL^2)}{\log_e (1 - f \cdot FL^2 \cdot SL^2)} \qquad (32)$$

The Function, $\bar{F}$, is defined by Equations 25 and 27. It appears from these expressions that $\bar{F}(L) = 0$; that is, catastrophic failure is predicted by Equation 31 when κ becomes κ_{cr} as predicted by Equation 18.

Equation 31 may be approximated by

$$\frac{dt}{dU} \cong - \frac{\bar{F}(U)/U}{(2f - 1) f\, FL^2 \cdot SL^2} \quad ; \quad (U = \frac{A}{\kappa}) \qquad (33)$$

which for constant or stepwise constant load level forms the exact limit solution when $f \to 1$ (single crack situation) - and also describes correctly crack propagation at small loads, $\sqrt{f}FL \to 0$.

The state of crack propagation (κ, t) is given by Equations 31 or 33 applying the following limits of integration

$$(L, A_o, t_s) \to (\kappa, U, t) \to (\kappa_{cr}, L, t_{cat}) \qquad (34)$$

where t_{cat} is the time when catastrophic failure occurs.

Strength Levels, $FL \leq 1/(3\sqrt{f})$

The expressions given above reduce considerably when small loads are considered. That is when $\sigma/\sigma_L = FL \cdot SL < 1/(3\sqrt{f})$.

Time to start of crack propagation:

$$\int_o^{t_s} C(t_s - \eta)\, \frac{d(SL^2)}{d\eta}\, d\eta \qquad (35)$$

Crack Velocity

$$\frac{dt}{d\kappa} = \frac{f_o/\kappa - (f_o - 1)\kappa}{f_o\, FL^2\, SL^2}\, \bar{F} \quad \frac{f_o/\kappa - (f_o - 1)\kappa}{SL^2} \qquad (36)$$

$$\frac{dt}{dU} = - \frac{\bar{F}(U)/U}{(2f-1) f\, FL^2\, SL^2} \quad ;$$

$$U = \frac{f_o/\kappa - (f_o - 1)\kappa}{SL^2} \qquad (37)$$

where the interaction factor, f, is given by Equation 20. Catastrophic failure occurs at $\kappa = \kappa_{cr}$ as given by Equation 21. At low crack intensities, Equations 36 and 37 reduce even more, that is by introductng $f = f_o = 1$.

APPLICATION

The fracture relations presented in the preceding sections will now be used to explain different features of wood behavior. That is, wood is considered to be a cracked, viscoelastic material, the viscoelastic properties of which are defined through the power law Equation 3.

Load and strength applied in the analysis are the relative quantities, load and strength levels, SL and FL, respectively, defined in Equations 9 and 10.

LIFETIME

Dead Load

A wood member is loaded at $t = 0$ to a constant load level, SL. Time to catastrophic failure, t_{cat}, is the sum of the time, t_s, it takes before crack propagation starts, and the time it then takes the crack to obtain a very high rate of propagation. These two contributions are determined by Equations 29 and 31, respectively. We get

$$t_{cat} = F(A_o) + \frac{1}{FL^2\, SL^2} \int_o^{\kappa_{cr}} \frac{\bar{F}(A/\kappa)}{f\kappa}\, d\kappa \qquad (38)$$

where the Function F, defined in Equation 25, has been used to derive t_s from Equation 29.

When power law creep is considered, Equation 38 reduces as follows

$$\frac{t_{cat}}{\tau} = (A_o - 1)^{1/b} + \frac{q}{FL^2\, SL^2} \int_o^{\kappa_{cr}} \frac{(\frac{A}{\kappa} - 1)^{1/b}}{f\kappa}\, d\kappa \qquad (39)$$

where q is given by Equation 28.

At very low crack intensities ($f \cong 1$), we may reduce Equation 39 as follows

$$\frac{t_{cat}}{\tau} = (A_o - 1)^{1/b} + \frac{q}{FL^2\, SL^2} \int_1^{A_o} \frac{(U-1)^{1/b}}{U}\, dU \qquad (40)$$

with A_o from Equation 30 with $f_o = f_L = 1$.

For certain values of b this equation can be solved analytically. With b = 1/4 we get

$$\frac{t_{cat}}{\tau} = (A_o-1)^4 + \frac{3.91}{FL^2\ SL^2}\left[\frac{1}{4}(A_o-1)^4 - \frac{1}{3}(A_o-1)^3 + \frac{1}{2}(A_o-1)^2-(A_o-1)+\log_e A_o\right] \quad (41)$$

Graphical representations of Equations 39 and 41 are shown in Figures 5, 6 and 7 for large, medium, and small size cracks, respectively. (The size indications refer here to low crack intensity strength levels at FL = 0.1, 0.2 and 0.4, respectively.)

The following conclusions can be drawn on the basis of Equation 39 and Figures 5 - 7:

1. Lifetime is decreasing at increasing strength level, FL < 0.5. This feature is most pronounced when few cracks are present (low crack intensity).
2. Lifetime increases at increasing strength level, FL > 0.5, and there will be practically no influence of crack intensity.
3. Increasing "brittleness" is predicted at increasing strength level, FL > 0, and/or increasing crack intensity. That is, the fracture process, Phase 2, illustrated in Figure 4 becomes less dominant at increasing FL.

Statement 1 is clearly demonstrated experimentally in Figure 2.

Curiosa:

The influence of eventually having a threshold on creep is illustrated in Figure 8 where Equation 5,

$$F(X) = \tau\left[\alpha \log_e\left(\frac{\alpha}{1+\alpha-X}\right)\right]^{1/b} \quad (42)$$

and $\bar{F}(X) \cong qF(X)$ have been the basis of evaluating Equation 38.

It is noticed that a threshold, SL_t, on stress levels is predicted at $SL_t = (1+\alpha)^{-1/2}$. When $SL < SL_t$, no failure will ever happen.

Ramp Load

A wood member is loaded at t = 0 to a load level, SL, which increases proportionally to time, that is

$$SL = \frac{t}{t_s} SL_s = \frac{t}{t_{cat}} SL_{cat} \quad (43)$$

where indices s and cat denote the situations of start of crack propagation and catastrophic failure, respectively.

Again lifetime, t_{cat}, is determined by the sum of the life, t_s, it takes before crack propagation starts, and the time it then takes the crack to obtain infinitely high rate of propagation. As for the dead loads, we may find these two contributions using Equation 29 and Equation 31, respectively. The analysis of lifetime at ramp load will be demonstrated by looking at low load and low crack intensity examples. That is $f \cong 1$ and FL < 1/3 such that Equations 35 and 36 replace Equations 29 and 31, respectively.

It is easily shown that Equation 35 implies that time to start of crack propagation is given by

$$t_s = \bar{F}(SL_s^{-2}) \quad (44)$$

where $\bar{F}$ is the function defined in Equation 27.

At $f \cong 1$, Equation 36 becomes

$$\frac{dt}{d\kappa} = \frac{1}{FL^2\ \kappa SL^2}\ \bar{F}\ \frac{1}{\kappa SL^2} \quad (45)$$

or for ramp load, by means of Equation 43

$$\frac{dSL}{d\kappa} = \frac{SL_s}{t_s\ FL^2}\ \frac{1}{\kappa SL^2}\ \bar{F}\ \frac{1}{\kappa SL^2} \quad (46)$$

from which the ramp load strength, SL_{cat} is determined by letting $1 \rightarrow \kappa \rightarrow \kappa_{cr} = SL_{cat}^{-2}$, while $SL_s \rightarrow SL \rightarrow SL_{cat}$.

The corresponding time to catastrophic failure is then determined by Equation 43 as

$$t_{cat} = \frac{SL_{cat}}{SL_s}\ t_s \quad (47)$$

An alternative way of determining ramp load strength and lifetime is to make use of the observation made on Equation 44 that one may treat ramp load as dead load when replacing the creep function, C(t), by the weighted creep function $\bar{C}(t)$, defined in Equation 26.

That is, use Equation 45 to determine $t_{cat} - t_s$ introducing the "constant load level, SL_{cat}, together with the inverse function

$$\bar{\bar{F}} = \bar{C}^{-1} \quad ; \quad (\bar{\bar{F}}(X) = q^2F(X)) \quad (48)$$

of the "double weighted" creep function

$$\bar{\bar{C}}(t) = 1 + \int_o^t (1-\frac{\eta}{t})^2\ \frac{d\bar{C}}{d\eta}\ d\eta\ ; \quad (\bar{\bar{C}}(t) = C\ \frac{t}{q^2}) \quad (49)$$

The expressions in parenthesis are the respective functions applying when creep is defined by the power law expression previously referred to.

Now, following the procedure described above, one obtains

$$t_{cat} - t_s = \frac{1}{FL^2\ SL_{cat}^2} \int_1^{SL_{cat}^{-2}} \frac{\bar{\bar{F}}(1/\kappa SL_{cat}^2))}{\kappa}\ d\kappa = \frac{1}{FL^2\ SL_{cat}^2} \int_1^{SL_{cat}^{-2}} \frac{\bar{\bar{F}}(u)}{u} du \quad (50)$$

or introducing the information of Equations 43 and 44

$$\frac{SL_{cat}}{SL_s} - 1\ \ \bar{F}(SL_s^{-2}) = \frac{1}{FL^2\ SL_{cat}^2} \int_1^{SL_{cat}^{-2}} \frac{\bar{F}(u)}{u}\ du \quad (51)$$

This expression gives the ramp load strength. As before, ramp load lifetime is then determined by Equation 47.

As an example consider wood exhibiting power law creep with b = 1/4. Then Equation 51 becomes

$$\frac{SL_{cat}}{SL_s} - 1 \qquad \frac{1}{SL_s^2} - 1 \quad ^4 = \frac{3.91}{FL^2\, SL_{cat}^2}$$

$$\frac{1}{4} \quad \frac{1}{SL_{cat}^2} - 1 \quad ^4 - \frac{1}{3} \quad \frac{1}{SL_{cat}^2} - 1 \quad ^3$$

$$+ \frac{1}{2} \quad \frac{1}{SL_{cat}^2} - 1 \quad ^2 - \quad \frac{1}{SL_{cat}^2} - 1$$

$$+ \log_e \quad \frac{1}{SL_{cat}^2} \qquad (52)$$

some results of which (together with Equation 47) are shown in Figure 9.

Naturally, ramp load lifetime is greater than dead load lifetime (Figure 7) because the effective, averaged "constant" load level is causing less creep. It is noticed that ramp load lifetime is influenced by strength level in the same way as dead load lifetime (Figures 5 - 7). That is, lifetime increases with decreasing strength level in the range $FL \leq 0.4$.

CREEP FUNCTIONS

Stress-strain relations for cracked viscoelastic materials are produced applying Equation 1 together with an elastic strain history given by

$$d\epsilon_{el} = \frac{1}{E^*}\, d\sigma + \sigma d \quad \frac{1}{E^*} = \frac{1}{E}\,(D\, d\sigma + \sigma\, dD) \qquad (53)$$

where the moduli, E^* and $D = D(\sigma,\kappa)$ are explained through Equations 23 and 15.

Equation 53 can also be written as

$$\frac{d\epsilon_{el}}{dt} = \frac{1}{E}\; D\; \frac{d\sigma}{dt} + \sigma\, \frac{dD}{dt} \qquad (54)$$

which can be used directly in Equation 1.

Creep functions are strain response due to a constant load, σ_o, applied at $t = 0$. That is, a creep function is produced by Equations 1 and 54 introducing $\sigma = \sigma_o H(t)$ where H(t) denotes the Heaviside's unit step function. Therefore,

$$\frac{d\epsilon_{el}}{dt} = \frac{\sigma_o}{E}\; D\; \delta(t) + \frac{dD}{dt} \qquad (55)$$

where $\delta(t) = dH/dt$ is the Dirac's delta function.

When Equation 55 is introduced into Equation 1, we get

$$\epsilon = \frac{\sigma_o}{E}\,[\bar{D}\; C(t) + \int_o^t C(t-\eta)\, \frac{dD}{d\eta}\, d\eta] \qquad (56)$$

where

$$\bar{D} = \frac{1}{\sigma_o} \int_o^{\sigma_o} D(\sigma,L)\, d\sigma$$

$$= \frac{1}{SL_o} \int_o^{SL_o} D(SL_o,L)\, dSL \qquad (57)$$

appears in Equation 1 when integrating the first term of Equation 55. That is,

$$\sigma_o \int_o^t C(t-\eta)\; D(\sigma,\kappa)\eta\delta(\eta)\, d\eta$$

$$= C(t) \int_o^{\sigma_o} D(\sigma,L)\, d\sigma \qquad (58)$$

The initial strain, $\epsilon(0)$, of $\epsilon(t)$ is given by

$$\epsilon(0) = \frac{\sigma_o}{E^{**}} \qquad E^{**} = E/\bar{D} \qquad (59)$$

where E^{**} could be named the material's "secant" Young's modulus. The influence of strength, stress level and crack interaction on E^{**} is demonstrated in Figure 10.

Introducing $\epsilon(0)$ into Equation 56, and remembering that cracks start running first at $t = t_s$, we get the following relation expressing a normalized creep function for a cracked viscoelastic material

$$C^*(t) = \frac{\epsilon}{\epsilon(0)}$$

$$= C(t) + \frac{1}{\bar{D}} \int_{t_s}^t C(t-\eta)\, \frac{dD}{d\eta}\, d\eta \qquad (60)$$

where the second term is first included when $t > t_s$.

When D is introduced according to Equations 23 and 15, we get

$$C^*(t) = C(t) + \frac{10}{\theta\bar{D}} \int_{t_s}^t C(t-\eta)$$

$$\frac{f-1}{\kappa}\, \frac{d\kappa}{dt}\Big|_{t=\eta}\, d\eta \qquad (61)$$

where f still is the interaction factor as given by Equation 15.

When wood is considered with power law creep, see Equation 3, we may approximate, according to (3)

$$\frac{1}{\kappa} \cong \frac{1}{\kappa_{cr}} + \quad 1 - \frac{1}{\kappa_{cr}} \quad \frac{t_{cat} - t}{t_{cat} - t_s} \quad ^b \qquad (62)$$

which reduces Equation 61 as follows

$$C^*(t) \cong C(t) + \frac{10b}{\theta\bar{D}} \int_{t_s}^t C(t-\eta)$$

$$\left\{(f-1)\, \frac{1 - \kappa/\kappa_{cr}}{t_{cat} - t}\right\}_{t=\eta} d\eta \qquad (63)$$

which applies directly when a lifetime analysis has been performed. That is, when we know κ_{cr}, t_{cat}, and t_s.

An example of the application of Equation 63 is shown in Figure 11. The shaded area represents tertiary creep as a result of running

cracks, that is the strain described by the integral term in Equation 63. Tertiary creep is a highly non-linear phenomenon. Note that Figure 11 compares well with the experimentally determined creep function shown in Figure 1.

Theoretically, creep of cracked materials is also a non-linear process because of the stress level dependency of the initial strain described by Equation 59 and Figure 10. The effect is, however, relatively small such that $\overline{D} \cong D(SL_o = FL/2,L)$ is sufficiently accurate.

Figure 12 is also based on Equation 63. Stress-strain bounds are shown for approximately linear and non-linear behavior of a cracked material under a dead load.

Figure 12 indicates that stress-strain relations predicted by the present theory show a stress maximum, and then decreasing stress at increasing strain. This means that experimentally determined stress-strain relations which exhibit such features do not necessarily reveal genuine material properties. A decreasing branch of the stress-strain relation may very well be a result of competition between speed of testing and rate of crack propagation. That is, at slow testing the cracks run relatively fast, resulting in a low stress maximum. Under fast testing, crack speed is exceeded by loading speed, thus the material exhibits more elastic and brittle behavior, with a high stress maximum as a consequence. The author is examining this subject at present.

SHORT-TIME STRENGTH AS INFLUENCED BY TIME UNDER LOAD

The lifetime theory developed gives the possibility of evaluating the influence of time under load on the short time strength, $\sigma_{cr,t}$.

This feature will be demonstrated here for dead loading of a power law creep material with low strength level and low crack intensity; that is, $FL < 1/3$ and $f \cong 1$.

From Equation 6

$$\Gamma_{cr} = \frac{\sigma_{cr}^2 \pi L_o}{E} = \frac{\sigma_{cr,t}^2 \pi L}{E} \qquad (64)$$

or

$$R = \frac{\sigma_{cr,t}}{\sigma_{cr}} = \sqrt{\frac{1}{\kappa}} \qquad (65)$$

where R denotes remaining strength relative to initial strength.

When κ from Equation 62 is introduced, Equation 65 becomes

$$R = \frac{1}{\kappa_{cr}} + \left(1 - \frac{1}{\kappa_{cr}}\right) \left(\frac{t_{cat} - t}{t_{cat} - t_s}\right)^{b\ 1/2} \qquad (66)$$

or because $\kappa_{cr} = 1/SL^2$ at the assumptions given

$$R = [SL^2 + (1 - SL^2)(1 - T)^b]^{1/2} \qquad (67a)$$

$$\cong SL + (1 - SL)(1 - T)^{b/(1+b)} \qquad (67b)$$

where the "fractional decay time", T, is defined by

$$T = \frac{t - t_s}{t_{cat} - t_s} \qquad (68)$$

Time to a given remaining strength, R, is determined by solving Equation 67b with respect to T, yielding

$$T = 1 - \left(1 - \frac{1 - R}{1 - SL}\right)^{(1+b)/b} \qquad (69)$$

Some results of Equation 67b are demonstrated graphically in Figure 13. It is noticed that strength reduction first takes place at times $t > t_s$. After that serious reduction first occurs when 75 percent of the residual time to catastrophic failure has elapsed. This statement, however, should be considered together with the comments on "brittleness" made in the "Lifetime" section. That is, the absolute time where strength reduction occurs reduces at increasing strength levels.

STRENGTH AS RELATED TO ELASTICITY

Under fast loading this relationsnip is non-viscoelastic. The subject is, however, included here because of its practical relevance to strength grading based on measurements of elasticity.

The relevant expression has already been presented in a preceding section, as Equation 24. Figure 14 is based on this expression. The influence of the geometrical factor, θ, defining the placing of cracks in the multi-crack model described in the text immediately before Equation 14 is shown in the figure. MOR and MOE designate modulus of rupture and modulus of elasticity, respectively.

STRONGLY VARYING LOADS, FATIGUE

It has been mentioned before that the model presented in this paper does not consider theoretically correct load variations, where Equation 31 predicts negative crack velocity. It is, however, possible to generalize the model also to include the problems of crack closure, in a relatively simple way. Figure 15 demonstrates some results of this generalization, details of which are explained in a research progress report (Nielsen, 1985).

The above figure illustrates a situation where the effects of load variations with a cycling time, $T < 10^{-4}\tau$, can be treated according to elastic fatigue theory; that is, the "cycling" energy dissipation in the front zone of a crack overrides the energy dissipation caused by creep. The symbol τ is still the doubling time in the power law representation of creep, Equation 3. At $T > \tau$, the effects of load variations are mainly a matter of energy dissipation caused by creep. In between these two situations we have a situation of viscoelastic fatigue.

INFLUENCE OF MOISTURE CONTENT AND TEMPERATURE

The time dependent, mechanical properties of wood considered in this paper are extremely sensitive to changes in moisture content and temperature. This has already been indicated in the introductory section on viscoelasticity.

At equilibrium such changes in climatic conditions are easily taken care of in the analysis applying the procedure described in the section just mentioned. That is, the reference doubling time, τ, of the creep in Equation 3 is replaced by $a\tau$, where "a" is the climate factor given in Equation 4. This factor is 1 at the reference state, moisture content (by weight), $u = 0.15$, and temperature, $T_e = 20°C$. As time has been kept dimensionless in the article, all figures are valid irrespective of climatic conditions. Only the numbers of the time axis are changed very simply by multiplication or shifting.

In lifetime analysis time has been given in $\log_{10}(t/\tau)$. Here the numbers, x, of the time axes are shifted according to

$$x \Rightarrow x + [10(0.15 - u) + (20 - T_e)/15] \qquad (70)$$

For example, the moisture content of a wood member has been changed from $u = 0.15$ to 0.30 (wet), while the temperature is still $T_e = 20°C$. Then,

$$x \Rightarrow x - 1.5 \qquad (71)$$

therefore, lifetime at (FL,SL) = (0.1,0.6) in Figure 5 changes from $\log_{10}(t/\tau) = 3.25$ to $\log_{10}(t/\tau) = 1.75$ at the moisture change assumed.

Figure 16 demonstrates experimentally that Equation 71 is at least qualitatively correct.

The simple procedure just described to consider the influence of temperature and moisture content on lifetime assumes constant fracture mechanics parameters, σ_L and δ_{cr} (see text immediately following Equation 6). If environmental conditions change these qualities, appropriate modifications have to be made in the basic relations 29 and 31. In this respect the latter equation describing crack velocity is most directly involved, because of its dependency on strength level, $FL = \sigma_{cr}/\sigma_L$.

Some topics relevant to the above mentioned environmental influence on the fracture parameters have been discussed earlier (Nielsen, 1982a).

FINAL REMARKS

The presnt article has shown that the concept of considering wood as a cracked viscoelastic material is a realistic concept. It presents a unified description of certain features of wood behavior which cannot be described in traditional ways; that is, by assuming wood to be either a cracked elastic material or a homogeneous viscoelastic material alone.

An inteesting point is that the theory presented is valid not only for crack defects, but for dislocation defects also. Thus, the hypothesis can be made that the theory presented is valid for explaining the behavior of wood influenced by a variety of defects; from large defects like cracks, to small defects which are not visible to the naked eye.

These comments on the generality of the theory are the reasons why the "defect ratio", , is introduced in Equation 11. This quantity is not necessarily a dimensionless crack length. The defect ratio can be thought of as a defect accumulating parameter, which runs from an initial value of one to a critical value, dependent on load situation.

An important consequence of the theory is that short time strength at any time is a sufficient "fingerprint" of the immediate mechanical wood condition. That is, for example, when recycling wood members we do not need to know the pre-load history of the members in order to predict their remaining lifetime under a given load.

Certain aspects of the importance of parameter "A" used in the viscoelastic crack analysis have been discussed in connection with Equation 7. An additional advantage of applying this parameter in the analysis is that the question of orthotropy becomes less important (Nielsen, 1982a) as long as the modes of short time failure and long time failure are similar. This is usually the case. Thus, when cleavage along the grain is the mode of failure, τ_L in the creep function (Equation 3) is relevant. When failure across the fibers is the failure mode, τ_t is the relevant τ-magnitude (see text immediately following Equation 3).

Finally, the main Equations 29 and 31 of the theory are not generally suitable for simple hand calculations. They are, however, not too complicated for a small calculator. Indeed, every result presented in this paper has been generated by a Hewlett Packard 15C. These equations could be simplified in a number of ways which, however, would "hurt" somewhat the generality of the method.

In certain cases, where a generalized version of the theory is not needed, the equations can be simplified considerably; for example, when lifetime studies are considered exclusively. In this respect, readers are referred to Nielsen (1979) and Nielsen and Kousholt (1980) from where Figure 17 is reproduced.

REFERENCES

Dugdale, D.S. 1960. Yielding of steel sheets containing slits. J. Mech. Phys. of Solids. 8:100.

Griffith, A.A. 1920. The phenomenon of rupture and flow in solids. Trans. Royal Soc. of London. 222:163.

Krebs, Hans, J. 1984. The Influence of Moisture Content on the Long Term Mechanical Properties of Wood. Thesis (in Danish). Building Materials Laboratory, Technical University of Denmark, Report No. 105.

Madsen, B. 1979. Time-strength relationship for lumber. First Int. Conf. on Wood Fracture, Banff, Alberta, Canada, 1978. Proc. Western Forest Products Lab., Vancouver, B.C. Canada. 111p.

Madsen, B. and J.D. Barrett. 1976. Time-Strength Relationship for Lumber. Univ. of British Columbia, Vancouver, B.C., Canada. Dept. of Civil Engineering, Structural Research Series, Report No. 13.

Madsen, B. and Johns, K. 1982. Duration of load effects in lumber. Can. J. Civil Eng. 9:502, 515, 526.

Nielsen, A. 1972. Rheology of Building Materials. Thesis. National Swedish Building Research Institute, Stockholm, Sweden. Document D6(1972).

Nielsen, A. 1981. Long time deflection of wood beams. (in Danish) Nord. Traetidsskr 7:201. (Alborg Univ. Center, Denmark.)

Nielsen, L. Fuglsang and Kousholt, K.K. 1980. Stress-strength-lifetime relationship for wood. Wood Sci. 12:162.

Nielsen, L. Fuglsang. 1978. Crack propagation in linear-viscoelastic materials. Bygningsstatiske Meddelelser. 49:1. (Danish with extensive English summary.)

Nielsen, L. Fuglsang. 1979. Crack failure of dead-, ramp, and combined loaded viscoelastic materials. First Int. Conf. on Wood Fracture, Banff, Alberta, Canada, 1978. Proc. Western Forest Products Lab., Univ. of British Columbia, Vancouver, B.C. Canada. 187p.

Nielsen, L. Fuglsang. 1982a. A lifetime analysis of cracked linear-viscoelastic materials--with special reference to wood. Meeting of Int. Union of Forestry Research Organizations, Wood Engineering Group, Borås, Sweden, 1982. Proc. IUFRO S5.02, Chalmers Univ. of Technology, Dept. of Struc. Eng., Gothenberg. 151 p.

Nielsen, L. Fuglsang. 1982b. On the mechanical behavior of materials with interacting cracks. Meeting of Int. Union of Forestry Research Organizations, Wood Engineering Group, Borås, Sweden, 1982. Proc. IUFRO S5.02, Chalmers Univ. of Technology, Dept. of Struc. Eng., Gothenberg. 141 p.

Nielsen, L. Fuglsang. 1983. On the concept of wood behaving like a cracked viscoelastic material. Meeting of Int. Union of Forestry Research Organizations, Wood Engineering Group, Madison, WI, U.S.A., June/July, 1983. Proc. IUFRO S5.02, Dept. of Civil Eng., University of British Columbia, Vancouver, B.C., Canada. 103 p.

Nielsen, L. Fuglsang. 1984. Power law creep as related to relaxation, elasticity, damping, rheological spectra and creep recovery--with special reference to wood. Meeting of Int. Union of Forestry Research Organizations, Wood Engineering Group, Xalapa, Mexico, December 1984. Proc. in press.

Nielsen, L. Fuglsang. 1985. Fatigue lifetime of viscoelastic materials--with special reference to wood. Building Materials Laboratory, Technical University of Denmark, Progress Report (1985, 11) on a research project (STVF 16-3179.8972) on the influence of varying load on the strength and lifetime of wood. (in Danish)

Walters, C.S. and Reiss, W.L. 1977. Predicting modulus of rupture from modulus of elasticity for small, clear specimens of oak and cottonwood. Forest Prod. J. 27:51.

Wood, L.W. 1947. Behavior of wood under continued loading. Engineering News Record. 139:24.

Wood, L.W. 1951. Relation of strength of wood to duration of load. U.S. Forest Products Lab., Madison, WI, USA. Report R-1916.

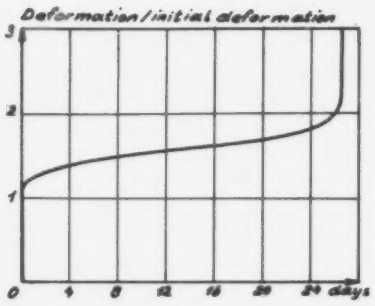

Figure 1. Deformation of a timber beam loaded to 75% of its short time strength. Based on data from Wood (1947).

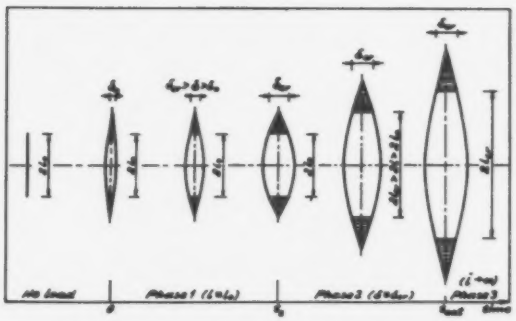

Phase 1: Constant length, $2l = 2l_0$, increasing front opening, $\delta < \delta_{cr}$
Phase 2: Constant crack opening, $\delta = \delta_{cr}$, increasing length, $2l < 2l_{cr}$
Phase 3: Critical crack length, $2l = 2l_{cr}$, has been reached. Crack velocity $\dot{l} = \infty$. Catastrophic failure occurs.

Figure 4. (Based on Figure 3 in Madsen and Johns, 1982) Crack development with time. Initial crack length $2l_0$. Loading at time t = 0.

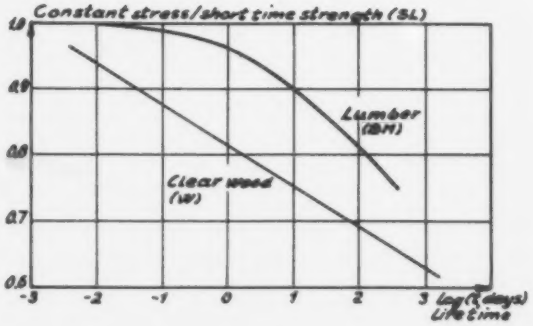

Figure 2. Lifetime of clear wood and lumber. Data denoted W and BM are from Wood, 1951 (straight line representation) and Madsen, 1979 (average representation), respectively.

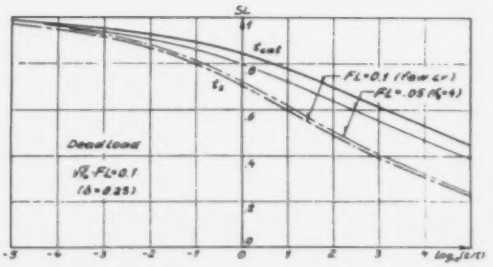

Figure 5. Dead load lifetime. Large Cracks: FL = 0.1 corresponds to very few cracks ($f_0 \cong 1$). At FL = 0.05 there are so many cracks (of the same size) that short time strength is decreased to 50%.

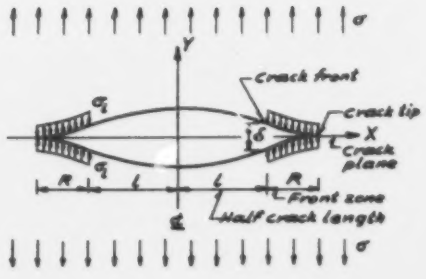

Figure 3. Dugdale single crack model.

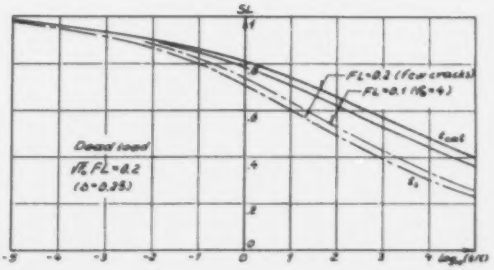

Figure 6. Dead load lifetime. Medium Size Cracks: FL = 0.2 corresponds to very few cracks ($f_0 \cong 1$). At FL = 0.01 there are so many cracks (of the same size) that short time strength is decreased to 50%.

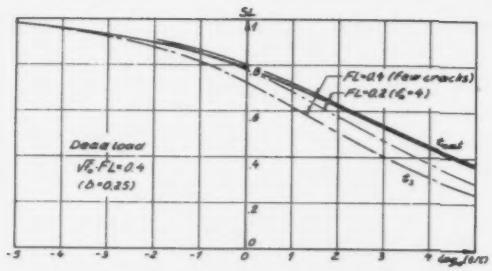

Figure 7. Dead load lifetime. Small Cracks: FL = 0.4 corresponds to very few cracks ($f_0 \cong 1$). At FL = 0.02 there are so many cracks (of the same size) that short time strength is decreased to 50%.

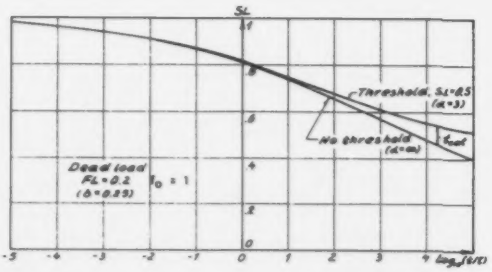

Figure 8. Dead load lifetime. The potential influence of having a threshold on creep. See Equations 3 and 5.

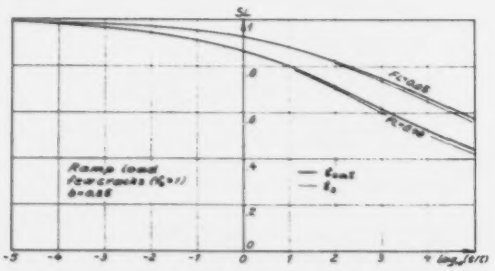

Figure 9. Ramp load lifetime according to Equations 52 and 47.

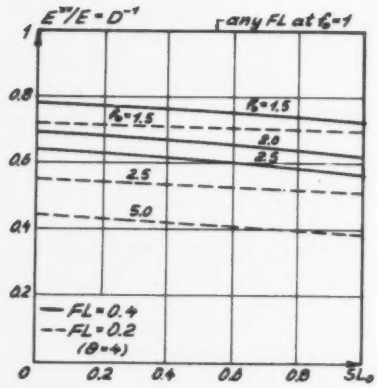

Figure 10. Secant Young's modulus of a cracked material loaded to stress level SL_0. Equations used are 57 and 59.

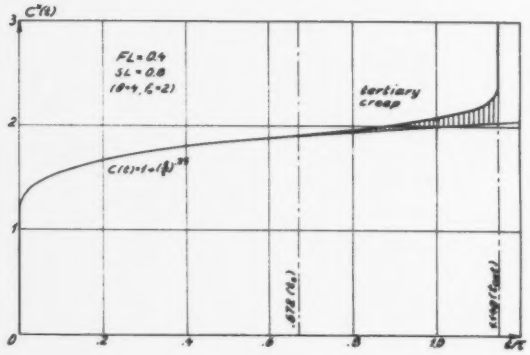

Figure 11. Normalized creep function of a cracked material according to Equation 63. For time, $t < t_s$, it is approximately equal to the normalized creep function of the uncracked material (see text). For $t > t_s$ the function becomes non-linear because of running cracks; that is, tertiary creep (shaded area) appears.

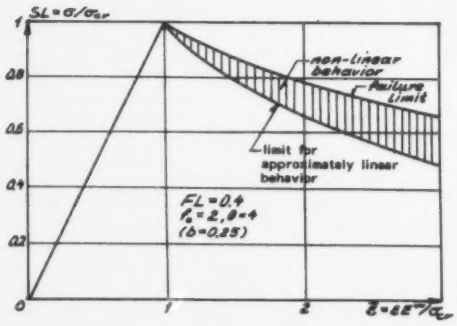

Figure 12. Bounds for approximately linear and non-linear creep behavior of a cracked viscoelastic material.

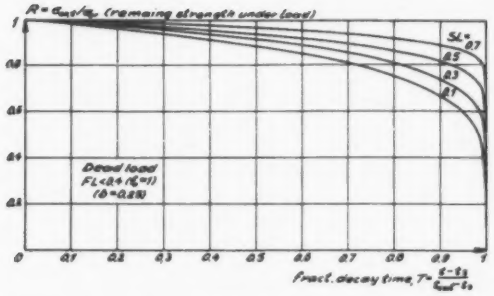

Figure 13. Short time strength reduction as a function of time under dead load.

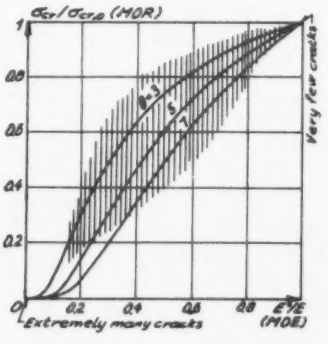

Figure 14. Strength as related to elasticity (Young's modulus) for a cracked material. Strength, σ_{cr}, is relative to strength at very few cracks (Griffith load capacity), $\sigma_{cr,o}$. Elasticity, E^*, is relative to elasticiy, E, at very few or no cracks. The shaded area covers roughly the MOR-MOE data for 1200 oak and cottonwood beams presented in Walters and Reiss, 1977.

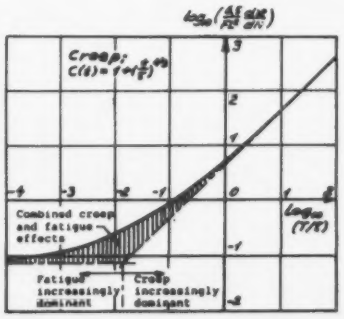

Figure 15. Crack velocity, increase of defect ratio/cycle (N), in a cracked viscoelastic material subjected to a square wave loading between SL = 0 and SL$\sqrt{\kappa}$ = 0.8, κ being the defect ratio defined in Equation 11. The cycling time is T. Time under load is T/2.

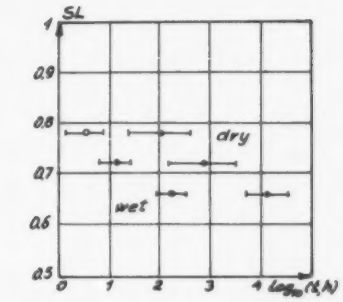

Figure 16. The influence of moisture content on lifetime of clear wood in bending. Data from Krebs, 1984. Dry and wet mean u ≅ 0.15 and u > 0.30, respectively, both at Te ≅ 20°C.

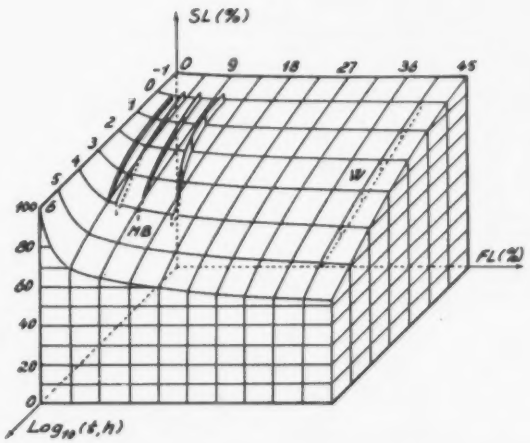

Figure 17. Dead load lifetime for wood as related to strength and load levels. Experimental data denoted W and MB are from Wood (1951) and Madsen and Barrett (1976), respectively. The lifetime surface predicted is based on power law creep with (b, τ) = (0.25, 81 days).

WOOD AS A CRACKED VISCOELASTIC MATERIAL

Part II: Sensitivity and Justification of a Theory

Lauge Fuglsang Nielsen
Building Materials Laboratory
Technical University of Denmark
Lyngby, Denmark

INTRODUCTION

In Part I (Nielsen, 1985) of the present study a theory was established which describes the mechanical behavior of wood on the basis of combining crack mechanics and viscoelasticity. The theory explains a variety of features which cannot be explained consistently by other known theories on wood behavior. For example, the theory successfully describes experimental results on tertiary creep and dead load lifetime of wood, as influenced by wood quality and moisture content. Experimental justification of the theory was also given on the ability of predicting MOE-MOR relations.

The present Part II of the study will give more experimental evidence which supports the concept of considering wood as a defective viscoelastic material. Some key points of the theory will be tested.

Before that, however, we will look at how variations in the parameters influence the theoretical predictions. This section will also discuss the effects of strength distribution.

Terminology and meanings of symbols are as given in Part I.

The theory presented in Part I is general in the sense that it considers any strength level and any number of defects (which, by the way, are not necessarily cracks).

For the present study the theory is simplified by assuming: (1) that the actual wood strength is relatively small compared to the theoretical ("uncracked") strength and (2) that the number of defects is relatively small.

Assumption (1) means theoretically that the strength level, $FL < 1/3$. Practically, however (see Nielsen, 1982), $FL < 0.5 - 0.6$ is sufficient. Assumption (2) means that the interaction factor, $f_0 \simeq 1$.

The simplified basic relations (Part I, Equations 29 and 31) become

$$\int_0^{t_s} C(t_s - \eta)\, \frac{dSL^2}{d\eta}\, d\eta = 1 \qquad [1]$$

giving the time, t_s, to start defect propagation - and

$$\frac{dt}{d\kappa} = \frac{\bar{F}\left(\frac{1}{\kappa SL^2}\right)}{FL^2 \kappa SL^2}; \quad (1 \longrightarrow \kappa \longrightarrow \kappa_{cr} = SL^{-2}) \qquad [2]$$

giving the defect velocity for $t > t_s$. Load level and defect ratio are denoted by SL and κ respectively. The normalized creep function is given by C(t). The function $\bar{F}(X)$ is related to the creep function as given in Part I, Equation 27. Throughout the paper creep is defined by the so-called power law expression, (Part I, Equation 3).

SENSITIVITY OF THEORY

The sensitivity of the theory presented in Part I of the present study will be evaluated for the dead-load lifetime of wood members.

Here Equations 1 and 2 predict

$$t_{cat} = \tau \left\{ \left(\frac{1}{SL^2} - 1\right)^{1/b} + \frac{q}{FL^2 SL^2} \int_1^{SL^{-2}} \frac{(\theta - 1)^{1/b}}{\theta}\, d\theta \right\} \qquad [3]$$

where

$$q = ((1 + b)(2 + b)/2)^{1/b} \qquad [4]$$

The first term of Equation 3 is the time, t_s, to start defect propagation. The other term, $t_{cat} - t_s$, is the additional time it takes a defect to develop a size which is critical; that is which makes the defect velocity infinitely high.

Material properties influencing lifetime are: creep doubling time, τ, creep power, b, strength level, FL, and then of course the distribution $\phi(FL)$ on strength level (which also involves the load level, SL).

In the following sections some comments and illustrations will be given on how variations in the above mentioned parameters will influence lifetime prediction by the theory.

CREEP DOUBLING TIME

It is seen from Equation 3 that lifetime is directly proportional to the doubling time, τ. This parameter is very sensitive to variations in climatic conditions. An expression is suggested in Part I which considers this feature at equilibrium. The expression is represented graphically in Figure 1. The influence of climatic changes may be considerably increased when non-equilibrium conditions are involved (Nielsen, 1984).

Experimentally τ can be determined (Nielsen and Hoffmeyer, 1985) with an accuracy of

$$\tau = \bar{\tau}\ (1 \pm \cdot 25) \qquad [5]$$

According to Nielsen (1984) the orders of magnitudes are $(\bar{\tau}_\perp, \bar{\tau}_\parallel)$ = (10-100,10000-100000) days at temperature $T_L = 20°C$, and a moisture content (by weight) of $u = 0.15$. The symbols $\perp$ and $\parallel$ refer to actions perpendicular and parallel to grain, respectively.

CREEP POWER

This parameter, b, can be considered independent of climate (Nielsen, 1984). Experimentally, b can be determined (Nielsen and Hoffmeyer, 1985) with an accuracy of

$$b = \bar{b}\ (1 \pm \cdot 25) \qquad [6]$$

Orders of magnitudes are $(\bar{b}_\perp, \bar{b}_\parallel)$ = (0.33-0.25, 0.25-0.20) with the overall average being $\bar{b} = 0.25$. The influence of variations of b on start to defect propagation and on time from initial defect propagation to catastrophic failure is shown in Figures 2 and 3.

STRENGTH LEVEL

Only the second term in Equation 3 is dependent on the strength level, FL, which is the lifetime part associated with defect propagation. This influence is inversely related to the second power of the strength level, FL.

DISTRIBUTION OF STRENGTH

The distribution of strength for a group of wood members may be described by the factor, $F(\phi)$, defined and illustrated in Figure 4, where ϕ is the accumulated strength distribution. The strength has been normalized to the 50th percentile, $\sigma_{cr,50}$. The figure also represents the distribution of strength level relative to the level, FL_{50} at $\phi = 50$ percent. The parameters, a, and especially α characterize the variation of strength (and strength level).

When the group of wood members is loaded relative to $\sigma_{cr,50}$ we have

$$FL = FL_{50} \cdot F(\phi) \qquad [7]$$

$$SL = FL_{50}/F(\phi) \qquad [8]$$

where $FL_{50} = \delta_{cr,50}/\delta_L$

The distribution with $\alpha = 0.5$ shown in Figure 4 is close to the strength distribution of the lumber population I used by Madsen and Barrett (1976) in experimental lifetime studies of beams under dead load. The distribution with $\alpha = 0.1$ shown in Figure 4 is close to a normal distribution, characterized by a coefficient of variation of 15 percent.

The latter distribution is applied in Figures 5 and 6 to demonstrate how Equations 1 to 3 reflect strength distribution in predicting dead load lifetime. The example chosen has a 50th percentile strength level of $FL_{50} = 0.10$. The creep has been assumed to develop according to $b = 0.25$. The symbol, BOL, means "broke on loading". Load is referred to strength at $\phi = 50$ percent, that is, $SL_{50} = \sigma/\sigma_{cr,50}$. Figure 6 indicates that an approximately log-normal distribution of lifetimes is approached at decreasing load levels. An important feature characterizing both Figures 5 and 6 is that time is kept dimensionless. That is, the figures apply practically for any creep function with $b \simeq 0.25$.

Figure 7 demonstrates the influence on lifetime of the strength distribution shown in Figure 4 with $\alpha = 0.5$. As mentioned previously, this distribution approximates the strength distribution of Test Group 1 outlined by Madsen and Barrett (1976).

Figure 7 considers additionally creep with $b = 1/3$ and $\tau = 10$ days. That is because the experiments by Madsen and Barrett (1976) included creep tests from which $b_f \simeq 1/3$ and $t_f \simeq 10000$ days could be deduced. Considering Equations 5 and 6, including the associated text, the values applying to flaking (1), relevant for the experiments by Madsen and Barrett (1976) and used in Figure 7, were estimated.

It is evident from Figure 7 that a wood group broadly varying in quality exhibits an enormous scattering of lifetimes, when exposed to a constant load. This experience is also demonstrated in Madsen and Barrett (1976), Figure 4.

JUSTIFICATION OF THEORY

DEAD LOAD LIFETIME, MADSEN AND BARRETT (1976)

The results obtained in the tests reported by Madsen and Barrett are presented graphically by Madsen, 1979, and Madsen and Johns, 1982. Quite an ingenious data treatment was used in order to maximize the information which could be extracted from each single lifetime observation. The samples were assumed to fail in the same order as given by the ranking (accumulated strength distribution, ϕ). In this way the influence on lifetime of several load levels, $SL = \sigma/\sigma_{cr}(\phi)$, could be illustrated on the basis of a constant load experiment. In principle this data treatment is consistent with the concept of wood behaving as a cracked material.

The data treatment just described corresponds to transferring an experimental data point, D, in Figure 7, to point B. The procedure, however, disregards the influence of strength level, which in Figure 7 corresponds to shifting point B to point T. As a consequence of that, the data presentation in Madsen (1979) and Madsen and Johns (1982) will show a lifetime which varies too steeply at decreasing load levels. That is, each trend of data "contains" increasing strength levels, FL, at increasing time.

In order to test the author's theory, and also to evaluate the data treatment used in Madsen (1979) and Madsen and Johns (1982), the theoretical data of Figure 7 have been "translated" according to these two articles. The results are shown in Figure 8 together with the results from Madsen (1979).

Good agreement between these data supports the model considered for wood behavior. In the time considered (10^{-4} - 10^5 days), the strength level varies from FL = 5 percent to 11 percent and 26 percent for the lower and higher loads respectively. That is, higher strength level promotes shorter lifetime as predicted by the theory (when FL < ca. 0.5).

The error made by treating the experimental data according to Madsen (1979) and Madsen and Johns (1982) depends somewhat on what reference strength level is chosen. For practical use, the error seems to be unimportant when referring to a strength level which is the simple average of FL considered in the time period of testing. As an example Figure 8 shows a theoretical graph corresponding to FL = 0.15 which is not too different from the graph representing $SL_{50} = 0.70$ when t < 10 years.

DEAD LOAD LIFETIME, NIELSEN AND HOFFMEYER, (1985)

As previously mentioned, the proposed theory predicts lower lifetime at increasing strength level. This is a critical point which would reject the theory, if not verified by experiments.

A lifetime experiment was reported in Nielsen and Hoffmeyer (1985). Tests were made on small, 60-cm-long beams made of clear wood (spruce) with a centrally placed kerf. The sides of the cross section, 2 x 2 cm, were cut parallel-perpendicular to the annual rings. The kerf was placed in the "perpendicular to annual ring" side. Carefully matched twin-beams were made so as to ensure that tests could be made on series having the same load level (relative to the strength of the twin-beam). The load was constant bending with the

kerf in the tension side. Test conditions were at equilibrium at temperature, $T_L = 19 \pm 1°C$, and relative humidity, $RH = 64 \pm 2$ percent.

Ranking of the specimens tested according to lifetime provides the basis for evaluating the strength level influence on lifetime. Such an analysis yields the results shown in Table 1. It is evident from the table that the theoretical statement previously made, that lifetime decreases at increasing strength level, is justified.

Figure 9 presents graphically the lifetime results of the tests reported by Nielsen and Hoffmeyer (1985). Apparently, kerf depth has no significant influence on lifetime (which is close to the one predicted by the Madison curve). That is because strength level is dependent mainly on cleavage in both test populations. This feature is discussed in detail in Nielsen and Hoffmeyer (1985).

Creep measurements were taken on all beams. From thse data "parallel-values" of $b = 0.25$ and $\tau = 2500$ days could be determined. The theoretical (heavy) line depicted in Figure 9 is calculated by Equation 3 using the creep parameters shown in the figure. The "perpendicular" τ is 0.003 times the "parallel" value, while the b value remains the same.

DRY-WET DEAD LOAD LIFETIME, KREBS (1984)

Dead load lifetime tests were made by Krebs (1984) on small beams made of artificially defected clear wood. The tests were made at two equilibrium moisture levels, dry ($u = 0.15$) and wet ($u > 0.30$). The experiment is explained in more detail by Hoffmeyer et al. (1985), from which the data shown in Figure 10 are reproduced. Creep measurements were taken which showed "parallel" (dry) quantities of $b = 0.23$ and $\tau = 11250$ days.

The theoretical predictions shown in Figure 10 are made from Equation 3 and Figure 1 applying the "perpendicular" (dry) quantities of b and τ indicated in the figure. That is, b is unchanged while τ is given the value of 0.001 times the "parallel" value. Apparently, lifetime prediction by Equation 3 is good; and the moisture modifying procedure suggested by Nielsen (1985) and Figure 1 works fairly well.

SHORT TIME STRENGTH - DURATION OF LOAD, SPENCER AND MADSEN, (1984)

A strong justification of the proposed model may be established if the theory can explain the short time strength of wood as influenced by time under load. This follows from Madsen and Johns (1982) and Spencer and Madsen (1984) who suggested that the onset of crack propagation may be identified by the point where short time strength of survivals in a lifetime experiment touches the strength control curve.

As an example we will consider the results in Figure 11 reproduced from Spencer and Madsen (1984). This figure is a "by-product" of dead shear-load lifetime experiments on relatively small samples of clear wood (Douglas-fir). Short time strength was determined on surviving samples - and compared with the control strength distribution.

Figure 12 illustrates the theoretical prediction which can be made by applying Equation 3 and (Part I, Equation 67b). The figure reads, for example: A lifetime experiment at 800 psi load was interrupted when 73 percent of the samples were still surviving. That is, 27 percent have experienced Phase 3 behavior (catastrophic failure), see Part I, Figure 4. Short time strength was then determined on the survivals. Forty-two percent of the original samples did not show strengths different from the strength control curve. These specimens correspond to Phase 1 (resting cracks) in Part I, Figure 4. The test samples between $\phi = 27$ and 58 percent in Figure 12 behave according to Phase 2 in Part I, Figure 4; that is, crack propagation has occurred, but the cracks have not yet reached their critical lengths.

It is noticed that the agreement between Figures 11 and 12 is fairly good, which, as previously indicated, is a strong justification for the proposed model. Implicitly, this means also that the data treatment used by Madsen (1979) and Madsen and Johns (1982) is a practical way of rationalizing lifetime test information, when considering the comments made in this paper concerning the associated strength level.

RATE OF LOADING EFFECTS ON STRENGTH, SPENCER, (1979)

The rate of loading effect on strength (ramp load strength) can be determined theoretically using Part I, Equations 47 and 51 or Equation 52 when $b = 0.25$. Figure 13 depicts the results of such an analysis. The strength distribution applied approximates fairly well, for $0.1 < \phi < 0.9$, the distribution characterizing the sample used by Spencer (1979, Group 4) in his ramp load experiments on Douglas-fir lumber beams. Spencer's data (1979, Figure 11) are compared in Figure 13 with the theoretical results when a doubling time of $\tau = 10$ days has been estimated together with a 50th percentile strength of $\sigma_{cr,50} = 5700$ psi (Spencer, 1979, Group 4).

Good agreement is noticed between the two data sets--except eventually at $\phi = 90$ percent and $\dot{\sigma} = 100000$ psi/sec. which characterize high speed testing of high quality wood. At $\phi = 95$ percent, Spencer derived the remarkably high strength of 14000 psi obtained in 0.1 sec. That is (as indicated also by Nielsen and Kousholt, 1980) a situation where dynamic effects will influence strength determination. Spencer was aware of that and used specially designed equipment for the high speed tests.

The writer believes that strength determined at high speed testing is not only influenced by dynamic effects. We are also faced with shift of fracture modes (because creep has no time to develop). That is, a cleavage mode in bending at moderate rates of loading may change to crack propagation perpendicular to grain at high speed testing which would yield higher strength. The topic of mode shift has been discussed by Nielsen (1982).

In order to predict the whole range of ramp load strengths, the proposed model should consider a continuous change (in the range of $\dot{\sigma} \simeq$ 100-10000 MPa/sec.) of material properties from the "perpendicular" creep- and fracture parameters to the corresponding "parallel" quantities.

FINAL REMARKS

The theory presented in Part I of the present study has been shown to reflect in a simple way the influence of different climatic conditions and strength distributions on wood

behavior. Figures presented, like Figures 5 and 6 combined with Figure 1, are useful when designing lifetime experiments for wood members.

Orders of magnitudes for the creep parameters of wood needed in the theory have been given. It seems that $b = 1/4$ and $\tau = 10$ days are reasonable estimates at temperatures, $T_L \simeq 20°C$, and moisture contents, $u \simeq 0.15$ (by weight), when no creep parameters are experimentally determined.

The choice of strength parameters depends on the wood quality considered. Throughout both Part I and Part II of this study, strength levels are: $FL > 0.25$ for clear wood, $FL \simeq 0.15$ for wood with small defects (relative to structural dimensions) and $FL < 0.10$ for wood with large defects. These values have also been based on theoretical considerations in Nielsen and Hoffmeyer (1985). The comments just made refer to wood failure by cleavage. When other fracture modes are considered, creep- (and fracture-) parameters should be modified correspondingly.

The theory has been tested in some detail; see Figures 8 to 13, Table 1, and the associated comments in the text. In the author's opinion, these tests--and also those from Part I on the applicability of the theory to predict tertiary creep and MOE-MOR relations--represent sufficient evidence for the concept of wood as a defective viscoelastic material.

Finally, it should be repeated from Part I (Nielsen, 1985) that detailed studies of the wood material (like derivation of tertiary creep and relations correlating strength and stiffness) especially for very high quality wood, need the application of the full general theory given in Part I. Other wood behavior, like the lifetime of normally appearing structural wood and wood members can usually be adequately modelled by a simplified theory used in the present article; that is, by Equations 1 to 3, for which relevant auxiliary relations are given in Nielsen (1982).

REFERENCES

Hoffmeyer, P., H.J. Krebs, L.F. Nielsen. 1985. Duration of Load Tests with Notched Spruce Beams at Two Moisture Levels. Paper presented at the international workshop on Duration of Load held at Forintek Canada Corp. in Vancouver, B.C. Canada. September 12-13, 1985.

Krebs, H.J. 1984. The Influence of Moisture Content on the Long Term Mechanical Properties of Wood. Thesis (in Danish). Building Materials Lab., Techn. Univ. Denmark Technical Report No. 105.

Madsen, B. and J.D. Barrett. 1976. Time-Strength Relationship for Lumber. Civ. Eng. Struc. Res. Series, Report No. 13. University of British Columbia, Vancouver, B.C., Canada.

Madsen, B. 1979. Time-Strength Relationship for Lumber. IN: Proc. of First Int. Conf. on Wood Fracture, Banff, Alberta, Canada. Western Forest Products Laboratory, Vancouver, B.C., Canada. 111p.

Madsen, B. and K. Johns. 1982. Duration of Load Effects in Lumber. Can. J. Civil Engineering 9:502, 515, 526.

Nielsen, L.F. and K.K. Kousholt. 1980. Stress-Strength-Lifetime Relationship for Wood. Wood Science 12:162.

Nielsen, L.F. 1982. A Lifetime Analysis of Cracked Linear-Viscoelastic Materials--With Special Reference to Wood. IN: Proc. of Meeting of Intl. Union of Forestry Research Organizations, Wood Engineering Group, Boras, Sweden. IUFRO S5.02, Chalmers Univ. of Technology, Dept. of Struc. Eng., Gothenburg. 151p.

Nielsen, L.F. 1984. Power Law Creep as Related to Relaxation, Elasticity, Damping, Rheological Spectra and Creep Recovery--With Special Reference to Wood. IN: Proc. of Meeting of Intl. Union of Forestry Research Organizations, Wood Engineering Group, Xalapa, Mexico.

Nielson, L.F. 1985. Wood as a Cracked Viscoelastic Material (Part I). Building Materials Lab., Techn. Univ. Denmark Technical Report No. 153.

Nielsen, L.F. and P. Hoffmeyer. 1985. Lifetime of Loaded Wood--Viscoelastic Fracture Theory (in Danish). Building Materials Lab., Techn. Univ. Denmark Technical Report No. 149.

Spencer, R. 1979. Rate of Loading Effect in Bending for Douglas-fir Lumber. IN: Proc. of First Intl. Conf. on Wood Fracture, Banff, Alberta, Canada. Western Forest Products Laboratory, Vancouver, B.C., Canada. 259p.

Spencer, R.A. and B. Madsen. 1984. IN: Proc. of Meeting of Intl. Union of Forestry Research Organizations, Wood Engineering Group, Xalapa, Mexico.

Table 1

Strength Increase with Decreasing Lifetime*

Kerf	Series	SL (%)	N	ϕ - (1 - ϕ)		
				$\bar{\sigma}_{cr}(T < T_{\phi}) /$	$\bar{\sigma}_{cr}(T > T_{1-\phi})$ - 1	
6 mm	2	85.4	20	50 - 50	30 - 70	10 - 90
				24%	28%	79%
	5	80.3	20	50 - 50	30 - 70	15 - 85
				17%	59%	86%
	8	75.1	20	50 - 50	45 - 55	5 - 95
				30%	36%	49%
	11	70.0	40	50 - 50	43 - 57	3 - 97
				33%	34%	58%
	Average		100	27 %	38 %	66 %
11 mm	1	89.6	40	50 - 50	25 - 75	15 - 85
				27%	52%	51%
	4	85.9	40	50 - 50	30 - 70	10 - 90
				14%	27%	24%
	7	82.3	40	50 - 50	30 - 70	15 - 85
				29%	31%	45%
	10	78.6	50	50 - 50	36 - 64	4 - 96
				22%	29%	46%
	Average		170	23 %	34 %	42 %

* The data from Nielsen and Hoffmeyer (1985) have been ranked according to lifetime. The table compares the average (twin) strength at lifetime, $T < T(\phi)$, with that at lifetimes, $T > T(100\% - \phi)$.

The averages were determined with a coefficient of variation between 10 and 25 percent--concentrating mainly in the area 15 percent.

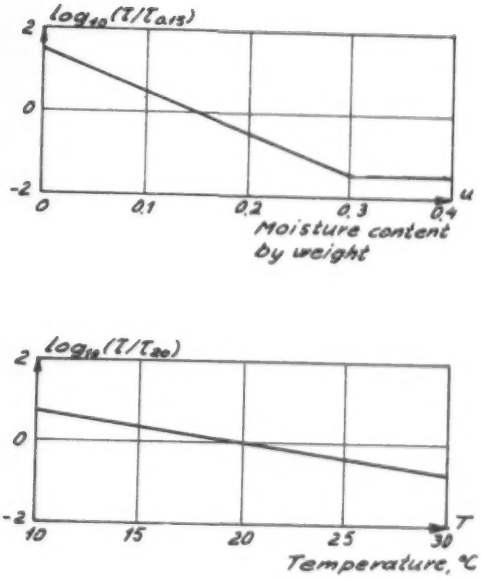

Figure 1. The influence of moisture content and temperature on creep doubling time (and dead load lifetime). Equilibrium conditions.

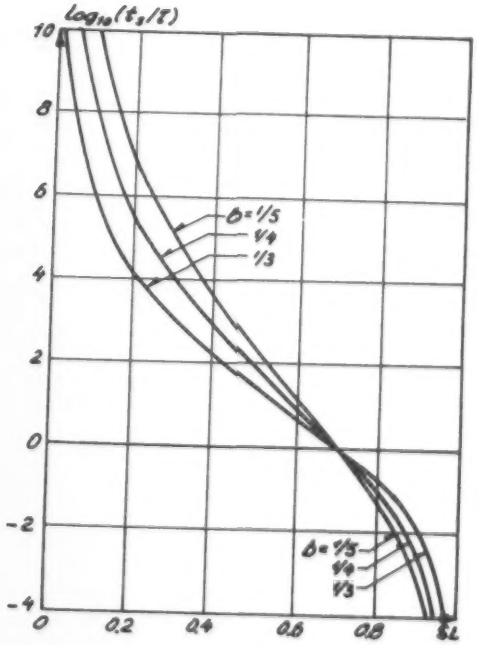

Figure 2. The influence of the creep power, b, on time to start of defect propagation in dead loaded wood.

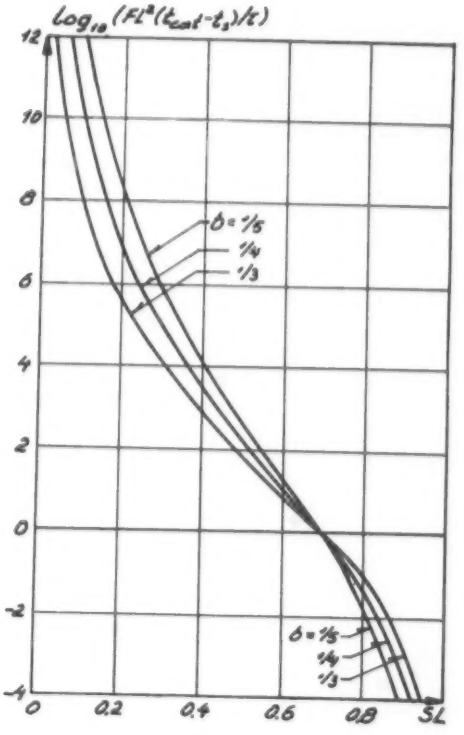

Figure 3. The influence of the creep power, b, on the time from start of defect propagation to catastrophic failure in dead loaded wood.

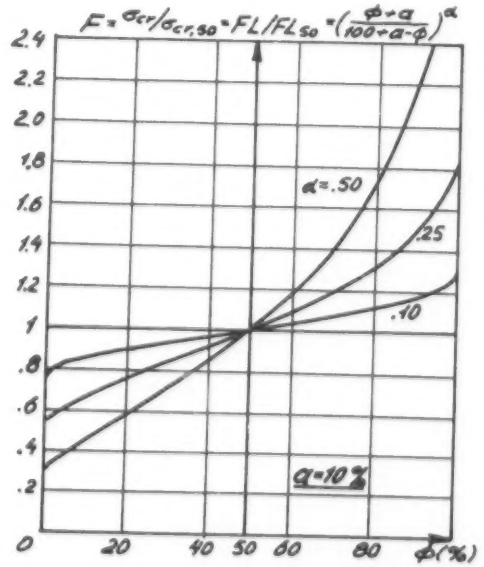

Figure 4. Normalized strength (and strength level) distributions.

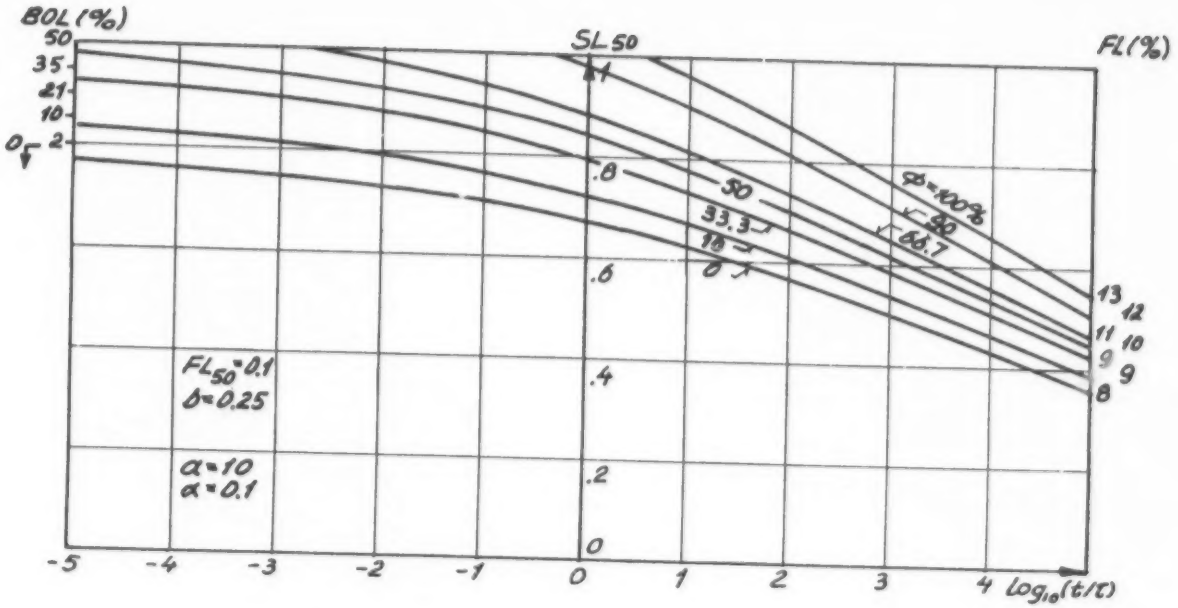

Figure 5. Dead load lifetime as a function of load- and strength distribution.

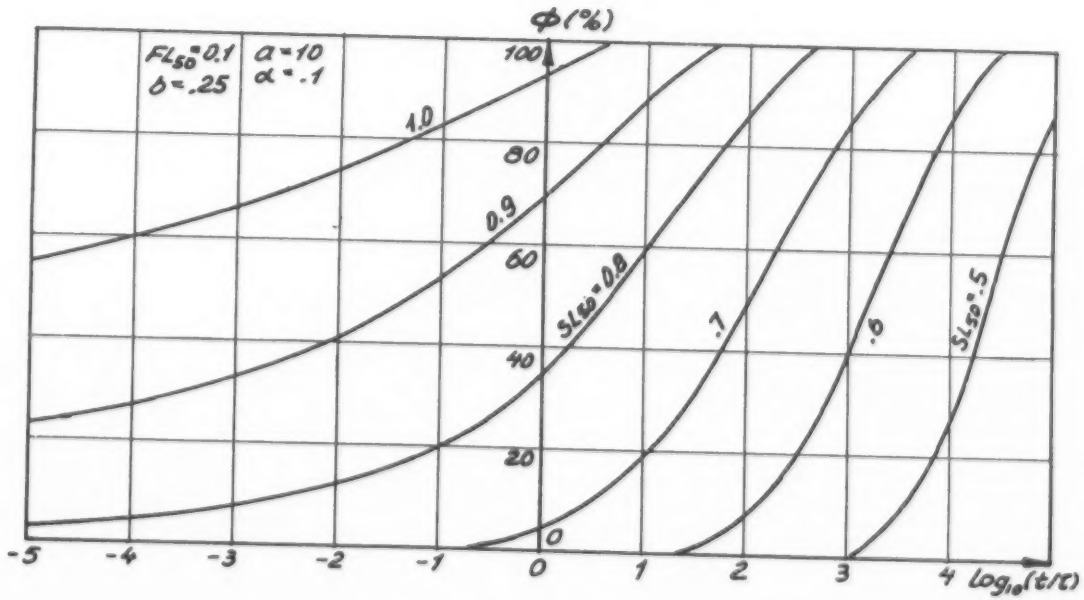

Figure 6. Distribution of lifetime as a function of load level.

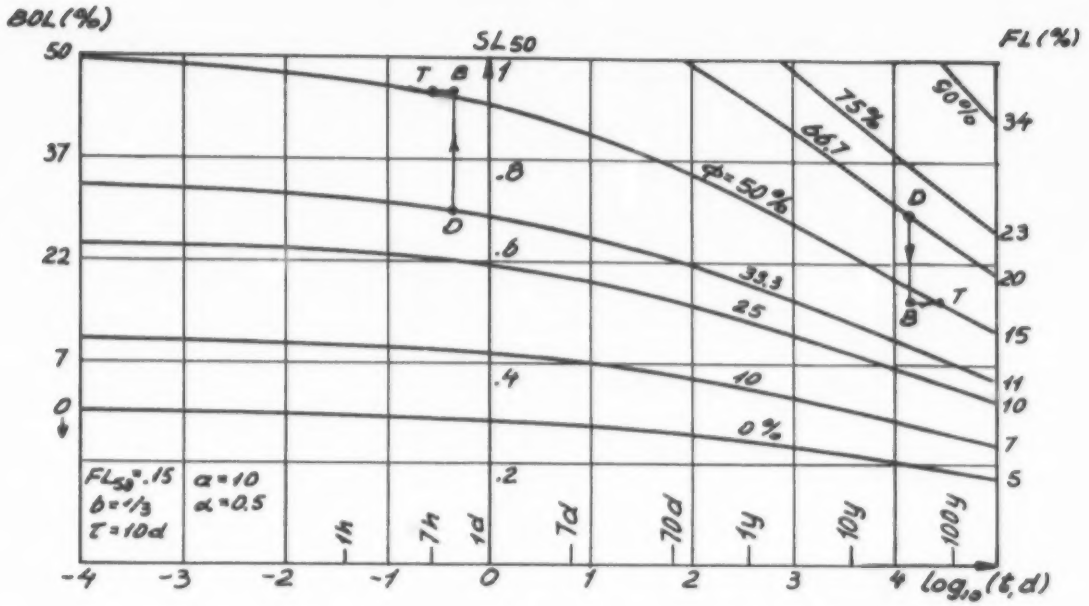

Figure 7. Dead load lifetime as a function of load- and strength distribution. The materials and distribution parameters used correspond approximately to population 1 applied in the beam tests reported in Madsen and Barrett (1976), Madsen (1979), and Madsen and Johns (1982).

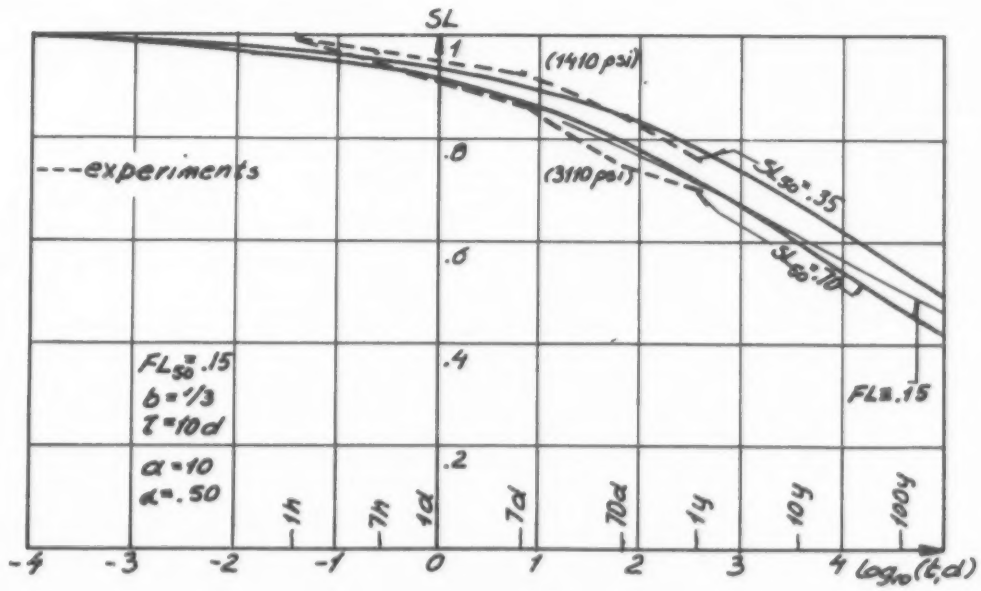

Figure 8. Experimental data (treated according to Borg Madsen) for population 1 in Madsen and Barrett (1976) compared with theoretical data (treated like the test data). SL(.35) and SL(.70) correspond to σ = 1410 and 3110 psi in Madsen and Barrett (1976), respectively.

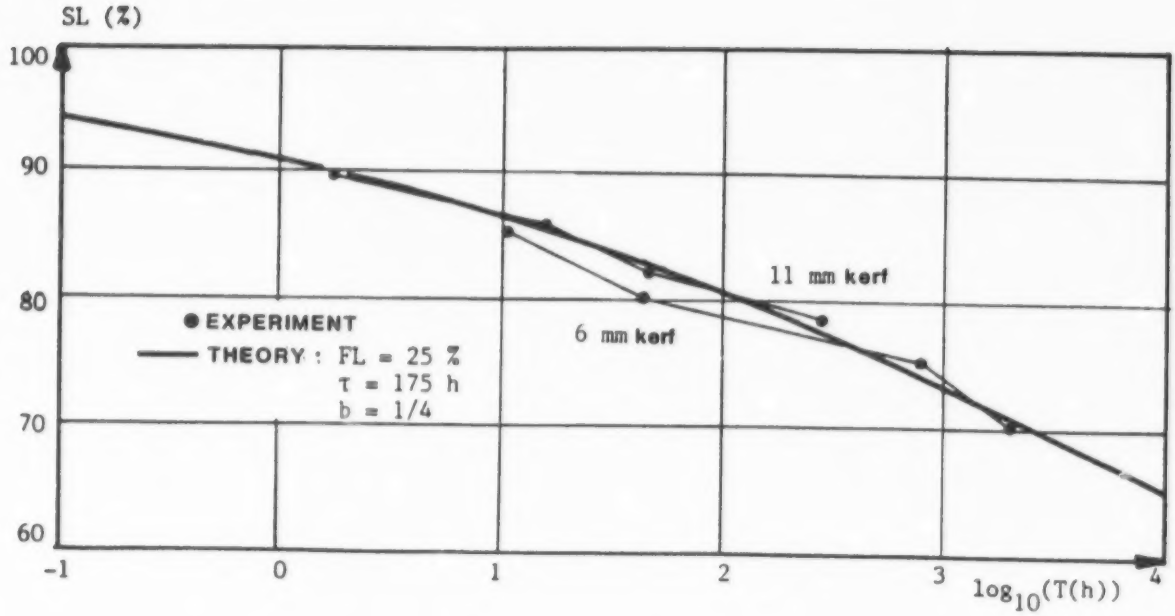

Figure 9. Dead load lifetime from the tests (Nielsen and Hoffmeyer, 1985) described in the text. Each experimental point is an average as determined by the theory of truncated populations. The heavy line is lifetime as predicted by Equation 3.

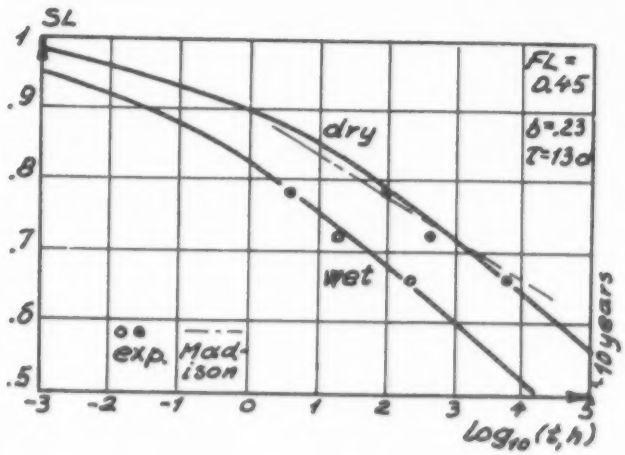

Figure 10. Dead load lifetime for dry and wet small beams made of artificially defected clear wood (Krebs, 1984; Hoffmeyer et al., 1985). Theoretical predictions by Equation 3 and Figure 1.

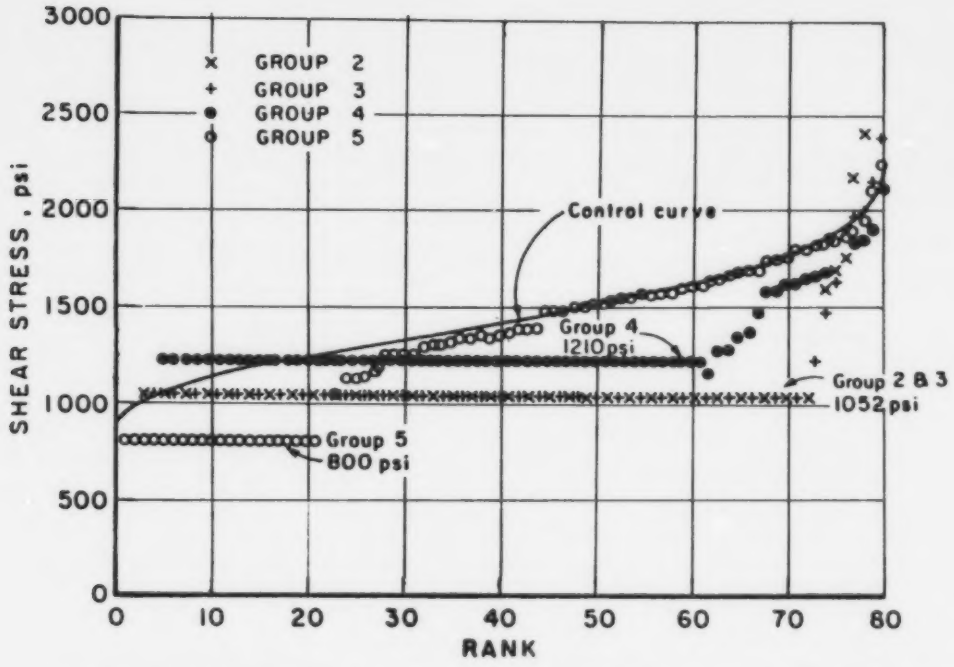

Figure 11. Shear strength as influenced by load history. The figure is reproduced from Spencer and Madsen (1984) which reports lifetime results from shear loaded, relatively small samples of clear wood (Douglas-fir).

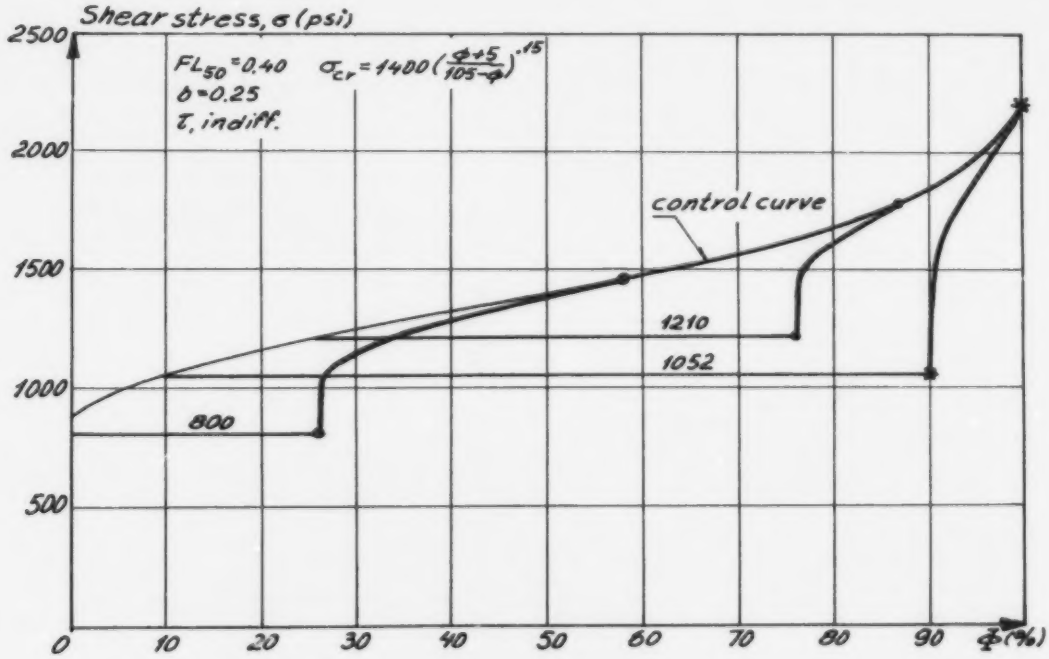

Figure 12. Theoretical prediction made by Equation 3 and Part I, Equation 67B, of the strength behavior observed in Spencer and Madsen (1984) on shear loaded clear wood members (see Figure 11).

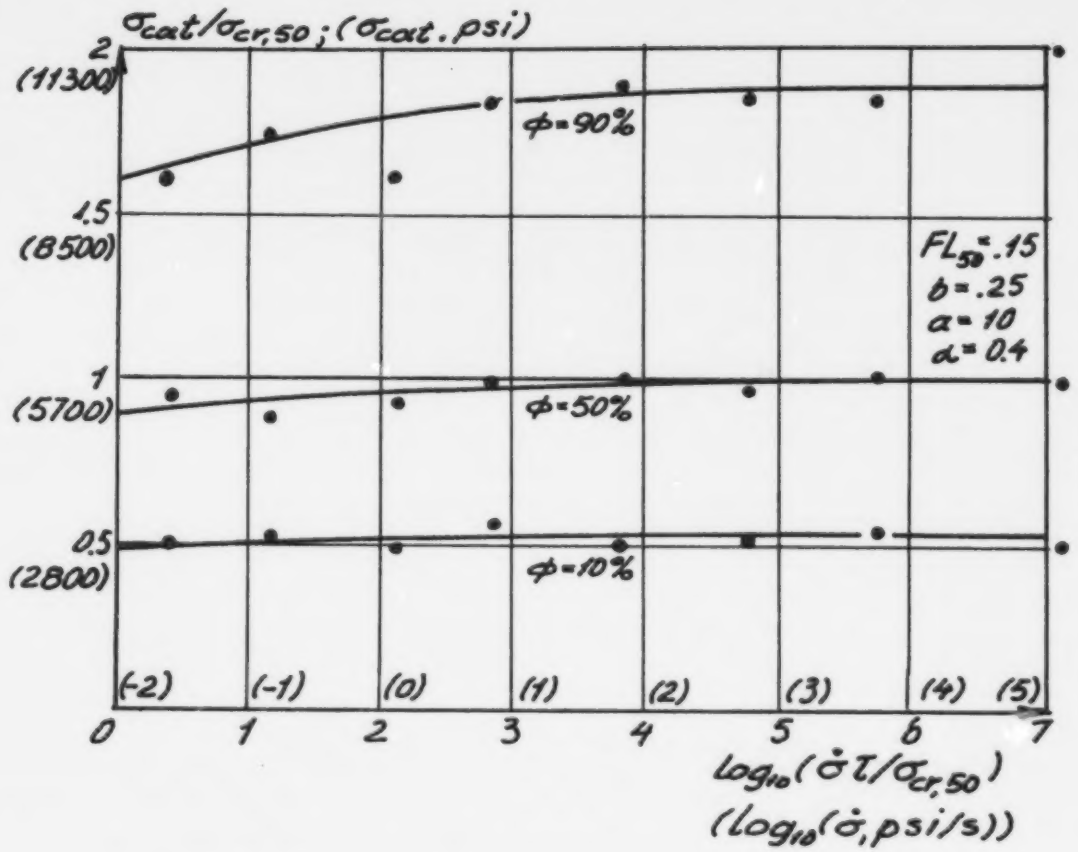

Figure 13. Ramp load strength, σ(cat), as related to rate of loading, $\dot{\sigma}$. Theoretical data (heavy lines) are predicted using Equation 52 of Part I with estimated (b,τ) = (0.25, 10 days) and a strength distribution (a,α) = (10,0.4) with σ(cr,50) = 5700 psi which for $0.1 < \phi < 0.9$ is close to the distribution found for Group 4 in Spencer (1979). The experimental values are from Spencer (1979, Figure 11).

RELIABILITY OF WOOD STRUCTURAL SYSTEMS

Ricardo O. Foschi

Prof., Civil Engineering Dept., University of British Columbia, Vancouver, B.C.

ABSTRACT

A methodology for the study of reliability in wood structural systems under load is presented. The approach implements duration of load effects by means of a damage accumulation model, and combines it with a structural analysis of the system. The reliability under a random, varying load is then calculated at the end of the intended service life for the structure. Both strength and serviceability limit states are considered. As an example, the reliability of a flat roof under snow loads is studied. Weather data from two Canadian cities (Vancouver and Quebec) are used, and allowable roof spans are derived to satisfy a target reliability at the end of 30 years. Load sharing and load duration adjustment factors are derived in relation to a design equation in Limit States Design format, with the condition that a prescribed reliability be associated with the resulting span.

INTRODUCTION

The implementation of reliability-based structural design presents a challenge to the utilization of wood in structural applications. Reliability assessment methods developed for other materials like steel cannot be applied directly to wood products (Foschi, 1979). This problem stems from special mechanical characteristics of wood, particularly the relationship between strength and the time under load. This "load duration" effect implies that the strength of a joist, for example, cannot be quantified until one defines the type and duration of the loads to which it is subjected. Thus, the joist might not fail immediately upon loading, but could fail over time if the same load is sustained. Load and strength are thus not independent variables, and their relationship is currently being investigated for special loading functions (Foschi and Barrett, 1982).

The reliability assessment for a wood structure requires that the load duration behavior be predictable for loading histories that occur in service. Thus, a mathematical model for extrapolation of test results to any loading function is required, and damage accumulation models have received substantial attention for the case of lumber (Foschi and Barrett, 1982; Gerhards, 1977).

Another aspect of reliability assessment in wood structures is that, because of the usually large variability in material properties, it is important to focus on the structural system rather than the single member. For example, to study the reliability of lumber joists in a realistic manner, one should consider their behavior in a floor system in combination with sheathing and a given type of fastener. Comprehensive structural analyses are required that, coupled with models for damage accumulation, allow the consideration of safety in the system during the prescribed service life.

The static structural analysis presented by Foschi (1982) for systems such as those shown in Figure 1 has been combined by the writer with the damage accumulation model examined in Foschi and Barrett (1982). This paper presents results from a study that, using this combination, considered the reliability of a flat roof under snow in two different locations in Canada. A direct implication of the results is the value of the performance, load sharing and duration of load adjustment factors to be used in a Limit States Design equation to ensure a target reliability at the end of the service life for the structure.

THE LIMIT STATES DESIGN EQUATION

It is customary to design the structure shown in Figure 1 using an equation that disregards the contribution of the sheathing and the fasteners to the overall strength and stiffness. The design equation for the reliability-based Limit States Design Canadian code, has form

$$\psi_D G_D R_D + \psi_L G_L R_C = \phi \tau_s(0.05) \qquad (1)$$

in which R_D = the permanent or dead load acting per joist or rafter; R_C = the live load, acting per joist or rafter and based on the Code-specified live load; ψ_D and ψ_L = load factors; G_D and G_L = geometric factors to transform loads into stresses; ϕ = the resistance or performance factor; and $\tau_s(0.05)$ = the characteristic strength for the material, which in the case of lumber has been defined as the 5th percentile of the "short-term" strength distribution.

The load factors ψ_D and ψ_L are specified for all materials, and the values adopted in Canada are ψ_D= 1.25 and ψ_L = 1.50. The factors, G_D and G_L, depend on the type of loading; for uniformly distributed loads, for example, G_D = 0.75 $L/(BH^2)$, where L = the span of the structure, B = joist or rafter width and H = its depth.

The performance factor, ϕ, must be determined so that the design achieves a desired reliability level. In the case of wood structures, the computation of ϕ must take into account the load history, the duration of load effect, the load sharing in the system and the intended service life. The target reliability can be specified in terms of a reliability index, β, as used for steel structures.

The following sections describe the calculation of the performance factor, ϕ, and its relationship to the reliability index, β, for the structure of Figure 1, under snow loading for the cities of Vancouver and Quebec and for an intended service life of 30 years.

LOADING

Snow is an intermittent load of a cyclic, random character. The distribution for the annual maximum load in a given location, as well as the mean number of days of ground snow, can be determined from weather data. However, there is little information on the duration of the load cycle, its actual shape or the probability of combination of snow and rain loads.

Nevertheless, and without loss of generality, consider the simplified load cycle of Figure 2. R_D = a permanent or dead load and R_i = the intensity of the live load cycle of duration Δ. Both R_i and Δ are considered to change randomly from cycle to cycle, and the duration of

the complete load cycle is Δ_c. In the case of snow, Δ_c is the duration of one year or 8,760 hours. The shape of the live load cycle is assumed given by

$$R_L = R_i \left(\frac{2z}{\Delta} \right)^m \qquad (2)$$

where R_L = the live load and z, as shown in Figure 2, = the time measured from the beginning of cycle Δ. Different cycle shapes can be represented by changing the exponent m but, for simplicity, it is assumed that m = 1.0. This implies that all live load cycles have triangular shape with randomly varying intensity, R_i, and duration Δ.

The distribution of annual maximum snow depth, d_i, can be represented by means of a Gumbel Type I distribution function,

$$d_i = U + \frac{[-\ln(-\ln p)]}{C} \qquad (3)$$

in which U and C = distribution parameters; and p = a random number from zero to one, uniformly distributed, giving the probability of having snow depths less than or equal to d_i. The parameters U and C have been obtained from weather data for different cities across Canada and are listed in Table 1 for Vancouver and Quebec.

In general, the live load R_i is composed of snow and rain. Information on the distribution of rain loads is not available and only the maximum rainfall over a period of 24 hours can be extracted from weather data for different locations. Without loss of generality, it is assumed that this rain load is superposed to snow with a probability p_r. Thus, the live load R_i can be written as follows:

$$R_i = \delta_s \left[U + \frac{-\ln(-\ln p)}{C} + 5.2\, I_r\, Q(q_r) \right] \qquad (4)$$

in which δ_s = the snow weight per unit area and per inch of accumulation (approximately 1 psf/in.); 5.2 = the ratio of water and snow weights per inch of accumulation; I_r = the maximum rainfall over 24 hours (in inches); and $Q(q_r)$ = a factor depending on the uniform random number, q_r $(0 \leq q_r \leq 1)$ and such that $Q(q_r) = 0$ if $q_r > p_r$ and $Q(q_r) = 1.0$ if $q_r \leq p_r$.

A characteristic load, R_o, can be chosen for design purposes. Let R_o be the superposition of the load, R_i, corresponding to p = 29/30 and the rain load for the maximum rainfall over 24 hours. Thus, the variability in live loads can be expressed by the ratio R_i/R_o as follows:

$$\frac{R_i}{R_o} = \frac{C\,U + [-\ln(-\ln p)] + 5.2\, C\, I_r\, Q(q_r)}{C\,U + 3.384294 + 5.2\, C\, I_r} \qquad (5)$$

Only a mean value is available for the duration Δ. It is assumed here that there exists a relationship between snow depth, d_i and Δ, such that deeper snows correspond to longer winters. Without loss of generality, it is assumed that this is a linear relationship, but such that the duration Δ cannot exceed a maximum Δ_{max} nor be less than Δ_{min}. Thus, from Equation 3

$$\Delta = \Delta_{min} + [\Delta(0.5) - \Delta_{min}] \left\{ \frac{CU + [-\ln(-\ln p)]}{CU + 0.366513} \right\} \qquad (6)$$

in which $\Delta(0.5)$ = the median duration; and the constant 0.366513 corresponds to letting p = 0.50 in Equation 3. If the results of Equation 6 exceed Δ_{max}, then $\Delta = \Delta_{max}$. The durations Δ_{max} and Δ_{min} are not available from weather data. For the purpose of this work, these durations have been approximately estimated as shown in Table 1.

DAMAGE ACCUMULATION

A model developed for accumulation of damage (Foschi and Barrett, 1982) can be used to determine the relationship between time-to-failure and stress history. Damage is a state variable normalized to take the value $\alpha = 0$ in the initial state and $\alpha = 1$ at failure. The rate at which the damage α accumulates is given in this model by

$$\frac{d\alpha}{dt} = a e^{\omega_1 R_N} \left(\frac{\tau(t)}{\tau_s} - \sigma_o \right)^b + \lambda e^{\omega_2 V_N} \alpha \qquad (7)$$

in which $\tau(t)$ = the applied stress history; τ_s = "short-term" strength in the initial state; a, b, λ, ω_1 and ω_2 = model parameters; σ_o = a threshold stress ratio; and R_N and V_N = standard normal random variables, which permit the modeling of the variability in rate of damage accumulation between specimens and, thus, for example, the variability in short-term strength.

Equation 7 applies as long as the stress-ratio, $\tau(t)/\tau_s$, exceeds the threshold σ_o. Below such threshold damage does not accumulate and loads can be sustained indefinitely. The short-term strength is obtained in a ramp load test of short duration (median time-to-failure of one minute, for example).

As shown in (Foschi and Barrett, 1982), ramp and constant load tests have been used to determine the model parameters in the case of hemlock lumber, 2 x 6 nominal size and grade "No. 2 and better":

$$\begin{aligned} a &= 0.721568 \times 10^{14}\,\text{hour}^{-1} \\ b &= 34.0 \\ \lambda &= 0.15 \times 10^{-2}\,\text{hour}^{-1} \\ \sigma_o &= 0.50 \\ \omega_1 &= 0.40 \\ \omega_2 &= 1.50 \end{aligned} \qquad (8)$$

The value $\sigma_o = 0.50$ implies that damage accumulates only if the specimen is stressed to more than 50 percent of its initial short-term strength. Since such stress levels are rarely achieved under design load, the threshold stress ratio may have a marked importance for the reliability of the system.

Equation 7 can be integrated for any stress history $\tau(t)$, and the corresponding time-to-failure can then be derived from the failure condition $\alpha = 1$. Two load histories are of importance for the purpose of this paper: 1) the ramp load used to obtain short-term strength, τ_s; and 2) the load cycle shown in Figure 2.

The strength τ_s is obtained in a ramp load test with rate k_s, so that the time-to-failure T_s satisfies $\tau_s = k_s T_s$. As shown in Foschi and Barrett (1982), T_s can be computed by integration of Equation 7 for any given random pair R_N and V_N.

Equation 7 can also be integrated for the load cycle in Figure 2, and the damage α_{i+1} at the end of the ith-cycle can be expressed in terms of the damage α_i at the beginning using the factors K_1, K_2, K_3 and K_4 as

shown in Appendix I. The relationship between α_{i+1} and α_i depends on the stresses τ_D and τ_i produced, respectively, by the dead load and the maximum intensity of the live load. Appendix I shows this relationship for three cases, depending on whether all stresses are below the threshold, only the live loads produce damage or this is accumulated by both the dead and the live loads.

COMPUTER SIMULATION AND RELIABILITY ANALYSIS

The factors K_2, K_3 and K_4 of Appendix I require the ratios τ_D/τ_s and τ_i/τ_s. These ratios correspond to the actual stresses τ_D and τ_i in the structure of Figure 1. These stresses will change from rafter to rafter, reflecting not only the distribution of the applied load but also the load-sharing resulting from the different rafter stiffnesses.

The stresses can be determined by a structural analysis program like FAP, as discussed in Foschi (1982). For convenience, these stresses can be related to those computeed on the basis of simple beam equations, considering only the joist as the resisting element. Thus, let

$$\tau_D = \gamma_D \, G_D \, R_D \tag{9}$$

$$\tau_i = \gamma_L \, G_L \, R_i \tag{10}$$

in which γ_D and γ_L = the "load sharing coefficients" determined from the structural analysis and corresponding, respectively, to dead and live loads. These factors will change, in general, from joist to joist.

Furthermore, if $\tau_s(0.5)$ = the median short-term strength for the joists and $T_s(0.5)$ = the median short-term time-to-failure,

$$\tau_s = \tau_s(0.5) \; \frac{T_s}{T_s(0.5)} \tag{11}$$

Thus, the ratio τ_i/τ_s required for the computation of the factors K_2, K_3 and K_4 can be determined as follows:

$$\frac{\tau_i}{\tau_s} = \gamma_L \, G_L \, R_D \; \frac{T_s(0.5)}{\tau_s(0.5) \; T_s} \; \left(\frac{R_i}{R_D}\right) \tag{12}$$

in which R_i/R_D is obtained from Equation 5.

Similarly, the ratio τ_D/τ_s can be expressed in the form

$$\frac{\tau_D}{\tau_s} = \gamma_D \, G_D \, R_D \; \frac{T_s(0.5)}{\tau_s(0.5) \; T_s} \tag{13}$$

In the computer simulation the following were kept constant:

1) the population of rafters, which were assumed to be 2 x 8 (nominal) Western hemlock, visual grade No. 2 and better;
2) the number of rafters (12), with the roof supported on all four sides;
3) the spacing of the rafters, s = 15.75 in. (400 mm);
4) the sheathing material, 5/8 in. Douglas-fir plywood panels, oriented with their face grain perpendicular to the direction of the rafters, and with properties as shown in Table 2;
5) the nailing between sheathing and rafters, 8d Bright Common nails (2 1/2 in. Common nails), spaced 6.0 in. (152.4 mm) o.c.; and
6) the probability of combination of maximum snow loads and rain, p_r = 0.20.

Simulation results were obtained for eight different cases, combining snow and rain data for two cities (Vancouver and Quebec) and four roof spans, L = 12 ft., 13 ft., 14 ft., and 15 ft. (3.66 m, 3.96 m, 4.27 m, and 4.57 m). A simulation flow chart is shown in Figure 3.

For each city and roof span, the simulation proceeded as follows. For each realization:

1. Twelve (12) pairs of standard normal random numbers, R_N and V_N, were chosen. As shown in Foschi and Barrett (1982), 12 short-term times-to-failure, T_s, were calculated and, from Equation 11, the corresponding short-term strengths, τ_s, were determined. These values were assigned to the 12 rafters in the roof.

2. Using the correlation between short-term strength τ_s and modulus of elasticity, E, a value of E was randomly assigned to each τ_s (i.e., each rafter), as shown in detail by Equations 19 to 21 later.

3. The E values were used in the structural analysis of the roof under uniformly distributed load. The analysis program was FAP, as described in Foschi (1982). The load sharing coefficients, γ_D and γ_L, were thus determined for each rafter. On the assumption that snow loads were uniformly distributed, $\gamma_D = \gamma_L$.

4. For each load cycle a pair of random numbers, p and q_r, were chosen and Equations 5, 12 and 13 were used to obtain, for that cycle, the stress ratios required for the factors K_1, K_2, K_3 and K_4 of Appendix I. Damage was thus accumulated, cycle per cycle, rafter per rafter. The pair of random numbers R_N and V_N used in the calculation of K_1, K_2, K_3 and K_4 were the same as those used for the determination of T_s for the corresponding rafter. For each cycle, the duration of the snow was determined from Equation 6.

5. Damage was accumulated for a maximum of 30 cycles (30 years) with Δ_c = 8,760 hours.

6. Assuming that failure of one rafter implies the strength limit state for the roof ("failure of the system"), three outcomes were possible at the end of, in general, N cycles: 1) the roof had failed before the N cycles had elapsed; 2) the roof failed during the Nth cycle; or 3) the roof did not fail up to and including the Nth cycle.

7. If the roof survived (N-1) cycles (outcomes 2 or 3), the value $R = R_D + R_i$ (total load) that would produce failure of the roof at the Nth cycle was computed. This value R is the residual strength of the roof conditional on the survival of (N-1) cycles. If the outcome was 2), R must be smaller than the last applied total load, and it was computed by an iterative process decreasing the intensity of the last load R_i until $\alpha = 1$ for the most damaged rafter. The cycle duration Δ was also adjusted to R_i according to Equations 5 and 6. If the outcome was 3), R must be greater than the last applied total load, and it was determined by iterations increasing the last R_i until $\alpha = 1$ for the most damaged rafter.

8. The residual strength, R at the Nth cycle, conditional on the survival of the previous (N-1) cycles, was computed at N = 1, 15 and 30 cycles (years).

9. The process was repeated from Step 1 for another selection of 12 rafters (another realization). Thus, each realization consisted of a different roof with a different load sequence.

For each of the eight combinations of city and span, the distributions of residual strengths, R, were obtained from a sample of 5,000 realizations.

The distribution of the total applied load at any cycle is the distribution of the variable $T = R_D + R_i$, which does not change from cycle to cycle, and was also obtained by simulation using 5,000 replications. Comparing the distributions for T and R at the Nth cycle, it is possible to estimate the probability of failure at the Nth cycle, conditional on the survival of the previous (N-1). Let such probability be θ_n, and let the total probability of failure after N cycles be P_n. Since

$$P_n = P_{n-1} + (1.0 - P_{n-1})\,\theta_n \qquad (14)$$

with $P_1 = \theta_1$, Equation 14 can be solved to obtain the total probability of failure after N cycles:

$$P_n = 1.0 - \prod_{i=1}^{N} (1.0 - \theta_i) \qquad (15)$$

The simulation results allowed the computation of the conditional probabilities θ_1, θ_{15} and θ_{30}. These were estimated by calculating the conditional reliability index, β_i, for the corresponding distributions using the Rackwitz-Fiessler algorithm (Rackwitz and Fiessler, 1978; Thoft-Christensen and Baker, 1982). Thus, knowing β_1, β_{15}, and β_{30}, θ_1, θ_{15} and θ_{30} were obtained from the general relationship

$$\theta = \Phi(-\beta) \qquad (16)$$

in which Φ = the standard normal distribution function.

In order to compute the total probability of failure after N years, Equation 15 requires θ_i for i = 1,....,N. These probabilities were estimated by using Equation 16 with values of β_i linearly interpolated between β_1, β_{15}, and β_{30}.

Finally, the total probability of failure at 30 years could be used directly as a measure of reliability at the end of the service life, or a total reliability safety index, β, could be obtained from

$$\beta = -\Phi^{-1}\,(P_{30}) \qquad (17)$$

The Rackwitz-Fiessler algorithm requires distributions for the variables R and T, so that the value and the slope of the cumulative distribution functions can be computed for any given value of the variables. These calculations were performed numerically, working directly with the ranked data obtained from the simulation. The iteration for the most likely failure point was stopped when two successive β's differed less than 0.001.

The reliability index concept was also applied to the serviceability limit state of maximum short-term roof deflection. In this case, the variable R must be interpreted as that load which, when applied, produces the maximum tolerable roof deflection. This limit is usually given as a fraction of the span, L/K. It is possible to write R as

$$R = \frac{384\,E_o\,I}{5\,K\,L^2\,\gamma_d} \qquad (18)$$

in which γ_d = a load sharing coefficient derived from the structural analysis, relating maximum roof deflection under uniform load to a reference deflection obtained by simple beam theory and the assumption of a nominal modulus of elasticity E_o. I = the moment of inertia of the rafter cross-section . The structural simulation permitted the determination, from the sample of 5,000 realizations, of the distribution of γ_d. Equation 18 can then be used to calculate the distribution of R required for the analysis of the serviceability limit state.

The simulation process hinges on information about the relationship between short-term strength and modulus of elasticity of the rafters. The results shown in this paper were obtained using short-term strength data for 2 x 8 (nominal) Western hemlock lumber, visual grade "No. 2 and better." For a median time-to-failure $T_s(0.5)$ = 1 minute, the median strength $\tau_s(0.5)$ was 6,475 psi (44.66 MPa), with a strength coefficient of variation of 0.40. The median, E, was 1.6×10^6 psi (11.03×10^3 MPa), with a coefficient of variation for E of 0.22.

The variability in E for a fixed τ_s was assumed to be normal with mean $\bar{E}$ and coefficient of variation C_v, which were expressed as functions of τ_s as follows:

$$\bar{E} = 1.0 + 0.86 \times 10^{-4}\,\tau_s \qquad (19)$$

$$C_v = 0.305 \times 10^{-1} \left(\frac{\tau_s}{1{,}000 - 0.875}\right)^{0.2257} \left(\frac{16.6 - \tau_s}{1{,}000}\right)^{0.6466} \qquad (20)$$

with $\bar{E}$ in 10^6 psi (6.9×10^3 MPa) and τ_s in pounds per square inch (6.9×10^{-3} MPa). Thus, for a given τ_s,

$$E = \bar{E}\,(1.0 + K_N\,C_v) \qquad (21)$$

in which K_N = a standard normal variable randomly chosen. Equation 20 applies between the minimum strength of 875 psi (6 MPa) and the maximum of 16,600 psi (114.5 MPa). This range is representative of No. 2 and better grade of 2 x 8 hemlock lumber. Figure 4 shows the correlation between τ_s (modulus of rupture, MOR) and E which results from the formulations just described.

RESULTS AND ANALYSIS

RELIABILITY ANALYSIS AND ALLOWABLE SPANS

Table 3 shows the load sharing coefficients, $\gamma_D = \gamma_L$, for uniformly distributed loads as a function of the roof span. The same table also shows the load sharing coefficient, γ_d, for maximum roof deflection, corresponding to a reference modulus of elasticity $E_o = 1.55 \times 10^6$ psi (10.69×10^3 MPa). It is important to notice that the coefficients of variation corresponding to the system's behavior are much smaller than the 0.22 corresponding to modulus of elasticity of single members.

Tables 4 and 5 present reliability analysis results for the two locations, Vancouver and Quebec City. These cities were chosen because they represent a wide range of snow loads, from heavy, small-variability loads in the case of Quebec City to light, but more variable loads in the case of Vancouver. In all cases, the dead load was assumed to be 10 psf (0.48 kN/m^2) and the snow design load was taken from the National Building Code of Canada (1980): 40 psf (1.9 kN/m^2) for Vancouver, and 80 psf (3.8 kN/m^2) for Quebec City. In all cases, a factor of 0.8 was applied to the NBCC loads to account for roof slope.

N_f, in Tables 4 and 5 is the expected number of failures during the period of 30 years, obtained by using the total probability of failure derived from the β-algorithm and Equation 15. N_f may be compared with the failures N_{fs} observed in the simulation over 5,000 trials of 30 cycles each. Such a comparison gives an assessment of the procedure described for β versus straight Montecarlo simulation. The reliability index, β, was also computed for the serviceability limit state of maximum short-ter, deflection equal to 1/180, 1/240 or 1/360 of the span. In this case, the load producing the limit state was computed from Equation 18, assuming that the load sharing coefficient, γ_d, was normally distributed and with statistics from Table 3. The results are also shown in Tables 4 and 5.

The determination of allowable spans requires the definition of target reliability levels for both limit states. According to the provisions developed for steel structures, an average reliability index β= 3.50 should also be recommended for wood in order to maintain a nearly uniform safety level across materials. On the other hand, a lower reliability could be tolerated for serviceability limit states. Let us assume reliability targets β= 3.50 for strength and β= 2.50 for maximum short-term deflection. Allowable spans corresponding to these targets can be interpolated (or extrapolated) from the data in Tables 4 and 5. The following interpolating expression was taken to represent the relationship between span L and reliability index β:

$$L = L_0 \exp.(-L_1 \beta) \qquad (22)$$

in which L_0 and L_1 = non-negative constants. In each case, Equation (22) was fitted to the data from Tables 4 and 5 to determine the span corresponding to the target reliability, and the results are also shown in the same tables. Figure 5 presents these results for Vancouver.

Current allowable spans in Canada for this type of roof, according to the Residential Standards issued by the National Building Code, are 177.0 in. (4.50 m) for Vancouver and 128.0 in. (3.25 m) for Quebec City. These spans apply to roofs without ceiling, for which the deflection limitation is L/180. Under this condition, Tables 4 and 5 show that the spans would be controlled by strength and that the current spans compare very well with those obtained for a target strength reliability, β= 3.50.

EFFECT OF DIFFERENT ASSUMPTIONS FOR DURATION OF LOAD BEHAVIOR

The assumptions made for threshold stress ratio, σ_0, in the damage accumulation model may have a direct effect on the computed reliability of the structure. An estimate of this parameter from the tests described in Foschi and Barrett (1982) is σ_0 = 0.50. In order to assess the importance of this parameter, or of duration of load modelling in general, two cases were considered: 1) σ_0 was reduced to 0.25, adjusting the other parameters in the model to produce the same behavior under constant load up to two months of loading; and 2) σ_0 was increased to 0.99, to approximately simulate neglecting all effects of duration of load. In this last case, the rafters' strength is given by their short-term strength, since stress ratios lower than 0.99 will not produce failure. For σ_0 = 0.25, the model parameters were $a = 0.333 \times 10^{11}(hr^{-1})$; b = 55.0; $\lambda = 0.15 \times 10^{-2}(hr^{-1})$; ω_1 = 0.40; and ω_2 = 1.50. For σ_0 = 0.99, $a = 0.12 \times 10^{7}(hr^{-1})$; b = 1.0; and the remaining as for the case σ_0 = 0.25.

Table 6 shows the results of these calculations. The ratio Ω between the allowable span corresponding to a given threshold stress ratio and that for "ignoring duration of load effects" (σ_0 = 0.99) is shown in Figure 6. For the snow loadings studied and for the target reliability considered, Figure 6 shows that neglecting duration of load effects results in a span approximately 10 percent longer than that corresponding to the model described by Equation 8. Similarly, the span for "no duration of load effects" is approximately 20 percent longer than for the model with σ_0 = 0.25. Since these differences were obtained with three models differing drastically in σ_0, these results imply that, from a practical point of view, duration of load modelling need not be described with high precision. For example, the accuracy with which σ_0 = 0.50 was estimated in Foschi and Barrett (1982) (between 0.45 and 0.55) appears to be adequate in relation to the end applications of the model.

LOAD SHARING EFFECTS

How is the reliability affected by the number of rafters in the roof? Table 7 shows the results corresponding to a single rafter and the allowable spans that are obtained for the same target reliability β= 3.50. These data can be directly used to derive a "load sharing factor", K_{LS}, which can be applied to the performance factor ϕ of Equation 1 for a single member, to obtain the factor ϕ for a multiple member system. Since R_D and R_C are proportional to L, as are G_D and G_L for uniformly distributed loads, Equation 1 implies that the performance factor is proportional to the square of the span L. Thus, the load sharing factor is the square of the ratio of the allowable spans obtained, at the same target reliability, for the multiple and the single member roof. The factors K_{LS} thus determined, using Tables 4, 5 and 7, are shown in Table 9. It is apparent that, although K_{LS} is not the same for both cities, the variation is sufficiently small and an average of 1.20 could be used in design. The load sharing factor assumed in current design practice is 1.15.

It should be noted that these results apply to a system with 12 rafters and that somewhat different load sharing factors would be obtained for roofs with a different number of members. Also, the load sharing factor, K_{LS}, can be shown to be dependent on the target reliability used, increasing with the target β.

DURATION OF LOAD ADJUSTMENT FACTOR USED IN DESIGN

How does the roof reliability under snow loads for 30 years compare with the case of snow design load assumed constantly applied for 10 years? The latter case is defined as "normal load duration" in current design recommendations. Results of reliability calculations for this case are shown in Table 8, as well as the allowable spans corresponding to $\beta = 3.50$. These results can be used to define a "duration of load adjustment factor", K_{LD}, as the square of the ratio of the allowable spans obtained, at the same target reliability, for the case of snow loads and that of 10-year constant snow design load. The factors K_{LD} are shown in Table 9, and an average value, $K_{LD} = 1.35$, can be used for both cities considered. Current duration of load adjustment factor for snow is 1.15.

EFFECT OF RAFTER VARIABILITY WITHIN A ROOF

The previous results were obtained for roofs with rafters randomly selected from the population. It is possible, however, that lumber pieces arriving at a job site do not represent such a random sample, because the package may contain lumber that was cut from an homogeneous stand or even from the same tree. The effect of reduced variability in rafter properties within a roof was studied by selecting, in the simulation, lots of 12 rafters with the condition that all 12 had moduli of elasticity E within $\pm$ 10 percent of the E selected for the first rafter. This first E was selected at random from the entire population. Such a criterion approximately corresponds to a rather small within-roof coefficient of variation for E of five percent.

The results are shown in Table 10. It is apparent that, at the target reliability levels chosen for the comparison, the effect of selection policy on allowable span is relatively minor. There is a general trend for allowable spans to be reduced for the case of restricted lot selection. As shown in Foschi (1982), random selection generally leads to higher maximum bending stresses in the rafters. However, these higher stresses tend to occur in rafters with higher modulus of elasticity (which thus share more of the load) and these, in turn, are likely to be stronger lumber pieces. In a more homogeneous lot of rafters, all pieces are more uniformly loaded, increasing the probability of failure of those which are weaker. Thus, even if random selection leads to higher maximum bending stresses, a randomly selected roof is slightly more reliable and allows marginally longer spans. Restricted selection also leads to somewhat shorter allowable spans for the serviceability limit state, and this effect becomes more important for more heavily loaded roofs and the more stringent the deflection criterion is.

LIMIT STATES DESIGN EQUATION - PERFORMANCE FACTORS

Equation 1 is the format of the strength limit states design equation adopted for the National Building Code of Canada. For the serviceability limit state of maximum short-term deflection, in the case of uniform loads, the value

$$\delta_{max} = \frac{5\,(R_D + R_C)\,L^3}{384\,\phi_E\,\bar{E}\,I} \qquad (23)$$

cannot exceed a maximum deflection prescribed as L/K, (K = 180, 240 or 360). $\bar{E}$ = the mean value of the modulus of elasticity for the population; and ϕ_E is a performance factor.

Knowing the allowable spans corresponding to the target reliabilities for strength and deflection, Equation 1 and Equation 23 can be used to compute the value of the performance factors, ϕ and ϕ_E. The characteristic strength, $f_s(0.05)$, for the lumber in this study was 2,490 psi (17.2 MPa).

Using the corresponding allowable spans of 175.15 in. (4.45 m) and 129.88 in. (3.30 m) from Tables 4 and 5, Equation 1 can be used to compute:

$$\begin{aligned} &\text{for Vancouver, } \phi = 0.771 \\ &\text{for Quebec, } \phi = 0.759 \end{aligned} \qquad (24)$$

These performance factors will result in spans with an associated reliability index, $\beta = 3.50$. They apply to a multiple member system under snow load for a period of 30 years. The factor ϕ may also be expressed as follows:

$$\phi = \phi_0\, K_{LS}\, K_{LD} \qquad (25)$$

in which ϕ_0 = the performance factor for a single member, under normal load duration conditions (snow design load applied constantly for 10 years). Using the factors $K_{LS} = 1.20$ and $K_{LD} = 1.35$ derived in the previous section, ϕ_0 is found to be

$$\begin{aligned} &\text{for Vancouver, } \phi_0 = 0.476 \\ &\text{for Quebec, } \phi_0 = 0.468 \end{aligned} \qquad (26)$$

It is apparent from Equations 24 or 26 that the performance factor is nearly uniform between these two locations, and that an average value $\phi_0 = 0.47$ can be used. Thus, Equation 1 becomes

$$1.25\, G_D\, R_D + 1.50\, G_L\, R_C = 0.47\, f_s(0.05)\, K_{LS}\, K_{LD} \qquad (27)$$

with $K_{LS} = 1.20$ and $K_{LD} = 1.35$. Similar calculations can be performed to determine the performance factor, ϕ_E, for the serviceability limit state of maximum short-term deflection. These are listed in Table 11, showing a small variation with the limit state definition and slightly lower values for a more heavily loaded roof. The results of Table 11 also tend to approximately justify current use of the mean E to compute deflections under design load.

CONCLUSION

A methodology for the assessment of reliability in wood structural systems under load has been presented. The approach refers both to serviceability as well as strength limit states. In the latter case, the procedure involves the implementation of damage accumulation models for load duration effects in structural analyses, so that the reliability of the structure can be determined at the end of its intended service life.

Although based on Monte Carlo simulation to account for the complex interaction between system load-sharing, load sequence and damage accumulation, the method presented makes use of conditional reliability indices to estimate reliability for different service lives, without resorting to individual simulations for each one. The method represents a systematic approach to the problem and can be

used as a "benchmark" to assess the performance of simpler procedures that may be proposed to estimate reliability in design. There is a need, at the developmental stage of design recommendations, to have such a comparison tool. The methodology can serve two objectives: 1) the calculation of performance factors in reliability-based design equations; and 2) the determination of reliability levels for "baseline" structures accepted as safe and adequate, and to which the design of future structures could be calibrated.

The procedure described requires data on loadings and on material behavior that are not available at present. In particular, creep behavior for lumber should be incorporated into the study of serviceability limit states, but such data are very limited at the moment.

Finally, the method may be used to assess the influence that different materials (e.g., panel products, fasteners), construction techniques, or quality control procedures (e.g., machine graded lumber) may have on the reliability of the structural system. As such, the method represents a first step towards a comprehensive engineering analysis of a wood light-frame system, with the objective of optimizing the end use performance and achieving an efficient use of the resource.

ACKNOWLEDGEMENT

The work presented here was supported by a research contract awarded to Forintek Canada Corp. by the Canadian Forestry Service, Environment Canada, No. 41SS-KL229-1-4102.

This paper is a reprint from the Journal of Structural Engineering, Vol. 110, No. 12, December, 1984 with permission from the ASCE.

REFERENCES

Foschi, R.O. 1979. A discussion on the application of the safety index concept to wood structures. Canadian Journal of Civil Engineering 6(1):51-58.

Foschi, R.O. 1982. Structural analysis of wood floor systems. J. Structural Division, ASCE 108(ST7)(July).

Foschi, R.O. and J.D. Barrett. 1982. Load duration effects in western hemlock lumber. J. Structural Division, ASCE 108(ST7)(July).

Gerhards, C.C. 1977. Time-related effects of loads on strength of wood. IN: Proc. Environmental Degradation of Engineering Materials Conference, College of Engineering, VPI, Blacksburg, VI.

Rackwitz, R. and B. Fiessler. 1978. Structural Reliability under Combined Random Load Sequences. Comput. Struct. (9):489-494.

Thoft-Christensen, P. and M. Baker. 1982. Structural Reliability Theory and Its Applications. Springer-Verlag, New York, N.Y. p.108.

APPENDIX I - CYCLE DAMAGE ACCUMULATION RELATIONSHIPS

Let $$f = \sigma_0 \frac{\tau_s}{\tau_i} - \frac{\tau_D}{\tau_i} \tag{28}$$

and $$K_1 = \exp\left[\lambda e^{\omega_2 V_N} (\Delta c - \Delta)\right] \tag{29a}$$

$$K_2 = \frac{a e^{\omega_1 R_N}}{\lambda e^{\omega_2 V_N}} (K_1 - 1.0) \left(\frac{\tau_D}{\tau_s} - \sigma_0\right)^b \tag{29b}$$

$$K_3 = \exp\left[\lambda e^{\omega_2 V_N} \Delta \left(1 - \frac{2z_0}{\Delta}\right)\right] \tag{29c}$$

$$K_4 = a e^{\omega_1 R_N} \cdot \frac{\Delta}{4} \left(1 - \frac{2z_0}{\Delta}\right) \cdot \int_{-1}^{1} \left\{ \exp\left[\lambda e^{\omega_2 V_N} \cdot \Delta \left(1 - \frac{2z_0}{\Delta}\right) \frac{(3-\xi)}{4}\right] + \exp\left[\lambda e^{\omega_2 V_N} \cdot \Delta \left(1 - \frac{2z_0}{\Delta}\right) \frac{(1+\xi)}{4}\right] \right\} \left\{ \frac{\tau_D}{\tau_s} + \frac{\tau_i}{\tau_s} \left[\frac{2z_0}{\Delta} + \left(1 + \frac{2z_0}{\Delta}\right) \frac{(1+\xi)}{2}\right]^m - \sigma_0 \right\}^b d\xi \tag{29d}$$

Table 1

Snow Weather Data

City	C	U	I_r (in.)	Δ_{min} (hr.)	$\Delta(0.5)$ (hr.)	Δ_{max} (hr.)
Vancouver	0.181	2.69	2.69	48.0	168.0	984.0
Quebec	0.140	39.30	1.07	2520.0	3360.0	3888.0

Note: 1 in. = 25.4 mm.

Table 2

5/8 Inch Douglas-fir Plywood Properties

Property, per unit width	Parallel to face grain	Perpendicular to face grain
Bending stiffness, in pounds-square inches per inch	28,000	9,000
Torsional stiffness, in pounds-square inches per inch	1,800	1,800
Axial stiffness, in pounds per inch	430,000	340,000
Shear stiffness, in pounds per inch	60,000	60,000

Note: 1 lb. = 4.45 N; 1 in. = 25.4 mm.

Table 3

Load Sharing Coefficients,
Uniformly Distributed Loads

Span		$\gamma_D = \gamma_L$		γ_d [a]	
(in.)	(m)	Mean	C.O.V.[b]	Mean	C.O.V.
144.0	3.66	1.025	0.064	0.893	0.080
156.0	3.96	1.016	0.067	0.856	0.077
168.0	4.27	1.007	0.069	0.825	0.076
180.0	4.57	0.997	0.070	0.797	0.074

[a] Corresponding to $E_0 = 1.55 \times 10^6$ psi (10.7×10^3 MPa).

[b] C.O.V. = coefficient of variation.

Table 4

Reliability Analysis and Allowable Spans for Vancouver

Span		Conditional			β, Strength Limit State (30 years)	N_f	N_{fs}	Serviceability Limit State, β (Max. roof deflection)			Limit State	Reliability Index, β	Allowable Spans	
(in.)	(m)	β_1	β_{15}	β_{30}				L/180	L/240	L/360			(in.)	(m)
144.0	3.66	5.12	5.12	5.12	4.44	0	0	5.40	4.15	2.80	Strength	3.50	175.15	4.45
156.0	3.96	4.78	4.78	4.78	4.04	0	0	4.29	3.31	2.21	L/180 maximum deflection	2.50	193.15	4.91
168.0	4.27	4.40	4.40	4.41	3.60	1	0	3.75	2.81	1.73	L/240 maximum deflection	2.50	174.84	4.44
180.0	4.57	4.28	4.28	4.29	3.45	1	1	3.36	2.33	1.23	L/360 maximum	2.50	150.05	3.81

Note: N_f: predicted number of failures in 5,000; 30 years.
N_{fs}: number of failures observed in the simulation over 5,000 replications; 30 years.

Table 5

Reliability Analysis and Allowable Spans for Quebec

Span		Conditional			β, Strength Limit State (30 years)	N_f	N_{fs}	β, Serviceability Limit State (Max. roof deflection)			Limit State	Reliability Index, β	Allowable Spans	
(in.)	(m)	β_1	β_{15}	β_{30}				L/180	L/240	L/360			(in.)	(m)
144.0	3.66	3.68	3.81	3.76	2.83	12	37	3.26	2.08	0.11	Strength	3.50	129.88	3.30
156.0	3.96	3.24	3.44	3.42	2.32	51	82	2.47	1.18	-1.08	L/180 maximum deflection	2.50	154.98	3.94
168.0	4.27	2.91	3.13	3.33	1.91	140	194	1.67	0.22	-2.28	L/240 maximum deflection	2.50	139.91	3.55
180.0	4.57	2.49	2.82	2.92	1.38	421	465	0.83	-0.75	-3.45	L/360 maximum deflection	2.50	124.32	3.16

Table 6

Reliability Analysis, Influence of Threshold Stress Ratio σ_o

City	Threshold Stress Ratio σ_o	Span (in.)	Span (m)	N_f	N_{fs}	β, Strength Limit State (30 years)	Allowable Span (β = 3.5) (in.)	Allowable Span (β = 3.5) (m)
Vancouver	0.25	144.0	3.66	0	0	4.34	166.73	4.23
		156.0	3.96	0	1	3.73		
		180.0	4.57	4	6	3.16		
	0.99	144.0	3.66	0	0	4.97	195.33	4.96
		156.0	3.96	0	0	4.41		
		180.0	4.57	0	0	3.95		
Quebec	0.25	144.0	3.66	324	446	1.52	107.95	2.74
		156.0	3.96	987	984	0.85		
		180.0	4.57	2619	2681	-0.06		
	0.99	144.0	3.66	3	3	3.25	143.21	3.64
		156.0	3.96	3	3	3.24		
		180.0	4.57	69	65	2.20		

Table 7

Reliability Analysis, Single Member

City	Span (in.)	Span (m)	N_f	N_{fs}	β, Strength Limit State (30 years)	Allowable Span (β = 3.5) (in.)	Allowable Span (β = 3.5) (m)
Vancouver	144.0	3.66	0	0	3.91	162.12	4.12
	156.0	3.96	1	0	3.70		
	180.0	4.57	5	4	3.08		
Quebec	144.0	3.66	28	30	2.53	116.97	2.97
	156.0	3.96	102	96	2.05		
	180.0	4.57	368	350	1.45		

Table 8

Reliability Analysis, Constant Snow Design Load over 10 years

City	Span (in.)	Span (m)	β, Strength Limit State (10 years)	Allowable Span (β = 3.50) (in.)	Allowable Span (β = 3.50) (m)
Vancouver	144.0	3.66	3.75	149.92	3.81
	156.0	3.96	3.24		
	180.0	4.57	2.48		
Quebec	144.0	3.66	1.93	111.79	2.84
	156.0	3.96	1.41		
	180.0	4.57	0.54		

Table 9

Adjustment Factors for Load Sharing and Duration of Load

City	Reliability Index β = 3.50	
	K_{LS}, Load Sharing	K_{LD}, Duration of Load[a]
Vancouver	1.167	1.365
Quebec	1.233	1.350
Average	1.20	1.35

[a] From 10 years of constant snow design load to actual load over 30 years.

Table 10

Allowable Spans, in Inches, Random versus Lots Restricted Selection[a]

City	Selection Type	Strength (β = 3.5)	Serviceability (Max. Roof Deflection) (β = 2.5)	
			L/240	L/360
Vancouver	Random	175.15	174.84	150.05
	Restricted Lots	171.72	175.23	149.60
Quebec	Random	129.88	139.91	124.32
	Restricted Lots	127.11	136.96	116.87

[a] Stiffness coefficient of variation within a lot ≅ 5%.
Note: 1 in. = 25.4 mm.

Table 11

Serviceability Limit State - Performance Factor ϕ_E

City	Maximum Deflection (β = 2.50)		
	L/180	L/240	L/360
Vancouver	1.01	1.00	0.95
Quebec	0.92	0.90	0.88

Table 12

Cycle Damage Accumulation Relationships

If	$2z_0/\Delta$	Cycle Damage Accumulation	
$f \geq 1$	-	$\alpha_{i+1} = \alpha_i$	
$0 \leq f < 1$	$f^{1/m}$	$\alpha_{i+1} = K_3\alpha_i + K_4$	
$f < 0$	0.0	$\alpha_{i+1} = K_1K_3\alpha_i + K_2K_3 + K_4$	(30)

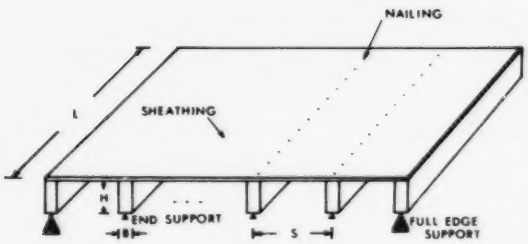

Figure 1. Roof structure.

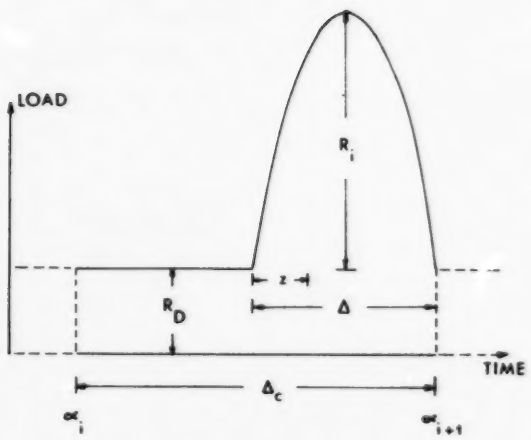

Figure 2. Dead and live load cycle.

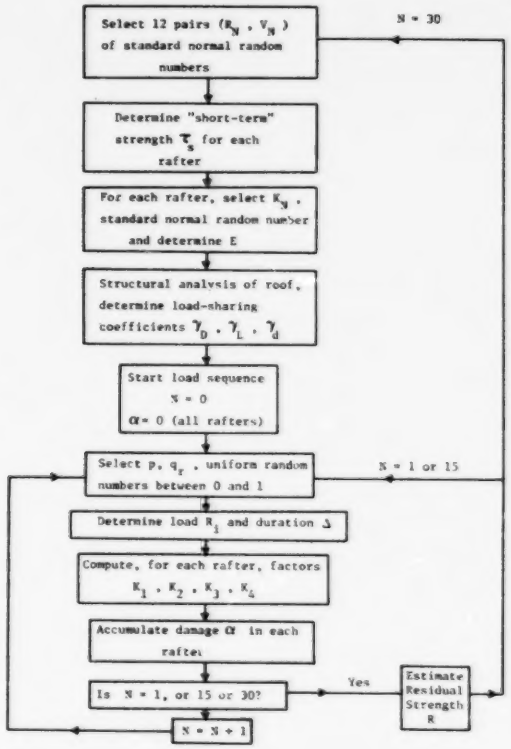
Select 12 pairs (R_N , V_N) of standard normal random numbers
N = 30
Determine "short-term" strength τ_s for each rafter
For each rafter, select R_N , standard normal random number and determine E
Structural analysis of roof, determine load-sharing coefficients γ_D , γ_L , γ_d
Start load sequence
N = 0
α = 0 (all rafters)
Select p, q_r , uniform random numbers between 0 and 1
N = 1 or 15
Determine load R_i and duration Δ
Compute, for each rafter, factors K_1 , K_2 , K_3 , K_4
Accumulate damage α in each rafter
Is N = 1, or 15 or 30?
Yes
Estimate Residual Strength R
N = N + 1

Figure 3. Simulation procedure - flow chart (per realization).

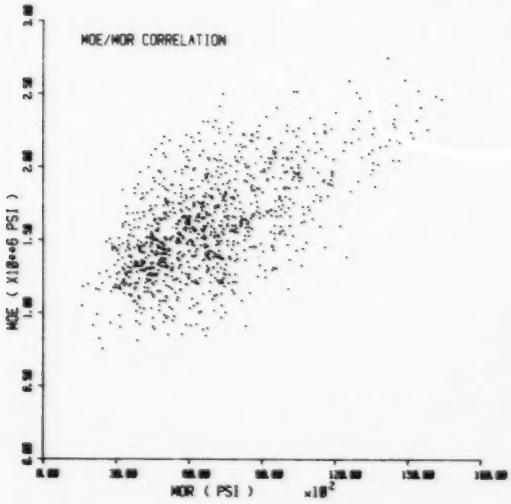

Figure 4. Correlation between bending strength (MOR) and modulus of elasticity (MOE).

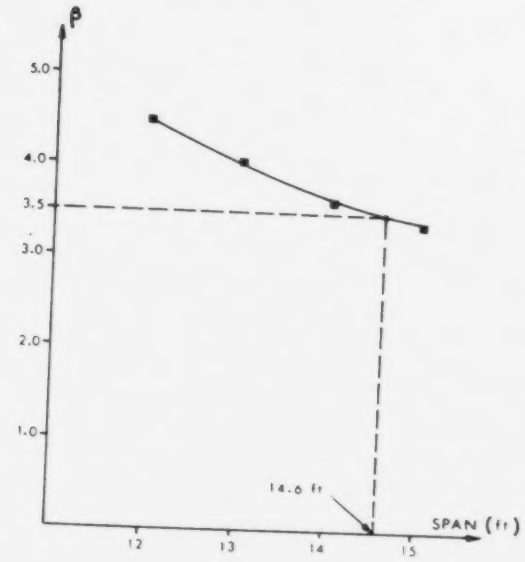

Figure 5. Reliability index versus span, Vancouver (1 ft. = 0.305 m).

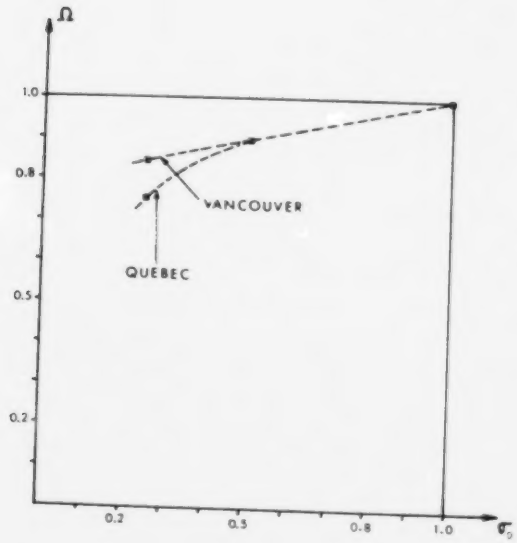

Figure 6. Ratio Ω between allowable spans for threshold stress ratio, σ_0, and for no duration of load effects ($\sigma_0 = 1$), $\beta = 3.5$.

APPLICATION OF DURATION OF LOAD INFORMATION TO TIMBER DESIGN CODES

Borg Madsen
Professor, Department of Civil Engineering
University of British Columbia, Vancouver

INTRODUCTION

Curves for experimental DOL data for lumber all appear to have a flat portion in the beginning followed by an increasing sloping line when the data was plotted using a logarithmic time scale. The curvature of these lines was opposite to the Madison curve. However, it is interesting to note that if Lyman W. Wood had interpreted the small, clear test results in isolation and not considered the impact tests or the rapid ramp load data he might well have arrived at the same conclusion.

Figure 1 shows the data from the 126 tests with matched clear specimens. The centroid of the points on each stress ratio is highlighted and a curve is drawn through these points. Amazingly, the curve has the same curvature as the one for lumber.

THE NATURE OF THE SPECIFIED LOADS

GENERAL

Most of the DOL research to date has been concentrated on investigating the long-term material behavior of lumber. Relatively little attention has been given to the duration of the loads. It may therefore be relevant to review the philosophy behind the establishment of the specified loads.

Steel and concrete engineers are not concerned with the length of time the loads act on the structure, thus only maximum loads are stated in the design code. It is left to the timber code to recommend the duration for the different types of loads acting on the structure. In order to provide such recommendations, it is vital for the timber engineer to fully understand how the magnitudes of the specified loads were derived. A short review is given below.

CLIMACTIC LOADS

a) Earthquake Loads. The maximum ground acceleration occurring with a return period of 100 years forms the basis for calculating the forces which will be created in the structure. On the simplest level of earthquake design, the mass of the structure is multiplied by a series of rather crude factors, each modeling one aspect of the site or the construction of the building including the acceleration, to obtain an equivalent static loading. Member forces are then obtained from normal structural analysis.

The chosen earthquake magnitude is of course a rare event and when it does occur it will last only for a few minutes. It is obviously a very short term loading even if the times that the structure experiences these maximum loads are added up over the lifetime of the structure.

b) Wind Loads. These loads are, for structural members, established from wind velocity measurements with a 30-year return period. The wind velocities are converted to approximate wind pressures by applying a series of crude factors representing different conditions occurring in the building being considered. The time that the maximum wind load will last, when it does occur, will be in the order of minutes and the accumulated effect over the life of the structure will be in the order of a few hours at the most.

c) Snow Loads. The specified snow loads are established from observations of the maximum accumulated ground snow which will occur with a 30-year return period. However, to that estimated mass is added the mass of the maximum 24-hour rainfall occurring in the same calendar month as the snow was observed to obtain the design ground snow load. The mass of the 24-hour rainfall can be substantial and if it is more than 50 percent of the accumulated snow only 50 percent of the snow load is added. To obtain an estimate of the design roof snow load the design ground snow load is multiplied by factors accounting for the shape of the roof, snow drifts, exposure to wind, etc.

The specified design load assumes that a maximum snow load accumulation with a 30-year return period will have a 24-hour maximum rainfall superimposed. This would be a rare event. However, the question is how long will that loading combination last on a roof. No doubt some of the rain will drain off over a period of a couple of days, thus reducing the intensity of the assumed load. It is not unreasonable to assume that the maximum snow load will last only a couple of days or may be a week at the most. (Structures in mountain passes or subjected to similar conditions may be considered exceptions.)

FLOOR LOADS

General

To discuss DOL as it relates to floor loads it is convenient to divide the floor loads into two groups. The first group (Group A) will be those floors where the presence of human beings has been taken into account, while the second group (Group B) consists of floors intended for storage.

Group A

In this group, three live load components exist in addition to dead loads. The first component would be furnishings associated with the occupancy. In an office that would be desks, filing cabinets, chairs, etc.; these loads are relatively constant over a long period of time but may change in magnitude when the space is leased to a new occupant.

A survey of 625 offices conducted for the National Bureau of Standards (Culver, 1976) showed that the average load was 0.43 kN/m^2 with a standard deviation of 0.26 kN/m^2. (Specified load for offices is 2.4 kN/m^2.) The survey also showed that filing cabinets and other heavy items most often are placed along the walls, so they may not contribute fully to the bending moments. However, during maintenance or moving of the tenant, these heavy items may well be moved to the centre of the floor, but only for a short time.

The second component is load caused by people during normal business conditions. This would be an intermittent load acting for about eight hours and absent for about 16 hours. It is a

very small load since 4 to 6 m^3 are required for each office worker, i.e. about 0.15 kN/m^2. In the vicinity of service counters, the load can be considerably higher.

The third component considered is from human beings under emergency conditions. It could happen that many people would have to crowd together during fire. Such an occurrence would last only for a short period of time. Figure 2 gives an impression of the number of people required to cause the stated loads. The people are contained within an area of 2 m x 2 m.

The point to be discussed here is not the magnitude of the specified floor loads--that decision is left to the committee on loads--but rather the length of time these specified loads can be expected to last. A residential floor, for instance, is to be designed for 1.9 kN/m^2 which means that about 54 persons would have to congregate in a 4 m x 5 m living room in order to achieve that load per m^2. It is an unlikely event. Should it ever occur, one can be sure that it would not last for a protracted period.

Similar considerations can be made for the other occupancies, where people loads are included. It is evident that these specified loads will only act for short periods of time.

Group B

Storage loads are different because they could act on the structure for extended periods of time. In these cases, a conservative approach is justified. Timber floors, however, are seldom used for such applications.

DURATION OF LOAD MODELS

Several DOL models were presented at the meeting. Two of them, the Foschi and Barrett cumulative damage model and the visco-elastic fracture mechanics model proposed by L. Fuglsang Nielsen, are shown in Figure 3 together with the Madison curve.

The differences between the two new models are not large. They both indicate that the Madison curve leads to conservative results for loads lasting less than about two years, but that the Madison curve is not conservative for loads lasting longer than two years. The Nielsen model predicts that the DOL effect is strength dependent, therefore it is presented with two curves; one for 10.0 MPa and another for 22.8 MPa. The curves are depicted using the traditional logarithmic time scale. This is an elegant way to present the trend, but it may be misleading for the reader not used to perceiving time as a logarithm. The curves are replotted in Figure 4 (a, b, c and d) using a real-time scale. In that presentation it can be seen that the curves are very flat. If an engineer makes the judgement that the specified loads will act on his structure for two weeks but it turns out that he had underestimated the time by a factor of five and that the load acted for 10 weeks, he would have made an error of only a few percentage points in the stress ratio.

DESIGN CONSIDERATIONS

An important design consideration is the length of time the member is loaded to a high stress ratio during the lifetime of the structure, since it is only at high stress ratios that significant damage occurs.

In the Limit States Design (LSD) format, the ultimate strength limit for lumber can be reached in two different manners:

a) A member could fail because the actual load is greater than the specified load anticipated by the design.

b) The member could fail because the specified load acts for a longer time period than anticipated by the design.

Condition (a) is common for all structural materials and is accounted for in the formulation of the LSD design criteria:

$$\omega \cdot R = 1.25\ D.L. + 1.5\ L.L.$$

where, ω = resistance factor
R = short-term strength
D.L. = dead load
L.L. = live load

Condition (b) is unique to timber and will be discussed in the following examples.

Example 1

A beam in a flat roof is carrying a snow load. Initially we assume that $\omega = 1$ and $R = 20$ MPa. The dead load is 0.6 kN/m^2 and the specified snow load is 1.8 kN/m^2, i.e.:

ground snow = 3.0 kN/m^2 exposed
ground snow = 2.3 kN/m^2 shielded

The beam will be designed for:

$$1.25 \times 0.6 + 1.5 \times 1.8 = 3.45\ kN/m^2$$

This factored load will last only for a short time should it occur due to some freak condition. The stress ratio (SR) for D.L. alone is equal to:

$$SR = \frac{0.6}{3.45} = 0.17$$

Using Figure 5, where the Nielsen model is presented, it can be seen that this stress ratio can be sustained by the beam for eons. (The Nielsen model has been chosen for this investigation because it is more conservative than the Foschi-Barrett model.)

The stress ratio created by the specified load is:

$$SR = \frac{0.6 + 1.8}{3.45} = 0.70$$

Figure 5 shows that this stress ratio can be sustained for 7.7 months. Keeping in mind that the specified load was established as the maximum snow accumulation occurring with a 30-year return period followed by a maximum 24-hour rainfall, it is not unreasonable to accept that the structure is all right, since the 7.7-month period is much longer than the duration over which the specified load will act.

In the example above, the resistance factor ω was kept equal to unity. In a real design case the resistance factor would be less than unity, which increase the time the load could be sustained. The times to failure, in years--or the time the load can be sustained--are shown in Table 1 for stress ratios caused by different percentages of the specified loads. Three values of ω are used in Table 1. The table shows that the length of time a specific load can be sustained is increased greatly by a lower resistance factor.

From this example it is evident that the governing design criterion is a sum of the specific loads multiplied by the load factors. Having designed the member for this short-term loading condition, it is shown that the stress ratios resulting from the specified loads (design criterion (b)) can be endured for a much longer time than the duration of specified loads. In other words, the DOL effect need not be considered in this case. The argument can be extended to all the other climactic loads, as well as to floor loads, where the presence of humans is part of the loading considerations.

STORAGE LOADS

An example of a floor beam used for a storage application is shown below. Again we start with $\omega = 1.0$ and $R = 20$ MPa. Let the dead load be $1.0\ kN/m^2$ and the live load $6.0\ kN/m^2$.

The beam will be designed for a factored load of:

$$1.25 \times 1.0 + 1.50 \times 6.0 = 10.25\ kN/m^2$$

so the stress ratio for the specified load will be:

$$SR = \frac{1.0 + 6.0}{10.25} = 0.68$$

That stress ratio can only be sustained for a nine-month period, which is unacceptable for storage occupations. To overcome this the following design procedure is suggested:

1) Estimate the total time the storage load will act on the structure. Let us assume that 10 years is the estimate.

2) Apply a factor α_{TIME} to reflect the time estimate. Let us use $\alpha_{TIME} = 3.0$.

3) Multiply the time estimate by α_{TIME}, i.e. $3 \times 10 = 30$ years.

4) Using the chart with 30 years and R = 20 MPa one finds a stress ratio of 0.48.

5) Design the beam using a revised strength equal to 0.48 R (0.48 x 20 MPa).

This method will satisfy design criterion (b) with an allowance for the uncertainty in the time estimate.

CONCLUSIONS

A few observations have been made in the above discussion which can be summarized under the following headings:

Loads

The specified loads have been selected to represent rare events. They will, when they occur, only last for a short period of time--a matter of a few days. (Exception: storage loads and extreme snow conditions.)

DOL Behavior

The DOL effect in timber is represented by a flat curve when stress ratio is plotted over real time. This shows that the DOL effect is rather insensitive to errors in the estimate of the length of time the load acts on the structure.

Design Criteria

The ultimate limit state for timber can be reached in two ways:

a) A member can fail because the actual load is greater than the specified load anticipated by the design.

b) A member can fail because the specified loads act for a longer time period than anticipated by the design.

Design for Short-Term Loads

An example showed that for short-term loads (climactic loads and loads based upon human congregation under emergencies) the design criterion (a) is governing, resulting in stress ratios for dead load only and for dead load plus the specified live load, so low that they can easily be sustained for time periods much longer than their duration on the structure.

Resistance Factor ϕ

The use of a resistance factor of less than unity lengthens the times that the loads can be sustained to a point where DOL considerations can be omitted.

Design for Long-Term Loads

A design method is proposed for those few cases (mainly storage applications) where the specific loads act on the structure for an extended period of time.

Summary

Based upon the newly developed models for predicting the long-term strength of lumber, it appears that the DOL phenomenon is of less importance than previously assumed.

Duration of load considerations can be ignored for most load cases, with the exception of storage loads and extreme snow loads. Therefore, most timber structures can be designed in the same manner as other structures.

REFERENCE

Culver, C.G. 1976. Survey Results for Live Loads and Live Loads in Office Buildings. Center for Building Technology, National Bureau of Standards, Washington, D.C. NBS Building Science Series Report No. 85.

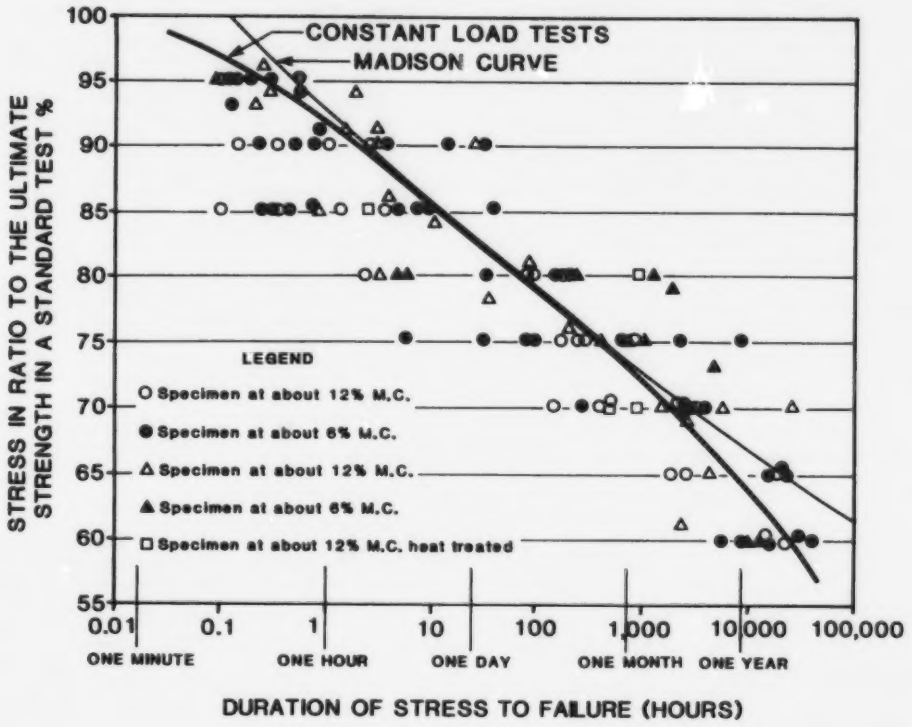

Figure 1. Madison constant load tests and Madison curve.

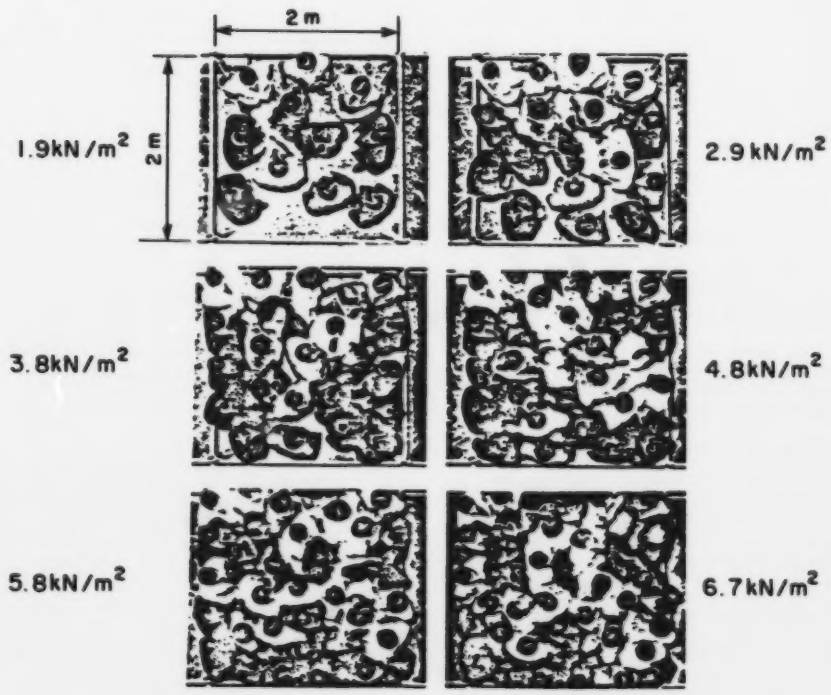

Figure 2. Human loads.

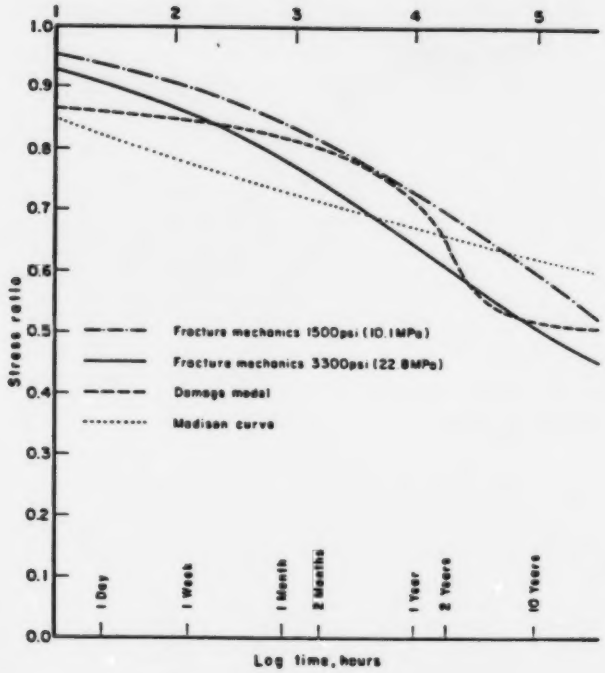

Figure 3. DOL curves with logarithmic time scale.

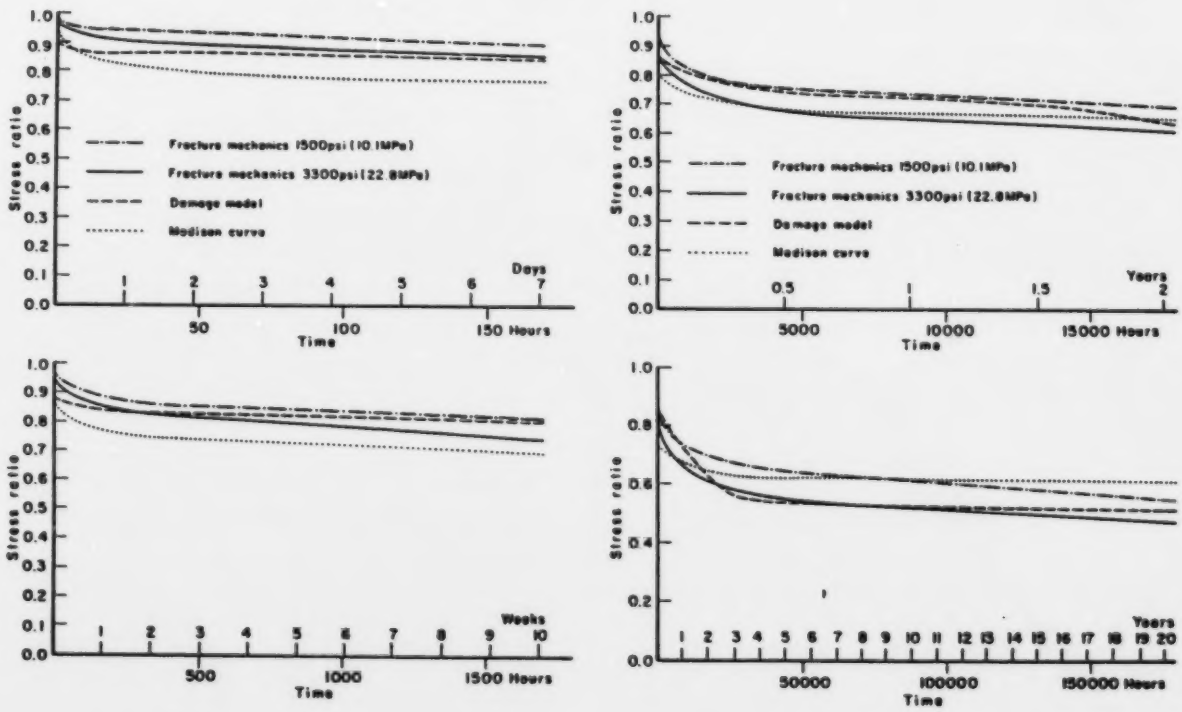

Figure 4. DOL curves with real time scale.

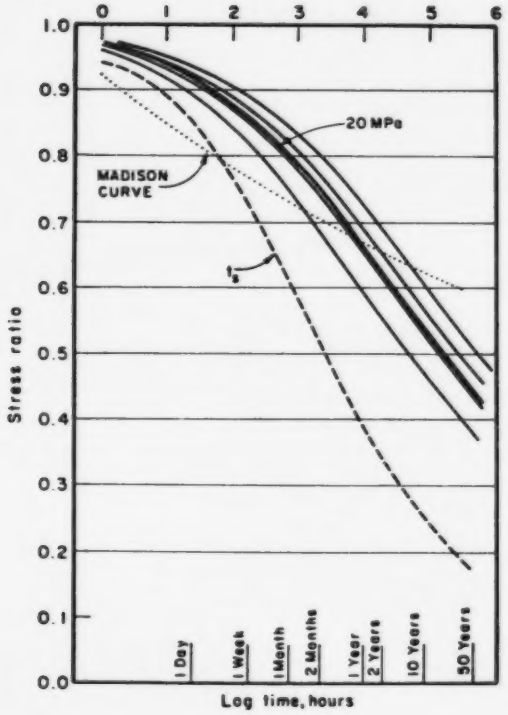

Figure 5. Nielsen DOL curve for 20 MPa.

Table 1

Times to Failure (years)

% Specified Load	ω = 1.0		ω = 0.9		ω = 0.80	
	SR*	TIME	SR	TIME	SR	TIME
100	0.70	0.8	0.63	5.5	0.56	34.5
90	0.63	5.5	0.57	28.7	0.50	154.
80	0.56	34.5	0.50	154.	0.45	720
70	0.49	217.	0.44	865	0.39	3780
60	0.42	1540	0.38	5720	0.34	23300
50	0.35	13400	0.32	46500	0.28	181000
40	0.28	161000	0.25	546000	0.22	2120000

* SR = Stress ratio

DURATION OF LOAD TESTS AT U.B.C.

Borg Madsen
Professor, Department of Civil Engineering
University of British Columbia, Vancouver

The basis for the Duration of Load (DOL) concept used in North America is presented by Lyman Wood (1951). This short report clearly describes how the DOL curve, often referred to as the "Madison Curve", was developed. It also outlines the arbitrary decisions the author had to make in order to make a single curve out of the data available to him at the time.

The mainstay of the investigation was a test in which small, clear, defect-free Douglas-fir specimens 1-in. x 1-in. x 14-in. were loaded to a specified stress ratio. Eight stress ratios from 0.95 to 0.60 were employed using an average of 16 specimens for each stress ratio. Some of the specimens were tested at six percent moisture content (MC), others at 12 percent MC. The stress ratios were established from matched specimens subjected to a standard static bending test of about five minutes duration. The results are shown in Figure 1.

These tests with constant load were then considered in conjunction with rapid ramp loading tested by Liska (1950). It was of course realized that the loading conditions were different, but they were combined nevertheless.

A third piece of information was obtained from some impact tests conducted in 1916 by A. Elmendorf, who found that Douglas-fir specimens subjected to impact tests had a strength roughly 75 percent greater than that obtained in a standard five-minute ramp loading test. This data point did not, however, fit the two previously mentioned tests and another point was chosen to represent the impact tests. The resulting "Madison Curve" was, due to lack of appropriate test results, applied to all other strength properties for wood except modulus of elasticity.

The purpose of recounting the thoughts which led to the presently used DOL concept is not to criticize past judgement, but to illustrate that our present DOL concept is not an unshakeable fact. Indeed, there is a great need for a physical understanding as underpinning of the duration of load phenomena.

STEPWISE RAMP LOAD TESTS

A DOL test program was commenced at U.B.C. in 1971. The purpose was to ascertain the DOL effect for lumber rather than for clear, defect-free wood. The reason for this was that the failure mode in lumber subjected to bending is very different from the failure mode found in clear wood subjected to bending.

Lumber often fails in the tension zone, usually in the vicinity of a knot where the grain is disturbed. The failure mode is associated with localized tension perpendicular to the grain stresses and has a brittle character. Clear wood, on the other hand, has a failure initiation mode consisting of wrinkles developing in the compression zone creating a somewhat ductile failure. Therefore, it was thought that the DOL effect could very well be different for the two failure modes and the DOL effect for lumber could therefore be different from the Madison curve.

It is, however, not possible to use the matched specimen technique used by Wood in his tests, since we cannot predict the strength of lumber very well. Therefore, we cannot obtain matched specimens with sufficient degree of accuracy. Instead, a matched sample technique is used. Two or more subsamples are created by randomly dividing the material from an original sample into the required subsamples. The aim is to get subsamples with strength distributions as similar to each other as possible. By using large sample sizes the strength distributions will indeed be similar.

By subjecting the subsamples to different loading conditions and observing the change in the strength distribution, one can make inferences of the effects of the different loading conditions. A sample size of 45 specimens 2-in. x 6-in. x 12-in. was used initially. This meant that a lot of full-sized specimens had to be loaded for a very long time at each of the stress levels, if Wood's technique was to be followed.

To overcome this, a stepwise ramp loading method was devised as shown in Figure 2. The load was applied in load increments equal to about one tenth of the short-term strength of the strong pieces in the strength distribution. The time interval between the application of the load increments was kept constant for an individual test but varied by a factor of 10 between the tests. In this manner all the specimens in a sample were broken. Tests were conducted with wet and dry lumber and with plywood subjected to different testing conditions as shown in Table 1. A total of 1,612 specimens of different kinds were tested. Details of the tests were reported by Madsen and Barrett (1976).

An example of the test results is shown in Figure 3 for 2 x 6 Douglas-fir tested dry in bending. Six load rates were used and the change in the strength distribution at the different rates is illustrated by joining the same percentiles of the strength distributions (10th, 25th, 50th 75th and 90th). A substantial change--30 percent decrease--is evident at the 90th percentile level where the ductile failure mode is predominating, while no change is indicated at the 10th percentile level where the failure is governed by a more brittle tension failure.

The overall conclusions drawn from these tests were:

1) The DOL effect in commercial material does not coincide with the Madison curve.

2) The DOL effect appears to be dependent on the strength of the material; strong material is affected more by DOL than weak material.

The above tests raised interest in developing a firmer foundation for the duration of load phenomena and the Canadian Forestry Service provided funding for a larger DOL experiment dealing with lumber.

CONSTANT LOAD TESTS

The primary aim was to establish if the Madison curve was applicable to lumber. In order to do that it was specified in the contract that the experiment should follow Wood's experiment as closely as possible, deviating only when necessary. As mentioned earlier, the matched specimen technique could not be used for lumber and the matched sample technique was used instead. However, the sample size was, after

statistical considerations, increased to 80 for each test condition and a few test conditions repeated.

The lumber was 2 x 6 kiln dried Douglas-fir, 12-feet long and of "No.2 and Better" grade. The allocation of the pieces to the subgroups was done more carefully than before in order to improve the similarity of the strength distributions of the subgroups. The modulus of elasticity (MOE) was measured on each board and the boards then ranked according to these values. The assignment to the subgroups was then done, starting with the board with the lowest MOE value. For a more detailed description of the process see Madsen and Barrett (1976).

Three groups were chosen to be used as the control sample, and their short-term strength distribution was established using a rate of loading that induced an average time to failure of about one minute. The 5th, 10th, 25th and 50th percentiles of this sample were calculated and used to establish the constant load to be used in the tests. The Madison curve predicts that the strength after seven days relative to a one-minute test should be 0.71, so the mentioned percentiles were multiplied by 0.71 and the load creating that stress calculated. Table 2 shows the different tests carried out. A second sample of material, but stronger, was obtained to broaden the range of test loads. This sample--called population II--was dealt with in the same manner as the first and the results are included in Table 2.

The constant load tests were conducted with a test setup as shown in Figure 4. The tests, originally planned to last 700 days, were extended to last six years before they were taken down. All the boards that survived the intended load period were subsequently broken using the same ramp loading test as for the control sample.

The test data were interpreted four different ways:

a) Number of survivors as percent of sample size;
b) Number of survivors as percent of boards stronger than the load level;
c) Stress ratio calculated using the control sample;
d) Stress ratio calculated using an assumed distribution deduced from the test results.

The last two methods will be discussed briefly.

In an ideal world the strength distribution for the control sample and the long-term test sample should be identical, as shown in Figure 5. The number of boards which broke on loading (BOL), i.e. at a stress less than the intended load level, should match the intersection point of the load level and the distribution curve. The distribution curve for the surviving boards which were subjected to the ramp load test subsequent to the constant load test should also coincide with the control curve. The stress ratio for the boards which broke while loaded by the constant load can then be calculated by dividing the applied stress with the control strength at the same rank. The implied assumption made is that the boards subjected to constant load fail in the order of their original short-term strength. This is not proven, but seems reasonable to assume.

If we cannot be certain that the strength distribution of the material used for the constant load test is identical to the control sample, a discrepancy may occur if we use the above method for establishing the stress ratio. The long-term data does, however, provide us with two pieces of information which help to establish the strength distribution of the long-term test.

We know the number of boards that broke at a stress less than the intended load level. This provides us with a point on the lower portion of the strength distribution of the long-term load sample. The short-term strengths of the surviving boards give us information on the high end of the strength distribution, assuming that damage did not taken place during the constant load test. Typically, one finds a couple of the surviving boards having a strength lower than expected and they are likely to have suffered damage but the rest of the material follows the general shape of the control curve.

In Method d the strength ratios were calculated assuming a short-term strength distribution going through the mentioned points as shown in Figure 6.

RESULTS

a) It was statistically proven that the Madison curve does not apply to the lumber samples tested here.

b) Constant loads applied for two months and one year reduced the short-term strength to 85 percent and 75 percent, respectively.

c) The curvature of the DOL curve for lumber is the opposite of that for the Madison curve.

d) An increase in strength with rapid loading was not observed.

e) The DOL effect appears to be strength dependent; largest for stronger material.

The results from these tests did not lead to changes in the North American timber codes, but the Swedish and Australian timber codes were modified.

The test data were, in addition, used to calibrate and verify a visco-elastic fracture mechanics model proposed by Dr. L. Fuglsang Nielsen for predicting the DOL behavior of timber as described in Johns and Madsen, (1982).

REFERENCES

Elmendorf, A. 1916. Stress in impact. Journal of the Franklin Institute 182(6).

Johns, K. and B. Madsen. 1982. Duration of Load Effects in Lumber--Parts I, II, and III. Canadian Journal of Civil Engineering 9(3):502-536.

Liska, F.P. 1950. Effect of Rapid Loading on the Compressive and Flexural Strength of Wood. U.S. Forest Products Laboratory, Madison, WI. Report No. 1767.

Madsen, B. and J.D. Barrett. 1976. Time-strength Relationships for Lumber. Structural Research Series. Report No. 13. University of British Columbia, Department of Civil Engineering.

Wood, L.W. 1951. Relation of Strength of Wood to Duration of Load. Forest Products Laboratory, Forest Service, U.S. Department of Agriculture. Report No. 1916.

Table 1

Testing Program for Stepwise Ramp Load Tests

	Number of rates	N	Avg. sample size	Species
Dry Bending				
Clear	6	203	34	Hem-fir
#2 Grade	6	285	47	Hem-fir
Wet Bending				
#2 Grade	6	210	35	D-fir
Shear				
Clear	6	89	15	D-fir
#2 Grade	6	180	30	D-fir
Tension Perp.				
Clear	6	76	13	D-f Glulam
Commercial	6	89	15	D-f Glulam
Plywood				
Edge Bending	4	160	40	Sheating
Flat Bending	4	160	40	Sheating
Rolling Shear	4	160	40	Sheating
TOTAL 1,612 specimens				

Table 2

Testing Program for Constant Load Tests. Sample Size.

		TIME				
	Load level (psi)	2 sec.	7 hrs	7 days	70 days	6 years
Population I						
	1070		80	160	80	80+
	1410	80	80	160	80	80+
	2110	80	80	80	80	80+
	3110	80	80	160	80	80+
Population II						
	2010			80	80	
	3000			80	80	
	3820			80	80	
	4600			80	80	
Total (including controls)						
	2800 specimens					

+Truncated sample.

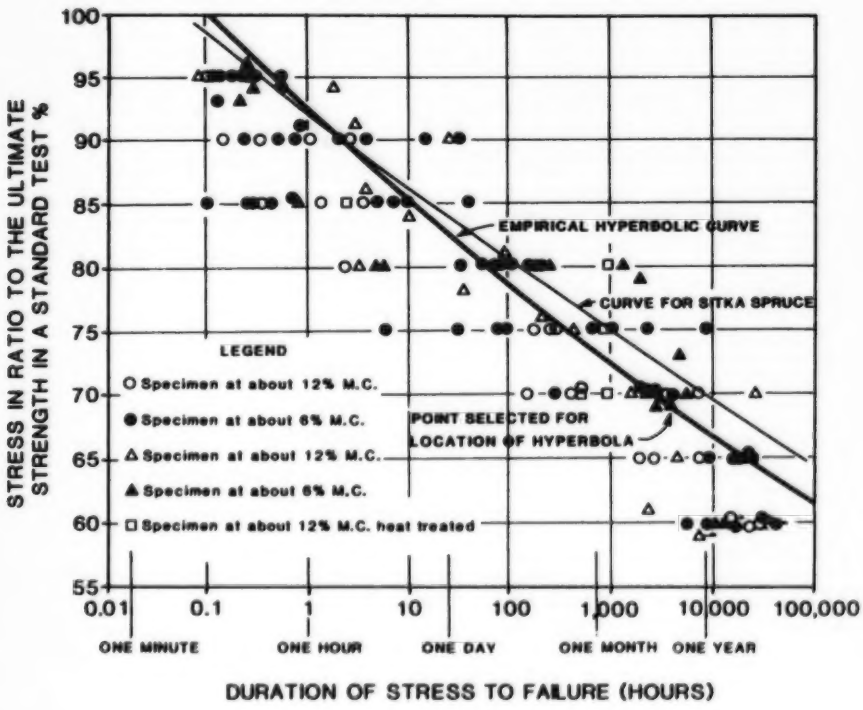

Figure 1. Madison Test - Results from small clear bending specimens.

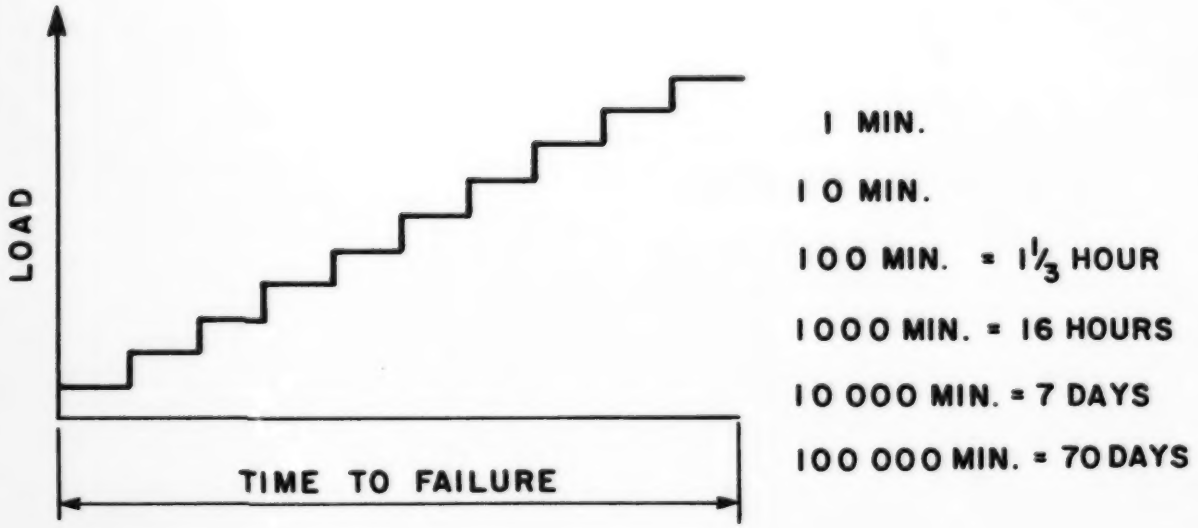

Figure 2. Stepwise ramploading tests.

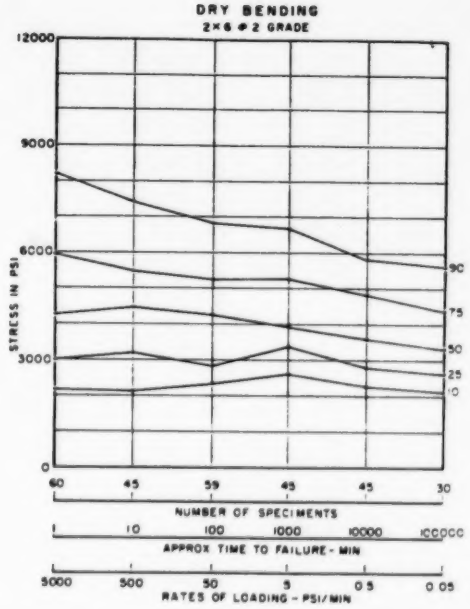

Figure 3. Change in strength distribution dry bending hem-fir #2 grade.

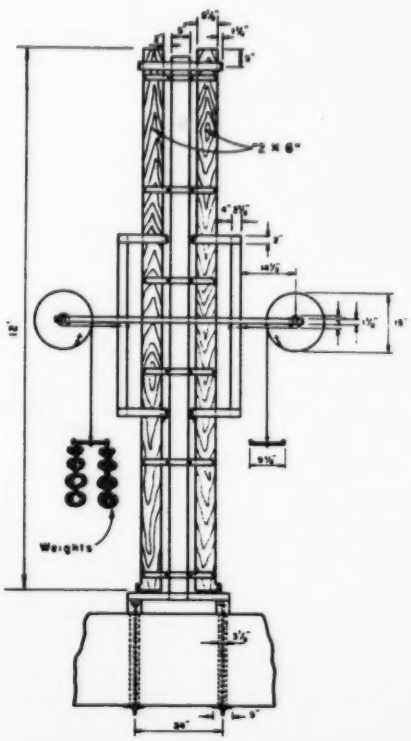

Figure 4. Test set up for constant stress 2" x 6" x 12' bending.

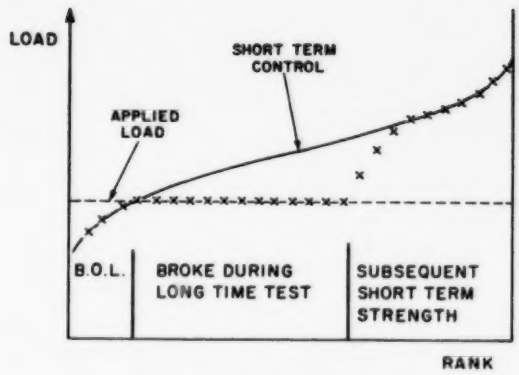

Figure 5. Strength distribution (ideal world).

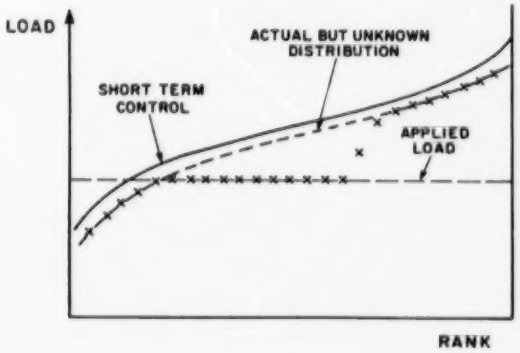

Figure 6. Strength distribution (real case).

LIST OF PARTICIPANTS

Mr. D.E.R. Anderson
Mr. E.N. Aplin
Mr. L. Bach
Dr. J.D. Barrett
Mr. Bendtsen
Mr. T.E. Brassell
Mr. M. Churchland
Mr. B. Craig
Dr. J.A. Dangerfield
Mr. D. Dolan
Mr. G.A. Dring
Mr. T.A. Eldridge
Mr. E. Elias
Mr. T. Fewell
Dr. R.O. Foschi
Mr. R. Fouquet
Mr. K.A. French
Dr. G. Gerhards
Mr. P. Glos
Mr. H. Griffin
Ms. A. Hejja
Mr. C.R. Henderson
Mr. R.A. Hewett
Dr. B. Hoffmeyer
Mr. A.P. Jessome
Mr. K.C. Johns
Mr. E.D. Jones
Mr. E. Karacabeyli
Mr. H.V. Koring

Professor J. Kuipers
Mr. K. Lakhani
Mr. F. Lam
Professor H.J. Larsen
Mr. T. Laufenberg
Ms. C. Link
Mr. J.Y. Liu
Mr. K.J. Lyngcoln
Professor B. Madsen
Dr. S.K. Malhotra
Dr. V.N.P. Mathur
Dr. L.F. Nielsen
Dr. B. Noren
Dr. L.C. Palka
Mr. F. Pienaar
Mr. A. Quaile
Mr. B.E. Rossborough
Professor J. Salinas
Dr. M. Samson
Mr. J. Sebelius
Mr. L. Soltis
Dr. C.K.A. Stieda
Mr. R. Stluka
Mr. J.G. Sunley
Mr. J.E. Turnbull
Mr. E. Varoglu
Mr. H.P. Vokey
Mr. J. Williamson
Dr. C.R. Wilson